Dendrimer-Fullerenes and Lipo-Fullerenes: Synthesis, Properties, and Organisation

Den Naturwissenschaftlichen Fakultäten
der Friederich-Alexander-Universität Erlangen-Nürnberg

zur

Erlangung des Doktorgrades

vorgelegt von

Francesc Xavier Camps Camprubí

aus Barcelona

Als Dissertation genehmigt von den Naturwissenschaftlichen Fakultäten der Universität Erlangen-Nürnberg

Tag der mündlichen Prüfung:

Vorsitzender der Prüfungskommission:	Prof. Dr. D. Kölzow
Erstberichterstatter:	Prof. Dr. A. Hirsch
Zweitberichterstatter:	Priv.-Doz. Dr. R. Schobert

Die vorliegende Arbeit wurde in der Zeit zwischen Oktober 1995 und April 1998 am Institut für Organische Chemie der Friederich-Alexander-Universität Erlangen-Nürnberg unter Anleitung von Prof. Dr. A. Hirsch angefertigt, dem ich für die Stellung des interessanten Themas, seine Unterstützung und sein stetes Interesse herzlich danke.

Table of Contents

1 General Part

1.1 Introduction

Fullerene ceased being a postulated molecule[1] and became true[2] in 1985, when H.W. Kroto, R. F. Curl and R.E. Smalley discovered its formation by focusing a pulsed laser beam onto a graphite target. The big expansion of fullerene chemistry, however, did not arrive until 1990, when Krätschmer and Huffmann described a method that made this third allotropic form of carbon available in suitable amounts to the scientific community for further research[3].

Fullerenes are built up of fused pentagons and hexagons. The pentagons, absent in the other two carbon allotropes graphite and diamond, provide the characteristic curvatures. The smallest and at the same time the most abundant fullerene obtained by usual preparation methods is the I_h-symmetrical buckminsterfullerene C_{60} (figure 1.1). The next stable homologue is C_{70} followed by higher fullerenes.

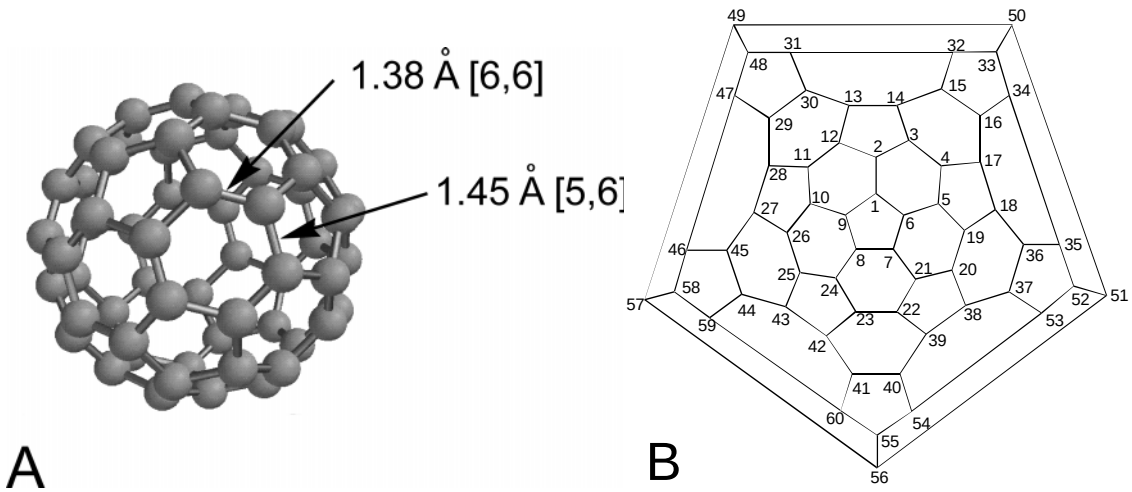

Figure 1.1. Schematic representations of [60]fullerene: (A) ball and stick model with the length of the two different bonds in the molecule, (B) Schlegel diagram of the lowest energy Kekulé structure with numbering of the carbon atoms.

Fullerenes, especially the C_{60} buckminsterfullerene (buckyball) with its soccer ball shape, derived their names from the similarity with the geodesic domes constructed by the American architect Richard Buckminster Fuller. In contrast to the extended structures of

diamond and graphite, the spherically defined carbon allotropes are soluble in a variety of organic solvents, thus facilitating their manipulation.

The accessibility of fullerenes in macroscopic amounts opened up the opportunity to develop a rich three dimensional chemistry of spherical and polyfunctional all-carbon molecules. Indeed, in less than a decade the basis of the fullerene chemistry has been established[4-6]. A large multitude of fullerene derivatives of both covalent addition products as well as fullerene salts can be imagined and a lot of them have been synthesized and studied. As a result, new materials with outstanding biological or materials properties have been discovered. Important events were the discovery of the superconductivity of certain fullerene derivatives[7] and the ferromagnetism of the charge transfer complex [TDAE]C_{60}[8]. Also, it has been shown that some modified water soluble fullerene derivatives exhibit biological activity like inhibition of HIV protease and transcriptase[9,10], DNA cleavage[11,12], and potential usefulness as neuroprotective agents[13].

1.2 [60]Fullerene: Structure and Properties

The term fullerenes is used to describe all carbon curved closed structures composed of five and six membered rings. Their construction principle follows Euler´s theorem, which says that for the closure of each spherical network of *n* hexagons, twelve pentagons are required, with the exception of n=1. As a consequence, each fullerene contains $2(10+n)$ carbon atoms (with *n* representing the number of hexagons).

[60]Fullerene is the most abundant as well as one of the most symmetrical fullerenes belonging to the highly symmetrical point group I_h (120 symmetry operations). [60]Fullerene contains twelve pentagons that are isolated by twenty hexagons obeying the *Isolated Pentagon Rule* (*IPR*)[14]. The *IPR* predicts fullerene structures with no adjacent pentagons to be more stable than those with adjacent pentagons. Resonance destabilization of pentalene-type 8π-electron systems and an increase of strain energy are the reasons why adjacent pentagons are not favored.

The bonds at the junctions of two hexagons ([6,6]bonds) are shorter than those at the junctions of a pentagon and a hexagon ([5,6]bonds). This bond length alternation shows that in the lowest Kekulé structure, the double bonds are located at the junctions of hexagons ([6,6]double bonds) and that there are no double bonds in pentagonal rings.

Although C_{60} has 60 conjugated π-electrons with isotropic conjugation, because of its deviation from planarity it cannot be treated as a "superarene" molecule, but rather as a poorly conjugated polyolefin consisting of [5]radialene and cyclohexatriene units.

The highly pyramidalized sp^2 carbon atoms in the spherical C_{60} cause a large amount of strain energy within the molecule. Mainly due to this strain energy, which is about 80% of its heat of formation (ΔH_f = 10.16 kcal/mol per carbon atom), [60]fullerene is thermodynamically less stable than graphite (ΔH_f = 0 kcal/mol)[15]. The response to this nonplanarity is a rehybridization from sp^2-σ and p-π orbitals. The π-orbitals exhibit no longer purely p-character and the σ-orbital no longer contains all the s-character[16]. This pyramidalization and rehybridization is mainly driven by the geometric constraint of the σ-system, whereas the fullerene still maintains a high degree of π-orbital alignment.

[60]Fullerene is an electronegative molecule, which can be easily reduced but hardly oxidized. This is reflected theoretically[17] by the MO diagram of C_{60} (figure 1.2) showing low lying triply degenerated LUMOs and a five-fold degenerated HOMO, as well as experimentally[18] by the ease of six reversible one-electron reduction steps. The electronic spectrum of C_{60} is characterized by several strong UV absorptions between 190 and 410 nm and by some forbidden transitions in the visible part of the spectrum which are responsible for the purple color of C_{60}. The assignment of the transitions has been carried out using theoretical calculations[19].

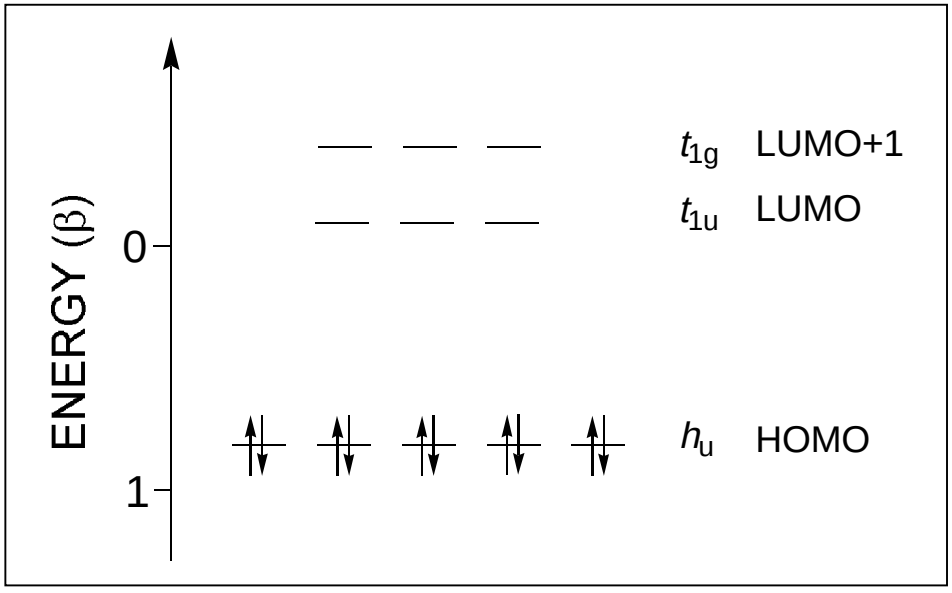

Figure 1.2. Schematic representation of the Hückel molecular orbital diagram for [60]fullerene (HOMO, LUMO, LUMO+1)[17].

Due to the high symmetry of C_{60}, from its 174 vibrational normal modes, only four are IR active (t_{1u}) and ten are Raman active (a_g, h_g)[20]. The ^{13}C-NMR shows a single peak at 143.2 ppm, about 15 ppm shifted downfield with respect to benzene as a result of the nonplanarity of the [60]fullerene molecule[21]. Mass spectra of C_{60} can be recorded easily with electron impact ionization (EI) giving a pronounced molecular ion (m/z=720). Minor fragment ions belonging to a series of C_2 cleavage (M^+-24, -48, -72, etc.) are observed.

These properties, together with the multitude of chemical transformations that have already been carried out with [60]fullerene, allow to postulate some rules to define its chemical behavior:

1. *The reactivity of C_{60} is that of a fairly localized electron deficient polyolefin.* The main reactions are nucleophilic or radical additions to the [6,6]double bond and cycloadditions.
2. *The major driving force for addition reactions is the relief of strain in the fullerene cage.* Reactions leading to saturated tetrahedrally hybridized sp^3 carbon atoms are strongly assisted by the strain of pyramidalization present in the fullerene (most addition reactions to C_{60} are exothermic).
3. *The regiochemistry of the addition is governed by the minimization of the formation of [5,6]double bond within the molecule.* The exclusive mode for typical cycloadditions and the preferred mode for additions of sterically non demanding segregated addends is 1,2 (addition to a [6,6]double bond), since in this case no unfavourable [5,6]double bonds within the fullerene framework have to be formed.

The chemical transformations that are possible with C_{60} could be classified in five main groups (figure 1.3):

a) *Addition reactions*. Formation of exohedral compounds by addition of nucleophiles or radicals, cycloadditions, complexations with transition metals and others.
b) *Electron transfer reactions.* Chemical reduction of fullerenes can easily be achieved by reaction with electropositive alkali and alkaline earth metals or organic donor molecules.
c) *Heterofullerenes.* Substitution of a carbon atom of the fullerene skeleton for a heteroatom, for example nitrogen or boron.

d) *Ring opening reactions*. Producing a hole in the C_{60} skeleton while breaking a discrete number of bonds.

e) *Formation of endohedrals*. Introducing and trapping of atoms inside the spherical carbon cage.

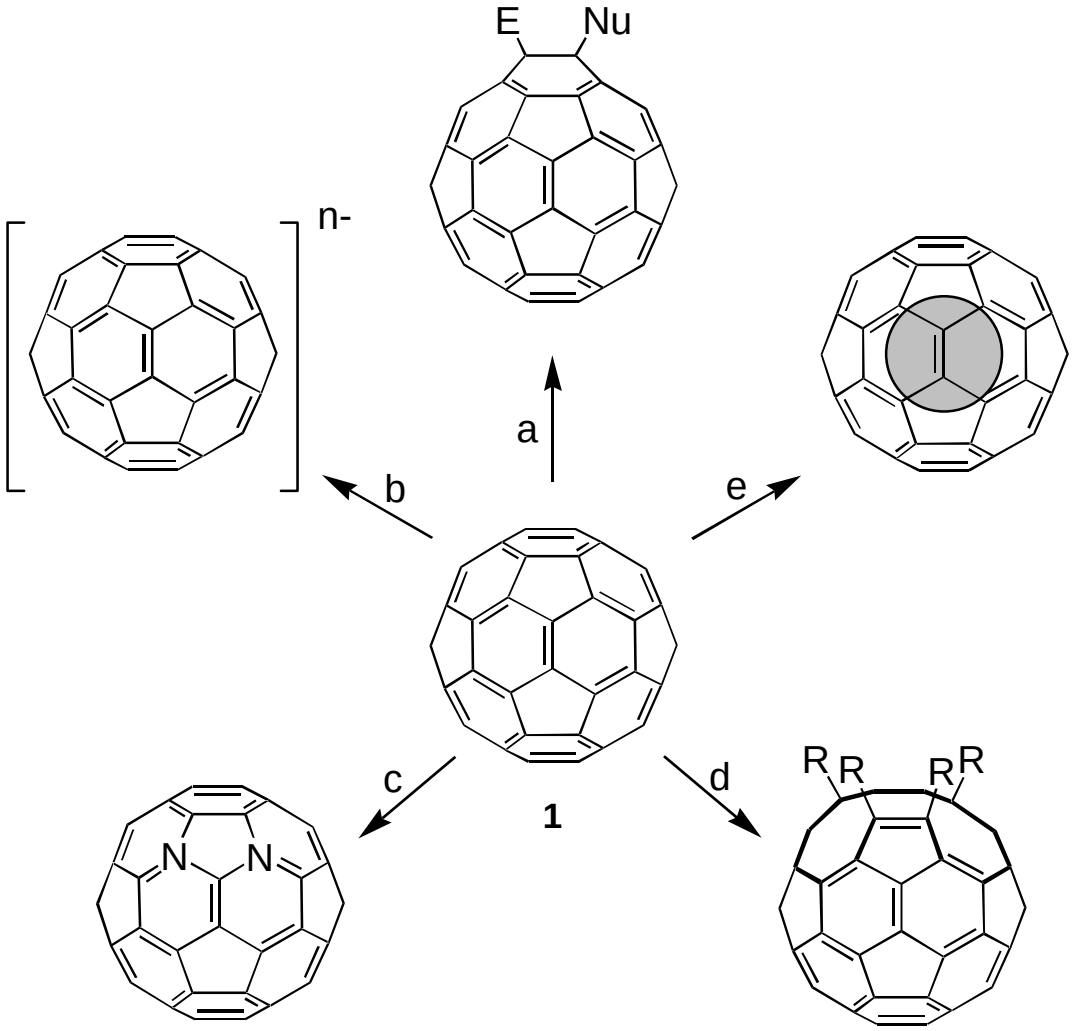

Figure 1.3. Different chemical transformations of C_{60}.

1.3 Multiple Additions to [60]Fullerene

From the beginning of fullerene chemistry it became clear that [60]fullerene with its perfect spherical shape represents a perfect building block for the synthesis of molecules with specific geometries. However, since C_{60} exhibits a workspace with 30 reactive [6,6]double bonds, a high number of polyaddition products are expected. This problem has been, and is still, extensively studied, not only because of the attempts to study the intrinsic differences in their physical and chemical properties, but also in order to exploit

the synthetic potential of [60]fullerene for the design of highly symmetrical and stereochemically defined oligoadducts.

For reversible reactions, processes have been described in which the most stable isomer is obtained as a single product[22,23]. For kinetically controlled irreversible reactions, however, mixtures of regioisomeric products are obtained. Cycloadditions to [6,6]double bonds of the fullerene framework[4,6], which are the most versatile and straightforward reactions in fullerene chemistry, belong to this last group. From these, cyclopropanation of fullerenes with α-haloesters or α-haloketones described by Bingel[24] is one of the most used due to its high yields and simple performance (scheme 1.1).

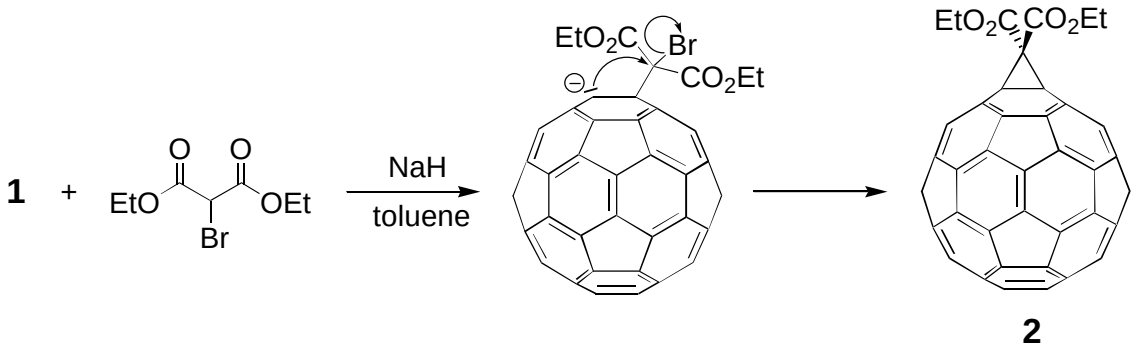

Scheme 1.1. Reaction mechanism of the cyclopropanation of [60]fullerene (**1**) with bromo diethylmalonate described by Bingel.

After the attachment of a first addend to a [6,6]bond of the fullerene, nine different reactive [6,6]bonds are available for a second attack (figure 1.4)[25,26]. Hence, for two different addends nine regioisomeric bisadducts are in principle possible, whereas for identical addends only eight isomers can be considered since attack at the *e'* and *e"* positions leads to the same product. Starting from different malonic systems, various series of bisaddition products have been extensively studied. Within this context it is of importance to emphasize that their characteristic UV spectra depend on the addition pattern regardless of the nature of the added moieties. Furthermore it should be noted that the three bisadducts in which the attached substituents are in *cis-3*, *trans-2*, as well as in *trans-3* relative positions possess C_2-symmetry and therefore are chiral.

The experimental results indicate that a second irreversible attack at a [6,6]bond proceeds with a regioselective preference for *e* and *trans-3* positions for sterically demanding addends and for *e*, *trans-3*, and *cis-1* positions for sterically less demanding

ones. Calculations have also shown that the coefficients of frontier orbitals are enhanced in these three positions (*e*, *trans-3*, *cis-1*)[27,28].

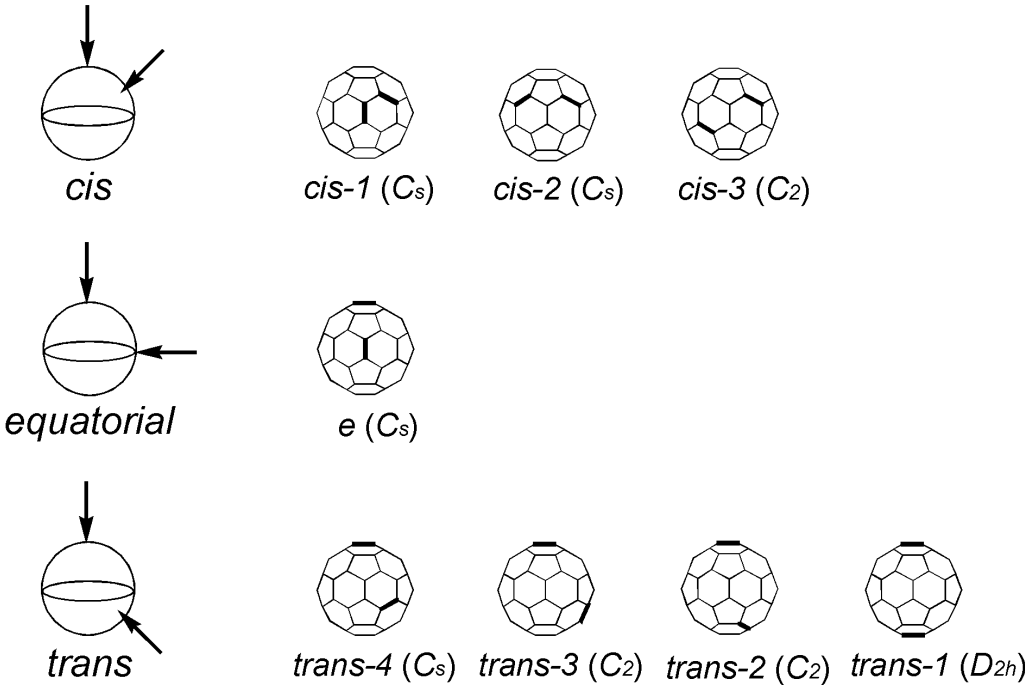

Figure 1.4. Relative positions of the [6,6]bonds carrying the two addends in the eight possible regioisomeric bisaducts and symmetries of the corresponding isomers considering identical addends.

In successive additions, the preference of attack at *e* positions becomes more pronounced, thus allowing the synthesis of T_h-symmetrical hexaadducts in considerably high yields[27]. Regioselective formation of T_h-symmetric [60]fullerene derivatives with an octahedral addition pattern is also achieved in one step via template activation with 9,10-dimethylanthracene (DMA) in high yields[29] (scheme 1.2).

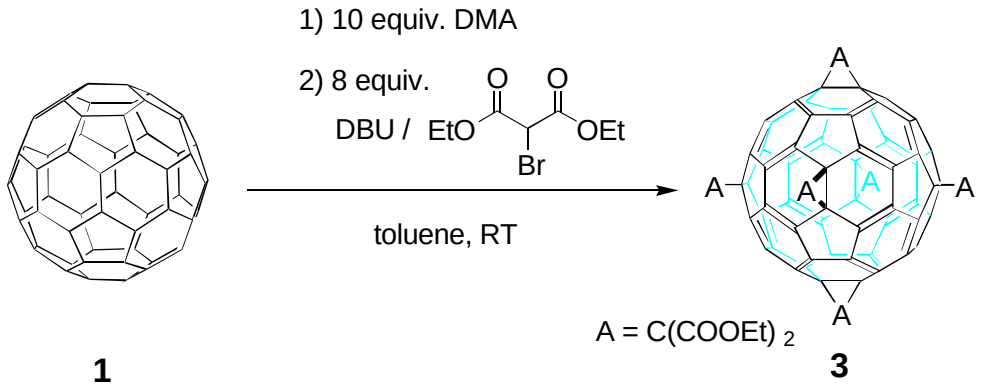

Scheme 1.2. Regioselective formation of [60]fullerene hexakisadducts with octahedral addition pattern via template activation with DMA.

Starting from monoadducts it is possible to prepare mixed hexakisadducts[30]. Triazoline **4** can be obtained by treatment of a concentrated solution of C_{60} in 1-chloro-naphthalene with one equivalent of methyl azidoacetate at 60°C (scheme 1.3). Since the triazoline group in **4** undergoes a facile cycloreversion, azides can be used as protecting groups for octahedral [6,6]double bonds, and therefore allow the synthesis of pentaadducts like **6** in comparatively high yields.

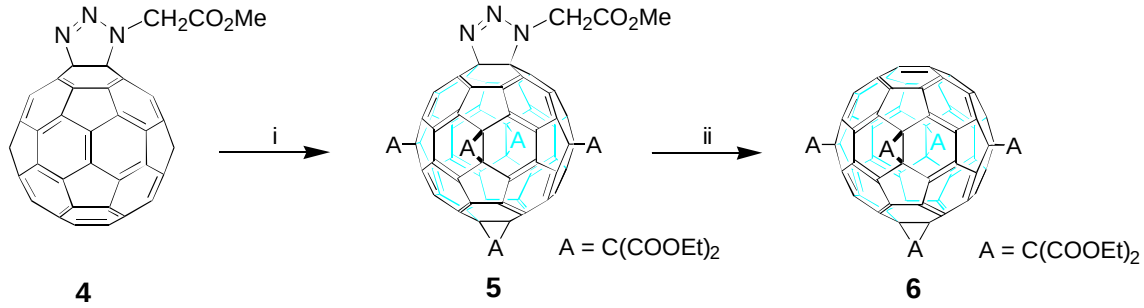

Scheme 1.3. i) 10 equiv. DMA, 10 equiv. bromo diethylmalonate/DBU, toluene, RT. ii) toluene, reflux.

Another strategy for the regioselective formation of higher adducts is the reversible tether directed remote functionalization developed by Diederich and coworkers (figure 1.5)[31].

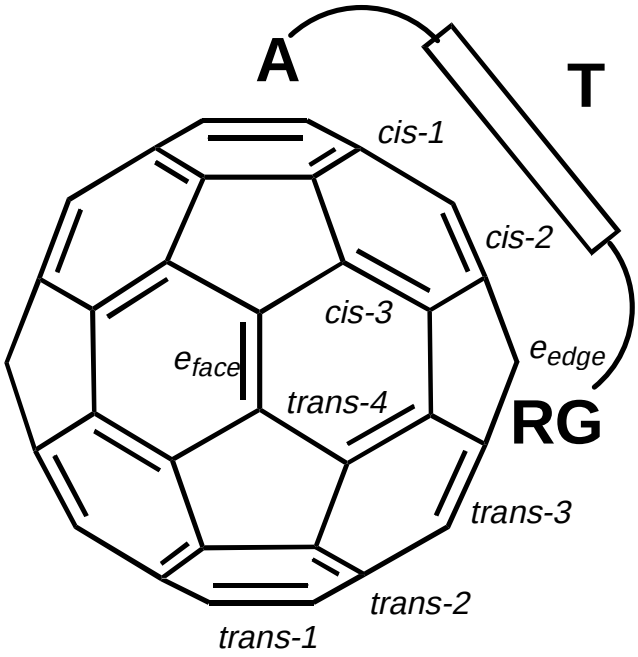

Figure 1.5. Schematic representation of the tether-directed remote bis-functionalization of C_{60} developed by Diederich and coworkers. A = anchor, T = tether, RG = reactive group.

To achieve regioselective multiple additions, the authors successfully applied the concept of tether-directed remote functionalization which had been introduced by Breslow for the regioselective functionalization of steroids and long chain alkanes[32]. This method is based on the introduction of an anchor group which contains one or more covalently bonded reactive groups. These groups react intramolecularily with C_{60} in a predetermined way according to the geometry of the tether between them and the anchor group. The choice of length and geometry of the handle between anchor and the reactive groups is critical to achieve regioselective attack.

Recently, an elegant topochemically controlled solid-state reaction providing access to a *trans-1* [60]fullerene bisadduct has been described (scheme 1.4)[33]. The crystalline [6,6]Diels Alder monoadduct from C_{60} and anthracene (**7**) undergoes a regiospecific and thermic exchange resulting in a solid mixture (1:1) of **1** and the [6,6]anthracene trans-1 bisadduct **8**.

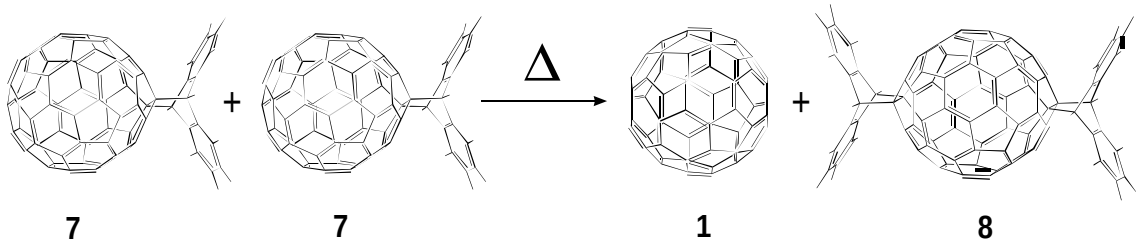

Scheme 1.4. *trans-1* Bisadduct **8** obtained through a topochemically controlled solid state reaction.

2 Proposal

2.1 Introduction

Recently, it has been shown that some fullerene derivatives exhibit biological activity[9-13]. In this respect, three properties of [60]fullerene based on its spherical skeleton or its electronic behavior are of special significance. The first one is its spherical shape, which can be used for molecular recognition. This property has been, for example, successfully exploited in inhibition of HIV protease (HIVP) studies[8,10]. The second one is the ability of the fullerene core to photosensitize efficiently the conversion of triplet oxygen to singlet oxygen, which can be used for DNA cleavage[11,12]. The third one is its radical-scavenger ability[34]. Prospective applications of [60]fullerene as neuroprotective agent are topics of current discussion[13].
In the last decade fullerene chemistry has been established and well developed. Nowadays, almost any class of compounds can be covalently bound to the fullerene core. Big efforts have been made to achieve control over addition patterns and the regioselectivity of higher adducts. No other building block offers such a versatility in organic chemistry as does C_{60}. It should enable chemists to synthesize structures with different functionalities spatially ordered similar to biomolecules like proteins, nucleics acids, etc. Therefore, it seems extremely rewarding to make use of [60]fullerene as a template building block (tecton) for the synthesis of globular macromolecules presenting functional groups in fixed positions with biological activity or impact in natural sciences. It is not only to take advantage of C_{60}´s own characteristics but to use it for the synthesis of molecules with very specific topologies in analogy to biomolecules.

2.2 Dendrimer-Fullerenes

Dendritic molecules[35,36] are well defined macromolecules topologically based on the structure of trees. These extremely branched molecules are synthesized from identical building blocks that contain branching sites via a repeatable synthesis strategy. By a judicious choice of these branched building blocks and functional group chemistry, one can precisely control properties of the target molecules such as shape, dimensions, density, polarity, flexibility, and solubility. Dendrimers combine typical characteristics of small organic molecules like defined composition and monodispersivity with those of polymers such as high molecular weight and their resulting multitude of physical properties. A similar combination of characteristics is present in

biopolymers like enzymes. Dendrimers consist of one or several cascades attached to a multifunctional central core, which can be an atom, molecule or an ion. The possibility to achieve different addition patterns in a controlled way turns C_{60} into a valuable synthon of incomparable characteristics to be used as a core.

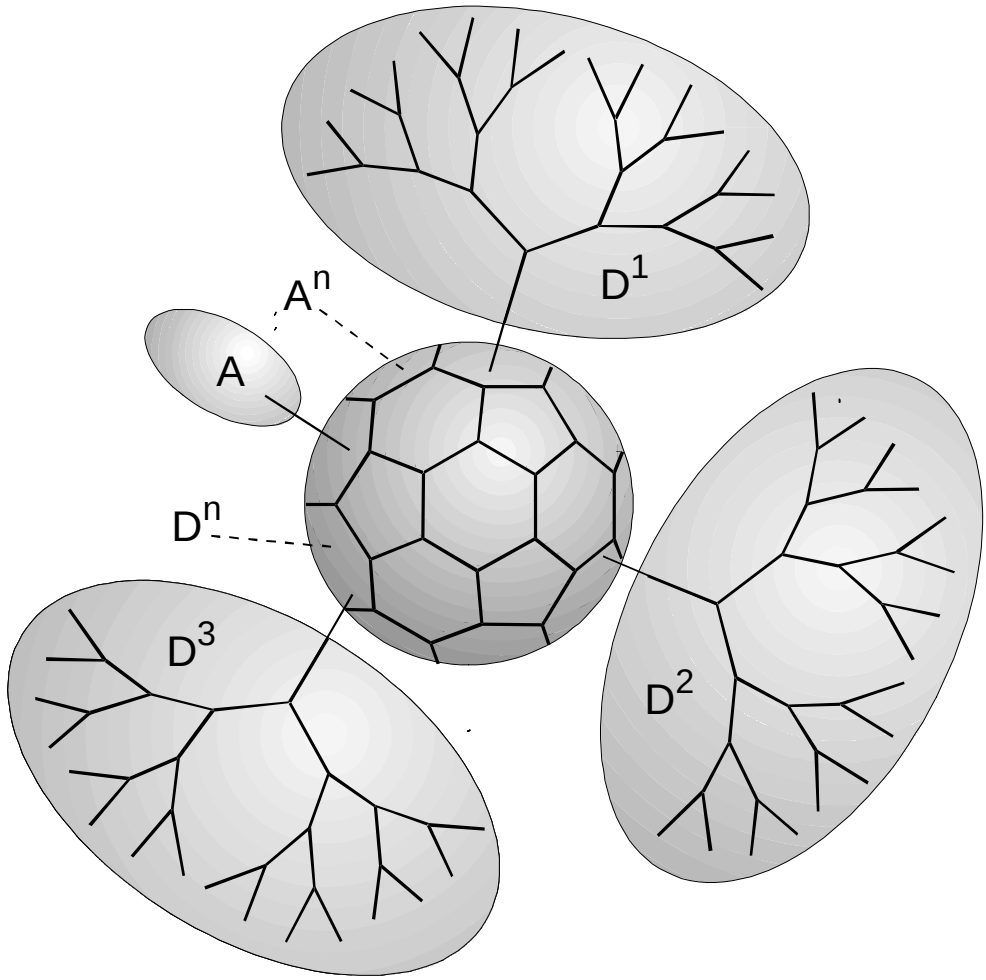

Figure 2.1. Schematic representation of possible dendrimer architectures with the C_{60} tecton as a central core. D_1, D_2, D_3...D_n denote identical or dissimilar dendrons attached to the fullerene framework. The A moieties are additional addends, which may also be attached to the fullerene framework. These addends may have specific physical or chemical properties or just be positional blockers to enable the construction of distinct addition patterns within the fullerene core. Furthermore they could influence the final conformation of the resulting dendrite molecule.

The aim of the present work is to build up globular fullerene based architectures containing dendrimers and additional functional groups mimicking the overall size and shape of natural biopolymers (figure 2.1). It is important to take advantage of all the characteristics that [60]fullerene presents for that purpose. Those are i) the possibility to easily accomplish variable degrees of addition within the fullerene core, especially mono- up to hexaadducts

obtained by cycloadditions, ii) the possibility to achieve spherical systems, and iii) the possibility of addition of similar as well as dissimilar addends in a stereochemically controlled manner.

2.3 Lipo-Fullerenes

Lipid bilayers, the basis of all natural membranes, are highly dynamic, two-dimensional, ordered systems. Their unique elastic properties lead to a number of applications as biomedical devices (e.g., biocompatibilization of surfaces, drug delivery). These properties derive from a unique double layer structure and the frictional drag between the two bilayer leaflets. The [60]fullerene shows extraordinary lubrication properties[37] and its diameter of 10.5 Å is just one fifth of the average bilayer thickness. Thus intercalation of C_{60} molecules between the two monolayers of a lipid bilayer may lead to interesting new material properties and may also affect the hierarchy of motion in a bilayer. To overcome the low solubility of plain C_{60} in bilayers[38], one could modify C_{60} by attaching long alkyl chains giving the so-called lipo-fullerenes. Although this chemical modification certainly alters the rotational dynamics of C_{60} and thus possibly its lubrication properties, it still retains its unique symmetry and may change the phospholipid bilayer to a composite system with new physical properties.
Also, this technology may offer the possibility to build up transmembrane systems consisting of fullerenes substituted with lipophilic and lipophobic substituents. The lipophilic part should stay inside the membrane and the lipophobic part should stand out. This strategy should permit the introduction of potentially biologically active moieties either inside or in the surface of the membrane opening extremely interesting new perspectives in this field.

3.1 Dendrimer-Fullerenes

3.1.1 Dendrimers: Branched Macromolecules. Synthesis Approach

The term dendrimer[35,36,39] is a composed word that derives from the Greek *dendr*on (*δενδρον* = tree) and oligo*mer*. The fundamental characteristics of these hyperbranched molecules are their well defined topology based on their construction principle. A dendritic system is composed of a central core (atom, ion or molecule) to which different dendritic branches are attached. These branches are synthesized from identical building blocks that contain branching sites via a repetitive synthetic strategy. Efficient nonlinear growth methodologies quickly provide access to high molecular weight, monodisperse globular structures with unique properties. With an accurate choice of the building block to be used, one can precisely control size, shape, density, polarity, solubility, flexibility and surface chemistry of the resulting macromolecules. All these parameters have been appointed as *critical molecular design parameters* (CMDPs)[35].

Since the first paper in this field, published in 1978 by Vögtle[40], the field of dendrimer research is increasingly attracting the attention of a broad cross-section of chemists. Dendrimers combine typical characteristics of small organic molecules like defined composition and monodispersivity with those of polymers such as high molecular weight and a resulting array of physical properties. A large number of dendritic systems has been synthesized and studied and as a result a broad variety of applications has been discussed[36,39,41]. Examples of these include encapsulation of guest molecules into dendritic *boxes* with potential use for drug delivery[42], nanoscale catalysis[43,44], applications in polymer technology, etc.

Two main methodologies are fundamental for the synthesis of dendrimers: the *divergent* and the *convergent approach*, although mixed approaches have been conceived as well[45,46].

In divergent[35,47-49] dendritic constructions growth occurs from the central core towards the macromolecule surface by successive stepwise addition and activation steps. The synthesis represented in the scheme 3.1 from Newkome et al.[50] of dendrimer **9** containing 36 carboxylic acid groups at the periphery provides a clear example for this approach. The first step consists of the attachment of the monomer unit to the polyfunctional core. Repetition of the two-step cycle, addition followed by activation, creates a new *generation*. The rapid increase of the number of reactive groups at the periphery of the growing macromolecule is a significant

feature of all divergent approaches. Any incomplete reaction of these terminal groups would lead to imperfections or failure sequences in the next generation. The probability of this occurrence increases with the growing of the macromolecule. To prevent side reactions and to force reactions to completion, large excesses of reagents are employed, thus causing purification problems.

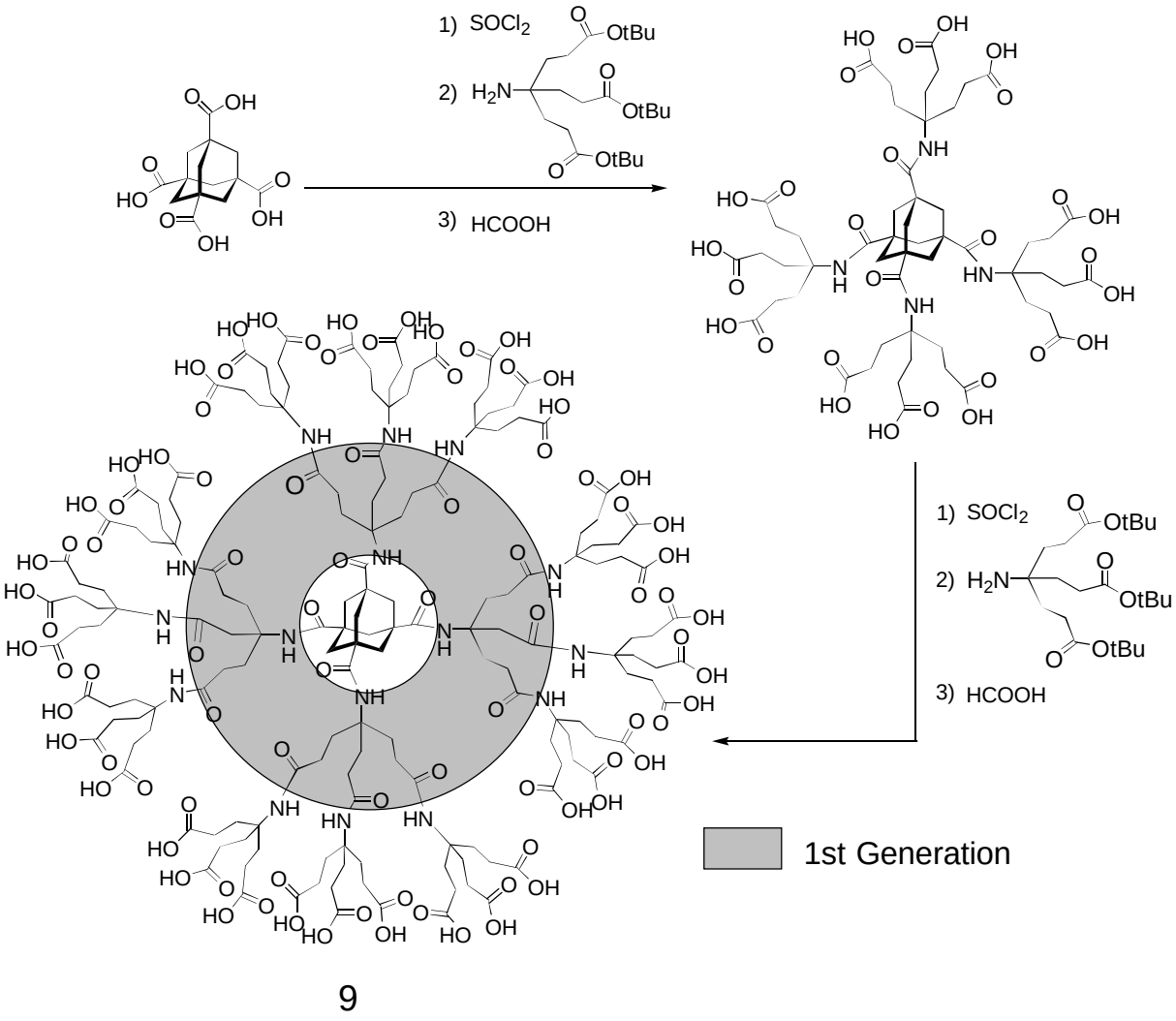

9

Scheme 3.1. Convergent synthesis of the 2nd generation dendrimer **9** with 36 carboxylic acids at the periphery using an adamantane based core[50].

In the convergent approach, developed by Hawker and Fréchet[51] and also by Miller and Neenan[52], growth begins at what will become the periphery of the final macromolecule and proceeds towards the interior. Dendrons are synthesized following the repetitive strategy depicted in figure 3.1. Once the synthesis of *monodendrons*[35] is accomplished, these are attached to the core in the last step. This approach offers as main features: the involvement of a very small number of molecules in each formation step, easy control of surface

functionality[53,54], the ability to dramatically change molecular architecture by using different cores for a given monodendron, and ease of purification and characterization of intermediates. However, the main limitation of this approach is that, as the size of the dendrimer increases, the focal point becomes more susceptible to steric inhibition. This limitation is not so significant in the divergent approach since the reactions are always taking place at the surface of the growing molecule.

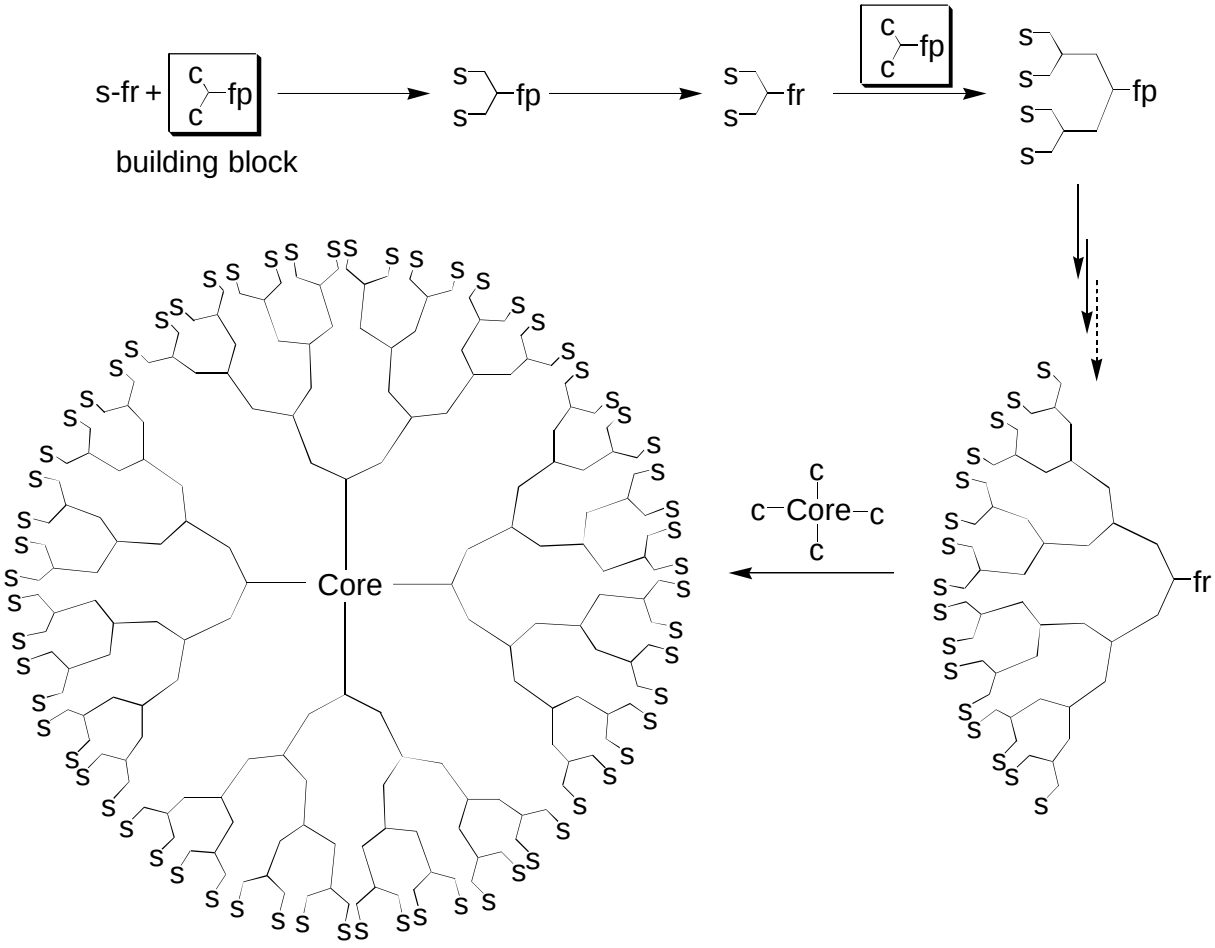

Figure 3.1. General schematic representation for the convergent approach. s: Surface functionality; f_r: reactive functional group; c: coupling site; f_p: protected functional group.

3.1.2 Dendrimer-Fullerenes: Background

Hawker and Fréchet[51,55] developed the convergent method to synthesize dendritic polyethers based on 3,5-dihydroxybenzyl alcohol (**10**) as a monomer unit up to the sixth generation (scheme 3.2). The synthesis involves a repetitive two-step process consisting of selective alkylations of phenolic hydroxyl groups and conversion of benzylic alcohols into benzylic bromides. The main advantages of this elegant work are the high yields in all steps and its simplicity in product purification and characterization. For this reason, many research groups

have made use of this benzyl ether-type dendrons in their first steps in macromolecular chemistry.

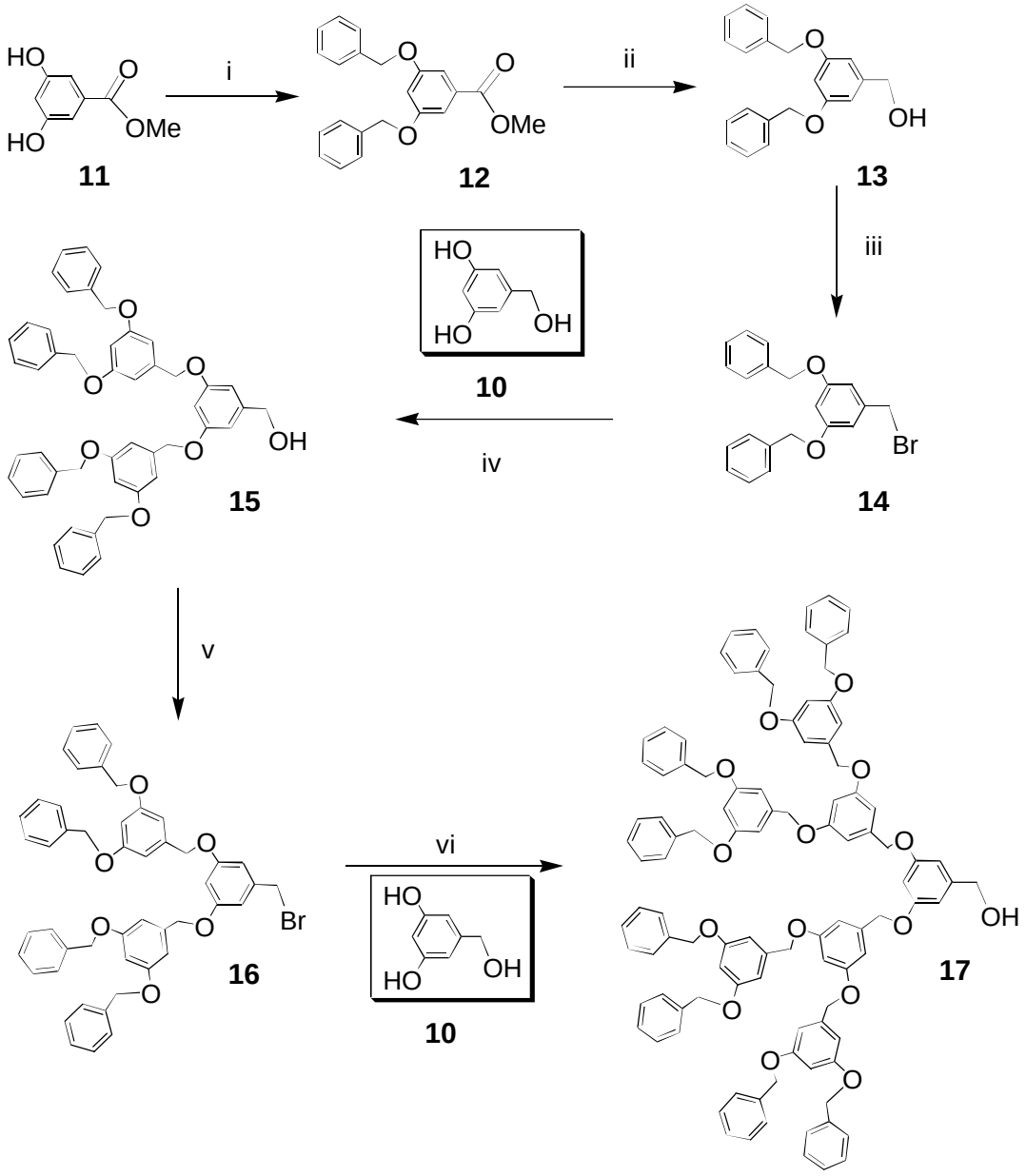

Scheme 3.2. Synthesis of dendritic polyethers based on 3,5-dihydroxybenzyl alcohol (**10**) by Hawker and Fréchet[51,55]. i) Benzyl bromide, K_2CO_3, [18]crown-6/acetone (93%); ii) $LiAlH_4/Et_2O$ (96%); iii) PBr_3/benzene (92%); iv) K_2CO_3, [18]crown-6/acetone (91%); v) CBr_4, PPh_3/ THF (93%); vi) K_2CO_3, [18]crown-6/acetone (88%).

At the beginning of the present work only two examples of dendritic molecules possessing a [60]fullerene molecule core were known[56,57]. These two works represent the connection between two of the most crucial subjects in supramolecular chemistry: dendrimer and fullerene chemistry. In the first example[56], two fourth generation benzyl ether-type bromide

monodendrons **18** were attached to a biphenol prefunctionalized C_{60} (**19**)[58] through a Williamson reaction (scheme 3.3).

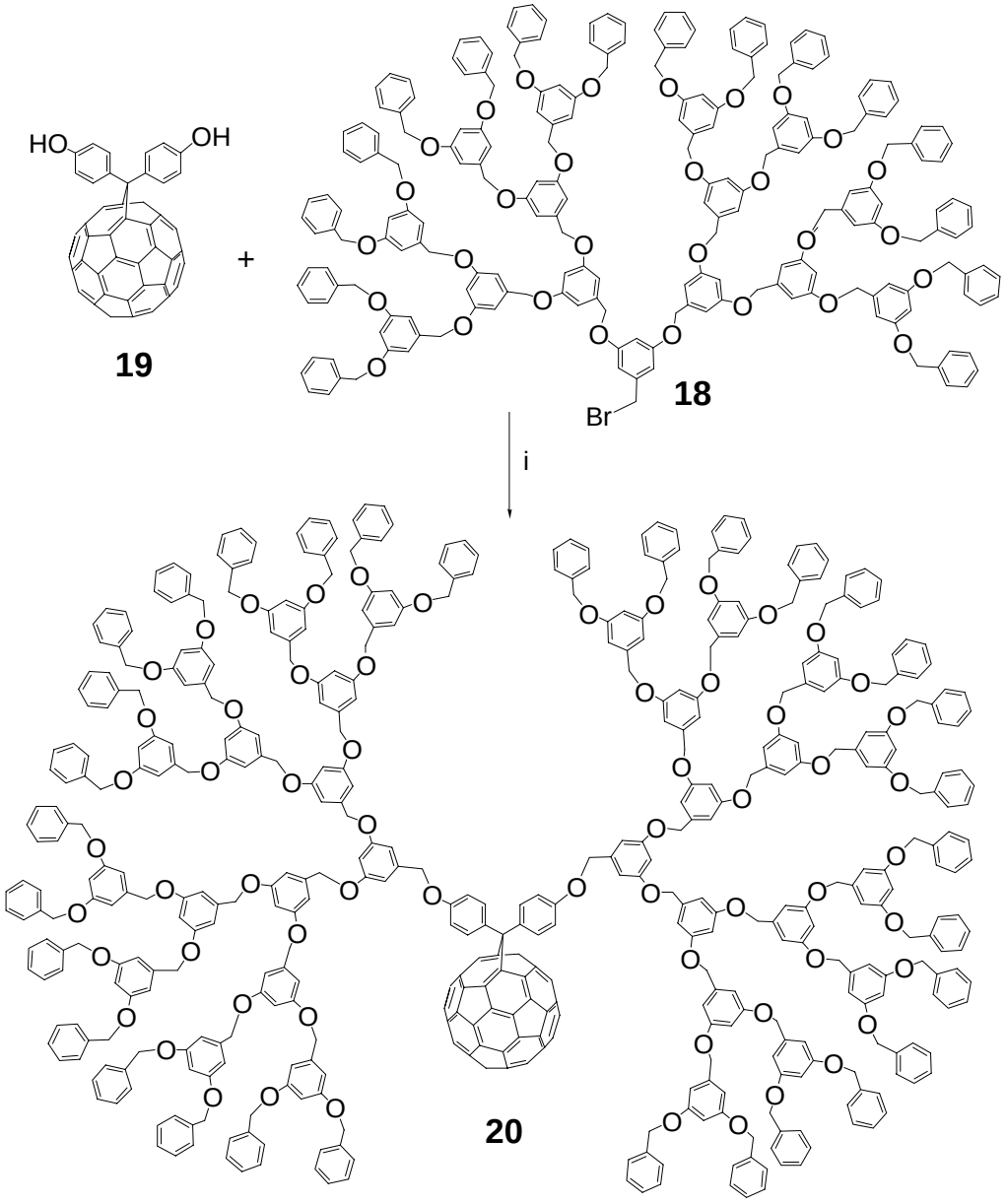

Scheme 3.3. i) K_2CO_3/THF (79%).

In the second one, Fréchet and coworkers[57] directly attached a single fourth generation dendron to a [60]fullerene molecule (scheme 3.4). First, the focal point of a Fréchet type dendron was converted into an azide. Subsequent treatment of the azide **21** with C_{60} in refluxing chlorobenzene afforded the substituted azafulleroid **22** containing an open annulene structure[59].

In both cases the dendrimers were fully characterized and the authors were reporting on the encapsulation of the fullerene moiety with the dendrons, a fact that could alter its physical properties.

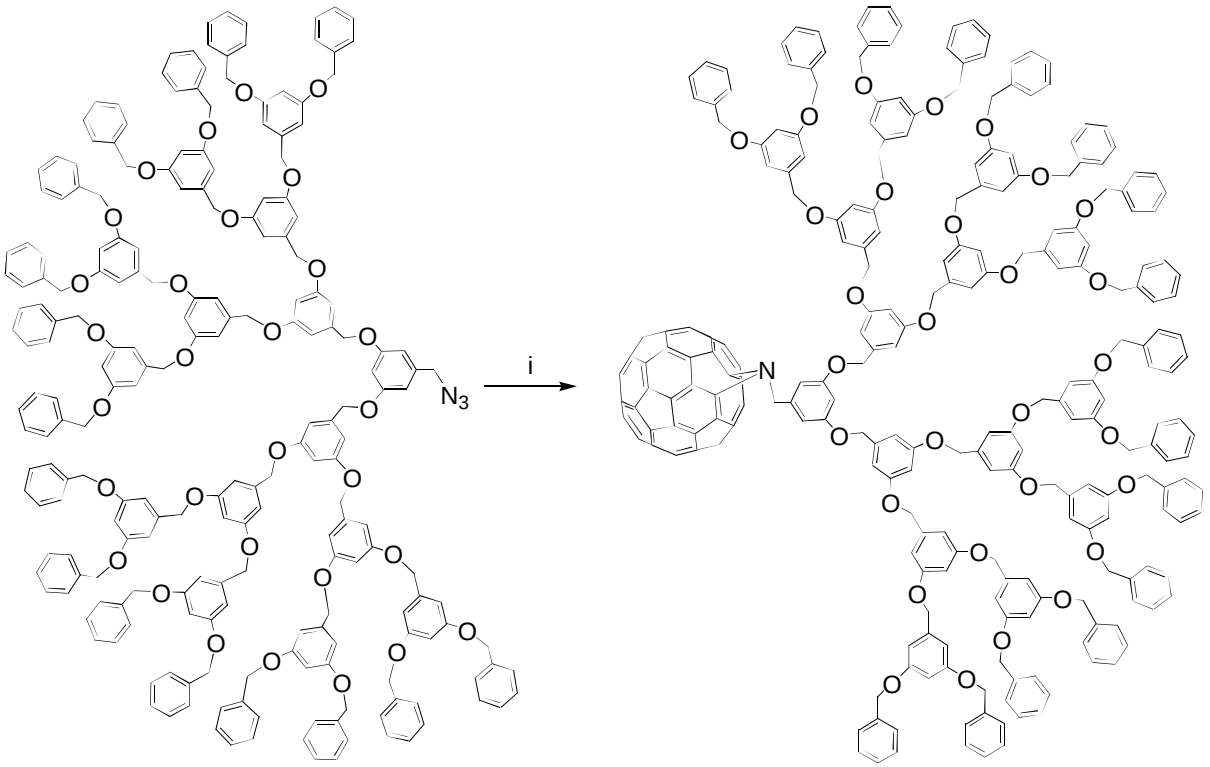

Scheme 3.4. i) C_{60} (**1**)**,** refluxing chlorobenzene (68%).

3.1.3 Synthetic Approach to Dendrimer-Fullerenes

For the present work, Fréchet's benzyl ether-type dendrons represent a quick and easy access for the synthesis of globular macromolecules based on C_{60} as a core. Although no previous considerations about the CDMPs[35] desirable for the resulting dendrimer have been made, this dendritic material should be a valid system to confirm that the pursued aim is feasible.

Once the dendritic system is chosen, another question which arises automatically is how to connect the branches to the fullerene core. It will be necessary to find a way of anchoring the dendrons to the fullerene core that allows the achievement not only of low pattern additions but also of higher functionalized derivatives. It would be of great interest to choose a reaction that leads to multiple addition products with high symmetry. This would be very helpful for an easy characterization of the resulting compounds.

The cyclopropanation reaction of fullerenes with bromo malonic esters described in the first chapter seems to fulfill all these requirements. This addition reaction is among the most elegant

and reliable reactions in fullerene chemistry, since it provides only [6,6]addition products in fairly good yields and proceeds with a large variety of malonates and related systems. Also the possibility to achieve higher adducts, especially T_h-symmetrical hexakisadducts with comparatively high yields turn this reaction into the best candidate to introduce dendritic branches to the fullerene core. Then, the first synthetic aim is to transfer the dendrons into a suitable malonic system capable of undergoing reaction with C_{60}.

3.1.4 Synthesis of Dendrimer-Fullerenes

3.1.4.1 Dendritic Bromo Malonates

The preparative work began with the synthesis of the benzyl ether-based dendrons [G1]-OH[60] (**13**), [G2]-OH (**15**) and [G3]-OH (**17**) introduced by Fréchet et al. and their subsequent conversion to the corresponding bromo malonates. The synthesis of the dendrons **13**, **15** and **17** (scheme 3.2) was carried out according to the described procedures[55,61] with reproducible results in all cases. Reaction of benzyl bromide with 3,5-dihydroxy-methylbenzoate (**11**) followed by exhaustive reduction gave the first generation alcohol [G1]-OH (**13**), which was easily converted to the related bromide [G1]-Br (**14**). Reaction of first generation bromide **14** with the monomer unit 3,5-dihydroxybenzyl alcohol (**10**) in the presence of potassium carbonate and [18]crown-6 in acetone afforded the second generation alcohol [G2]-OH (**15**). The third generation alcohol [G3]-OH (**17**) was obtained by repeating the last two steps: conversion of the benzylic alcohol **15** to bromide **16** followed by selective alkylation of the two phenolic hydroxyl groups of the monomer unit **10**.

The preparation of the bromo malonates **23-25** followed the procedure described by Diederich et al.[62] used for the synthesis of related systems. The dendritic alcohols **13**, **15**, and **17** were treated with malonyl dichloride in the presence of pyridine (scheme 3.5) to afford the corresponding malonic diesters **23-25**. As expected, the yield of the reaction decreases as the alcohol generation increases, with values going from 87.6 % to 65.9 %. This is a consequence of the increase of sterical hindrance at the focal point with every new generation. The subsequent bromination to **26-28** was performed by treatment of the corresponding malonates **23-25** with CBr_4 in the presence of 1,8-diazabicyclo[5.4.0]undec-7-ene (DBU). This procedure was slightly modified in order to minimize the formation of undesired dibromo malonates. The amount of CBr_4 was adjusted to 1 mol per mol of malonate instead of 1.2 as it was used in the original work. The first generation bromo malonate **26** was isolated in 71.5 % yield using flash chromatography. Unfortunately, the second (**27**) and the third (**28**) generation bromo

malonates could not be isolated as pure compounds. No suitable chromatographic conditions were found to separate the crude mixtures made up of starting material and the respective bromo and dibromo malonates. In both cases, the content of bromo malonate in the crude mixtures was determined by ^{1}H-NMR spectroscopy as higher than 60%. Since malonates and dibromo malonates are inert towards C_{60} under the conditions for the base-catalyzed coupling reaction, the crude mixtures had not to be purified and were used directly for the subsequent reaction with [60]fullerene.

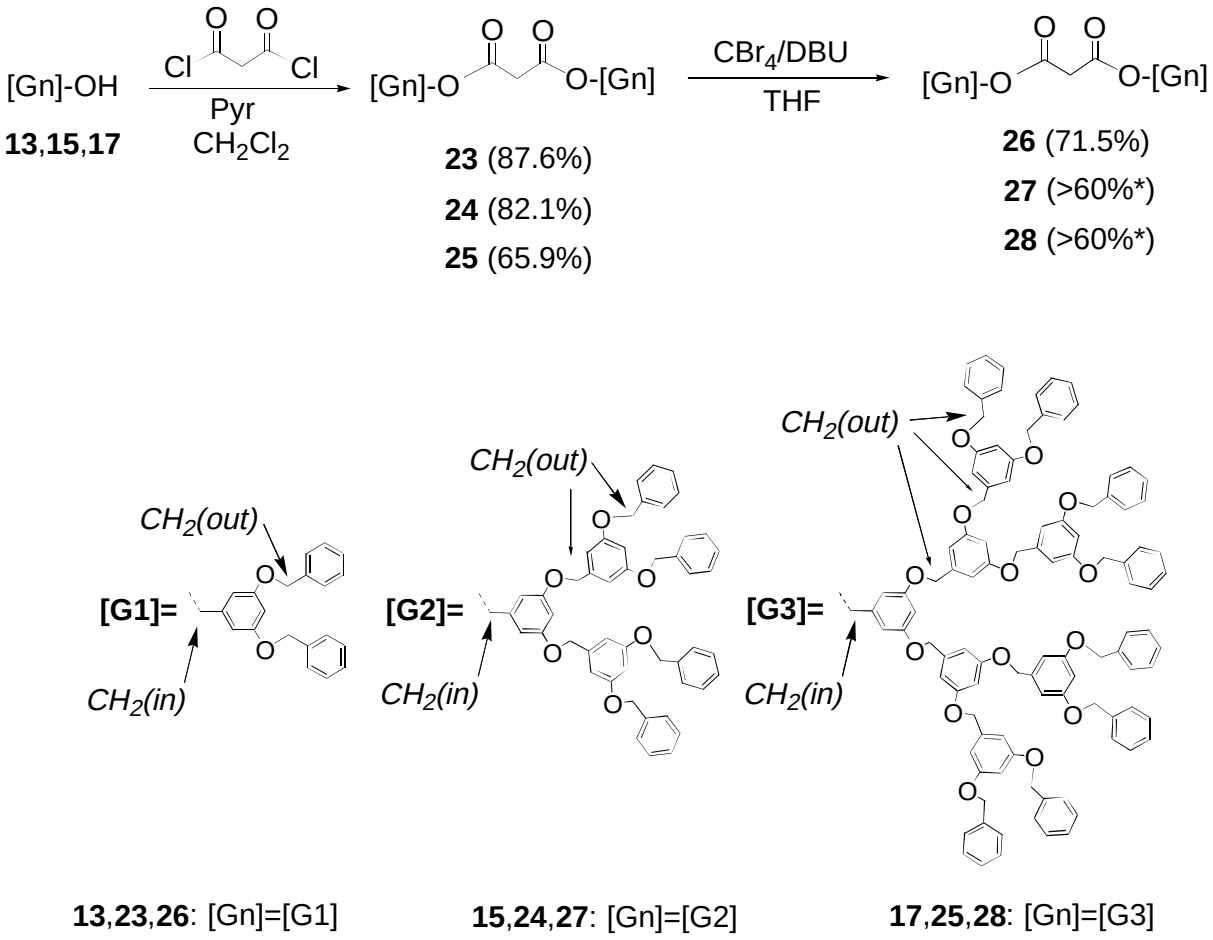

Scheme 3.5. Conversion of benzyl ether-based dendrons **13**, **15**, **17** into the bromo malonates **26**-**28**. (*Content of compounds **27** and **28** in the respective crude mixture was determined by ^{1}H-NMR spectroscopy).

3.1.4.2 Dendrimer-Fullerenes

The synthesis of the dendrimer **29** with two dendritic side chains was performed by treatment of C_{60} with bromo malonate **26** in toluene in the presence of sodium hydride (scheme 3.6). The isolation of **29** (52%) from unreacted C_{60} (5%) and a regioisomeric mixture of bisaddition products (21%) was achieved by flash chromatography on silica gel using toluene as eluent.

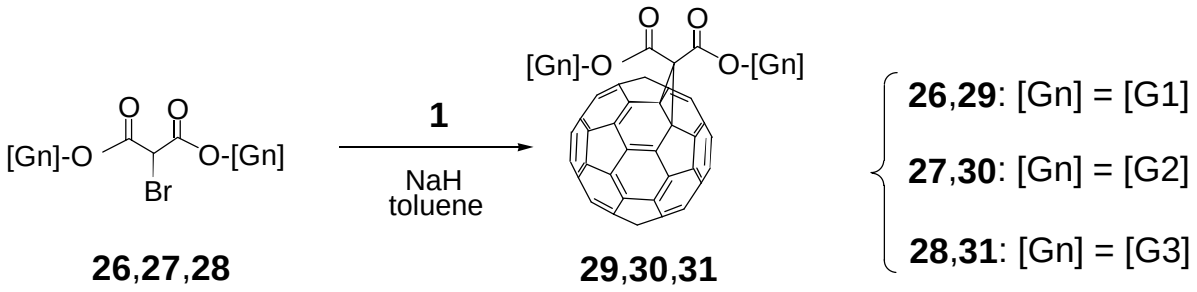

Scheme 3.6. Synthesis of [60]fullerene-dendrimer monoadducts **29**-**31**.

The dendrimer **29** was completely characterized by common spectroscopic methods. The NMR and UV/Vis spectra of this compound are typical for [6,6]bridged monoadducts of C_{60}. Due to its C_{2v}-symmetry, **29** presents in its ^{13}C-NMR spectrum 16 signals between δ = 139 and 145 ppm and one signal at δ = 71 ppm corresponding to the 16 different types of sp^2-carbon atoms and the two equivalent sp^3-carbon of the fullerene core, respectively. The signals of the ^{1}H- and ^{13}C-NMR spectra which belong to the dendritic branches appear clearly resolved at about the same position as those of the corresponding dendron (figure 3.6.a). The electronic absorption spectrum shows the characteristic band for [6,6]bridged [60]fullerene monoadducts appearing at about 425 nm[4] (figure 3.2). FAB mass spectrometry gave a molecular peak (m/z = 1427) together with a fragment peak at m/z = 720 corresponding to $(C_{60})^+$. Ether, aromatic, carboxylates, and fullerene (526 cm^{-1})[4] moieties were identified by IR spectroscopy.

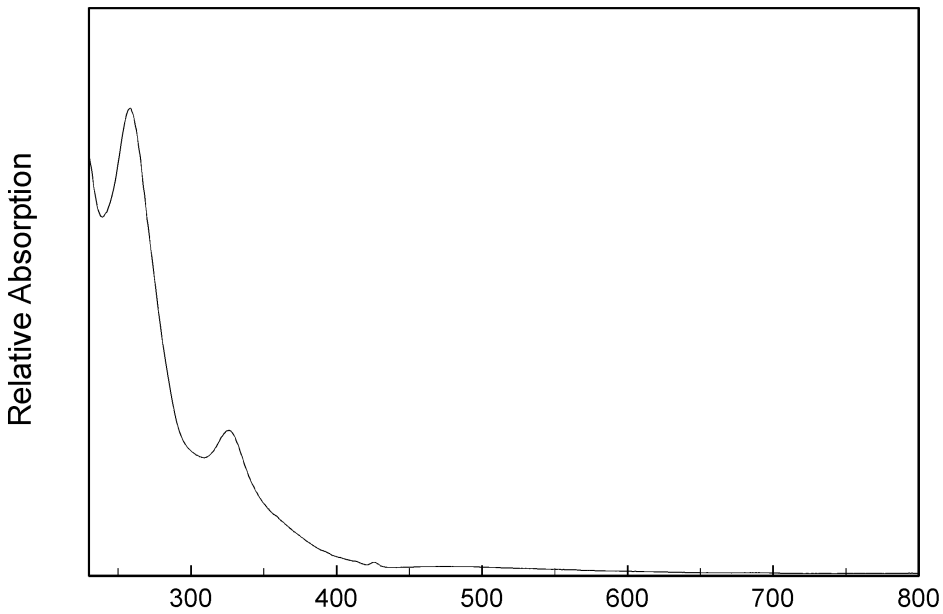

Figure 3.2. UV/Vis spectrum of **29** in methylene chloride.

For the synthesis of the globular hexakisadduct **32** (scheme 3.7) with 12 dendritic branches attached to the fullerene core, the efficient template activation method described above was used. This method, developed by Hirsch et al.[29,30], takes advantage of the activation of [6,6]double bonds in octahedral sites relative to the addends already bound resulting from reversible binding of DMA. This procedure guarantees the regioselective formation of oligoadducts of C_{60}, especially that of hexakisadducts, with octahedral addition pattern, in comparatively high yields.

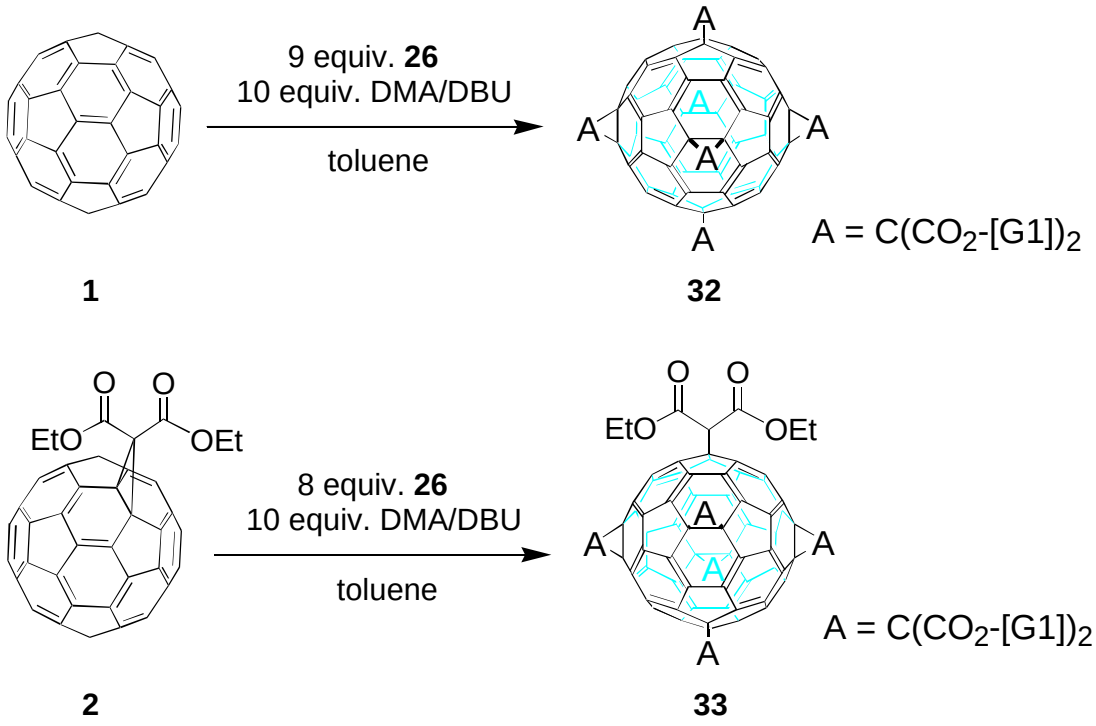

Scheme 3.7. Synthesis of dendrimers **32** and **33** using the template addition method.

Despite the bulkiness of the dendrons being attached to the core, this one-pot method afforded the desired dendrimer **32**. Nevertheless, the yield of the reaction was not very satisfactory (5.4%) and its purification needed the use of different methodologies including flash chromatography, preparative HPLC and size exclusion chromatography. The high symmetry of this dendrimer was made clear by the extreme simplicity of the ^{13}C-NMR and ^{1}H-NMR spectra considering the molecular formula of the macromolecule: $C_{330}H_{228}O_{48}$. In the ^{13}C-NMR spectrum (figure 3.3) only three signals at δ = 145.97, 141.29 and 69.42 ppm appear corresponding to the three types of magnetically equivalent fullerene carbon atoms. The ^{1}H-NMR spectrum of **32** (figure 3.7) shows only two peaks in the range of the methylene benzylic protons region at 4.78 ppm and 4.98 ppm which correspond to the two different sets of benzylic protons: *CH_2(in)* and *CH_2(out)* in a ratio 1:2 (scheme 3.5).

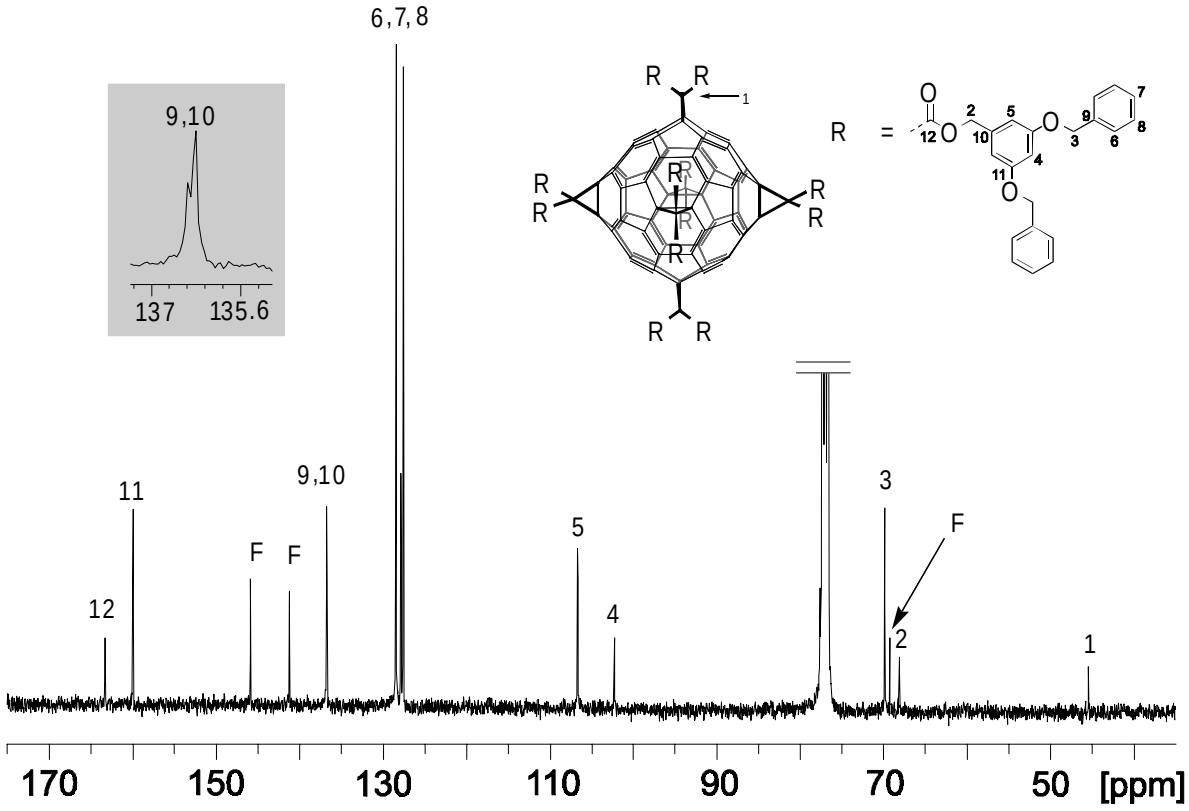

Figure 3.3. ^{13}C-NMR (100.5 MHz, RT, $CDCl_3$) spectrum of **32**. F denotes the signals for the fullerene carbon atoms.

The dendrimer **32** is a yellow solid, and its UV/Vis spectrum is characteristic for fullerene [6,6]hexakisadducts (figure 3.4). It shows only weak absorption bands in the visible region of the spectrum according to the reduction of the π-electron number of the fullerene core[29]. The characteristic bands associated with the octahedral pattern of **32** are the absorptions at 280, 320, and 340 nm.

In this case, FAB mass spectrometry was another suitable method that clearly proved the expected composition. Together with the molecular peak at m/z = 4961 (M^+), three fragment ions corresponding to the fragmentation of one (m/z = 4254), two (m/z = 3547) and three (m/z = 2840) dendritic malonates were recorded.

Once the possibility to gain highly packed globular architectures based on C_{60} as a central core with twelve pendant first generation benzyl ether-type dendrons was demonstrated, the formation of mixed structures combining dendrons and other addends was studied. The synthesis of dendrimer **33** (scheme 3.7) was planned as a preliminary example. Starting from 1,2-[di(ethoxycarbonyl)]methano-1,2-dihydro[60]fullerene[24] (**2**) and following the same successful strategy used in the synthesis of the dendrimer **32**, the hexakisadduct **33** with five dendritic malonates attached was obtained. The product was isolated after flash

chromatography and preparative HPLC on silica gel in 15.3 % yield. This yield represents a large increase in comparison with that previously obtained in the synthesis of the dendrimer **32** (5.4 %) and it seems to be a direct consequence of the smaller steric hindrance which results from the exchange of two dendrons for two ethyl groups.

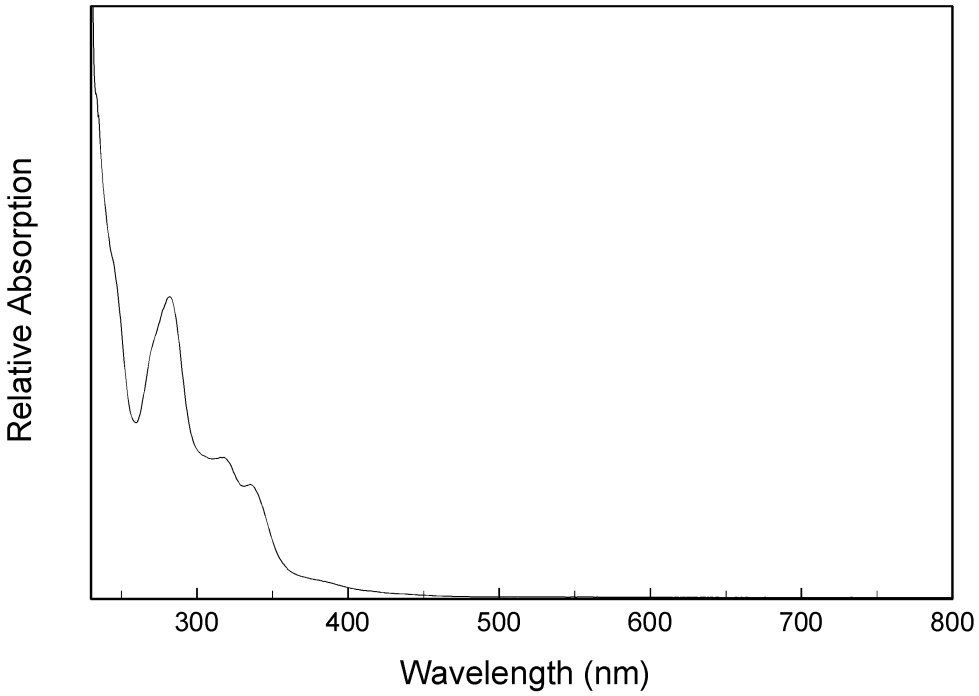

Figure 3.4. UV/Vis spectrum of **32** in methylene chloride.

The electronic absorption spectrum displays the typical profile for a hexakisadduct of [60]fullerene. FAB mass spectrometry gave the cluster molecular ion $(M+Na)^+$ with m/z = 4435. The ^{13}C-NMR spectrum of **33** (figure 3.5) reveals the local T_h-symmetry of the fullerene core showing a broad peak at 68.1 ppm corresponding to the four almost magnetically equivalent sp^3-carbon atoms of C_{60}. Two sets of signals with fine resolution appear at about 141.3 and 145.9 for the two different magnetically equivalent groups of fullerene sp^2-carbons. The global C_{2v}-symmetry of the molecule is perfectly reflected in the ^{1}H-NMR spectrum (figure 3.6) with the resonance of the four inequivalent methylene bridges at the interior, *CH_2(in)*, and the four different methylene bridges outside, *CH_2(out)* (scheme 3.5).

Of special interest is the comparison of the ^{1}H-NMR chemical shifts for the methylene protons CH_2*(in)* and CH_2*(out)* in dendrimers **29**, **32** and **33** (figure 3.6). In the monoadduct **29** these signals appear as two singlets at δ = 5.43 and 4.95 for CH_2*(in)* and CH_2*(out)*, respectively (figure 3.6.a). In dendrimer **32** these two types of methylene protons give rise to two singlets

which appear at δ = 4.98 and 4.78, nicely reflecting the T_h-symmetry of the spherical hexakisadduct (figure 3.6.b). Significant high field shifts of δ = 0.45 for the CH_2*(in)*-protons

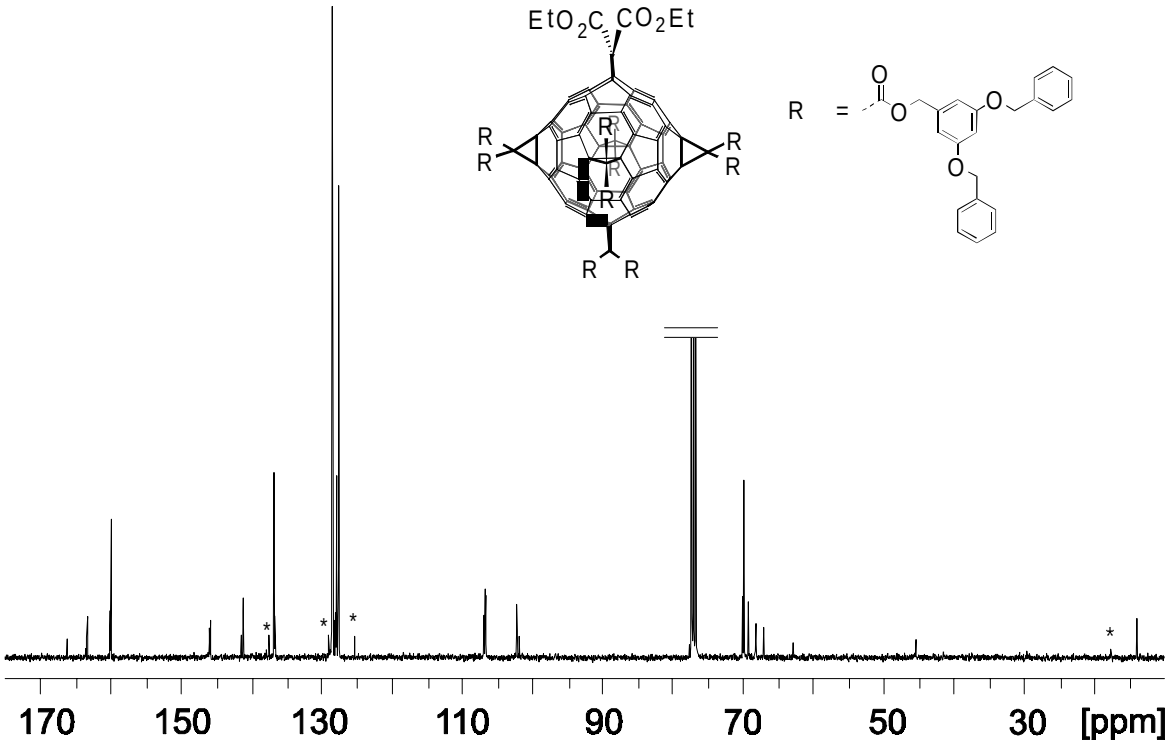

Figure 3.5. ^{13}C-NMR (100.5 MHz, RT, $CDCl_3$) spectrum of **33**, (* toluene).

and δ = 0.17 for the CH_2*(out)*-protons are observed in comparison with the parent monoadduct. These high field shifts are certainly caused by the influence of diatropic ring currents of proximate aromatic rings within neighboring dendrons. Obviously, the dense packing of the benzylic type dendrons in **32** is the reason for this phenomenon. In the ^{1}H-NMR spectrum of **33** the expected number of signals for the corresponding groups within the branches is found, which are for example, four signals for each of the four magnetically different CH_2*(in)*- and CH_2*(out)*-protons with the correct intensity ratio of 1:1:1:2 (figure 3.6.c). In analogy to **32** considerably high field shifts compared to the monoadduct **29**, especially for the signals of the CH_2*(in)*-protons within **33**, are observed. However, since the shift of the center of gravity for the various signals of **33** is somewhat less pronounced compared to the singlets of **32**, less dense packing of the dendrons is revealed. Especially, for those dendrons that are located next to the diethylmalonate addend at the equator a sterically less constrained situation can be expected.

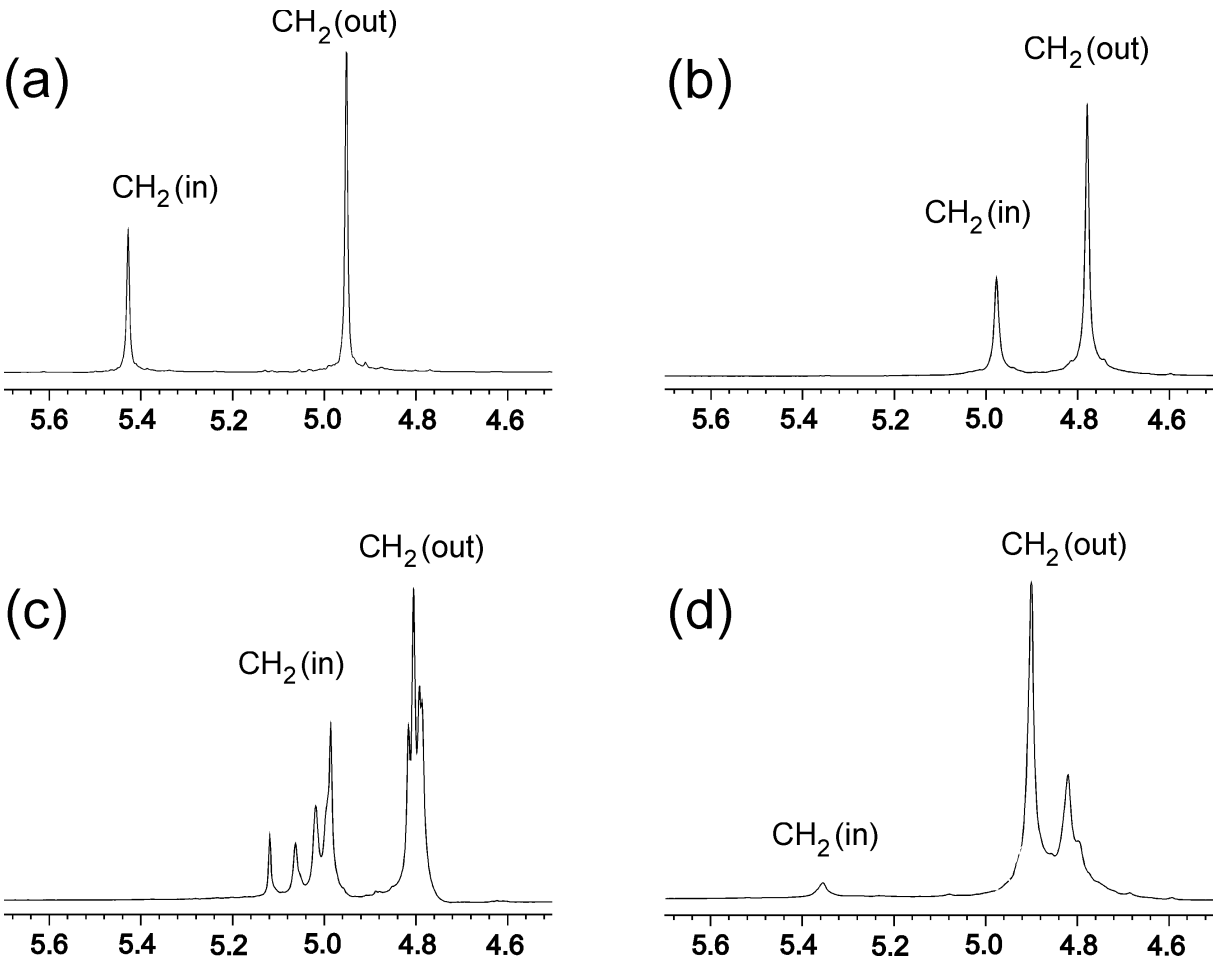

Figure 3.6. ^{1}H-NMR (400 MHz, RT, $CDCl_3$) spectra in the range of the methylene benzylic protons region of (a) **29**, (b) **32** ,(c) **33**, and (d) **31**.

The second and the third generation dendrimer-fullerenes **30** and **31** were prepared in analogy to the corresponding first generation homologue **29** (scheme 3.6). As was mentioned before, in both cases a crude mixture of the corresponding bromo malonate was employed for that purpose since it was not possible to separate these compounds from the starting malonates and the dibromo malonates side-products of the reactions. For the purification of **30** and **31** flash chromatography was not sufficient, so the use of a size exclusion chromatography on a polystyrene GPC column attached to a preparative HPLC was necessary. In both cases, this method was efficient for the separation of the dendrimers **30** and **31** from starting material and higher addition products due to their large difference in size.

The red-brownish glassy dendrimer **30** was obtained in about 20% yield and its spectroscopic characterization revealed the C_{2v}-symmetry of the compound. This second generation monoadduct dendrimer presents an electronic absorption spectrum nearly equivalent to that of the lower generation homologue **29** (figure 3.2). All expected signals for the C and H atoms of

the dendritic branches within **30** appear clearly resolved at about the same position as for the corresponding dendrons in the ^{13}C-NMR and ^{1}H-NMR spectra. Its ^{1}H-NMR spectrum reveals an increase of the line broadening for the signals with respect to that observed in the dendrons but no remarkable shifts to high field occur. The molecular ion at m/z = 2276 together with the fragmentation ion corresponding to the dendritic arms $(M\text{-}C_{60})^{+}$ were recorded by FAB mass spectrometry.

Unfortunately, it was impossible to synthesize the second generation dendrimer **34** (figure 3.7), the analogue of **32**. From the crude mixture obtained following the standard procedure, no clear-cut compound could be identified. Not even traces of hexakisadduct **34** could be detected by various MS techniques including MALDI-TOF and ESI spectrometry.

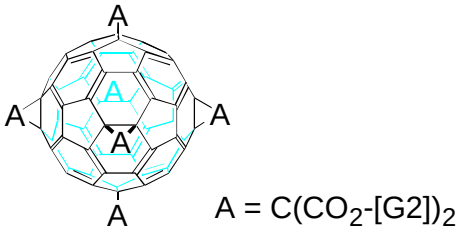

34

Figure 3.7. 2nd Generation dendrimer-fullerene hexakisadduct **34**.

Similar observations are reported by Fréchet et al.[57] who did not detect the formation of adducts higher than bisadducts of C_{60} with fourth-generation dendrons, even if an excess of the dendritic coupling component was used. Molecular modelling calculations supported also the difficulty to build up this molecule using a convergent approach[63].

The third generation monoadduct dendrimer **31** was synthesized in 43% yield as a red-brownish glassy composite. The UV/Vis spectrum confirmed the structure of a [6,6]bridged fullerene monoadduct. ^{13}C-NMR (figure 3.8) and ^{1}H-NMR (figure 3.6.d) gave all the expected signals. In the ^{1}H-NMR spectrum four broad bands with intensities 1:2:4:8 between 4.7 and 5.4 ppm corresponding to the four different types of methylene groups present in the dendrimer were found. In this case, FAB mass spectrometry also was a successful technique to detect the molecular ion peak (m/z = 3974).

3.1.4.3 Computational Investigations

For a computational determination of minimum energy structures at 0 °K of dendrimers **29**-**33**, molecular dynamics (MD) simulations using the MM^{+} force field implemented in the software

package HYPERCHEM[64] were carried out in collaboration with Hubert Schönberger[63]. The structures obtained from these simulations are represented in figure 3.9. Of interest is the dense packing of the branches around the core observed in all the dendrimers. For the monoadducts **29-31** face to face arrangements of the fullerene core with

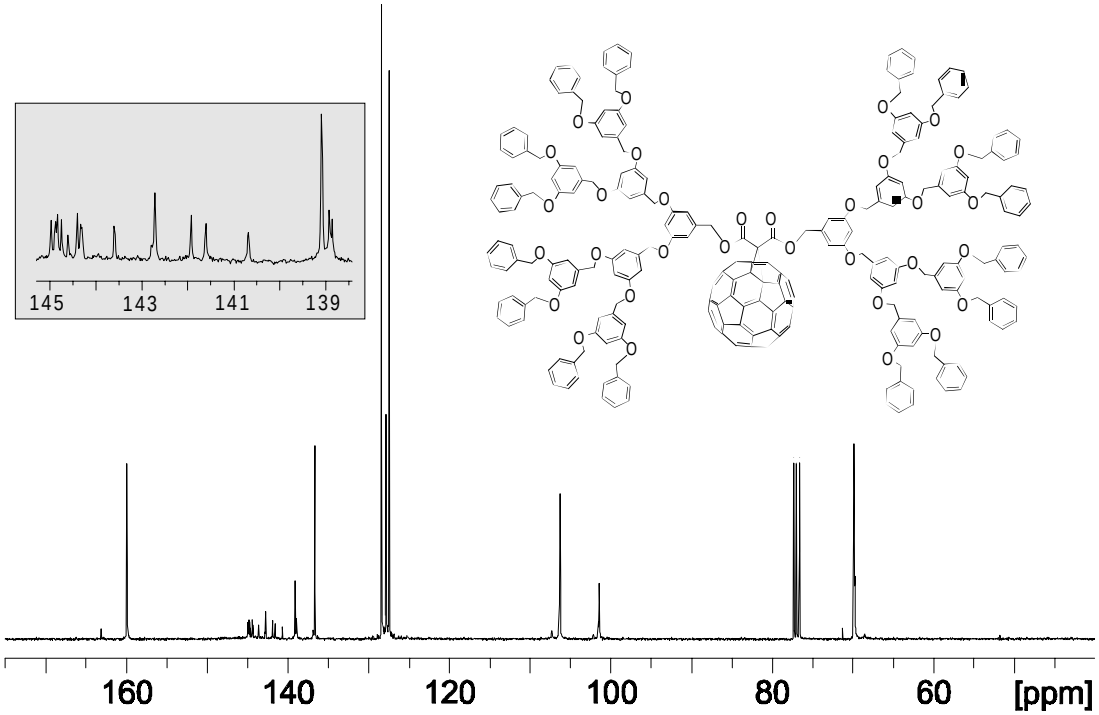

Figure 3.8. ^{13}C-NMR (100.5 MHz, RT, $CDCl_3$) spectrum of **31** and expansion of the fullerene sp^2-carbon atoms region.

several aromatic rings of the branches indicate favorable π-π-stacking interactions, which leads to a very pronounced wrapping of the branches around the fullerene sphere. Such favorable π-π interactions are a well known phenomenon in fullerene chemistry, which is clearly reflected, for example, by the enhanced solubility of fullerenes in polycyclic or electron rich aromatic compounds[4] as well as by the analysis of a variety of single-crystal structures of [60]fullerene derivatives with aromatics in the side chain[33,65]. These solid state structures nicely reveal the face to face arrangements between the fullerene core and the aromatic groups in the side chain. Within the dendrimers **32** and **33** several stacking arrangements between phenyl rings of the branches are present in the calculated structures. The dendrons are densely packed and in the case of **32** partially interpenetrating. More space is available in the region of the sterically less demanding di(ethoxycarbonyl)methylene addend of **33**.

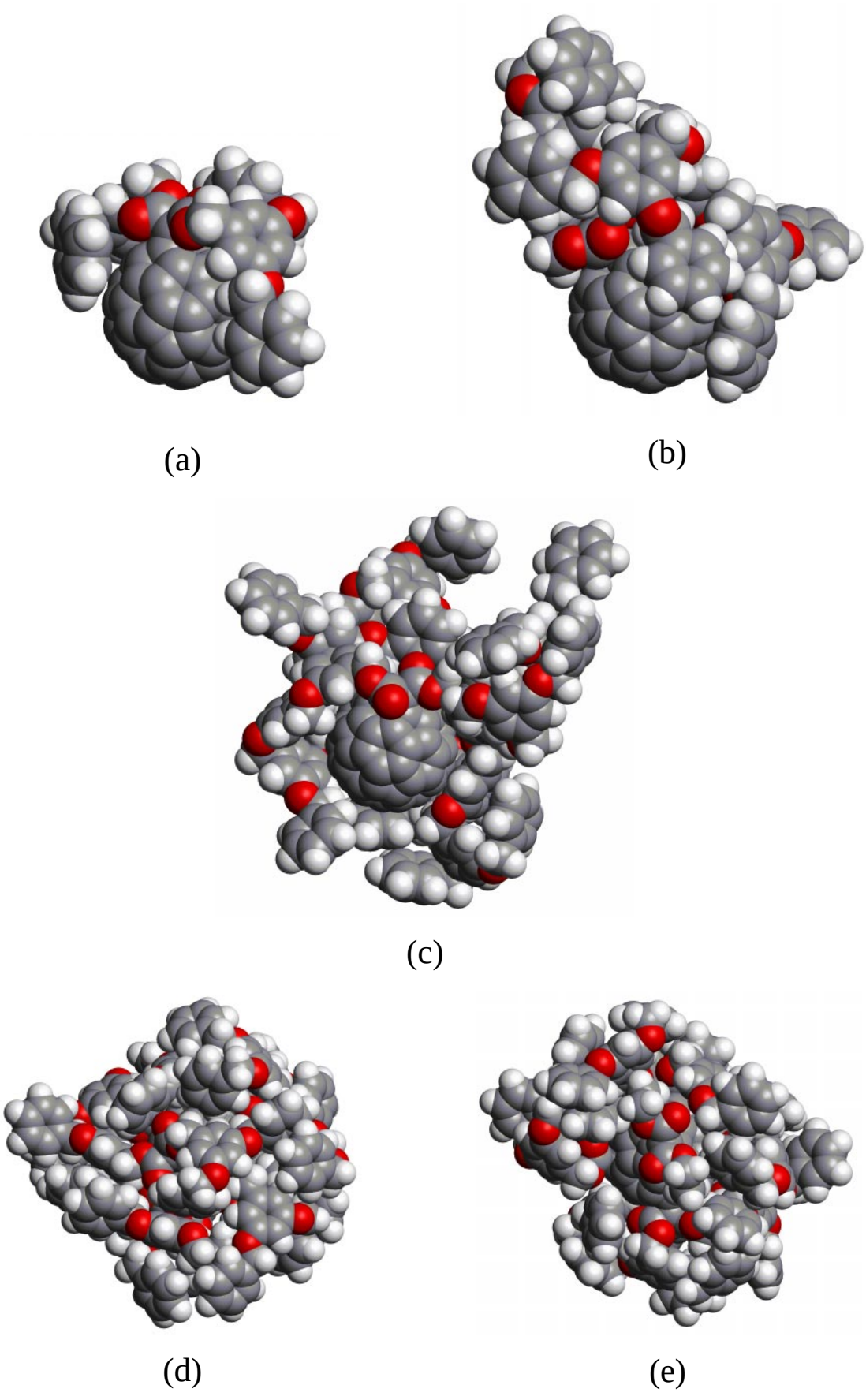

Figure 3.9. Minimum energy structures at 0 °K of the dendrimers **29** (a), **30** (b), **31** (c), **32** (d), and **33** (e) according to molecular dynamics (MD) simulation[66].

Of course, since solvent effects are neglected and 0 °K structures are considered, these modelling investigations reflect only partially the driving forces that are responsible for the geometrical expression of the structures of dendrimers **29**-**33** at the applied experimental conditions. In solutions at higher temperatures, the crystallinity of branch packing around the core is certainly substantially reduced. However, it is reasonable to assume that the sterical constraints associated with core branching multiplicity of 12 in **32** as well as the possibility to achieve conformations with energetically favorable π-π-interactions account also for a comparatively dense structure in solution at room temperature.

3.1.5 Fullerene Adducts as Cores for the Synthesis of Dendrimer-Fullerenes

3.1.5.1 Diethylmalonate Methano [60]Fullerene Derivatives

Fullerene-dendrimer **33** represents a first example in which dendritic branches are attached to a [60]fullerene core containing already one addend. The strategy followed permits the synthesis of mixed systems containing dendritic branches and other functionalities bound to a [60]fullerene molecule. To develop this topic diethylmethano [60]fullerene derivatives **35**, **36**, **37**, and **6** were chosen as starting points (figure 3.10) because of their facile accessibility[25,27].

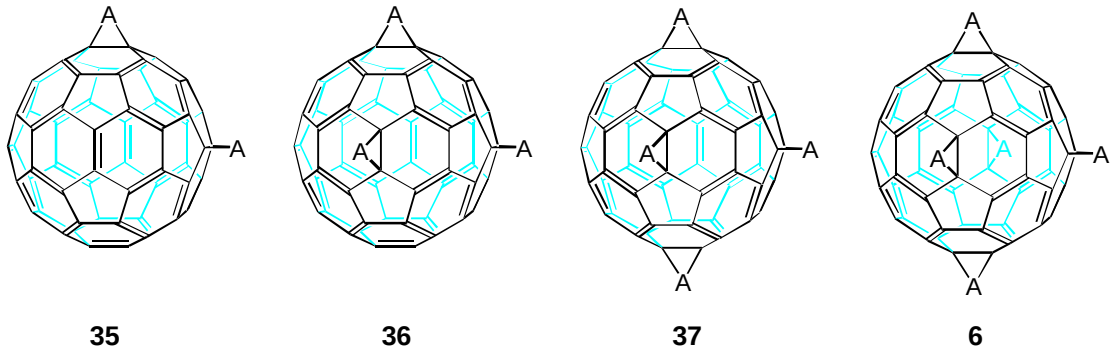

Figure 3.10. Diethylmethano [60]fullerene derivatives **35**-**37** and **6** [A = $C(CO_2Et)$].

[60]Fullerene derivatives **35**-**37**, and **6** contain two, three, four, and five diethylmalonate addends respectively. Thus, four, three, two, or one octahedral double bonds which can undergo reaction with dendritic bromo malonates remain still intact. Apart from their function as *protecting groups*, these non-sterically demanding diethyl malonic rests can also play an important role in activating the remaining free octahedral positions in order to introduce the dendritic branches afterwards. This project has been developed in collaboration with Andrea

Herzog. In the current chapter only a general trend and the qualitatively obtained results will be reported. More experimental and spectroscopic details will be given elsewhere[67].

Compounds **35**-**37** were synthesized step by step starting from **2** after tedious chromatographic purification steps[25,27]. It should be emphasized that **36** owns C_3-symmetry and thus is chiral. Therefore, compound **36** is in fact a racemate. Pentakisadduct **6** was prepared according to the procedure described in scheme 1.3[30].

Dendritic malonates were attached to the different fullerene cores **35**-**37**, and **6**, similarly to the processes described above for the synthesis of dendrimer **33** (scheme 3.7). Activation with DMA was not necessary when starting from **6** or **37**. In these cases, the remaining octahedral free positions are highly activated due to the presence of the substituents already bounded to the cage[27,28].

Dendrimers **38**-**43** (figure 3.11) were obtained according to the described strategy in yields ranging from good (**38**: 78.2%) to moderate (**42**: 25%). All compounds were isolated by chromatography on silica gel using mixtures of toluene/ethyl acetate as eluent, and were completely characterized.

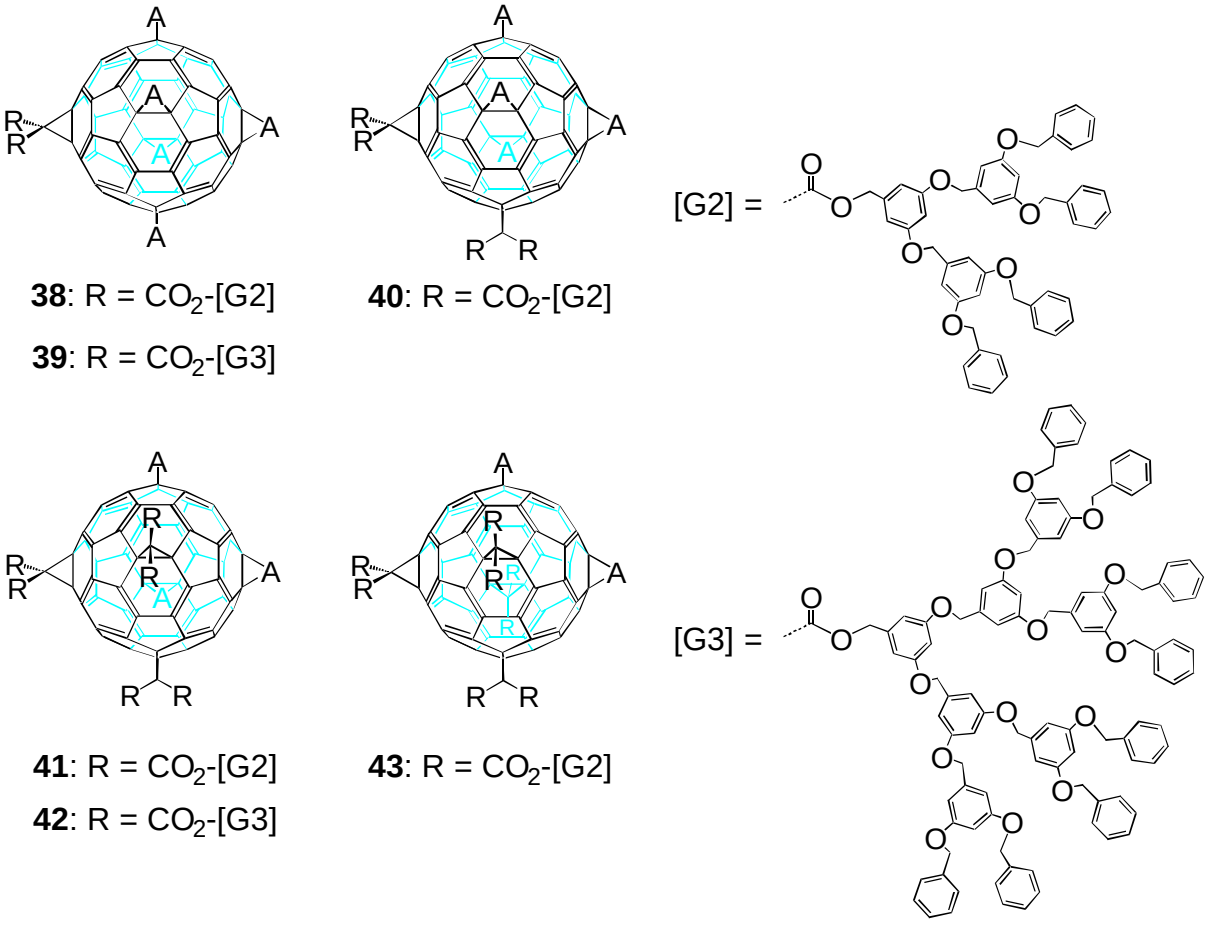

Figure 3.11. Dendrimers **38**-**43**.

The attachment of three second and third generation dendritic malonates to **36** yielded the desired fullerene-dendrimers **41** and **42**. Like their parent fullerene derivative, **41** and **42** possess C_3-symmetry and therefore are chiral. Starting from **35** and following an analogous strategy, the synthesis of the second generation fullerene-dendrimer **43** containing eight second generation dendritic branches was attempted. Although the target product was detected in the crude mixture by means of analytical HPLC equipped with an UV detector, its purification was not possible.

3.1.5.2 Bisoxazoline-Dendrimer-[60]Fullerene Derivatives: Potential Chiral Catalysts with Dendritic Coverage

The synthesis of the dendrimers **38**-**43** has demonstrated the synthetic potential of the applied methodology. The introduction of one, two or three second and third generation dendritic malonates to the diethylmethano [60]fullerene derivatives **35**, **36**, and **6** has proceeded satisfactorily. The diethylmalonate methano bridges are acting only as positional blocks allowing the construction of specific architectures, but do not possess other particular properties. Of special interest are the dendrimers **41** and **42**, because of their structure-inherent chirality. These compounds therefore represent racemic mixtures[25,68].

Great efforts have been made in order to isolate enantiomerically pure fullerene derivatives with an inherent chiral addition pattern. Recently, the racemate **36** has been resolved by HPLC using a chiral Welk-O1 phase on a semipreparative scale[69]. Other strategies have been involved in the attachment of chiral addends to fullerenes thus obtaining diasteroisomeric mixtures which can be more easily separated than racemates[26,62,70,71]. The possibility to reach [60]fullerene derivatives with axial chirality reinforces the exceptional characteristics of [60]fullerene as a new building block in organic chemistry.

Recently F. Djojo and A. Hirsch have synthesized and studied the chiroptical properties of several enantiomerically pure bis- and trisadducts of [60]fullerenes with an inherent chiral addition pattern[72]. Multiple additions of chiral C_2-symmetrical bisoxazolines to [6,6]bonds of the [60]fullerene cage by nucleophilic cyclopropanation and subsequent chromatographic separation of the corresponding diasteromers on achiral stationary phases provided a facile access to enantiomerically pure compounds like **44**-**47** (figure 3.12). CD spectroscopy revealed that it is the chiral arrangement of the conjugated π-electron system within the fullerene core itself that predominantly determines the chiroptical properties of **44**-**47**. The CD spectra of

related pairs of diastereomers **44**-**45** and **46**-**47**, the addition patterns of which represent pairs of enantiomers, revealed pronounced Cotton effects and mirror-image behavior.

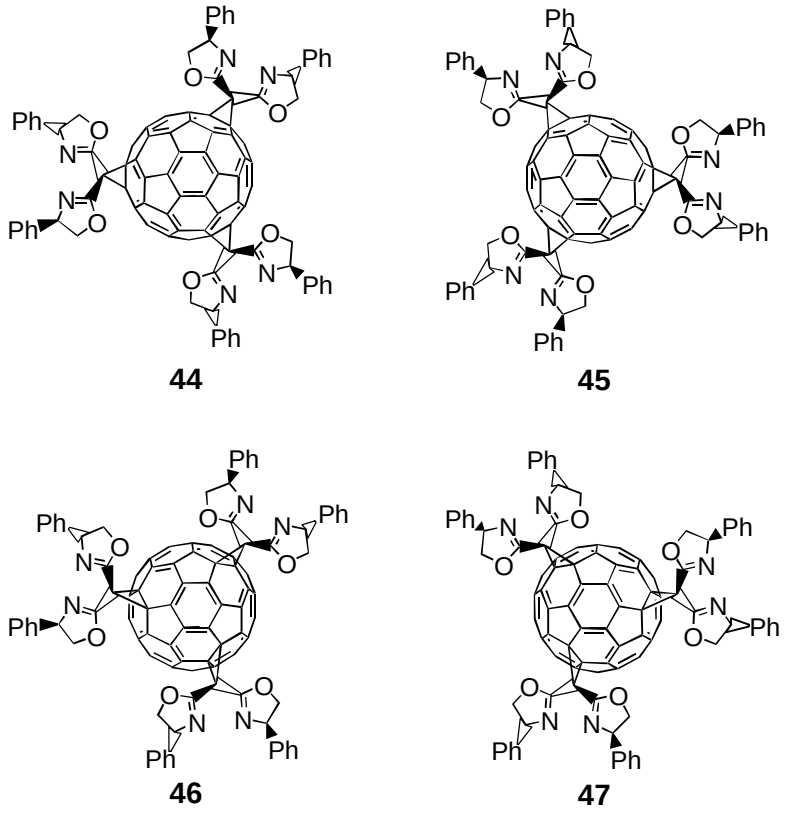

Figure 3.12. Bisoxazoline-fullerene trisadducts **44**-**47**.

In agreement with the synthesis of dendrimers **38**-**42** introduced earlier, it was decided to prepare fullerene-dendrimers containing bisoxazoline moieties. Starting from any of the four C_3-symmetrical [60]fullerene trisadducts **44**-**47**, it would be possible to prepare the mixed C_3-symmetrical hexakisadducts following an analogous procedure described above. This project has been developed in collaboration with Francis Djojo, and in this work only a brief overview will be given. Further considerations and experimental details will be presented elsewhere[73]. Second generation C_3-symmetrical dendrimers **48**-**51** (figure 3.13) were prepared from **44**-**47** via template activation with DMA[25,30] followed by cyclopropanation with second generation dendritic bromo malonate **27** under basic conditions. All compounds were isolated in a yield of about 40% by flash chromatography on silica gel using mixtures of ethyl acetate/toluene.

^{1}H-NMR and ^{13}C-NMR spectra of dendrimers **48**-**51** presented the expected peaks according to their symmetry. At present, further spectroscopic and chiroptical investigations are being carried out to fully characterize these compounds.

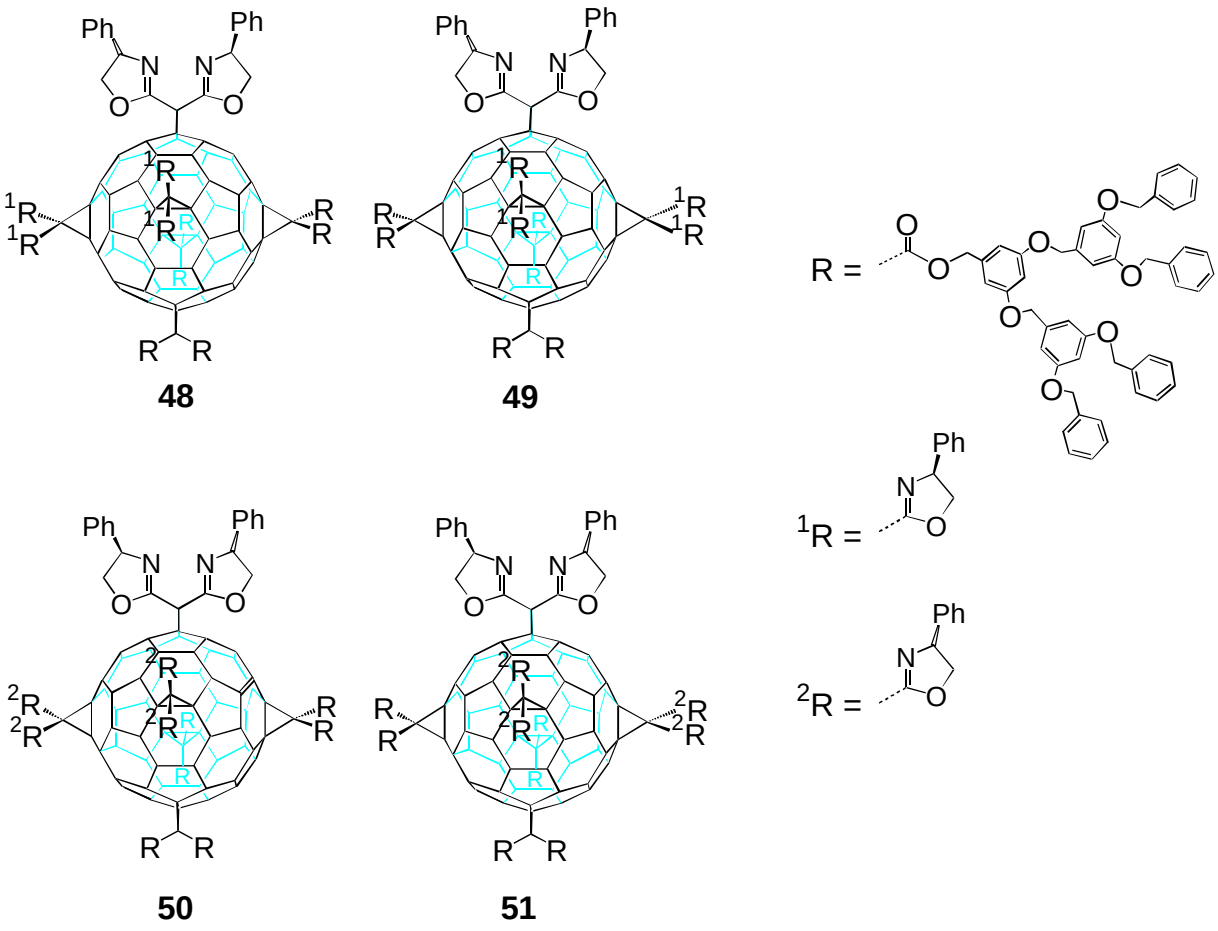

Figure 3.13. Bisoxazoline-dendrimer-fullerenes **48**-**51**.

The use of 4,4´-disubstituted bis(oxazolines) as chiral ligands in asymmetric catalysis has been extensively developed[74]. Their synthetic potential is based upon their easy accessibility from readily available chiral amino alcohols, the high enantioselectivity generally obtained in catalysis, and the enhanced reactivity of the metal catalysts in asymmetric transformations.

Dendritic bis(oxazolin)metal complexes have been synthesized and their use as catalysts for Diels-Alder reaction studied. Kinetic investigations revealed that the catalyzed reaction followed an enzymatic Michaelis-Menten relationship, thus demonstrating fast reversible formation of the *dendrizyme*-dienophile complex, prior to the rate-limiting conversion to the Diels-Alder adduct[43].

Dendrimers **48**-**51**, which remaining [6,6]double bonds are comparatively inert, could be interesting catalysts for all those enantioselective reactions that are catalyzed by bisoxazolines themselves. In addition to the local C_2-symmetry of the chiral addends, their screw-like C_3-symmetrical arrangement within the fullerene core provides a further effective scenario for chiral discrimination. Next to the role as protecting groups for the fullerene surface against addition reactions, the dendritic addends provide solubility and could also discriminate

substrates in the chiral regions. The ability of dendrimers **48**-**51** as potential *chemzymes* for different processes is currently under investigation.

The preparation of related systems possessing high generation dendritic branches attached would also be of high interest. The resulting nanoparticle would offer the advantages of a homogeneous catalyst and could be removed from the reaction mixture by physical operations (dialysis, etc.) as easily as a heterogeneous one.

3.1.6 Porphyrin-Dendrimer-Fullerenes

3.1.6.1 Porphyrin-Dendrimers and Porphyrin-Fullerenes

Porphyrins have been applied as central building blocks (*cores*) in dendrimer chemistry[75-78]. Dendrimer **52** described by S. Inoue et al. provides a spectacular example where eight fourth generation dendritic branches are connected to a central porphyrin (figure 3.14)[75].

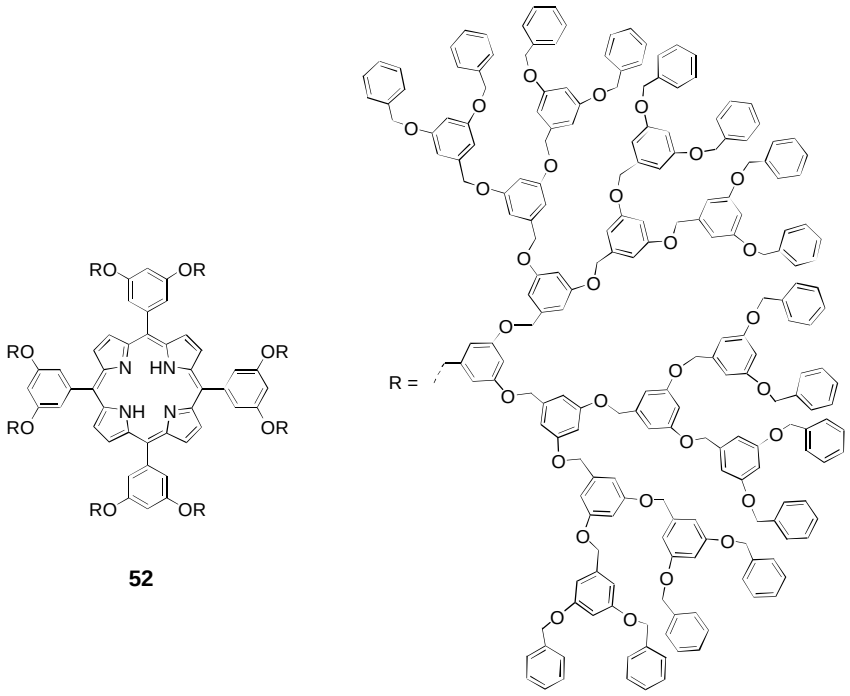

52

Figure 3.14. Dendrimer-porphyrin **52** with branching multiplicity equal to eight.

It has been suggested that dendritic porphyrins could act as a model systems for natural electron transfer hemoproteins like cytocrome C or hemoglobin[76]. With a proper choice of the branches it is possible to modulate the electrochemical redox activity of the inner electrophore. This modulation is attributed to strong microenvironmental effects and differences in solvatation imposed on the electroactive core by the densely packed dendritic surroundings.

High valent metalloporphyrins have been employed as catalysts for the oxidation of organic substrates[79]. Introduction of bulky dendritic polymers at the peripheral positions of a metal porphyrin results in steric protection of the metal center and was thought to provide for regio- and shape-selective catalysis[78]. Although dendrimer-porphyrins showed significantly greater regioselectivity than the corresponding unhindered parent metalloporphyrin, the selectivity was not as high as those achieved with other crowded bis-pocket porphyrins like 5,10,15,20-tetrakis(2´,4´,6´-triphenylphenyl)porphyrin[80].

Recently, many papers have been published concerning the synthesis and photophysical properties of fullerene-porphyrin systems[81]. The main subject of study in these reports is the charge transfer process where the porphyrin serves as a donor and the [60]fullerene moiety as an acceptor.

3.1.6.2 First Example of a Porphyrin-Dendrimer-Fullerene

The synthesis of a porphyrin-dendrimer-fullerene was planned in a joint project with Elke Dietel. Starting from a porphyrin-fullerene monoadduct, five dendritic malonates could be attached afterwards in order to generate the corresponding high compact globular dendrimer-porphyrin-fullerene structure. The fullerene core would only act as a building block since no acceptor properties remain in its skeleton after its complete octahedral functionalization. The dendrons would provide solubility to the system and interact with the porphyrin, thus modulating its electrochemical properties. The main advantage of this system is that the metal center is not as shielded as in the so-called porphyrin-dendrimers, where the metal is placed in the interior of the macromolecule. The porphyrin-fullerene distance can be fine-tuned by choosing the proper linkage between them. Different types and numbers of dendritic branches can be introduced in the neighborhood of the metal site. This approach points out a very promising method to develop new models with potential applications as hemoproteins or catalysts. With the right combination of building blocks, the porphyrin could be surrounded by dendrons but still be available for reaction substrates. This accessibility might be very useful to design catalysts or to mimic hemoproteins like cytochrome 450 which regulate oxygen activation and insertion into organic substrates.

Starting from the porphyrin-fullerene monoadduct **53**[82,83] and via template activation with DMA, the synthesis of the first generation dendrimer **54** was achieved (scheme 3.8).

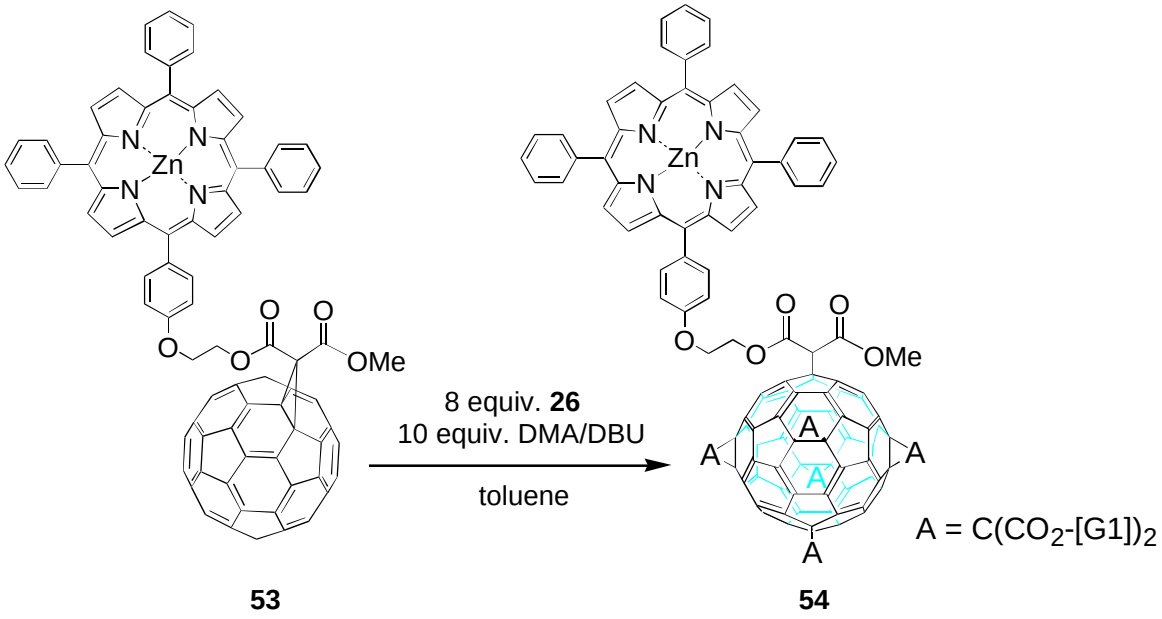

Scheme 3.8. Synthesis of the dendrimer-porphyrin-fullerene **54**.

The hexakisadduct **54** was isolated after laborious flash chromatography on silica gel and preparative HPLC on silica gel using mixtures of ethyl acetate/toluene as eluent. After the purification steps a yield of 2 % was estimated. The small amount of **54** obtained made its characterization difficult. The UV/Vis spectrum of a pink solution of dendrimer **54** displays the typical bands in the visible region for both active moieties present in the dendrimer: the fullerene core and the porphyrin (figure 3.15). Pronounced are the Soret band at 413 nm and the three Q-bands at 510, 548 and 586 nm of the porphyrin and the characteristic bands at 281, 308 and 348 nm for the hexasubstituted fullerene core.

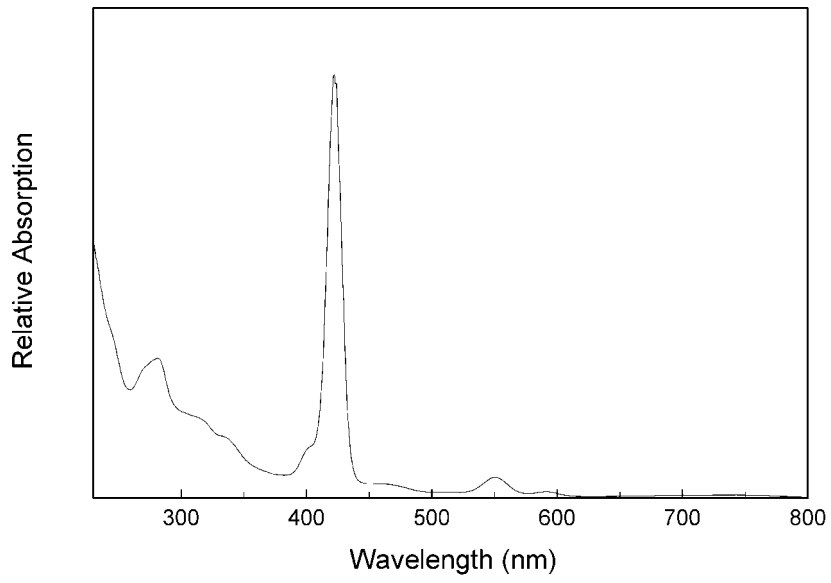

Figure 3.15. UV/Vis spectrum of **54** in methylene chloride.

The nearly I_h-symmetry of **54** is shown clearly in its ^{1}H-NMR spectrum (figure 3.16). The peaks corresponding to the dendrons show nearly the same positions as in the homogeneous hexakisadduct case (**32**). The methylene benzylic protons appear as two singlets with intensity 2:1, as a result of the quasi octahedral symmetry of the resulting compound. In comparison to the parent dendrimer-fullerene monoadduct **29** a pronounced high field shift was also observed for these protons (figure 3.6). All the expected peaks coming from the porphyrin moiety appear completely resolved at approximately the same position as they did in the dyad **53**[83] with two significant differences to be mentioned. First, the ethylene protons are experiencing an important shift to high field. They show two triplets, one at 4.40 ppm and another broader at 4.16 ppm shifting from 4.91 and 4.48 ppm in the starting monoadduct **53**. Second, the singlet corresponding to the methyl group is missing. In the parent dyad **53**

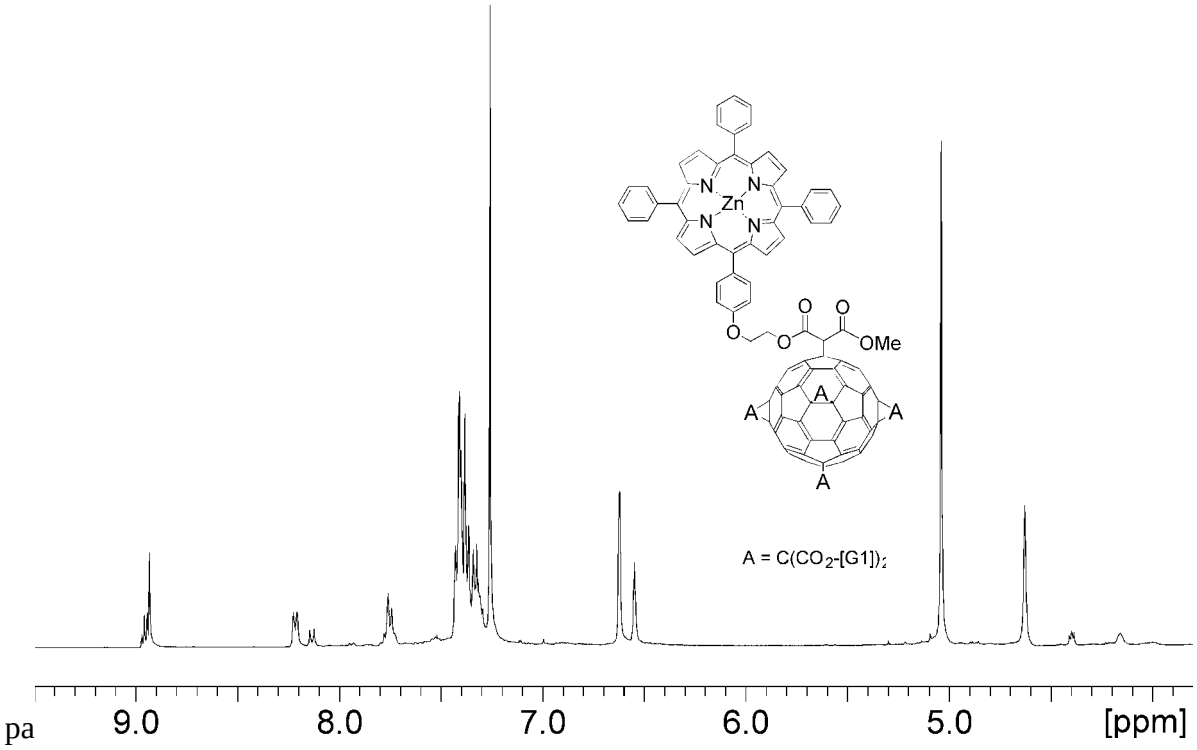

Figure 3.16. ^{1}H-NMR (400 MHz, RT, $CDCl_3$) spectrum of **54**.

these protons resonate at 4.08 ppm. Both effects are probably caused by the influence of diatropic ring currents of the neighboring dendrons. For the methyl group this phenomenon could be even more accentuated since its protons could be lying just above one of the aromatic rings. The chemical shift in this case could vary quite a lot and the signal positioned under some impurity peaks at the region from 1.7 to 1.2 ppm or even appearing at higher field.

The ^{13}C-NMR spectrum of **54** recorded after more than 30,000 scans gave a partial information. Only the peaks corresponding to the dendritic branches and some peaks from the phenyl rests attached to the porphyrin were observed. All equivalent carbons from different branches give a single peak showing pseudo-T_h-symmetry of the dendrimer **54**. MALDI-TOF mass spectrometry afforded the quasimolecular peak at m/z = 5093 (calculated for $C_{222}H_{336}NO_{45}Zn$, m/z = 5091).

The low yield in dendrimer **54** did not allow the performance of electrochemical studies which would give an idea about the influence of the dendritic branches to the redox properties of the porphyrin. Although the relative failure of this first attempt in constructing porphyrin-dendrimer-fullerene systems, the perspectives opened with this new class of materials were so promising that different approaches were tried.

3.2 A New Type of Dendrons. Synthesis of Dense Dendrimer-Fullerenes

3.2.1 Introduction

The synthetic strategy for the construction of fullerene-dendrimers developed till now, in spite of its success has presented some limitations. The synthesis of highly compact hexakis-adducts [60]fullerene containing up to ten (**33**, **54**) and twelve (**32**) first generation benzyl ether-type dendrons has been accomplished. Nevertheless, these compounds were obtained only in low yield as a consequence of the sterical hindrance involved in their formation processes. The attempted convergent synthesis of **34**, the second generation hexakis-adduct analogue to **32**, gave no hints of its formation, being undetectable even by spectroscopic methods applied to the crude mixture. Less crowded second and third generation fullerene-dendrimers **38**-**42** and **48**-**51**, have been obtained by attaching up to six dendrons to several [60]fullerene derivatives. In order to build up globular fullerene based architectures mimicking the size and the shape of natural macromolecules, it is crucial to develop an alternative methodology to synthesize highly dense [60]fullerene hexakis-addition analogues to **32**, **33** and **54** containing higher generation dendritic branches. Two different approaches were conceived with regard to this matter. First, the use of looser and more flexible dendritic systems might solve the above mentioned synthetic problem. The second alternative, which will be discussed in the next chapter, consists in changing the synthetic strategy from convergent to divergent.

3.2.2 Hypercores and Spacers

Fréchet and coworkers developed the concept of hyperbranched cores (*hypercores*)[46]. These hypercores may consist of flexible segments providing for ample spacing between the reactive groups at each chain end. As a result, the coupling of dendritic fragments to these loose cores is facilitated and less subject to steric constraints when coupled to more compact and rigid cores. Seebach and coworkers successfully developed the same idea in their elegant work on chiral dendrimers[61,84,85]. Chiral tris(hydroxymethyl)methane derivatives were synthesized and used as central cores in dendritic constructions (figure 3.17). First, the chiral triols were further

elaborated to give building blocks in which the distance between the three hydroxyl groups was increased so that steric hindrance during the attachment of branches was decreased[86].

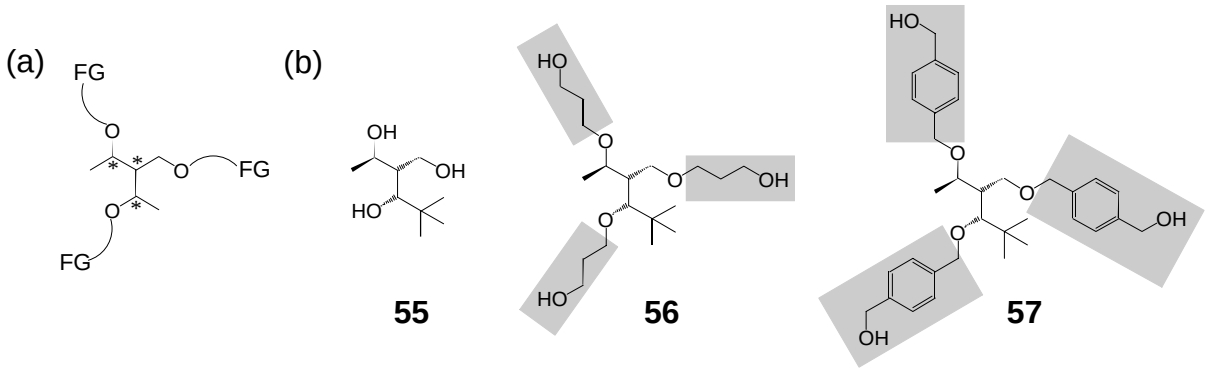

Figure 3.17. (a) General representation of the chiral hypercores developed by Seebach et al. (b) Hypercores 56 and 57 are synthesized from **55** after introduction of spacing units at each reacting group of **55**.

In a similar way, the conversion of Fréchet's benzyl ether-type dendrons into a less bulky system was planned. The designed modification consisted in the formal introduction of a spacing 3-oxypropane chain between the aryl-benzyl bond of Fréchet's dendrons (figure 3.18).

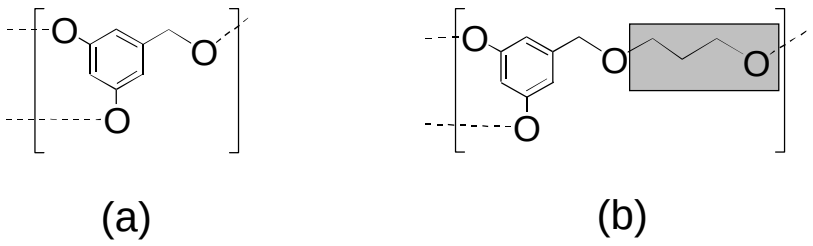

Figure 3.18. Schematic description of: (a) Fréchet's dendrons; (b) new dendritic system developed from the former after the introduction of a *spacer* unit marked with a gray rectangle.

The typical aryl-benzyl cadence of Fréchet's dendrons becomes aryl-alkyl-benzyl in the proposed ones. The synthesis of the targets was planned according to the convergent approach developed by Fréchet and coworkers[46], taking into account the preparation of extended cores developed by Seebach's group[61,84].

Two new additional steps per generation must be introduced in Fréchet's synthetic pathway route: the O-allylation of benzylic alcohols and the subsequent transformation of the introduced allyl moiety into a terminal alcohol via hydroboration. Although two extra steps are required to reach a new generation, both are expected to run with high yields and the resulting products are expected to be easily purified and characterized.

3.2.3 Synthesis of a New Dendritic System

The first and second generation dendritic alcohols **59** and **63** were obtained according to the synthetic pathway showed in scheme 3.9. Alcohol **13** was O-allylated using sodium hydride as a base and a two-fold excess of allyl bromide in refluxing THF to afford the liquid allyl ether **58** in almost quantitative yield. Hydroboration of the allyl group in **58** with

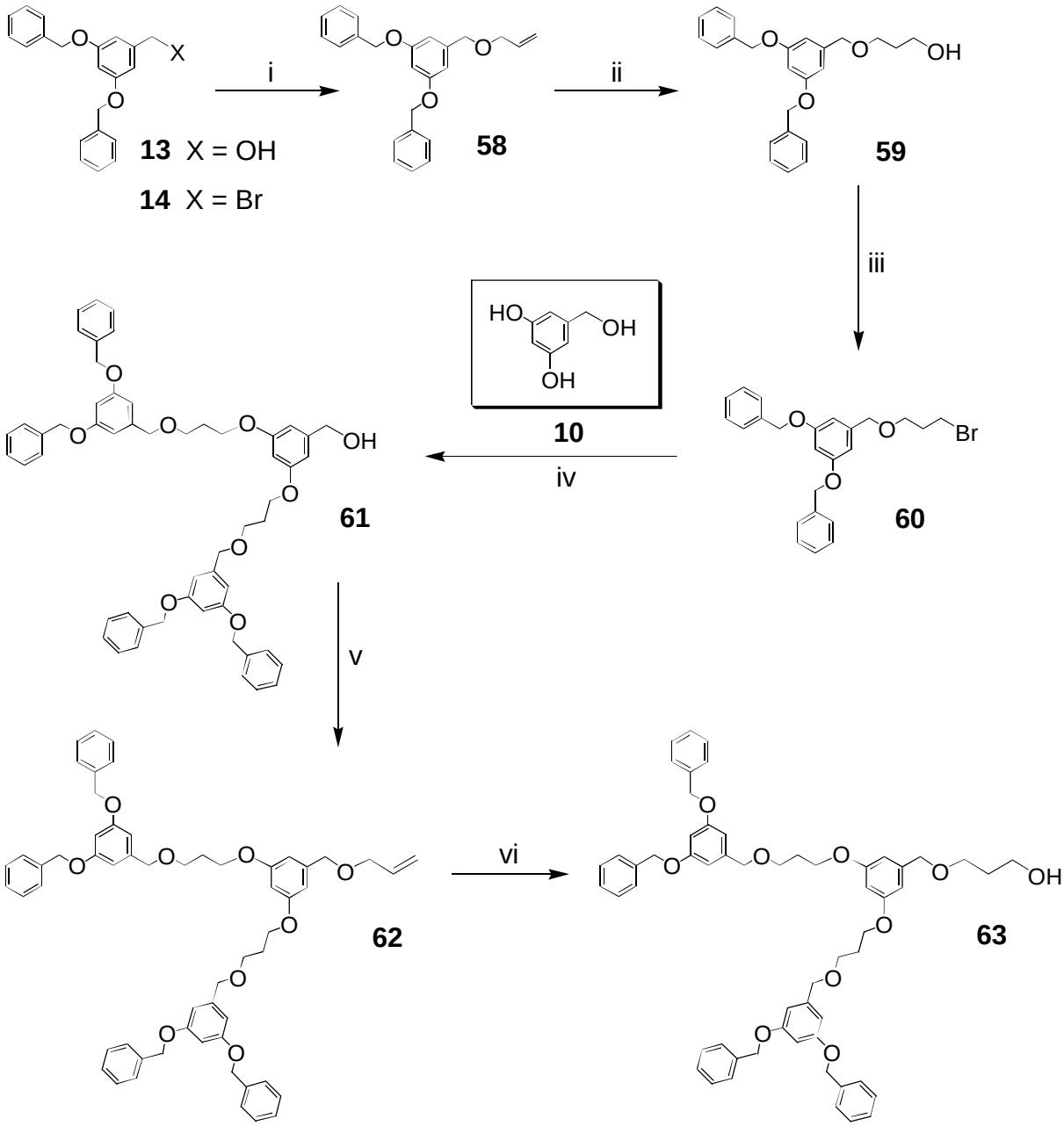

Scheme 3.9. Synthesis of dendritic polyethers alcohols **59** and **63**. i) allyl bromide, NaH/THF (98.5 %); ii) (a) 9-BBN/THF; (b) EtOH, H_2O_2, NaOH (90 %); iii) CBr_4, PPh_3/THF (94 %); iv) K_2CO_3, [18]crown-6/acetone (96.6 %); v) allyl bromide, NaH/THF (97 %); vi) (a) 9-BBN/THF; (b) EtOH, H_2O_2, NaOH (87 %).

9-borabicyclo[3.3.1]nonane (9-BBN), and subsequent oxidation of the intermediate borane with EtOH/NaOH/H_2O_2, furnished the corresponding first generation alcohol **59** in a 90 % yield. The hydroboration was completely regioselective, giving no secondary alcohol. The conversion of **59** to its respective bromide **60** was first tried with phosphorus tribromide. Under these conditions, the desired target **60** was only obtained in a 12 % yield, whereas the main product of the reaction was the bromide **14** (65 %). The breaking of the activated benzylic C-O bond in **59** could take place by direct action of PBr_3 or may be due to the presence of HBr resulting from its hydrolysis. Finally, the synthesis of bromide **60** was achieved treating the alcohol **59** with 1.3 equivalents of CBr_4/PPh_3 in THF[55]. In this case the reaction worked satisfactorily, producing the desired bromide **60** in a 94 % yield. Selective alkylation of both phenolic hydroxyl groups of 3,5-dihydroxybenzyl alcohol **10** afforded the alcohol **61** in excellent yield after a reaction time of 2 days. When the same sequence of O-allylation and oxidative hydroboration, described above, was applied to **61** the formation of the second generation alcohol **63** as a pale yellow liquid was achieved. The purification of both intermediate **62** and product **63** was easily accomplished by flash chromatography on silica gel.
The syntheses of these targets fulfill the necessary requirements in dendrimer chemistry: i) all reactions are high yielding, and ii) isolation and characterization of the consecutive dendritic wedges are both reliable and sensitive to the occurrence of impurities and defects.
Once the new dendritic first and second generation alcohols **59** and **63** were obtained, they were transformed into the corresponding malonate capable to be attached to C_{60} (scheme 3.10). When the first generation alcohol **59** was treated with malonyl dichloride and pyridine in methylene chloride under the same conditions employed before, the reaction did not proceed successfully. Control by thin layer chromatography (TLC) showed no progress even after heating the reaction mixture to 40 °C for 24 hours. The reaction was quenched and the starting alcohol **59** recovered in a 82 % yield after flash chromatography on silica gel. The desired malonate **64** was also isolated from the crude mixture but its yield was less than 5 %. It was suggested that the reason for such low reactivity would lie in the existence of an intramolecular hydrogen bonding in **59** between the hydroxyl group and the close ether oxygen. This interaction would stabilize the alcohol **59**, becoming inert under the reaction conditions. It was intended to perform the same reaction in a more polar solvent that could interact with the hydroxylic group of **59**, thus breaking the postulated intramolecular hydrogen bond. On the other hand, the solvatization of the hydroxylic group might also reduce its reactivity towards malonyl chloride. The reaction was performed in THF under the same conditions, but

unfortunately, the same result as previously was obtained and malonate **64** was found in a yield lower than 5 %. Nevertheless, the starting material could be partially recovered (75 %). The use of other solvents was not further investigated since a different approach was successfully attempted as it is described in the following paragraph.

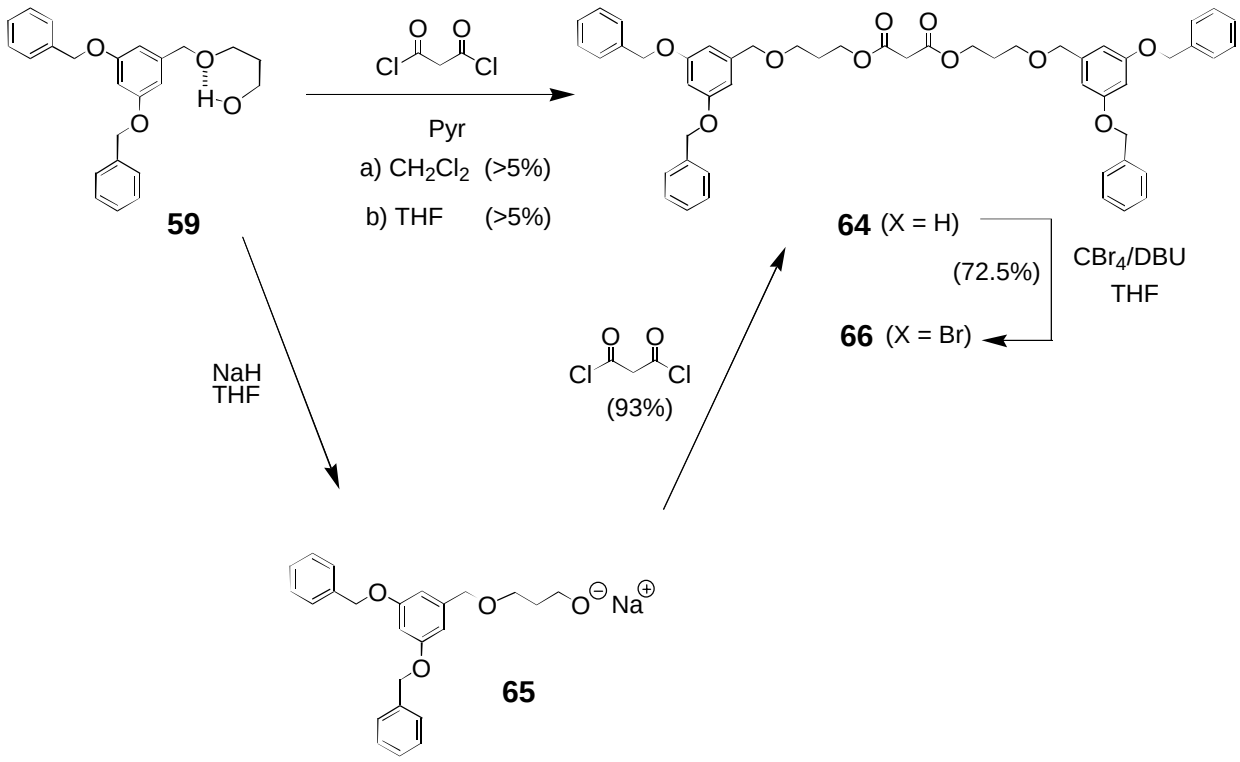

Scheme 3.10. Synthesis of **64** and **66**.

To circumvent the above problem, it was planned to deprotonate the alcohol **59** to yield the alkoxide **65** (scheme 3.10). Obviously, **65** contains no hydrogen bond and it should be possible to form the corresponding symmetrical malonate by reaction with malonyl dichloride. The hydroxylic proton of **59** was abstracted by treatment with one equivalent of NaH in THF. The resulting alkoxide **65** reacted with malonyl dichloride furnishing the expected malonate **64** in an excellent yield. Afterwards, the corresponding bromo malonate **66** was prepared following the same procedure used earlier[62].

The second generation malonate **67** (figure 3.19) was obtained in a not optimized process with a yield of 46 % following the same strategy.

Once the dendrons were transformed into the suitable form to be attached to C_{60}, the synthesis of fullerene-dendrimers proceeded.

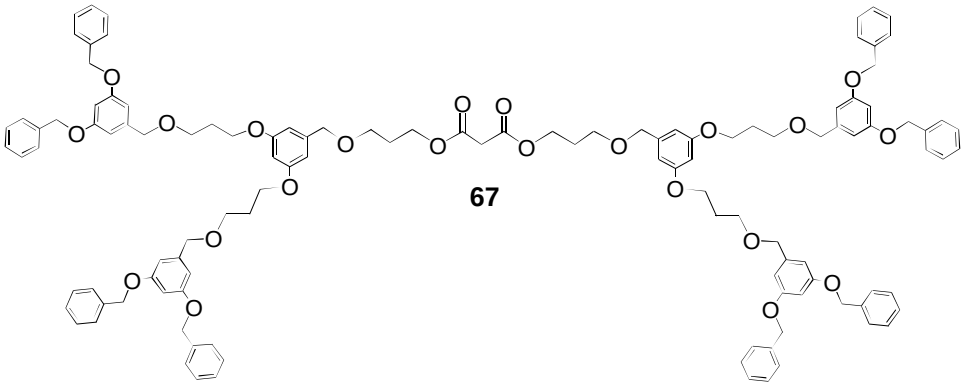

Figure 3.19. Second generation malonate **67**.

3.2.4 Synthesis of Dendrimer-Fullerenes

The synthesis of monoadduct **68** was achieved straightforward under classical Bingel reaction conditions[24] (scheme 3.11). The product was isolated by flash chromatography on silica gel in a yield close to 42 %, together with unreacted C_{60} (23 %) and a regioisomeric mixture of bisaddition products (15 %).

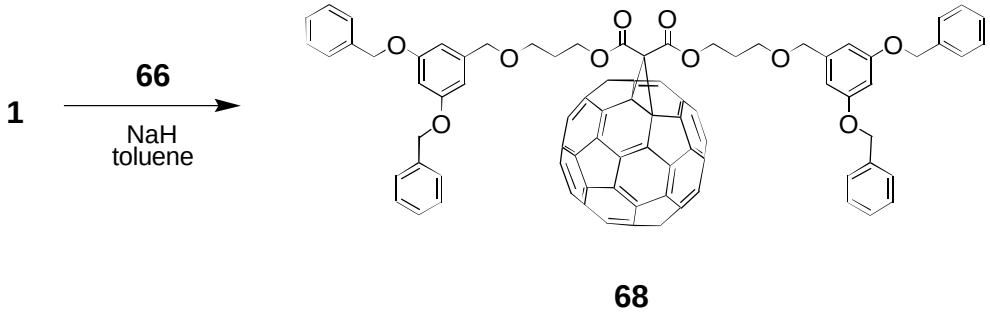

Scheme 3.11. Synthesis of monoadduct **68**.

The ^{13}C-NMR (figure 3.20) and ^{1}H-NMR (figure 4.22.a) spectra show all expected peaks clearly resolved. The signals corresponding to the dendritic branches appear at about the same position as in **64**, and all [60]fullerene carbons absorb at the usual position for [6,6]bridged [60]fullerene monoaducts. IR and UV/Vis spectra show the characteristic bands for this type of compounds according to previous experience. The molecular ion at m/z = 1543 was recorded with MALDI-TOF mass spectrometry.

The synthesis of the hexakis-adduct **69** was performed via template activation with DMA as described above (scheme 3.12). The glassy yellow dendrimer **69** was isolated using preparative HPLC on a silica column in a 12.7 % yield.

The comparison of this yield with that obtained in the preparation of **32** (5.4 %) indicated that

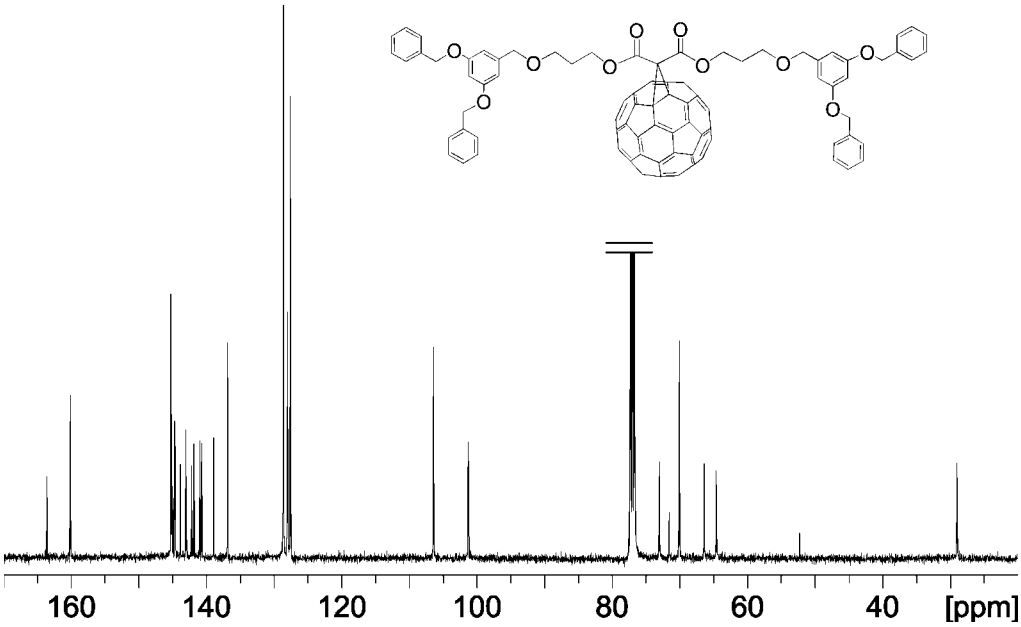

Figure 3.20. ^{13}C-NMR (100.5 MHz, RT, $CDCl_3$) spectrum of **68**.

the modification of the dendrimer clearly reduced the steric hindrance involved in the synthesis of these crowded systems. Also, the purification step was easier when the more flexible new dendrons were used instead of Fréchet ones, making a GPC purification step not necessary.

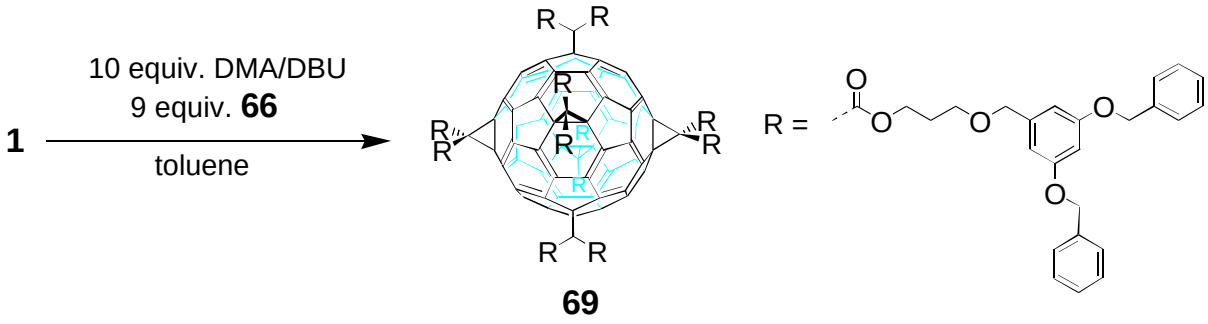

Scheme 3.12. Synthesis of the globular dendrimer **69**.

The ^{13}C-NMR of **69** shows the peaks corresponding to the dendrons together with three signals attributable to the fullerene core, clearly revealing the T_h-symmetry of **69** (figure 3.21). These three peaks appear at 145.89, 141.22, and 69.14 ppm. The ^{1}H-NMR spectrum of **69** (figure 3.22.b) also confirms its high symmetry. All the methylene protons in **69** are shifted to higher field with respect to their equivalent protons of the parent monoadduct **68** (figure

3.22.a). As was discussed in the previous chapter, the interactions between the methylene protons and the currents within the aromatic rings in the crowded hexakisadduct dendrimer **68** seem to be the reason for this effect.

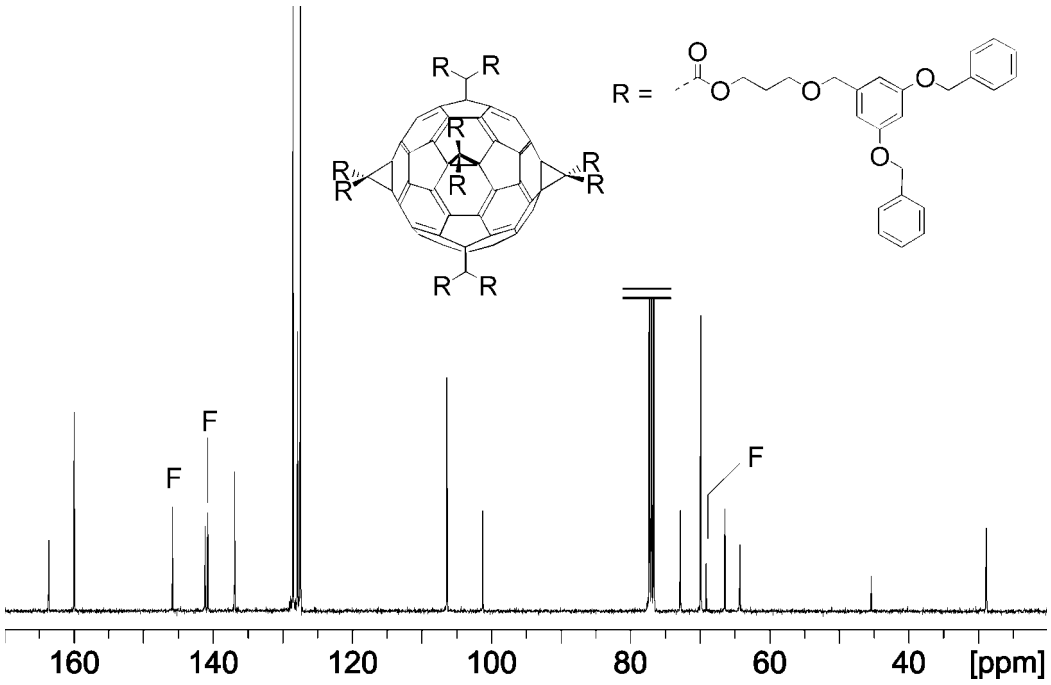

Figure 3.21. ^{13}C-NMR (100.5 MHz, 31°C, $CDCl_3$) spectrum of **69**. F denotes the signals for the fullerene carbon atoms.

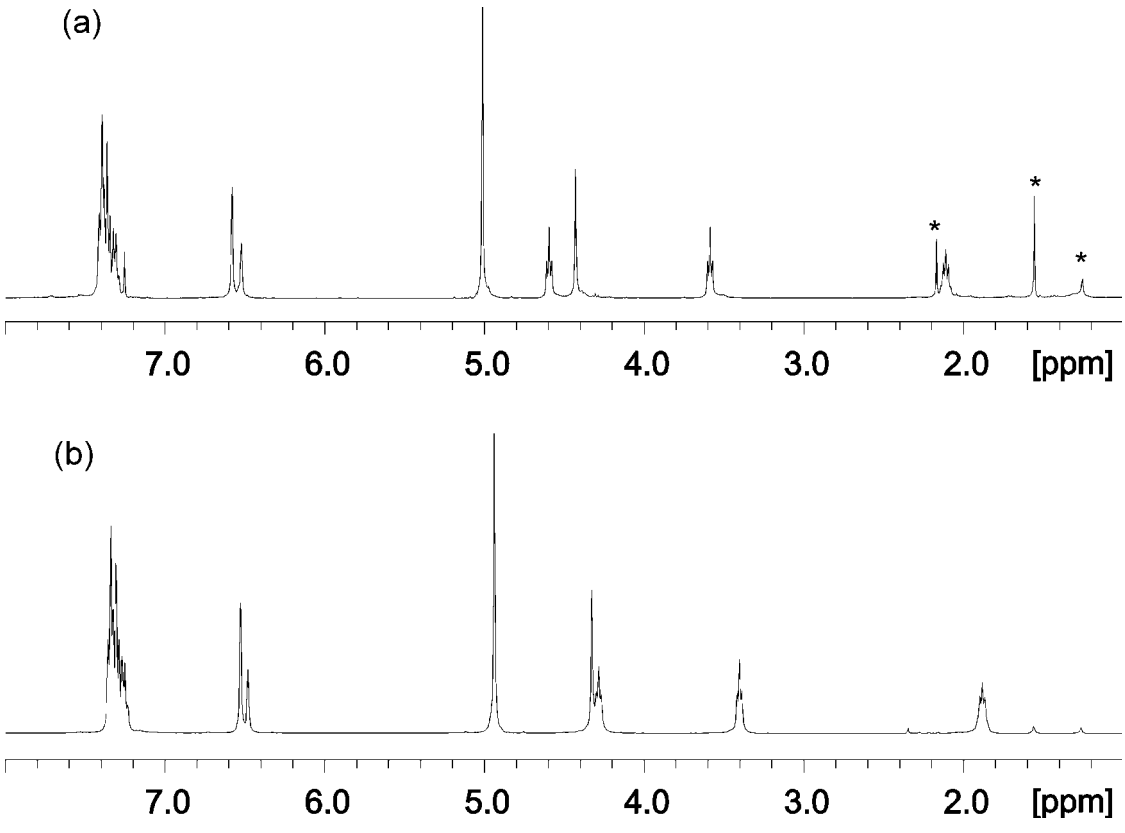

Figure 3.22. ^{1}H-NMR (400 MHz, RT, $CDCl_3$) spectra of (a) **68** (*toluene, H_2O), (b) **69**.

The UV/Vis spectrum of **69** gives the expected absorptions for a [60]fullerene hexakis-adduct. Its IR spectrum shows aliphatic, aromatic, ether, and carboxylate bands together with a sharp band corresponding to the fullerene core at 530 cm^{-1} (figure 3.23). MALDI-TOF Mass spectrometry was a suitable technique to corroborate the composition of **69** ($C_{366}H_{300}O_{60}$).

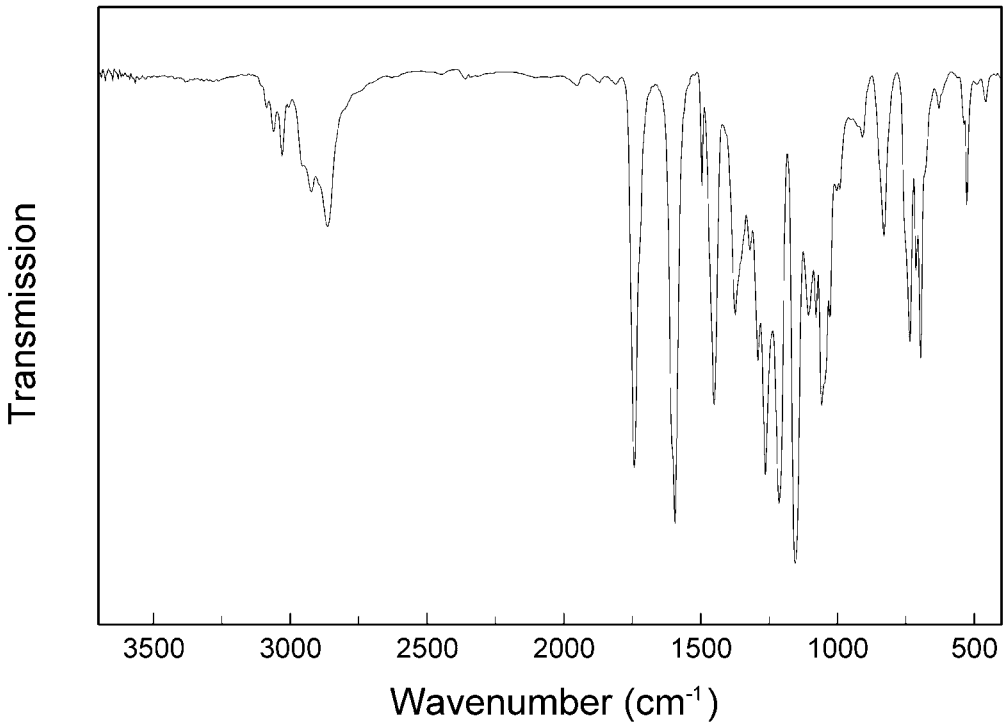

Figure 3.23. IR spectrum of **69**: the band at 530 cm^{-1} is characteristic for [60]fullerene derivatives.

Parallel to the development of this new type of dendritic system, a modification of the cyclopropanation reaction of fullerenes with bromo malonates described by Bingel[24] was conceived. This approach will be extensively discussed in the last chapter. Briefly, the improvement of this method consists of generating the reactive bromo malonic species in situ being able to cyclopropanate [60]fullerene starting directly from malonates.

Therefore, the second generation malonate **67** was not further transformed into the associated bromo malonate, and reaction with [60]fullerene was directly carried out.

[60]Fullerene was treated with equimolar amounts of **67** and CBr_4 and a little excess of DBU to yield the [60]fullerene monoadduct dendrimer **70** (scheme 3.13). Purification of **70** was achieved by flash chromatography on silica gel using toluene/ethyl acetate 9:1 as eluent in a 42 % yield.

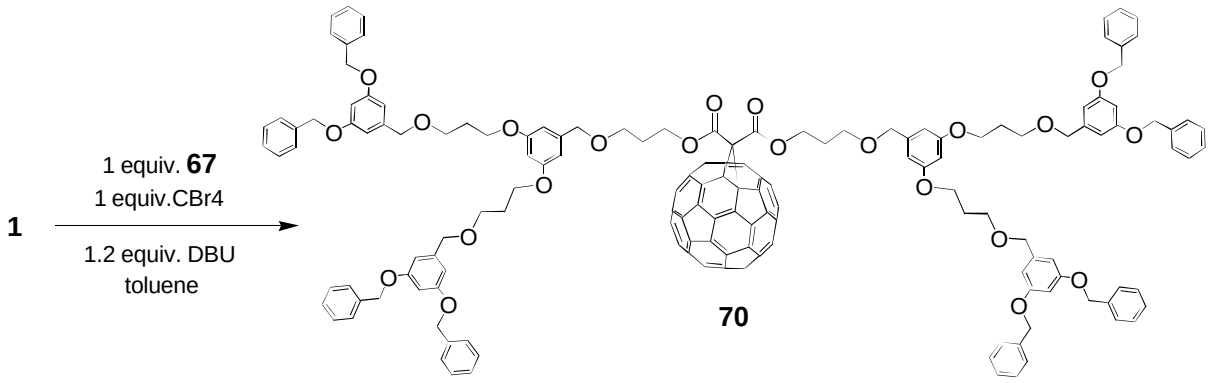

Scheme 3.13. Synthesis of **70** starting from malonate **67**.

The study of the ^{13}C-NMR and ^{1}H-NMR (figure 3.24) spectra revealed the C_{2v}-symmetry of the dendrimer **70** and all the resonance signals were assigned as reported in the experimental part.

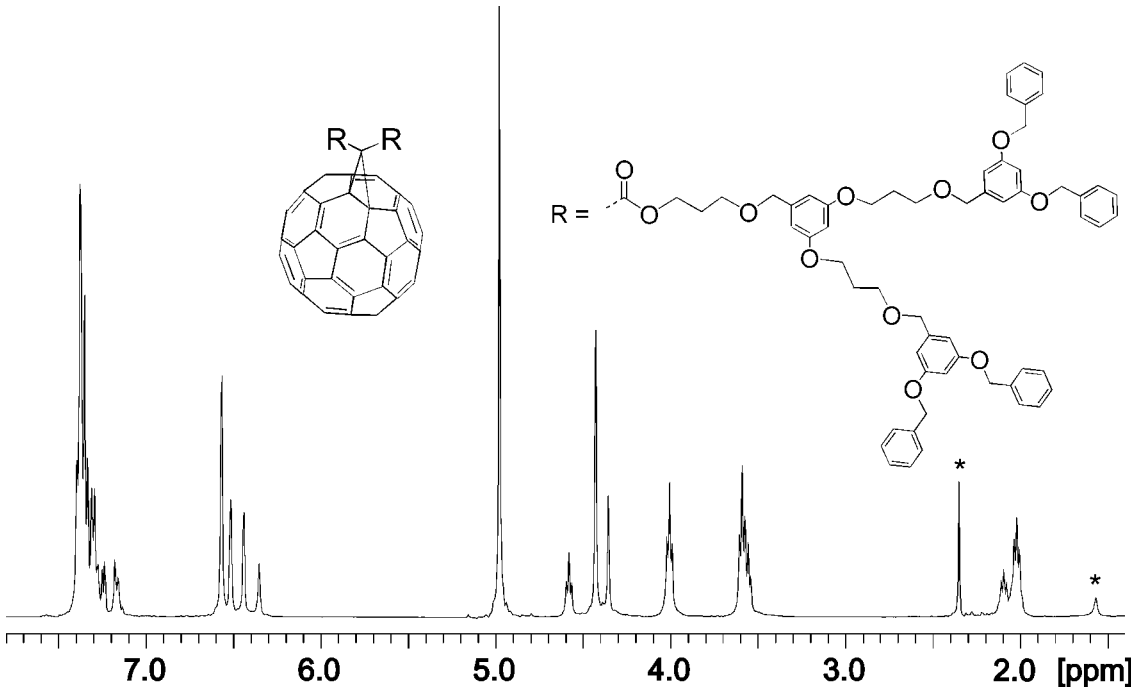

Figure 3.24. ^{1}H-NMR (400 MHz, RT, $CDCl_3$) spectrum of **70** (*toluene, H_2O).

UV/Vis and IR spectroscopies confirmed the structure of **70**. FAB Mass spectrometry recorded in the positive mode gave the $(M+Cs)^+$ ion at m/z = 2756 together with a fragmentation cluster corresponding to $(C_{60})^+$ at m/z = 720.

The synthesis of [60]fullerene hexakis-adducts containing only dendritic branches without any special additional functionality, is an example that shows the potential of the present strategy. Nevertheless, the synthesis of mixed systems like porphyrin-dendrimer-fullerenes is of utmost interest.

3.2.5 Porphyrin-Dendrimer-Fullerenes

3.2.5.1 Synthesis and Characterization of First and Second Generation Porphyrin-Dendrimer-Fullerenes

First generation porphyrin-dendrimer-fullerene **71** was prepared from porphyrin-fullerene **53** via template activation with DMA (scheme 3.14).

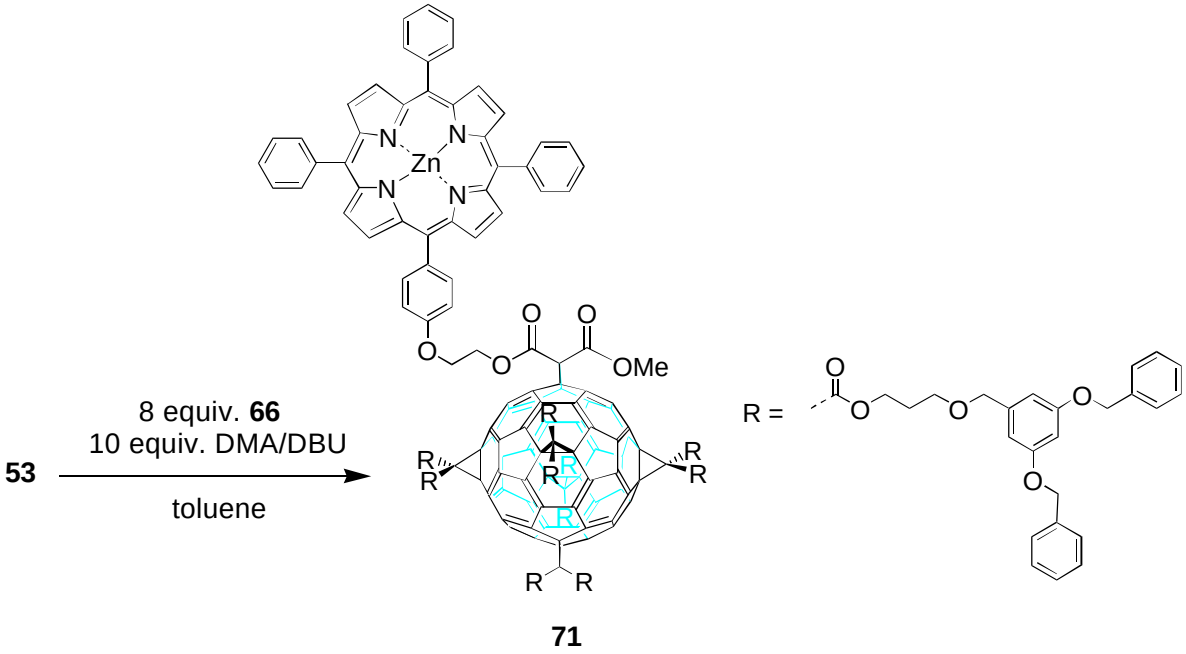

Scheme 3.14. Synthesis of first generation porphyrin-dendrimer-[60]fullerene **71**.

Dendrimer **71** was isolated from the crude mixture by HPLC in a 12.7 % yield. The compound was characterized by ^{1}H-NMR, ^{13}C-NMR (figure 3.25), UV (figure 3.28.a) and MS (figure 3.26) spectrometry. Using ^{1}H-^{13}C-COSY-NMR techniques it was possible to assign all peaks in ^{13}C-NMR and ^{1}H NMR spectra. *Pseudo*-T_h-symmetry of **71** is clearly manifest in its ^{13}C-NMR spectrum giving a single set of peaks with resolved structure for the ten dendritic branches together with three narrow distributions of peaks from the fullerene core. Peaks corresponding to the porphyrin appear at about the same position as in **53**. Figure 3.25 displays the ^{13}C-NMR spectrum and the complete proposed assignment for all the peaks is given in the experimental part.

The MALDI-TOF mass spectrum of **71** reveals a molecular ion at m/z = 5669 ($C_{365}H_{284}N_4O_{55}Zn$) and a fragment ion cluster at m/z = 4844 corresponding to the fragmentation of a dendritic malonate (figure 3.26).

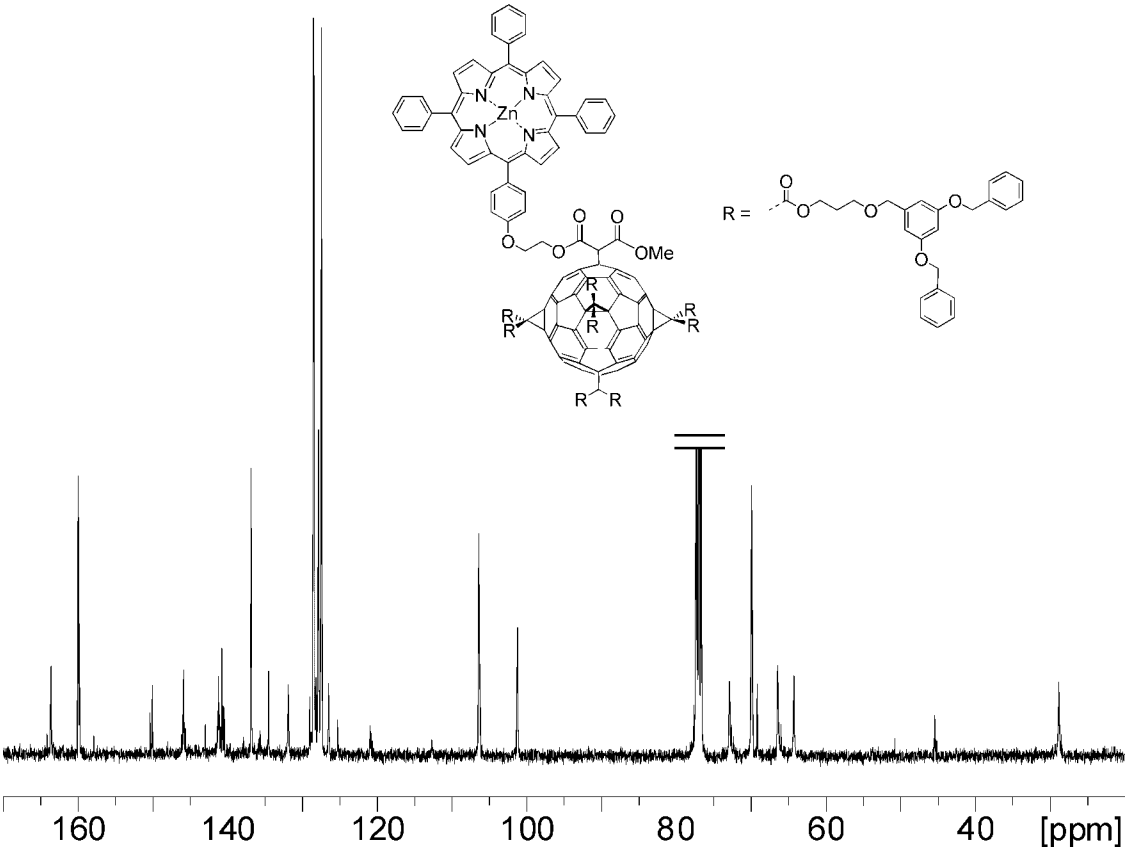

Figure 3.25. ^{13}C-NMR (100.5 MHz, RT, $CDCl_3$) spectrum of **71**.

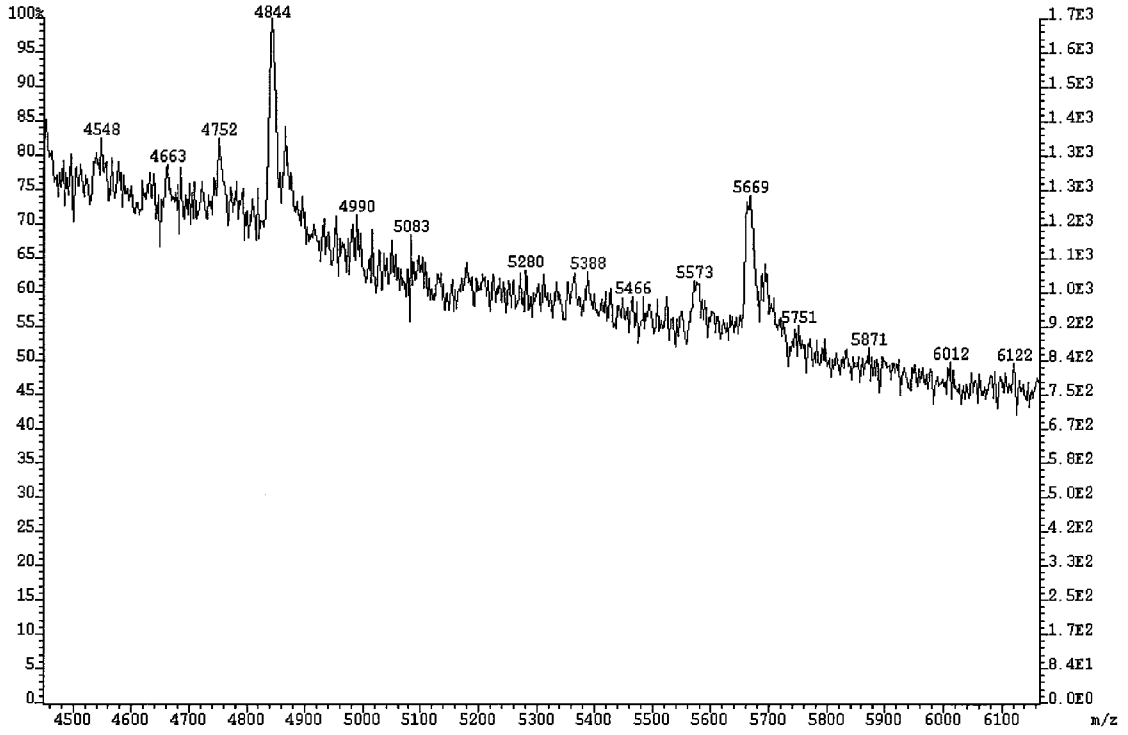

Figure 3.26. MALDI-TOFF Mass spectrum of **71**.

The second generation analogue **72** was obtained by exhaustive cyclopropanation of **53** via template activation directly from malonate **67** taking advantage of the Bingel reaction modification introduced above (scheme 3.15).

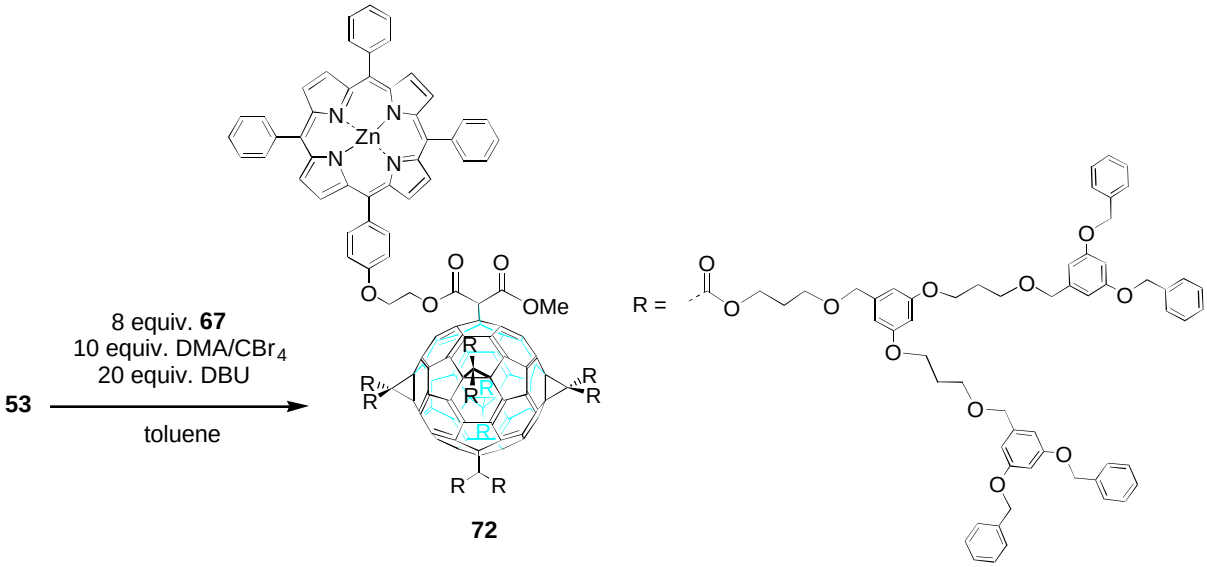

Scheme 3.15. Synthesis of second generation porphyrin-dendrimer-fullerene **72** from malonate **67**.

Purification of the crude mixture with HPLC afforded **72** in a 2 % yield. Dendrimer **72** was characterized by ^{1}H-NMR, ^{13}C-NMR and UV spectrometry (figure 3.28.b). The preparation of the second generation dendrimer **72** proved the success of the developed strategy. The introduction of spacing units has permitted the synthesis of a fullerene derivative containing ten second generation dendrons attached to it.

Molecular modelling[64,87] studies of **71** and **72** were performed. The conformers obtained are shown in figure 3.27. While in **71** the porphyrin group appears nearly naked, in **72** the dendrons are surrounding the metal center.

The study of the UV/Vis spectra of the dendrimers **71-72** and the parent porphyrin-[60]fullerene **53** manifested the different features of these compounds (figure 3.28). From 230-380 nm the absorption of the fullerene cores dominates the spectra. Thus, **53** displays two bands at 257 and 326 nm characteristic for [60]fullerene monoaddition, and both hexakisadducts **71** and **72** bands at 270, 285, 315 and 335 nm clearly demonstrating their addition pattern. Absorption below 300 nm is higher in **72** than in **71** as a result of the larger number of aromatic rings present in the second generation dendrimer **72** compared with the first generation product **71**. Starting from 380 nm the porphyrin moiety is responsible for the

(a)

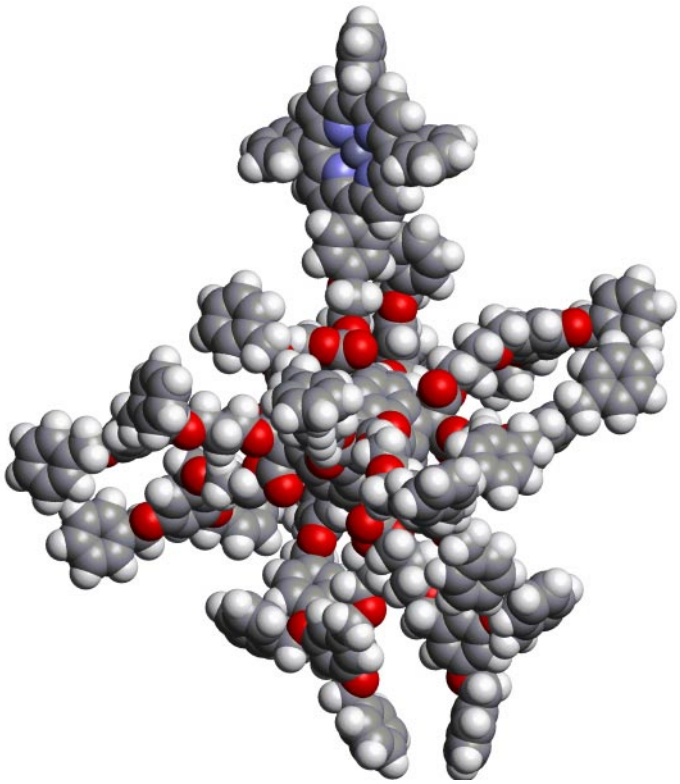

(b)

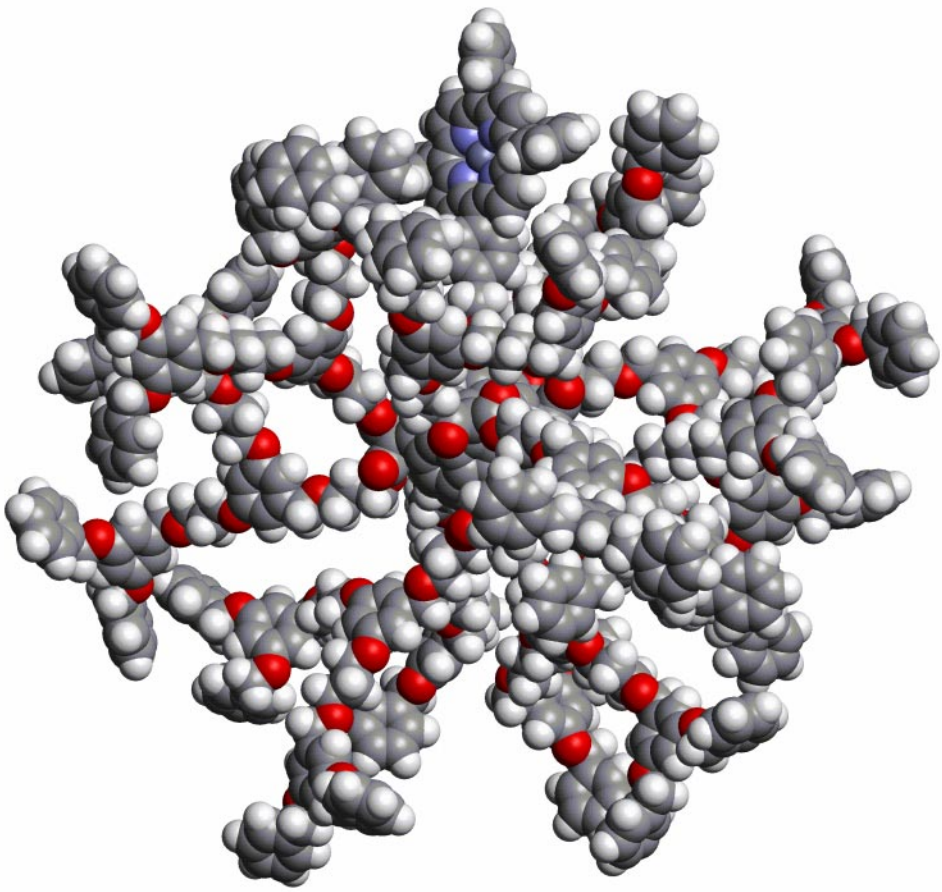

Figure 3.27. Optimized structures of the porphyrin-dendrimer-fullerenes (a) **71** and (b) **72**. All structures were minimized with the MM^{+} force field implemented in HYPERCHEM[64].

shape of the spectra since the extinction coefficient of the fullerene cores in this area are negligible compared with the porphyrin one. Characteristic in this area are the Soret band at about 400 nm and the Q bands at about 515, 550 and 590 nm. Bathochromic shifts of 7-4 nm for all these bands are observed in **72** relative to the parent dyad **53**, while shifts of 4-2 nm are observed for hybrid **71**. These shifts are unequivocally reflecting that interaction between the porphyrin and the dendrons occurs and that the magnitude of this interaction is increasing with the generation number as was expected. These shifts might derive from microenvironmental effects and/or from the deviation of planarity which the porphyrin could suffer in the resulting crowded surroundings.

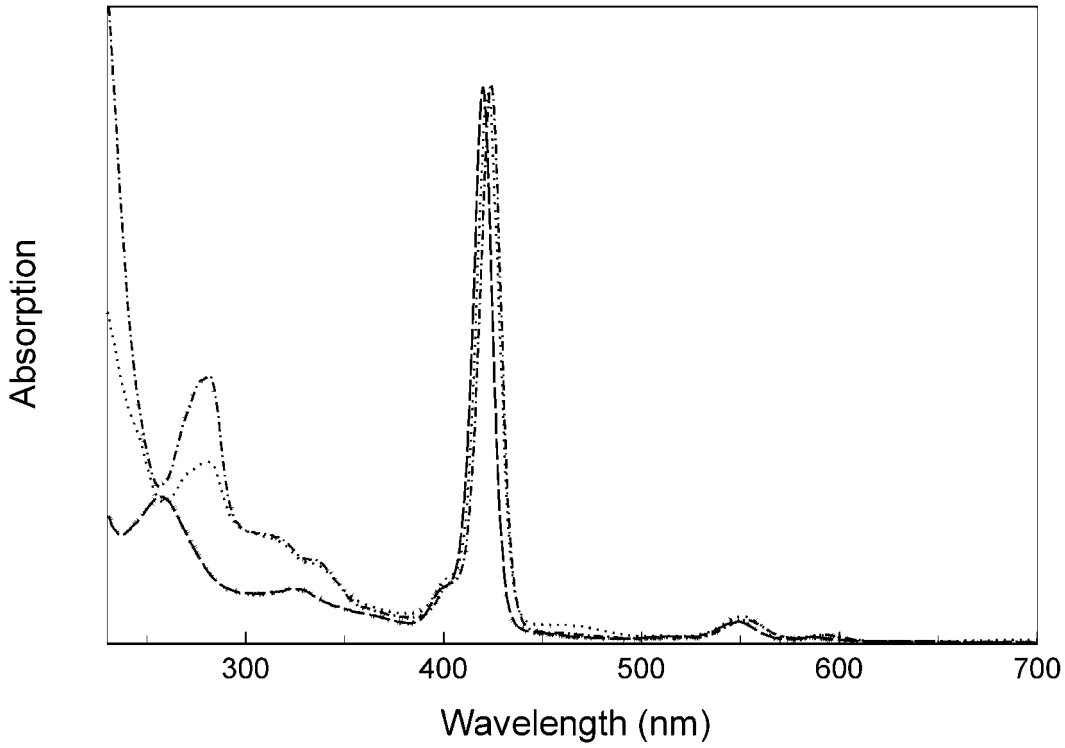

Figure 3.28. UV/Vis (CH_2Cl_2) spectra of porphyrin-dendrimer-[60]fullerenes (a) - - - - - - **71**;
(b) – – - – – - – – **72**, and (c) – – – – – – – – the parent porphyrin-[60]fullerene **53**.

3.2.5.2 Electrochemical Studies of Porphyrin-Dendrimer-Fullerenes. Preliminary Results

In a preliminary investigation the influence of the dendritic coverage in porphyrin-dendrimer-[60]fullerenes **71** and **72** on the redox potentials of the porphyrin moiety was studied. This project is part of a collaboration with Prof. Echegoyen at Miami University.

Cyclovoltammetric studies of compounds **53**, **71**, **72** and **73**[83] (figure 3.29) were performed[88].

These preliminary results are shown in table 4.1 and figure 3.30. The complete assignment of the redox potentials still needs to be corroborated in further studies.

	oxidation			reduction			
	E_1	E_2	E_3	E_1	E_2	E_3	E_4
53	0.760	0.957	1.095	-0.623	-0.997	-1.344	-1.432
73	0.778	0.982	1.115		-1.423		
71	0.783		1.133	-1.381			
72	0.668	0.909	1.209	-1.444			

Table 3.1. $E_{1/2}$ (V) values of compounds **53**, **71-73**. All values are based on the Ag/AgCl reference electrode.

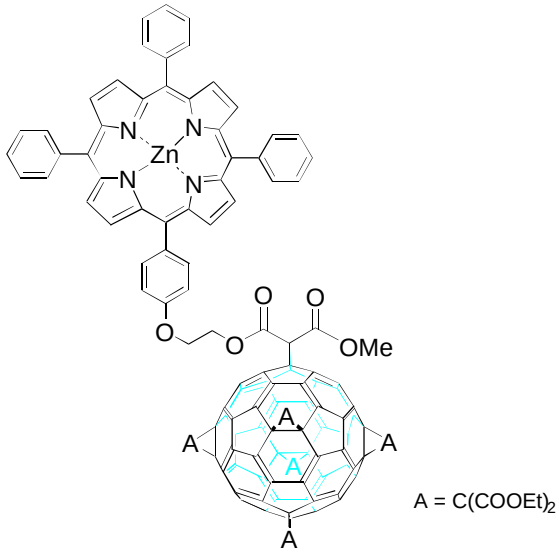

73

Figure 3.29. Fullerene hexakisadduct **73**.

The cyclovoltammogram of **53** presents two first reductions steps with potentials equal to -0.623 and -0.997 mV corresponding to two reversible reduction processes in the fullerene core. These two peaks are not present in **71-73**. In these cases the high substitution of the fullerene cage has decreased their number of π-electrons and disrupted its π-system, being not possible to achieve these low energy reduction steps. The first reduction potentials for **71-73** are assigned to the same reduction process at the porphyrin moiety. The tendency observed is that the values of the first reduction potential become more negative when increasing the size of the addends attached to the porphyrin-fullerene.

The first oxidation potential of these compounds are most likely due to the porphyrin group. In the most crowded porphyrin **72** it appears at 0.668 mV whereas in the naked dyad **53** its value is 0.760 mV.

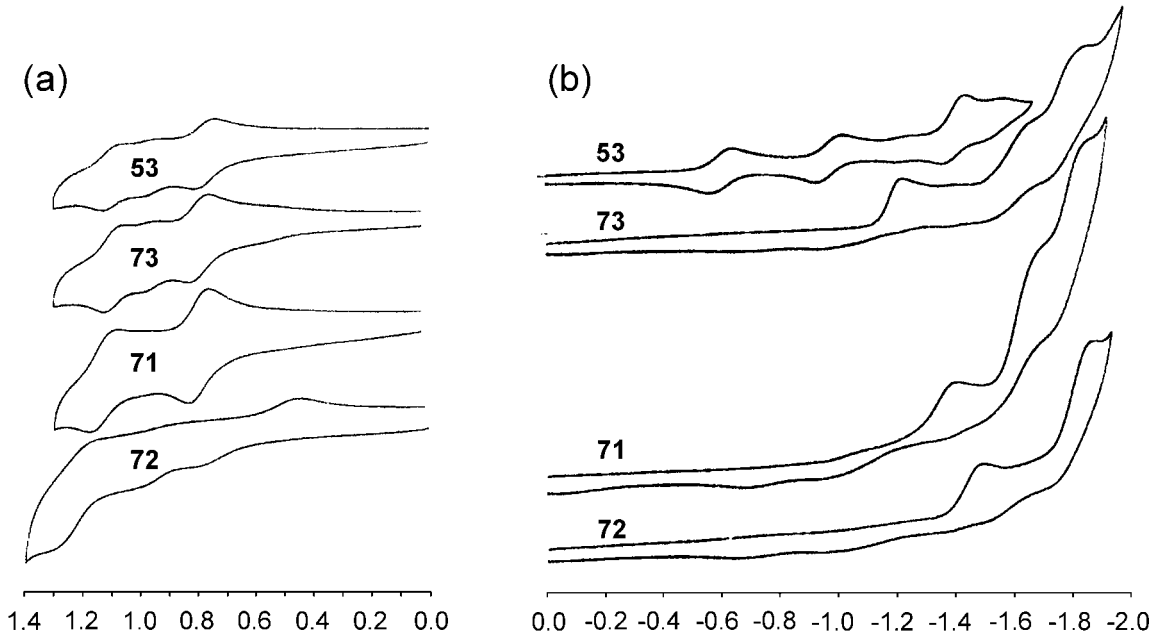

Figure 3.30. Cyclovoltammograms of **53**, **71**-**73**. (a) oxidation, and (b) reduction processes.

Further photochemical and photophysical investigation will help to understand the nature of the processes involved. A plausible interpretation of these results is that the polar microenvironment helps to attain the different oxidation states within the porphyrin. The numerous oxygen atoms of the dendritic branches apparently tend to stabilize a positive charge on the porphyrin[89]. For the same reason, the first reduction step within the porphyrin moiety is energetically more disfavorable with increasing the size of the addends attached to the fullerene core.

3.3 Divergent Approach

3.3.1 Synthetic Approach: Protecting Groups

The dendrimers presented so far have been synthesized through a convergent strategy. It was thought to make use of divergent methodologies[35,47-49] as an alternative approach to build up dendrimer-[60]fullerenes. Since in the divergent approach the reactions take place at the surface of the growing dendrimer, the steric inhibition encountered when using the convergent procedure may be avoided thus allowing for higher generations. However, the rapid increase in the number of reactive groups at the periphery of the growing macromolecule, which is characteristic for divergent methods, may cause difficulties. Potential problems which may arise as growth is pursued include incomplete reaction of the terminal groups, which would lead to imperfections in the next generation

Due to the own characteristics of the divergent method, surface functionalities able to be deprotected must be present in the growing macromolecule (figure 3.31). It was decided to develop this concept using a variation of the new dendritic system presented in the last chapter. The synthetic plan would include the introduction of protecting groups in the phenolic hydroxyls of the building block. These protecting groups should be stable during the construction of the dendrimer and easily removable once attached to the fullerene.

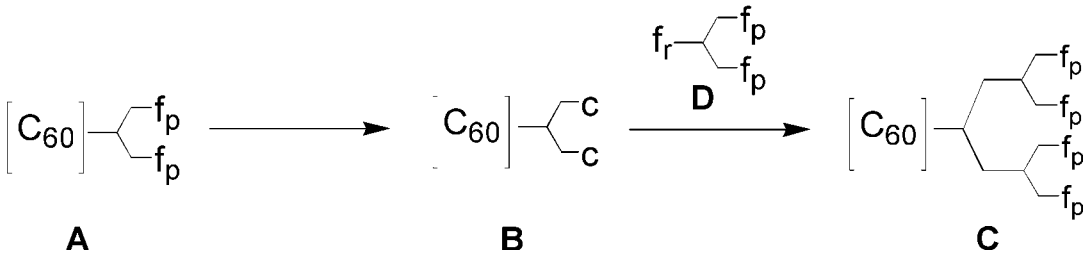

Figure 3.31. Divergent approach. First generation fullerene-dendrimer **A** contains several protecting groups. The attachment of first generation dendrons **D** to the surface coupling sites of the deprotected fullerene derivative **B** results in the formation of a second generation dendrimer **C** (f_p: protecting group; c: coupling site; f_r: reacting group).

Removal of the protecting groups is not only necessary to develop a divergent approach, but is interesting in itself. Of special importance would be the formation of water-soluble dendrimers

with potential abilities as molecular micelles[90] or as hosts for the transport of biological guests[42].

The protection of the hydroxyl groups of the starting compound methyl-3,5-dihydroxy-benzoate (**11**) was studied. The protecting groups must be stable under the reductive, oxidative, and basic conditions employed during the synthesis of the dendrimer. The protection of these hydroxyl groups as *tert*-butyl, tetrahydropyranyl and 2-methoxyethoxy-methyl ethers was studied (figure 3.32).

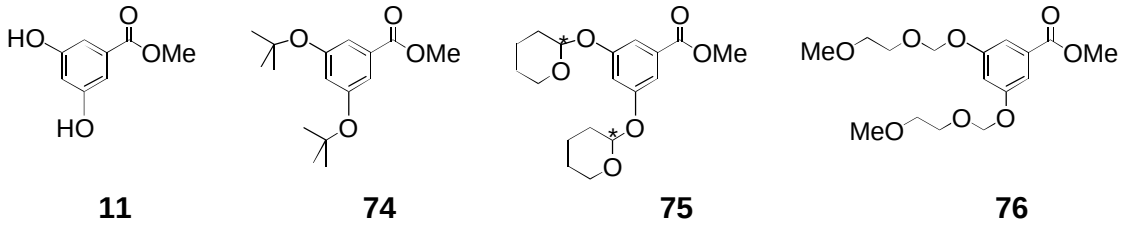

11 **74** **75** **76**

Figure 3.32. Synthons **74-76**.

Tert-butyl ethers should be stable under the reaction conditions and easily removable under acidic conditions. Unfortunately, the attempts to synthesize **74** failed. This included alkylations with 2-methylpropene under acid catalysis and alkylation with *tert*-butyl bromide in refluxing pyridine[91]. The formation of tetrahydropyranyl ethers was tested. Despite of the acceptable yields in the formation of **75** under classical conditions, this strategy was immediately rejected. The generation of a chiral center per THP group attached results in the formation of a diasteroisomeric mixture of products. Undoubtedly, this would complicate the isolation and identification of the dendritic system in the following steps.

Finally, it was decided to use 2-methoxyethoxymethyl ethers (MEM) as protecting group. This kind of ethers are stable under dendrimer formation conditions. A priori, MEM ethers should be easily cleaved under acidic conditions, while the rest of the dendrimer should be unchanged.

3.3.2 Divergent Synthesis of Dendrimer-Fullerenes

Ester **76** was obtained in a yield of about 92 % by alkylation of **11** with 2-methoxyethoxy-methyl chloride in a slurry of NaH in THF (scheme 3.16). Starting from **76**, the synthesis of malonate **80** was carried out in a way analogous to the preparation of **64** described in the previous chapter with comparable results. Different mixtures of solvent always containing 2 % of triethylamine were employed to the purify targets **76**-**80** by flash chromatography on silica gel in order to avoid the cleavage of MEM ethers.

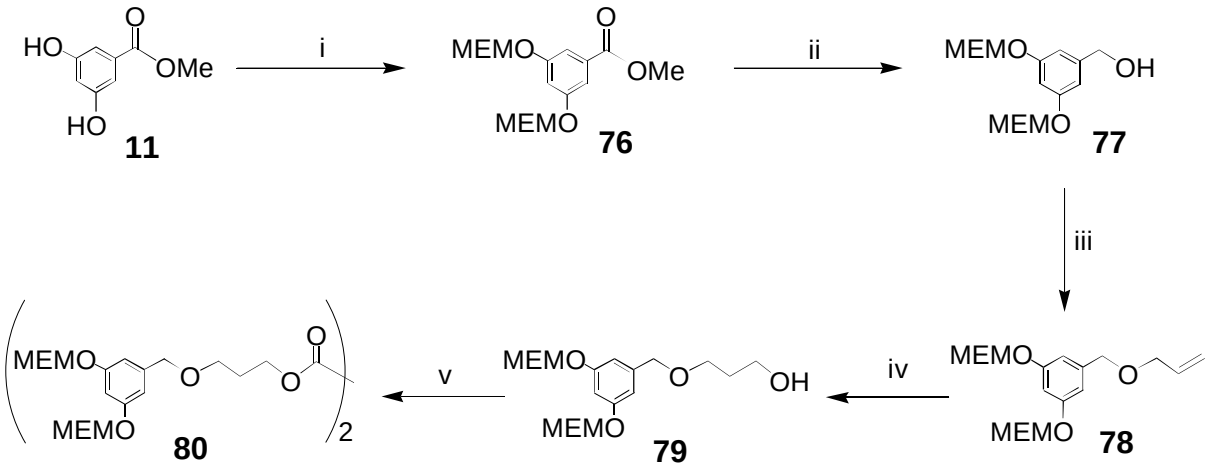

Scheme 3.16. Synthesis of malonate **80**: i) MEM-Cl, NaH/THF (91.6 %); ii) $LiAlH_4/Et_2O$ (93 %); iii) allyl bromide, NaH/THF (91 %); iv) (a) 9-BBN/THF; (b) EtOH, H_2O_2, NaOH (92.6 %), v) (a) NaH/THF, (b) malonyl chloride (48.6 %).

The [60]fullerene monoadduct **81** was obtained by treating [60]fullerene with the corresponding malonate **80** in the presence of CBr_4 and DBU (scheme 3.17).

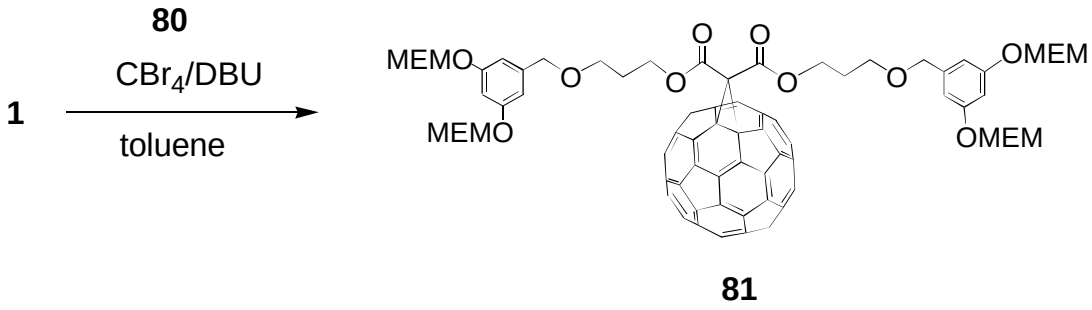

Scheme 3.17. [60]Fullerene monoadduct **81**.

The compound was completely characterized, and all the spectroscopic data recorded were in good agreement with a [6,6]bridged methano[60]fullerene structure. The ^{13}C-NMR spectrum (figure 3.33) reveals sixteen different types of sp^2-carbons (145-139 ppm) and one type of sp^3-carbon (72.8 ppm) of the fullerene cage according to the C_{2v}-symmetry of **81**. The rest of the peaks in ^{13}C-NMR and ^{1}H-NMR spectra appear at about the same position as in the parent dendritic malonate **80**. MALDI-TOF Mass spectrometry gave the molecular ion at m/z = 1536.

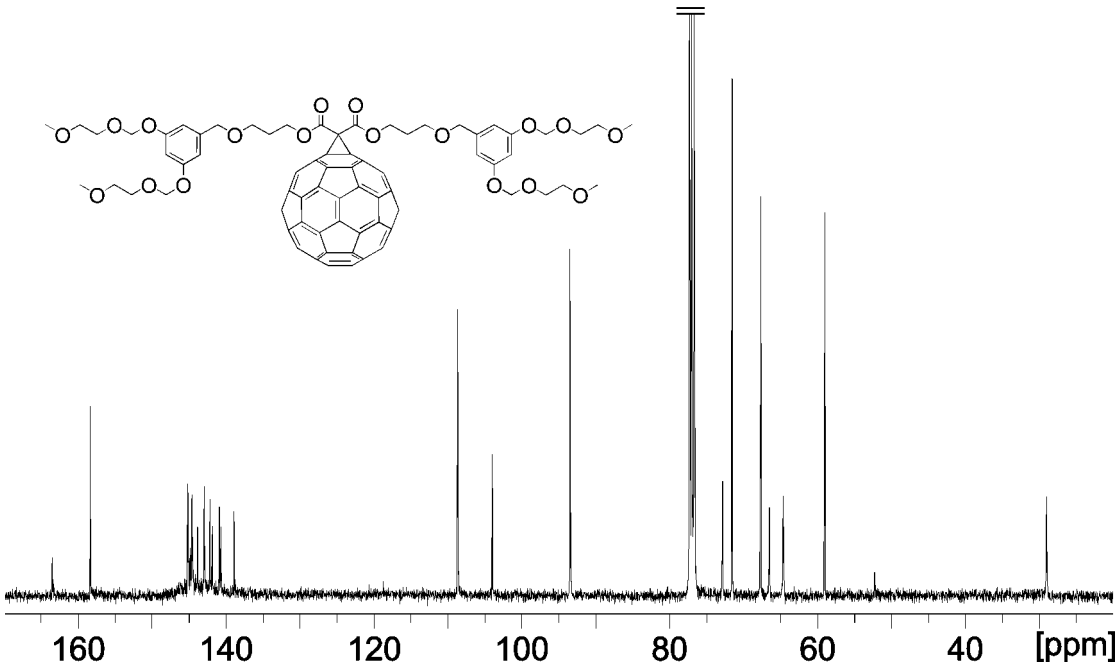

Figure 3.33. ^{13}C-NMR (100.5 MHz, 31°C, $CDCl_3$) spectrum of **82**.

It was tried to cleave the four protecting groups present in **81**. This would result in the formation of a molecule with four free hydroxyl groups (**82**) ready to undergo reaction with the bromide **83**, thus yielding the second generation dendrimer **84** (scheme 3.18).

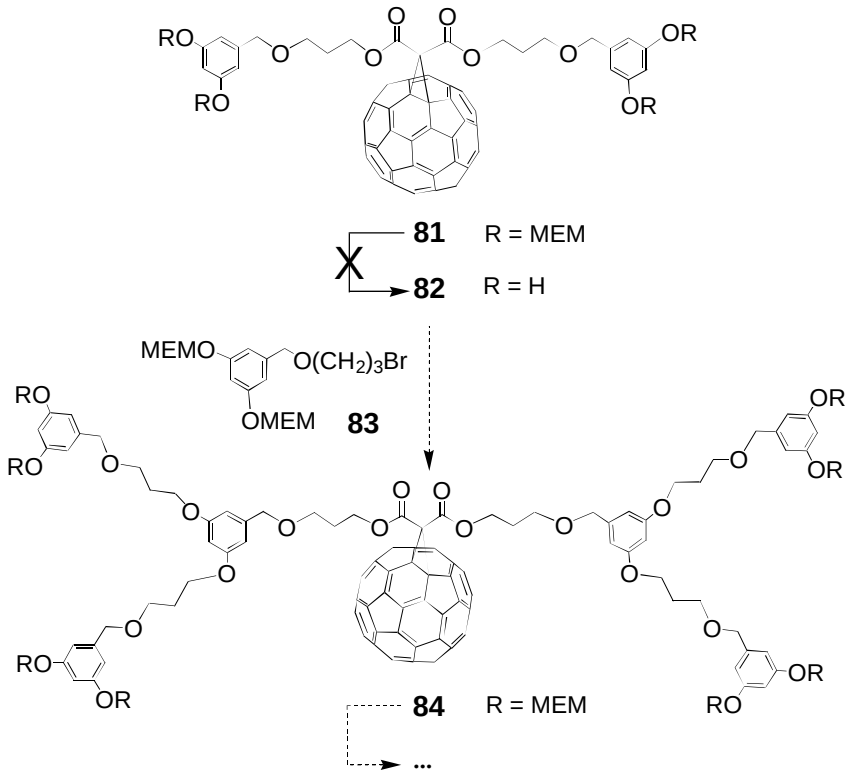

Scheme 3.18. Planed divergent synthesis of the second generation dendrimer **84**.

Unfortunately all the methods of cleavage applied failed. With 10 equivalents of trifluoroacetic acid no reaction took place, whereas with 50 equivalents, the formation of a dark brownish precipitate without defined composition was obtained[92]. With $TiCl_4$ a very slow progress was observed together with the formation of a precipitate that also could not be identified[93].

3.4 Lipo-Fullerenes in Membranes

3.4.1 Introduction

Natural membranes are organized sheetlike assemblies consisting mainly of lipids and proteins (figure 3.34). Phospholipids represent the main constituents of cellular membranes. They are relatively small molecules that have both a hydrophilic part, normally consisting of two long alkyl chains, and a hydrophobic moiety. These amphiphiles spontaneously form closed bimolecular sheets in aqueous media where the hydrophobic chains are in contact while the hydrophilic heads are exposed to the aqueous surrounding, thus constituting a barrier to the flow of polar molecules and ions. The proteins are embedded in the lipid bilayers, which creates suitable environments for their action. There are many processes occurring in biological membranes: membrane proteins can serve as ion pumps, gates, receptors, energy transducers and enzymes. The membrane composition in specific proteins varies according to the situation and role of the membrane in the cell. All constituents in membranes are hold together by many noncovalent cooperative interactions. In fact, membranes are fluid structures. Lipid molecules diffuse rapidly in the plane of the membrane, as do proteins. In contrast, they do not rotate across the membranes. Therefore, membranes can be regarded as two-dimensional solutions of oriented proteins and lipids.

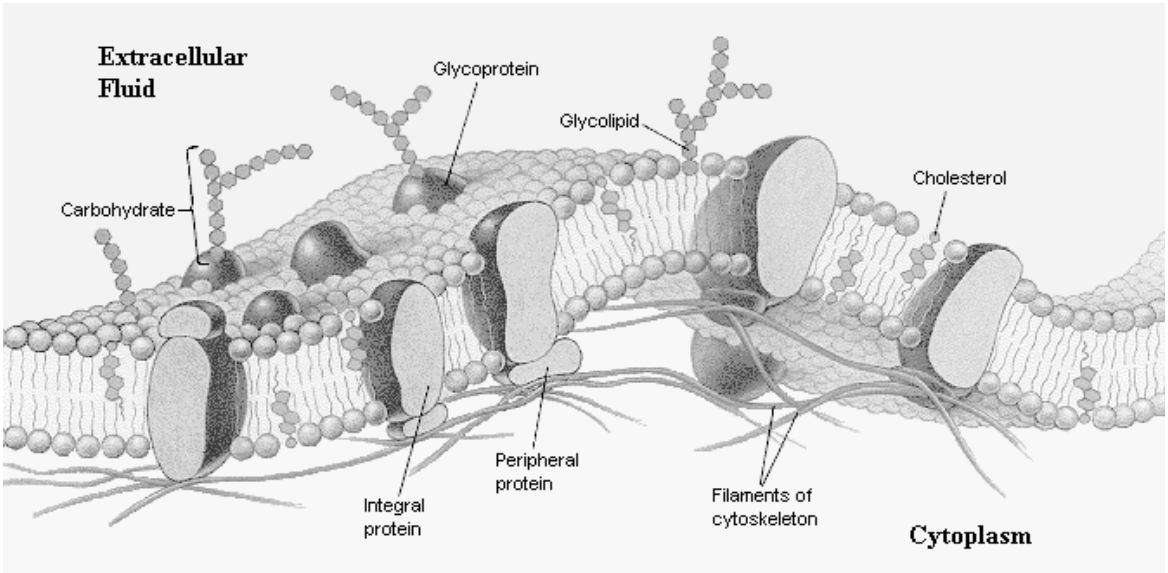

Figure 3.34. Schematic diagram of a cellular membrane[94].

Artificial lipid bilayers provide simplified systems to study the complex biological membranes and the processes that are occurring therein. Also, these quasi two-dimensional, partially ordered structures with their unique elastic properties have led to a number of applications in biomedical devices (e.g., biocompatibilization of surfaces, drug delivery)[90]. These properties are a result of a unique double-layer structure and of the frictional drag between the two bilayer leaflets. Usual studies in this field include the introduction of organic molecules in the membranes in order to affect the permeability as well as the physical and mechanical properties of the current system. In this context, [60]fullerene and [70]fullerene have been introduced in lipid bilayers and their ability as both photosensitizers for electron transfer from donor molecules, and mediators for electron transport across the lipid bilayer have been studied[38,95,96]. However, the main limitation for these studies is the low solubility of plain fullerenes in bilayers. [60]Fullerene shows extraordinary lubrication properties[37] and its diameter of 10.5 Å is just one fifth of the average bilayer thickness. The intercalation of [60]fullerene molecules inside a lipid bilayer may affect the motions and flexibility of the whole structure thus giving rise to new outstanding material properties.

To overcome the solubility problem of plain [60]fullerene in bilayers, it was decided to synthesize different fullerene derivatives by attaching long alkyl chains, giving the so-called *lipo-fullerenes*. It seemed appropriate to synthesize T_h-symmetrical [60]fullerene hexakisadducts containing six pairs of dodecyl (**85**) and octadecyl chains (**86**) (figure 3.35), corresponding to the chain length of lauric and stearic acid, respectively, using the efficient template method described above. Although this chemical modification certainly alters the rotational dynamics of the resulting molecules compared with plain [60]fullerene, and thus possibly its lubrication properties, it almost completely retains its unique symmetry, and may change the phospholipid bilayer to a composite system with new physical properties. It would also be of interest to study the intercalation of monoaddition products **87** and **88**. These compounds have still an almost intact C_{60} skeleton and thus may also lead to interesting electronical properties of the resulting system.

3.4.2 Synthesis and Characterization of Lipo-Fullerenes

Bromo malonates **91** and **92** were prepared from the commercially available 1-dodecanol and 1-octadecanol, respectively (scheme 3.19). Both were obtained in good yields after two steps.

[60]Fullerene monoadducts **87** and **88** were easily obtained under classical Bingel reaction conditions in high yields (scheme 3.19). Both targets were purified by flash chromatography

using mixtures of hexane/toluene. The spectroscopic characterization of lipo-fullerenes **87** and **88** confirmed their structure.

(a)

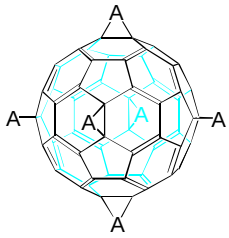

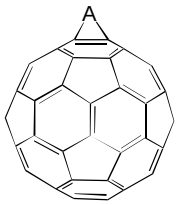

85 A = $C(CO_2C_{12}H_{25})_2$ **87** A = $C(CO_2C_{12}H_{25})_2$

86 A = $C(CO_2C_{18}H_{37})_2$ **88** A = $C(CO_2C_{18}H_{37})_2$

(b)

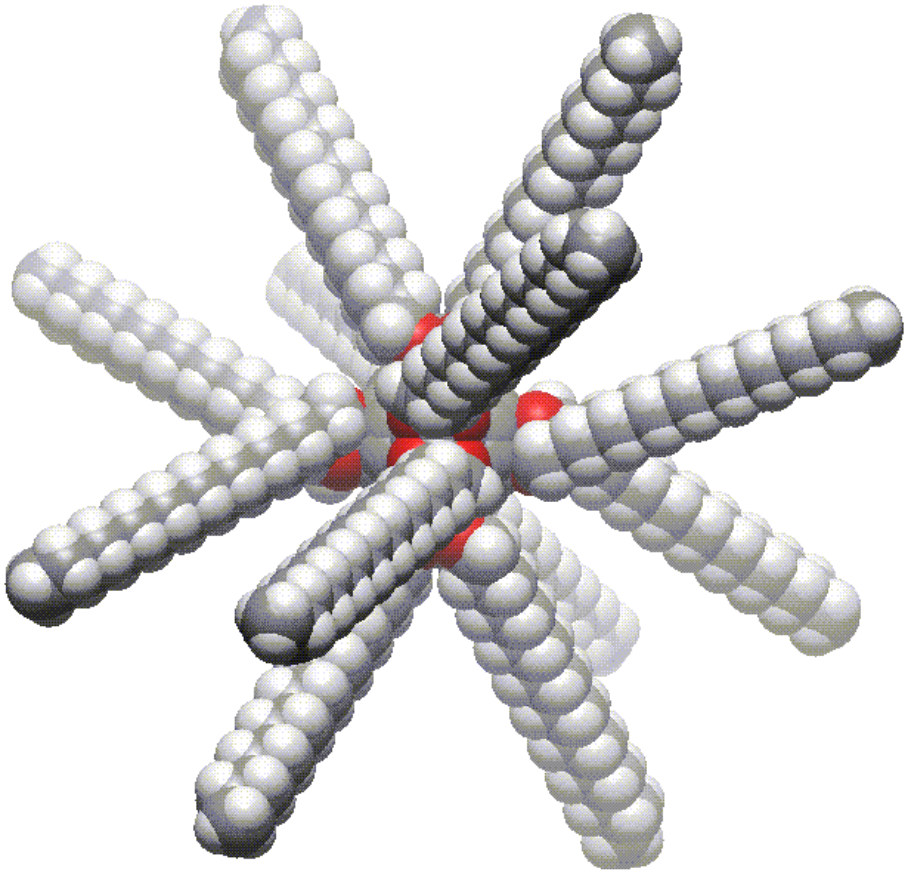

Figure 3.35. (a) Lipo-fullerenes **85-88**, (b) structure of the lipo-fullerene **86** optimized with the MM+ force field implemented in HYPERCHEM[64].

T_h-Symmetrical lipo-fullerenes **85** and **86** were synthesized via template activation of [60]fullerene with DMA and subsequent exhaustive cyclopropanation of the $[DMA]_n$-C_{60}

complex with the corresponding bromo malonate **90** and **91** under basic conditions (scheme 3.20).

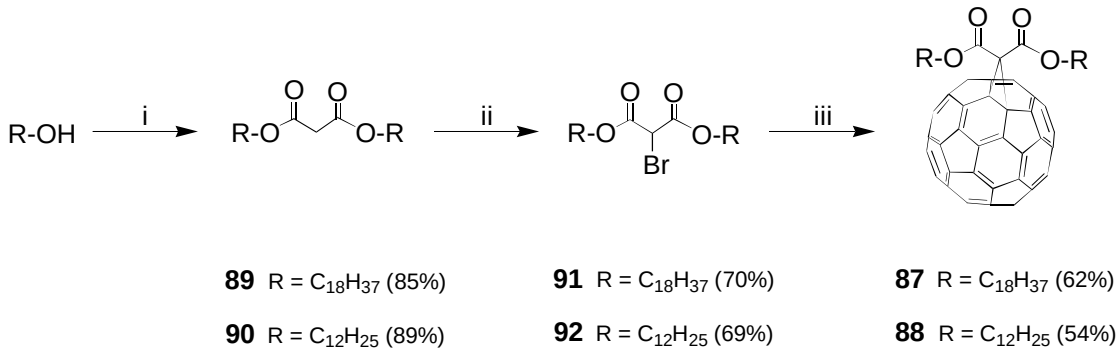

Scheme 3.19. Synthesis of lipo-fullerenes **87**-**88**. i) malonyl dichloride, pyridine/CH_2Cl_2; ii) DBU, Br_2/CH_2Cl_2; iii) C_{60}, NaH/toluene.

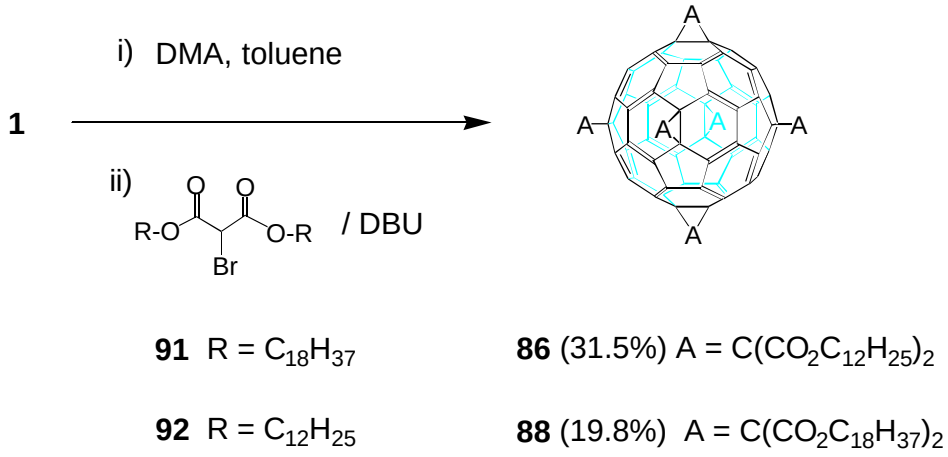

Scheme 3.20. Synthesis of T_h-symmetrical lipo-fullerenes C_{60}-HAC_{12} (**85**) and C_{60}-HAC_{18} (**86**).

Both lipo-fullerenes were purified by preparative HPLC on silica gel using mixtures of methylene chloride/hexane as eluent. Their T_h-symmetry is clearly proved by their NMR spectra (figure 3.36). For example, the ^{1}H-NMR spectrum of **86** displays a single set of peaks for all twelve aliphatic chains and its ^{13}C-NMR spectrum shows only two types of sp^2-carbons (141.17 and 145.83 ppm) and one type of sp^3-carbon (69.08 ppm) for the [60]fullerene cage, together with the expected signals corresponding to the malonate moieties.

As expected, the IR and UV/Vis spectra of both hexakisadducts **85** and **86** are almost identical. The low melting point of both compounds is noteworthy: 22 °C for C_{60}-HAC_{12} (**85**) and 65 °C for C_{60}-HAC_{18} (**86**).

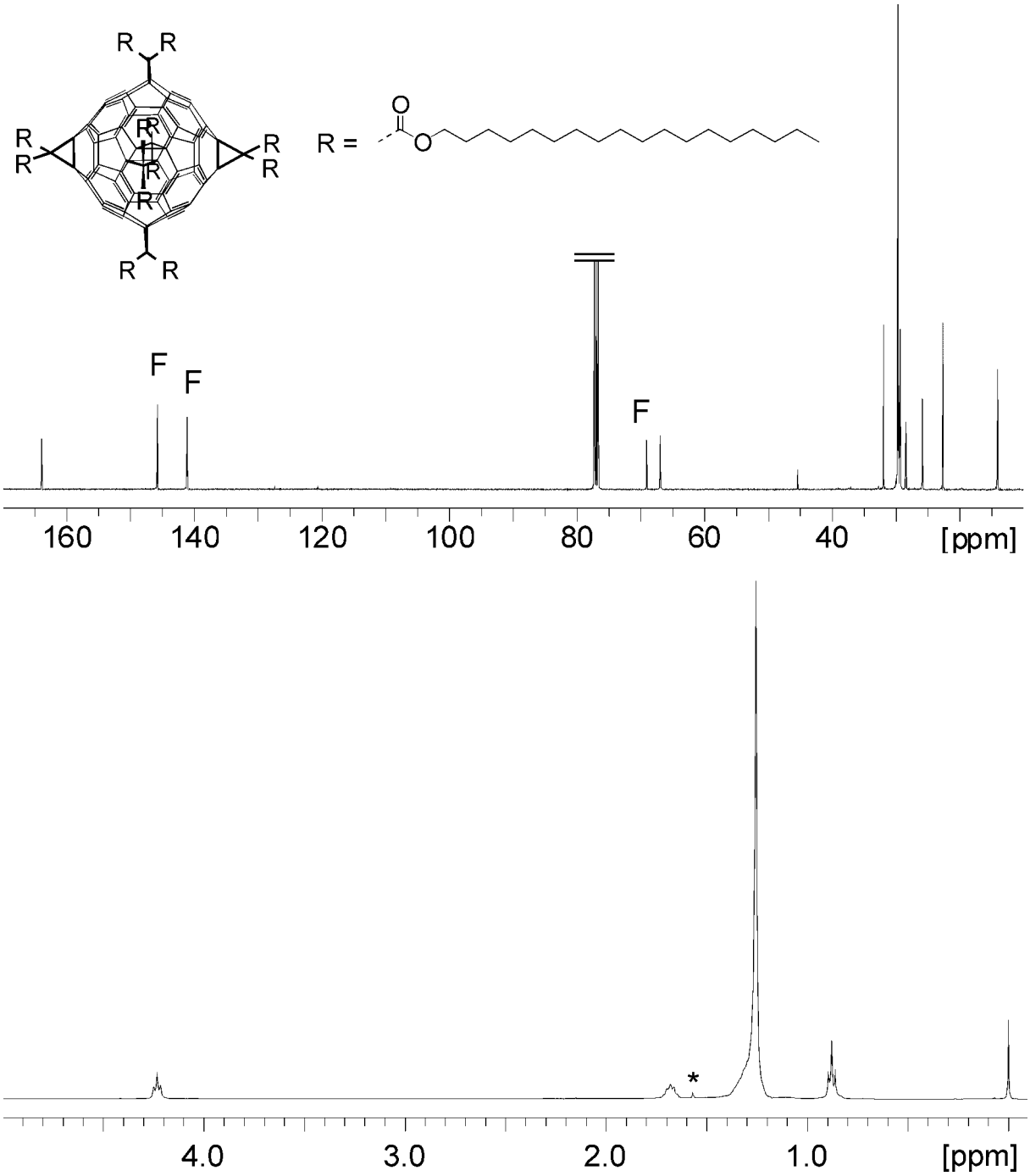

Figure 3.36. ^{1}H-NMR (400 MHz, RT, $CDCl_3$) and ^{13}C-NMR (100.5 MHz, RT, $CDCl_3$) spectra of lipo-fullerene **86** (* water). F denotes the signals for the fullerene carbon atoms.

In order to perform ^{2}H-NMR investigations (see chapter 6.3.4), the perdeuterated analogue to C_{60}-HAC_{18} (**86)** was required (scheme 3.21). For this propose, d_{35}-stearic acid was quantitatively reduced with lithium aluminum deuteride and further converted into the symmetrical malonate **94**. The target hexakisadduct C_{60}-HAC_{18}-d_{444} (**95)** was obtained after template activation of [60]fullerene and its subsequent cyclopropanation with malonate **94** according to the procedure introduced above.

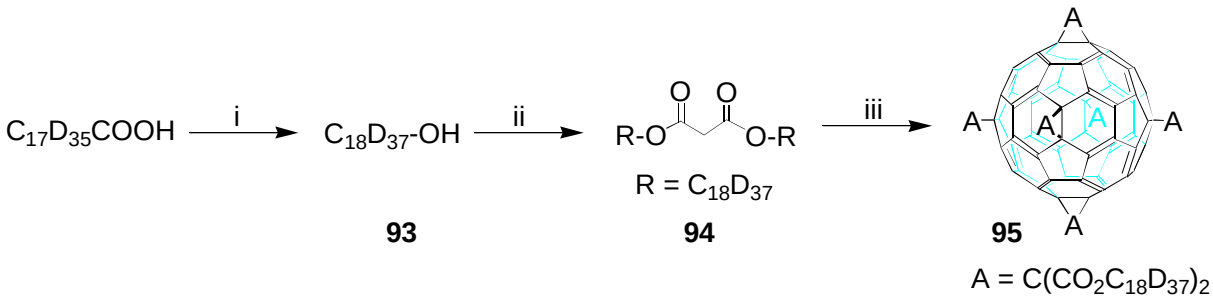

Scheme 3.21. i) $LiAlD_4$, THF (100 %); ii) malonyl dichloride, Pyr, CH_2Cl_2 (73.3 %); iii) (a) C_{60}, DMA, toluene; (b) **94**, CBr_4, DBU (22.3 %).

The ^{13}C-NMR spectrum of **95** (figure 3.37) showed five clearly resolved lines in agreement with the five different types of magnetically equivalent carbons not bounded to deuterium atoms. The signals corresponding to the carbons of the perdeuterated chain are not resolved as a consequence of the coupling of the ^{13}C and the ^{2}H nucleus.

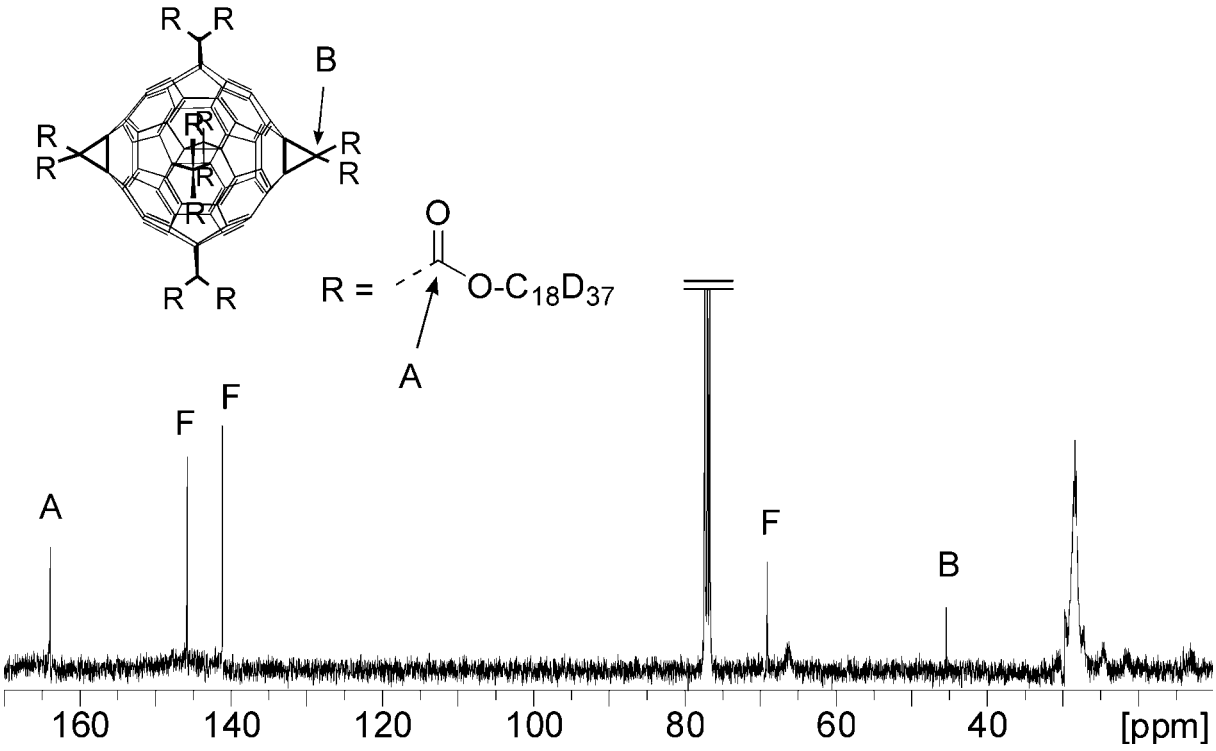

Figure 3.37. ^{13}C-NMR (100.5 MHz, RT, $CDCl_3$) of **95**. F denotes the fullerene carbon atoms.

No difference is found between the UV/Vis spectra of the d_{444}-lipo-fullerene **95** and that of its non-deuterated analogue **86**. In the IR spectra, new intense bands corresponding to the carbon-deuterium stretching vibration appear at 2200 cm^{-1} instead of 2900 cm^{-1}, which is the normal position for carbon-hydrogen stretching bands.

3.4.3 Fullerenes in Membranes: Structural and Dynamic Effects of Lipo-Fullerene Derivatives in Phospholipid Bilayers[97]

3.4.3.1 Preparation of MLVs Containing Lipo-Fullerenes

Multilamellar vesicles (MLVs) of dipalmitoyl-*sn*-glycero-3-phosphatidylcholine (DPPC) were chosen as membranoic model system due to their easy accessibility (figure 3.38). DPPC consists of an apolar, lipophilic molecule part (two palmitoic ester chains), as well as a polar, hydrophilic part (the phosphatidylcholine moiety). Multilamellar Vesicles of DPPC with onion-like multiple bilayer structures are formed by vigorous stirring or ultra-sonication of DPPC in water. It was planned to carry out the formation of MLVs of DPPC in the presence of the different lipo-fullerenes **85-88** in order to trap them in the lipophilic interior of the bilayers. All these experiments have been performed in collaboration with Prof. T. M. Bayerl and his group at the University of Würzburg.

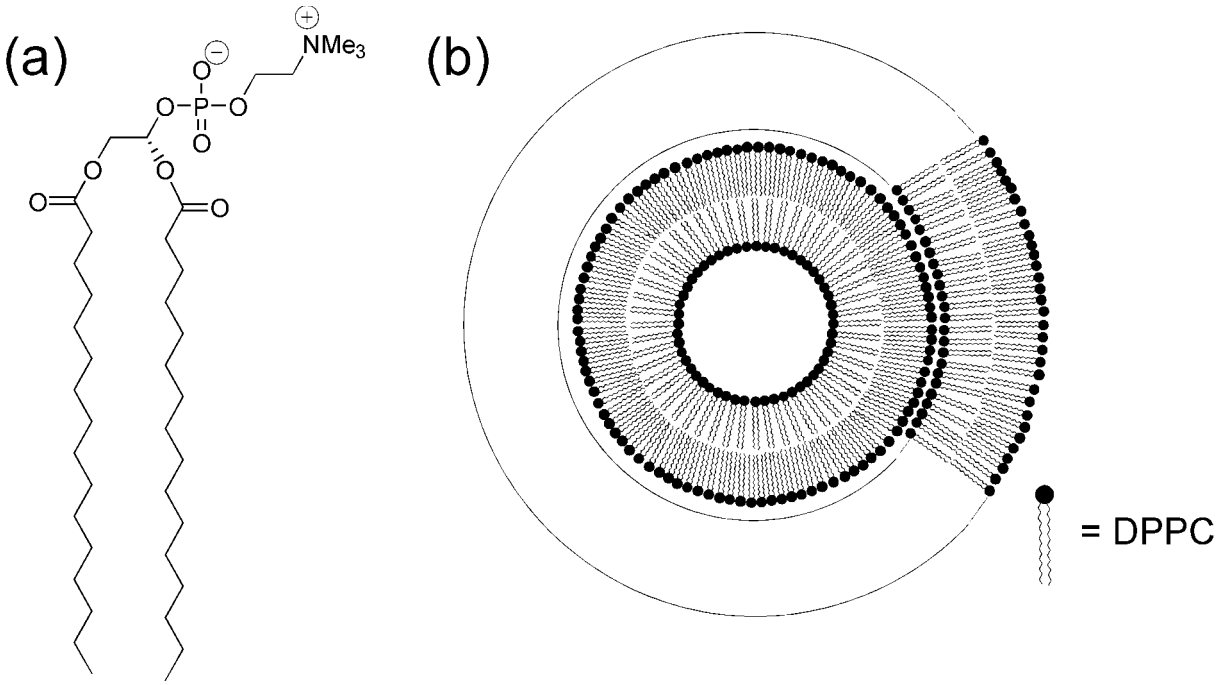

Figure 3.38. (a) dipalmitoyl-*sn*-glycero-3-phosphatidylcholine (DPPC); (b) schematic depiction of a multilamellar vesicle (MLV) of DPPC.

DPPC/lipo-fullerene MLV aggregates were prepared by mixing the two components in chloroform at room temperature, followed by lyophilization at liquid nitrogen temperature and a pressure of 15 hPa and overnight vacuum desiccation. The powder was then hydrated in water (5 mg of DPPC/lipo-fullerene mixture in 1 mL H_2O) at 50 °C and allowed to swell at this temperature for 1 h under gentle vortexing. The formation of MLVs containing either

C_{60}-HAC_{12} (**85**) or C_{60}-HAC_{18} (**86**) was successfully achieved. The resulting MLVs appeared yellow colored, as the parent lipo-fullerenes, and homogeneous by optical inspection. No precipitation of lipo-fullerenes was observed when up to 25 mol % of lipo-fullerene were employed, even after the samples were stored in the refrigerator for several weeks. Unfortunately, the formation of MLVs containing monoaddition lipo-fullerenes **87** or **88** was not accomplished under the same conditions. The samples appeared heterogeneous due to the presence of a brownish precipitate consisting of lipo-fullerenes.

3.4.3.2 DSC Studies of MLVs Containing Lipo-Fullerenes

Differential scanning calorimetry (DSC)[98] is a convenient method to study the thermodynamic properties of membrane model systems[99]. In that way it is possible to measure directly or indirectly parameters corresponding to the transition behavior of the sample (phase transition temperature, transition enthalpy, heat capacity, etc.), its purity, or the interaction between several components. Briefly, the calorimeter takes advantage of the *heat-leak principle*. DSC is based on the measurement of the difference in power requirements for a sample in comparison with a reference, both heating (or cooling) at the same constant rate.

Multilamellar vesicles (MLVs) of DPPC containing C_{60}-HAC_{12} (**85**) and C_{60}-HAC_{18} (**86**), respectively, were studied at different mixing ratios by DSC[100]. These results were compared with those obtained for pure samples of C_{60}-HAC_{12} (**85**) and C_{60}-HAC_{18} (**86**) (figure 3.39).

The DSC curve obtained for pure C_{60}-HAC_{18} (**86**) (figure 3.39.b) shows a peculiar profile. Heating the sample up from 20 °C to 70 °C causes the sample to undergo two major structural transitions. At 55 °C an exothermic transition, and at 64 °C an endothermic melting transition are observed. This phenomenon has been extensively studied by ^{2}H-NMR and X-ray scattering[101]. At 55 °C an exothermic transition from a low-temperature, hard sphere fashion packing state of the molecules with their separation distances (61 Å) slightly above the maximum diameter of the molecules, to a condensed one involving partial interdigitation of the alkyl chains belonging to adjacent molecules, is observed. This is preceded by a local melting of the chains, in order to tilt chains to bunches as a prerequisite for interdigitation. The interdigitation allows a denser packing with an average separation distance of 48 Å. The driving force for this process is the optimization of strong van der Waals interactions between the chains, which is hampered by the stiffness of the chains leading to a hard sphere packing at temperatures below 50 °C. At a temperature of 64 °C an endothermic melting transition from the interdigitated to a viscous fluid state with average separation distances of 28 Å is observed.

Cooling the sample from 70 °C causes a direct transition from the fluid into the low temperature state with no interdigitation in between.

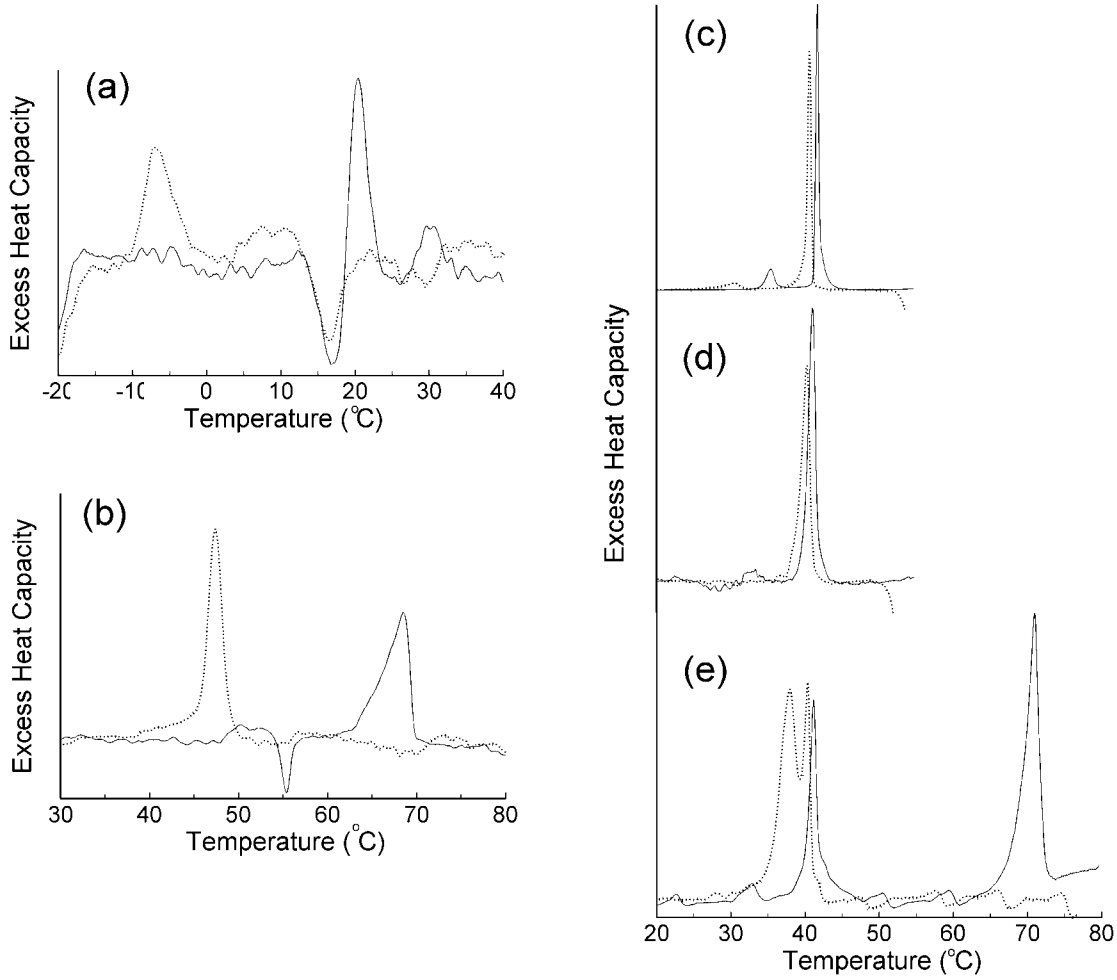

Figure 3.39. Endotherms (heating scans) and exotherms (cooling scans) corresponding to (a) pure **85**, (b) pure **86**, (c) MLVs of pure DPPC, (d) MLVs of DPPC containing 15 mol % of lipo-fullerene **85**, and (e) MLVs of DPPC containing 15 mol % of lipo-fullerene **86**. Solid curves correspond to the heating and the dashed ones to the cooling scans.

Comparing the results obtained from DSC measurements it was concluded that the effect of both lipo-fullerenes **85** and **86** on the phase transition behavior of the MLVs is surprisingly low. A broadening of the main phase transition corresponding to the melting of DPPC (T_m = 41°C) by a factor of 2-3 and a slight reduction of the phase transition temperature by 0.5°C were observed in MLVs containing lipo-fullerenes in comparison with homogeneous DPPC MLVs. Even the pre-transition of DPPC which can be observed for heating scans at T_p = 30.5°C was not completely eliminated by the presence of the lipo-fullerenes. In the case of

MLVs of DPPC containing 15 mol % of lipo-fullerene C_{60}-HAC_{18} (**86**) (figure 3.39.e) a second big peak was observed at 71°C (heating scan) and at 38°C (cooling scan). Since plain **86** exhibits a transition at nearly the same temperature and with similar hysteresis (figure 3.39.b), this peak was assigned to the chain melting transition of the lipo-fullerene **86**. In contrast, plain C_{60}-HAC_{12} (**85**) (figure 3.39.a) has a phase transition at 21 °C (heating scan) and -7 °C (cooling scan). Therefore, no lipo-fullerene transition was observed since the sample corresponding to MLVs of DPPC containing 15 mol % of lipo-fullerene **85** was not cooled below 0 °C and hence its chains were always fluid during the measurements.

Increasing the lipo-fullerene content of the sample up to 25 mol % did not change the DSC results significantly. The only remarkable changes were a gradual attenuation of the DPPC main transition (by a factor of 3 - 4 at 25 mol % compared to pure DPPC transitions).

From these results it is possible to conclude that the phase transitions of DPPC and of **85** or **86** are completely decoupled, indicating pronounced microscopic demixing. This is, the interaction between lipo-fullerenes and DPPC in the MLVs seems to be at least very small. The unusually large hysteresis of the C_{60}-HAC_{18} (**86**) transition is most likely a result of the rapid rotation of the [60]fullerene core in a microenvironment made up mainly of fluid octadecyl chains.

3.4.3.3 Electron Microscopy Studies of MLVs Containing Lipo-Fullerenes

Freeze fracture electron microscopy was employed to study the morphological changes in the MLVs caused by the lipo-fullerenes. Figure 3.40 shows freeze fracture replicas of DPPC-d_{62} MLVs without (figure 3.40.a) and with (figure 3.40.b) 15 mol % of lipo-fullerene C_{60}-HAC_{12} (**85**) under fluid phase conditions of the bilayer (samples quenched at 60°C). In both cases predominantly large MLVs with diameters up to 5 μm with the typical onion like structure were observed. However, while the plain MLVs showed smooth fracture faces in the bilayer plane, the inclusion of C_{60}-HAC_{12} (**85**) caused the formation of a rod-like surface structure that may look, at first glance, similar to the so called *ripple phase* of DPPC. Ripple phase was observed in plain DPPC MLVs at temperatures between 34 and 41 °C, i.e. below the main phase transition, and is shown in figure 3.40.c. However, it is clear for the following reasons that figure 3.40.b does not represent a ripple phase:

1) The bilayer exhibits a fluid state at 60 °C, and a ripple phase has never been observed under such conditions. Quenching the sample at even higher temperatures (70 °C) gave a similar result, thus ruling out the possibility that temperature artifacts during the freezing procedure were responsible for this behavior.

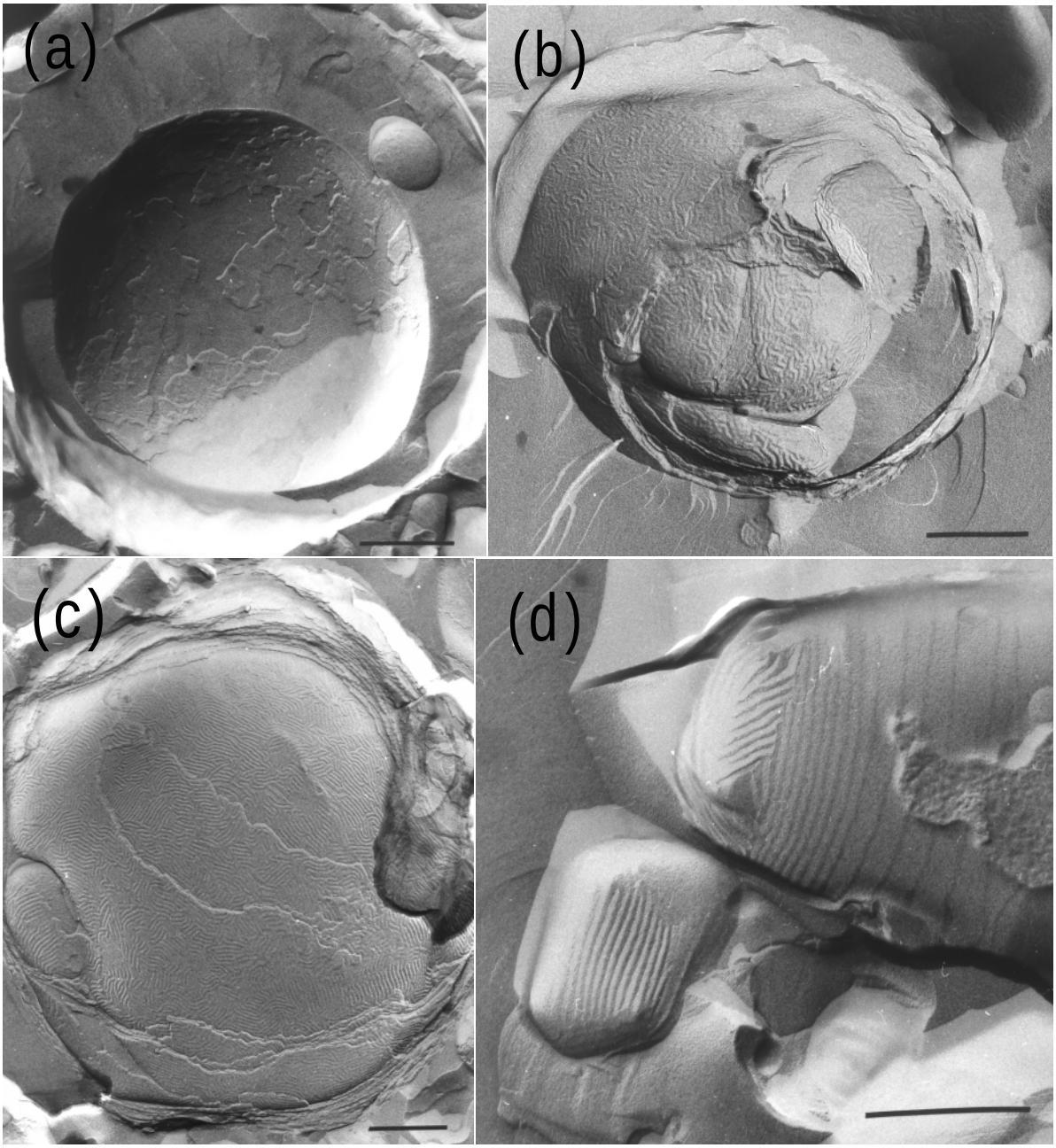

Figure 3.40. Freeze fracture micrographs of multilamellar vesicles of DPPC-d_{62} without (a) and (c), and with 15 mol % of the lipo-fullerene C_{60}-HAC_{12} (b) and (d). Samples (a) and (b) were quenched at 60 °C, (c) at 40 °C, and (d) at 25 °C respectively. The bars represent a size of 0.5 μm.

2) The diameter of the individual rods was 10-30 nm and thus does not agree with the known dimensions of ripples[102]. The diameter increased with increasing the lipo-fullerene concentration in the bilayer.

3) The structures in figure 3.40.b were not coherently in phase over the bilayers, as is typical for ripples in MLVs.

No significant differences to the above mentioned results were observed when lipo-fullerene C_{60}-HAC_{12} (**85**) was replaced by lipo-fullerene C_{60}-HAC_{18} (**86**); this holds also true when the quenching of the sample was carried out at 60 °C under conditions where the octadecyl chains were in all-*trans* conformation. A further interesting feature is the (reversible) long range ordering of the above mentioned rod-like structures under gel phase conditions of the bilayer (quenching the samples at 25 °C). Here, for both lipo-fullerenes a stratification of the rods over distances of several μm and the formation of superstructures that looked like bundles of individual rods are observed (figure 3.40.d). Again, the apparent rod diameter (up to 30 nm) increased with increasing the lipo-fullerene concentration.

3.4.3.4 ^{2}H-NMR Studies of MLVs Containing Lipo-Fullerenes

The dynamic of a lipid bilayer consists of several types of movements of the individual molecules composing the system. Intercalation of lipo-fullerenes between the two monolayers of a lipid bilayer may affect the hierarchy of motions in bilayer, which covers nearly twelve orders of magnitude in time from hertz to terahertz[103,104]. These motions include: internal chain movements (frequency range 10^{-9} to 10^{-14} s), flip-flop movements of the polar heads (10^{-9} to 10^{-12} s), lipid rotations (10^{-9} s), lateral diffusions (10^{-6} to 10^{-1} s), and collective undulations and related movements (10^{-6} to 10^{1} s). ^{2}H-NMR is a powerful tool to study changes to the molecular order in the bilayer resulting from the intercalation of lipo fullerenes[103,104]. Several studies were performed combining the use of C_{60}-HAC_{18}-d_{444} (**95**), C_{60}-HAC_{12} (**85**), C_{60}-HAC_{18} (**86**), DPPC, and DPPC with selectively (DPPC-d_8) and completely deuterated chains (DPPC-d_{62}). From these studies it was possible to conclude that:

1) The presence of the lipo-fullerene does not cause significant changes in the distribution of the methylene groups of the lipid chains from the DPPC, but the methyl group reveals some significant effect. The interactions between lipo-fullerene and DPPC in the MLVs seem to take place mainly in the extremities, i.e., the lipo-fullerenes are in contact between them and the methyl group of DPPC, while the rest of the DPPC molecules remains unaffected.

2) Plain DPPC MLVs exhibit a macroscopic magnetic field orientation due to the diamagnetic susceptibility anisotropy of the lipid[105,106], which results in an elliptical MLV shape, with its long axis parallel to the magnetic field. MLVs containing lipo-fullerenes do not experience this effect. The typical MLVs spherical shape remains unaltered in front of an external magnetic field. The lipo-fullerenes seem to stiffen the fluid bilayer without altering its molecular order.

3) The effect of lipo-fullerenes on bilayer dynamics was studied by measuring the ^{2}H-NMR longitudinal (T_{1z}) and transverse (T_{2e}) relaxation of the deuterated DPPC MLVs, with and without the lipo-fullerene in the fluid phase bilayer. The high frequency dynamics of the DPPC are not affected by the motion of the lipo-fullerenes, but some motions of the DPPC, which are slow on the NMR time scale (10^{-5} s), change significantly according to the reduction of the values of T_{2e}[107-109]. The most likely reason for the T_{2e} reduction, also in agreement with the microscopic results, is the formation of a wavy surface structure with a higher local curvature of the lipo-fullerene MLVs compared to the control experiment. It can be assumed that the lateral diffusion of the DPPC over this surface, and the resulting modulation of the molecular director axis, contribute to the 'slow motion' transverse relaxation mechanisms discussed previously.

3.4.3.5 Proposing a Model for MLVs Containing Lipo-Fullerenes

An arrangement of the lipo-fullerenes in the bilayer as depicted in figure 3.41 is suggested. In this model, which is capable of explaining all the experimental observations, the lipo-fullerenes form rod-like structures on their own, with the rods sandwiched between the two layers of the bilayer. The rods appear rather disordered in the fluid bilayer (figure 3.41.A), but become stratified and long range ordered (rod axis parallel to adjacent rods in the same plane) in the gel phase bilayer (figure 3.41.B). This is probably induced by the high order of the lipids in the host bilayer under gel phase conditions. The lipo-fullerene rods would stabilize the bilayer against deformation in a magnetic field in a similar fashion to the way a membrane cytoskeleton does, with the important difference that the former seems to be located between the two layer leaflets, while the cytoskeleton is attached at the outside of the membrane.

The data do not permit to distinguish directly between a hollow rod and a massive rod filled by lipo-fullerene molecules. However, the obviously high lipo-fullerene capacity of the bilayers, together with the observation of increasing rod diameter with increasing the lipo-fullerene concentration, strongly suggests massive rods. This would allow the bilayer to take up tremendous amounts of lipo-fullerene without enhancing significantly the DPPC-rod contact area. Considering that rods have a diameter of about 30 nm and a length of 1.5 μm according to the microscopy results, and that the volume of a molecule of lipo-fullerene C_{60}-HAC_{18} (**86**) is about 5 nm^3, it is possible to conclude that when the concentration of lipo-fullerene in the MLVs is 15 %, a maximum of 10-15 % of the bilayer is in close contact with the rods, while the remaining bilayer area is left undisturbed.

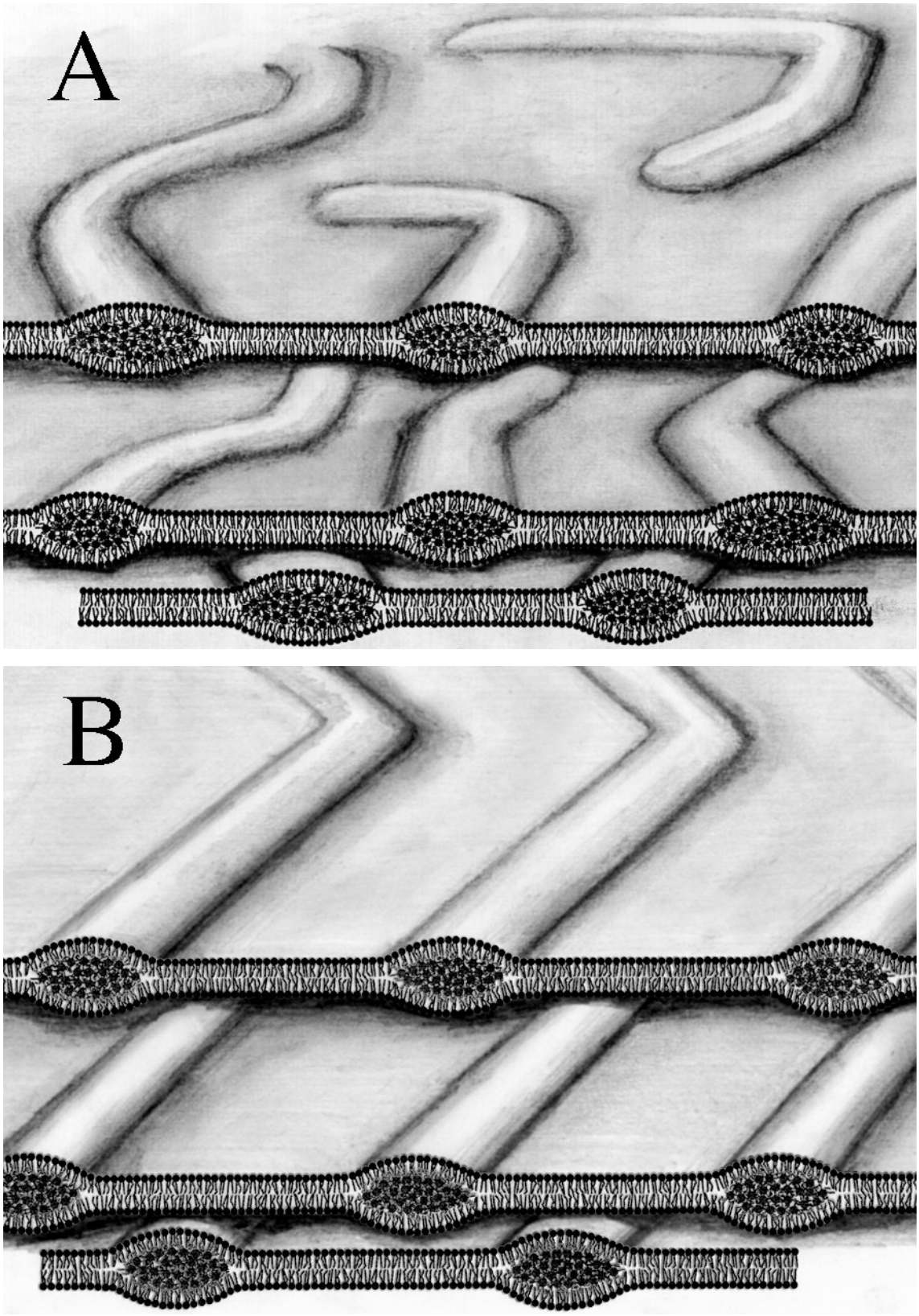

Figure 3.41. Schematic depiction of the suggested arrangement of lipo-fullerenes: (A) in a fluid bilayer, and (B) in a gel phase bilayer.

3.5 Polymers Based on Lipo-Fullerene Containing Butadiyne Units

3.5.1 Introduction

In phospholipid chemistry, big efforts have been made on the potential use of microstructures derived from this type of lipids to be applied in encapsulation, controlled drug release, biosensors, enzyme immobilization, etc. However, the main problem with the applicability of these systems is the lack of stability of lipid-based microstructures. Three different strategies could overcome these drawbacks: i) the incorporation of sugars, cholesterol and proteins mimicking the structure of natural membranes, ii) the use of long-chain phospholipids, which form highly robust structures, and iii) the modification of the phospholipid to enable them to form stabilized microstructures via polymerization[110]. In this context, phospholipids containing diacetylene units have been widely used.

Diacetylenes polymerize in a topochemically controlled way, being the efficiency of the process dependent on the correct alignment of the monomers according to a sequence of 1,4-additions investigated by Wegner[111] (figure 3.42). With these studies it was elegantly demonstrated that the distance and the angle between the chains is a critical factor for bringing about the polymerization process. According to EPR experiments, the formation of carbene-like structures as active species in the reaction mixture has been suggested[112,113].

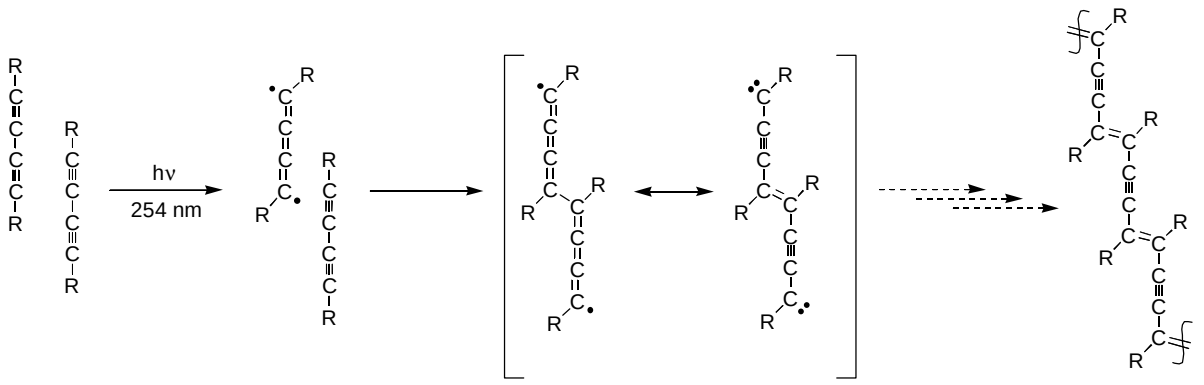

Figure 3.42. Polymerization of diacetylenes.

As has been reported in the last chapter, lipo-fullerenes C_{60}-HAC_{12} (**85**) and C_{60}-HAC_{18} (**86**) self-assemble into rod-like structures of up to 30 nm diameter and of several µm length upon intercalation into synthetic lecithin bilayers of DPPC. As a result, a composite of colloidal

dimensions is formed with interesting micromechanical properties. For a fluid-like bilayer, the rods show a lateral mobility and flexibility within the fluid bilayer plane, leading to collisions between adjacent rods. These rod-like structures consist of aggregations of the lipo-fullerenes. The introduction of diacetylene moieties in the lipo-fullerene chains would result in the formation of a three-dimensional arrangement of polymerizable units. The polymerization of the lipo-fullerene derivative during the collision processes could be initiated by irradiation with UV light. The MLVs should facilitate the collision between lipo-fullerenes especially at temperatures above the transition state of the DPPC MLVs, when the diffusion of lipo-fullerenes is faster.

3.5.2 Synthesis and Characterization of Lipo-Fullerenes Containing Butadiyne Units

The commercially available 10,12-octadecadiynoic acid was chosen as a starting compound for the synthesis of lipo-fullerenes containing butadiyne moieties. Quantitative reduction with lithium aluminum hydride followed by reaction with malonyl chloride afforded malonate **97**, a suitable precursor able to undergo reaction with [60]fullerene (scheme 3.22).

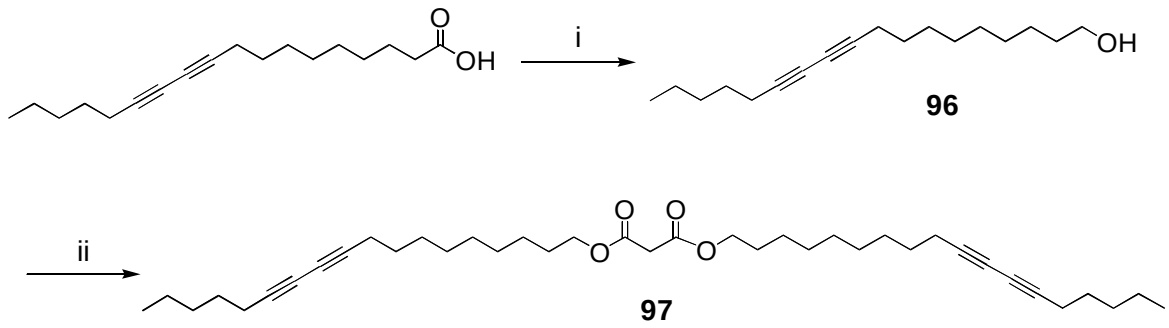

Scheme 3.22. Synthesis of di(10,12-octadecadiynyl)malonate **97**. i) $LiAlH_4/Et_2O$ (100 %); ii) malonyl dichloride, Pyr/CH_2Cl_2 (62.7 %).

The synthesis of the corresponding [60]fullerene monoadduct **98** and hexakisadduct **99** (figure 3.43) was performed starting from malonate **97** according to the procedures described above in yields of 38 % and 26 %, respectively. Both compounds were fully characterized by spectroscopic methods. The acetylenic moieties were clearly detected by NMR and IR spectrometry. For example, the ^{13}C-NMR spectrum of **99** allows to distinguish the four different types of acetylenic carbons (at 65.23, 65.26, 77.43, and 77.48 ppm) together with the

three types of fullerene carbons (two sp^2- and one sp^3-type) according to the T_h-symmetrical hexaaddition pattern (figure 3.44).

(a)

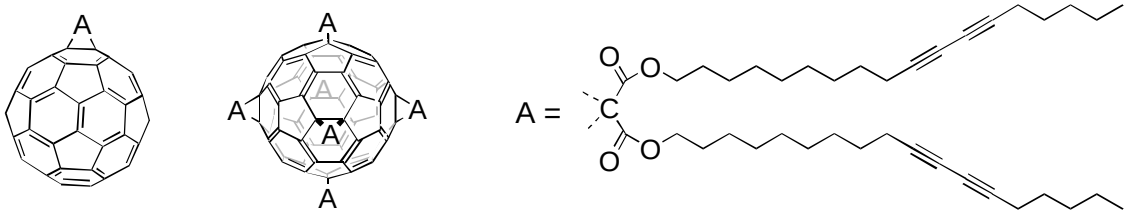

98 **99**

(b)

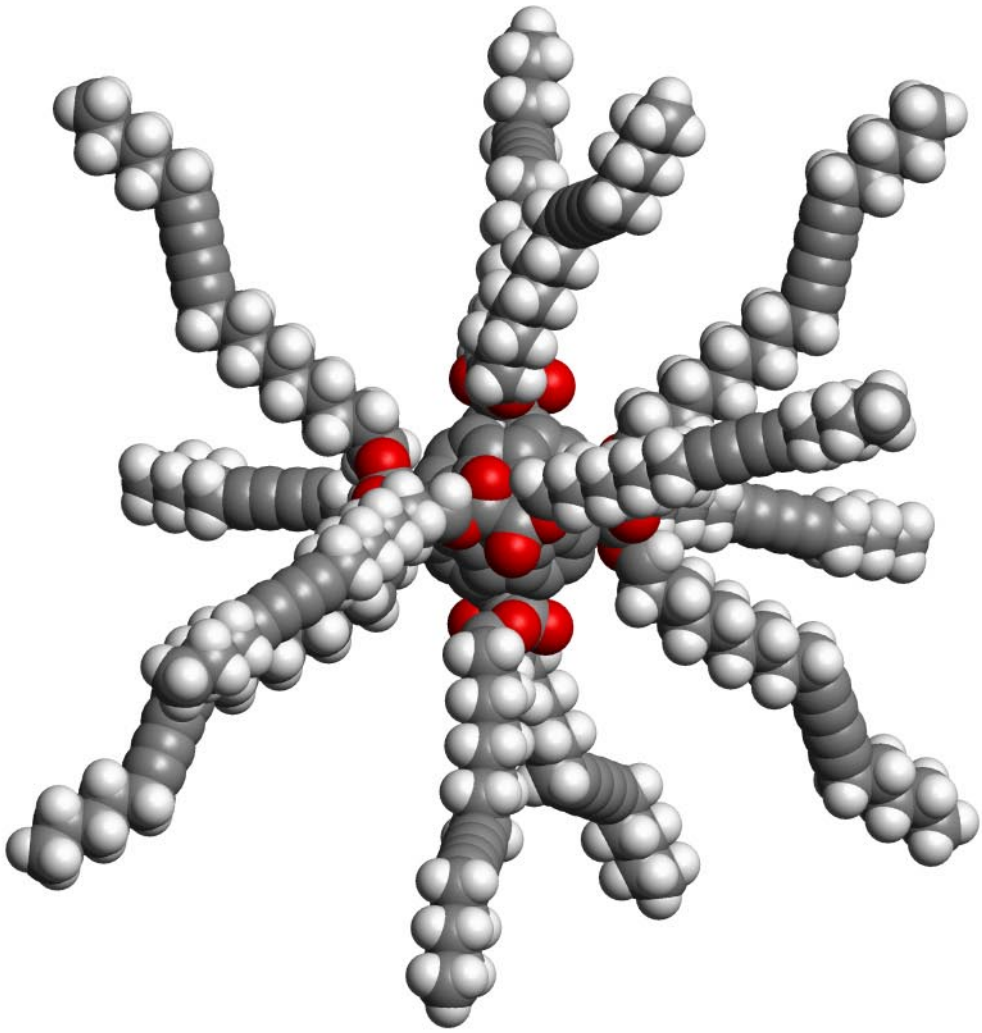

Figure 3.43. (a) Lipo-fullerenes **98** and **99** containing butadiyne moieties, (b) structure of lipo-fullerene **99** obtained with the MM^+ force field implemented in HYPERCHEM[64].

The IR spectrum of **99** shows week bands at 2256 and 2155 cm^{-1}, which are the characteristic bands for triple bond carbon-carbon stretching vibrations (figure 3.46.a). Also, the band corresponding to the fullerene core (530 cm^{-1}) appears in the spectrum.

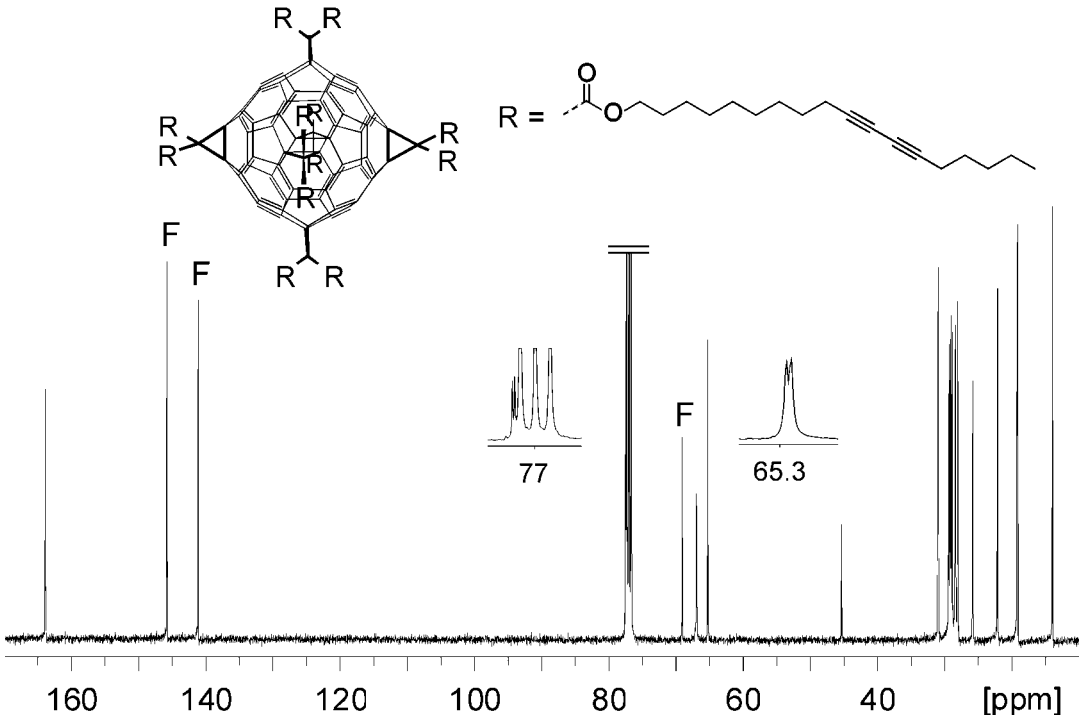

Figure 3.44. ^{13}C-NMR (100.5 MHz, RT, $CDCl_3$) spectrum of **99**. F denotes de fullerene carbon atoms.

3.5.3 Neat Polymerization of Lipo-Fullerenes Containing Butadiyne Units

The neat polymerization of **98** and **99** was studied. A film of [60]fullerene monoadduct **98** was deposited on a glass by evaporating the solvent of a concentrated solution in methylene chloride. After irradiation of the sample for 2 days with a standard 300 watt lamp, TLC experiments showed that no starting material was left. The polymerization afforded a crude mixture that surprisingly was partially soluble in chloroform. This mixture was studied by NMR, TLC, UV, and MS experiments, but no definite structure could be determined. The [60]fullerene properties as a radical-scavenger are well known[34]. The monoadduct **98** still has an almost intact [60]fullerene skeleton, and is thus able to trap radical species. Irradiation of **98** certainly yields radical species. These can react either with the fullerene cage or with butadiyne moieties giving a polymeric mixture with no homogeneous structure.

This complexity is not expected when considering the polymerization of hexaadduct **99**. In this case, the [60]fullerene core has been reduced to eight isolated benzenoid rings without any special radical scavenger properties. The polymerization of **99** was carried out as described for **98**. After two days of irradiating a neat film of **99** quantitative conversion was obtained. The

polymeric material **100** was insoluble in any common solvent and appeared as homogeneous red-brownish shining scales. According to the postulated polymerization mechanism the structure of **100** was proposed as depicted in figure 3.45.

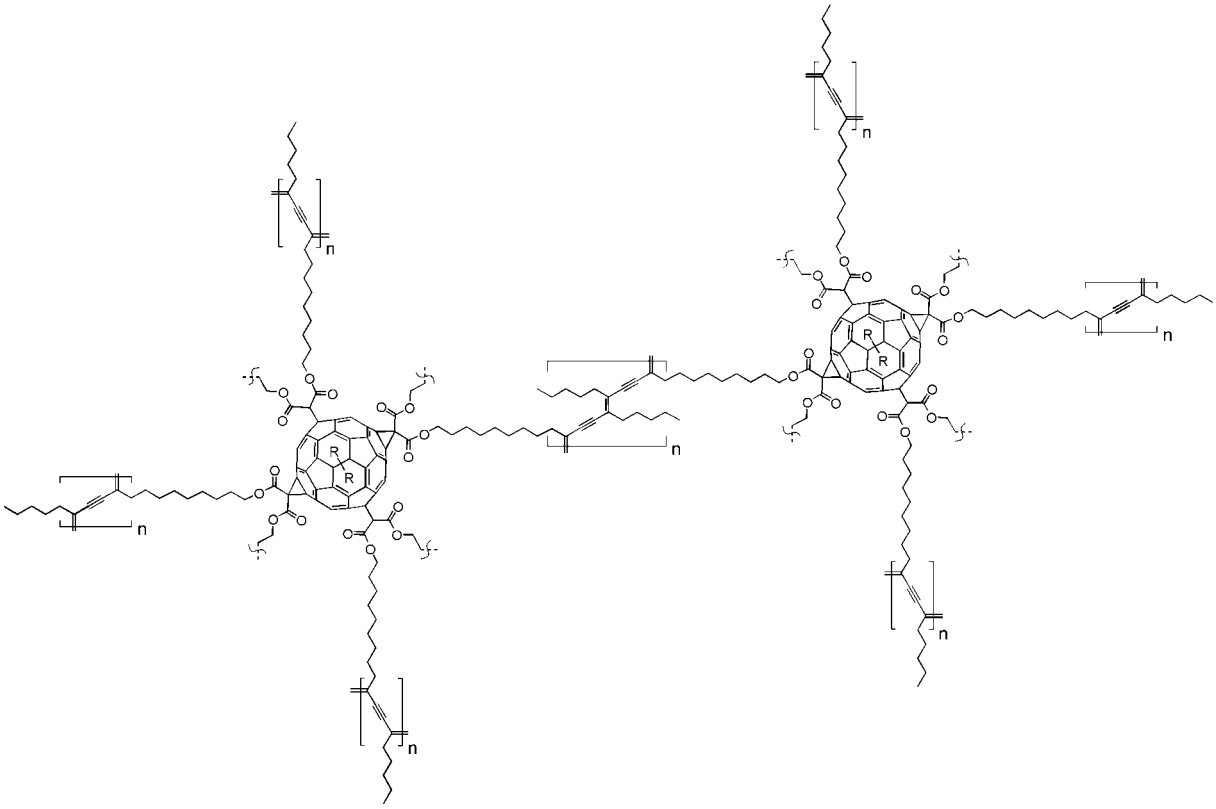

Figure 3.45. Proposed structure of polymer **100**.

Polymer **100** consists of a net of polydiacetylene chains with pendant pentyl rests and alkyl rests capped with substituted fullerenes. No tacticity is expected, since the butadiyne moiety is not polarized. The fullerenes provide the inter-cross-linking for the resulting polymer. It is not clear how the reaction is finished. The usual pathways for the quenching of active radical species could take place, including disproportion and radical recombination. Molecular modelling suggests that due to sterical reasons it is difficult to achieve long polydiacetylene chains and that, certanly, not all the butadiyne moieties can take part in the polymerization process. Chains containing 5 or 6 butadiyne units seem to be the most likely.

The IR spectrum of polymer **100** is shown in figure 3.46.b. The comparison of this spectrum with that corresponding to the monomer unit **99** (figure 3.46.a) afforded interesting structural information. The spectrum of polymer **100** shows a broad band centered at 2330 cm^{-1} corresponding to the acetylenic units. The band corresponding to the carboxylate groups presents a clear shoulder going down to 1600 cm^{-1} that may be due to the presence of conjugated double bonds formed during the polymerization process. The band characteristic

for the fullerene core is still present at about 530 cm^{-1}. The rest of the spectrum shows the same patterns as that of **99** although all the bands appear broadened. The huge band at 3440 cm^{-1} must be due to the presence of moisture in the sample.

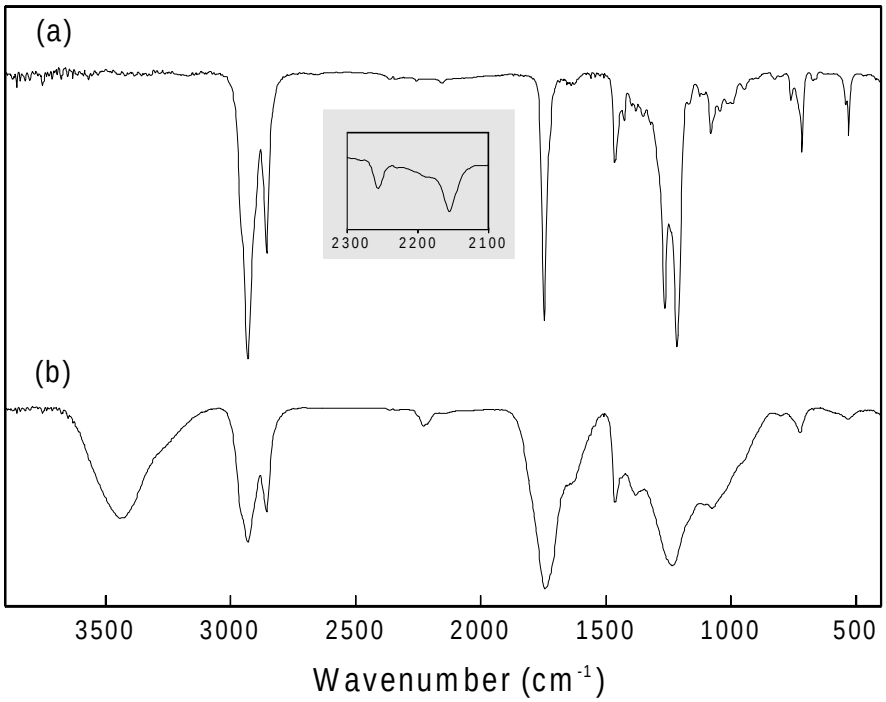

Figure 3.46. IR (KBr) spectra of: (a) monomer **99**; and (b) polymer **100**.

A solid state ^{13}C-NMR of the polymer **100** was performed by Prof. Albert in the University of Tübingen (figure 3.47). The spectrum displays broad bands due to the polymeric nature of the compound and the own characteristics of the technique. Of special relevance is the broad band ranging from 90 to 140 ppm, where no resonance appears in the ^{13}C-NMR spectrum of the monomer unit **99**. The presence of double bonds in the polymer structure is certainly responsible for these signals.

While the monomer melts at about 42 °C, the polymer does not melt below 280 °C. Further X-ray investigations are currently under way in order to prove the proposed structure and the extension of the polymerization reaction.

3.5.4 Long Polydiacetylene Chains Containing Pendant Fullerene Moieties

Polymer **100** is, according to its spectral and physical behavior an inter-crossed linked structure containing a multitude of short segments of polydiacetylene chains. Polydiacetylenes, with their conjugated carbon backbone, exhibit interesting nonlinear optical properties[114]. In this

context, it would be interesting to synthesize longer polydiacetylenes

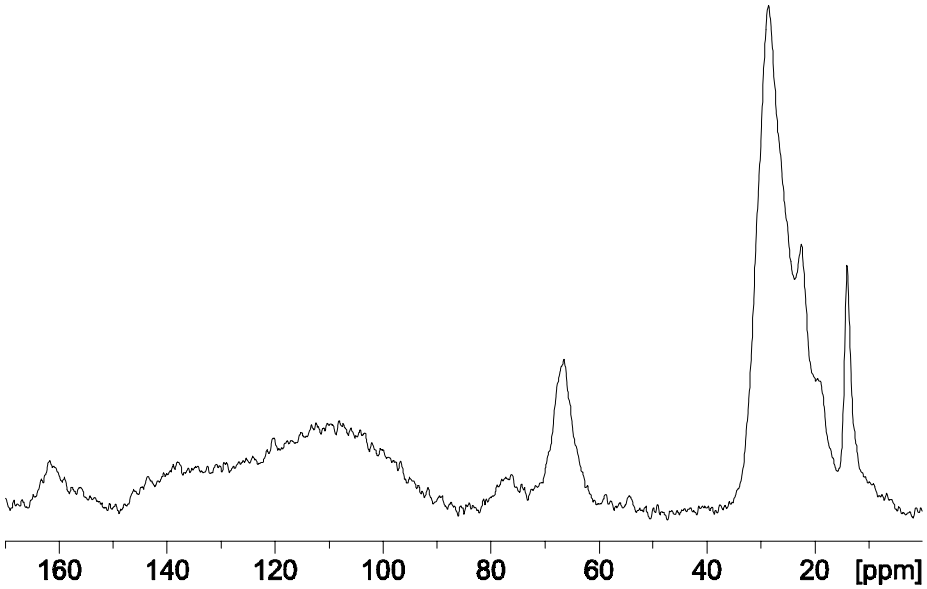

Figure 3.47. Solid state ^{13}C-NMR spectrum of the polymer **100**.

with pendant fullerenes. For this purpose the synthesis of a [60]fullerene derivative containing a single diacetylene moiety is required. According to the previous results, polymerization of a [60]fullerene monoaddition product with a unique butadiyne unit seems not reasonable, since the almost unaltered [60]fullerene skeleton would take part in the polymerization thus avoiding the possibility of achieving a long polydiacetylene chain.

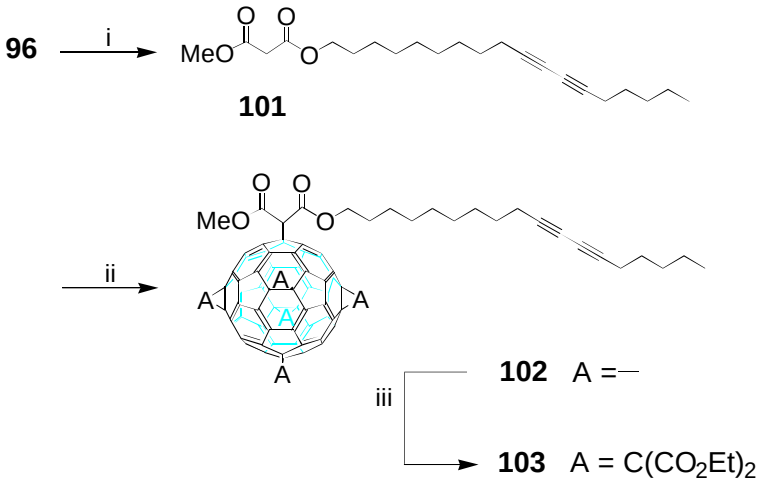

Scheme 3.23. Synthesis of hexakisadduct **103**. i) Malonyl chloride monomethyl ester, Pyr/CH_2Cl_2 (88.6 %); ii) CBr_4, DBU/toluene (55.0 %); iii) (a) DMA/toluene; (b) bromo diethylmalonate, DBU (35.2 %).

The monomer required should contain a single reactive butadiyne moiety and should own an inert [60]fullerene core towards radical attack like **99**. The synthesis of the C_s-symmetrical [60]fullerene hexakisadduct **103** was carried out according to the procedure described in scheme 3.23. [60]Fullerene hexakisadduct **103** was purified by flash chromatography followed by preparative HPLC, and it was completely characterized. Although the [60]fullerene hexakisadduct **103** is C_s-symmetrical, its ^{13}C-NMR spectrum shows the typical profile for a pseudo-T_h-symmetrical compound displaying only three bands with a hyperfine structure for the [60]fullerene core (figure 3.48). Two of the acetylenic bands are under the $CDCl_3$ peak, whereas the other two appear at about 65 ppm.

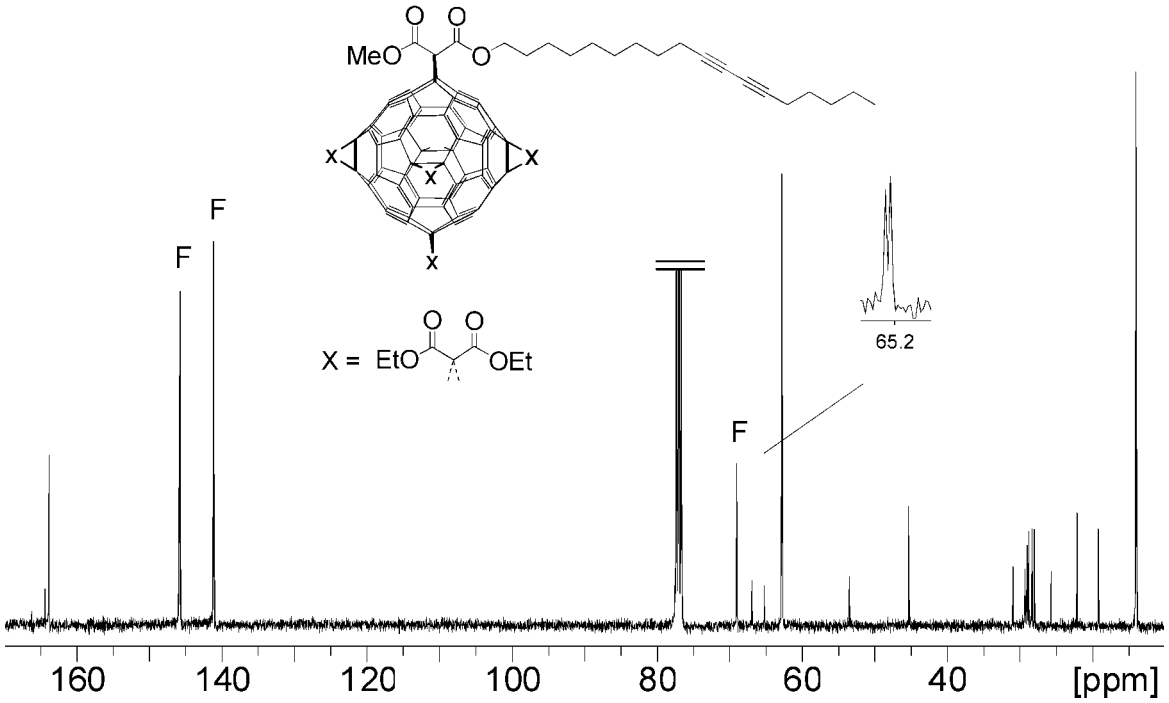

Figure 3.48. ^{13}C-NMR (100.5 MHz, RT, $CDCl_3$) spectrum of **103**. F denotes the signals for the fullerene atoms.

Polymerization of **103** was carried out by irradiating a neat film of monomer with a standard 500 watt lamp. After 5 days, an orange insoluble polymer (**104**) was obtained together with circa 5% of the unpolymerized monomer (**103**). The expected structure for polymer **104** should consist of a polydiacetylene chain with pendant aliphatic chains, half of them capped with a polyfunctionalized [60]fullerene (figure 3.49). Also in this case, polymerization is expected to be atactic since the monomer butadiyne is again not polarized.

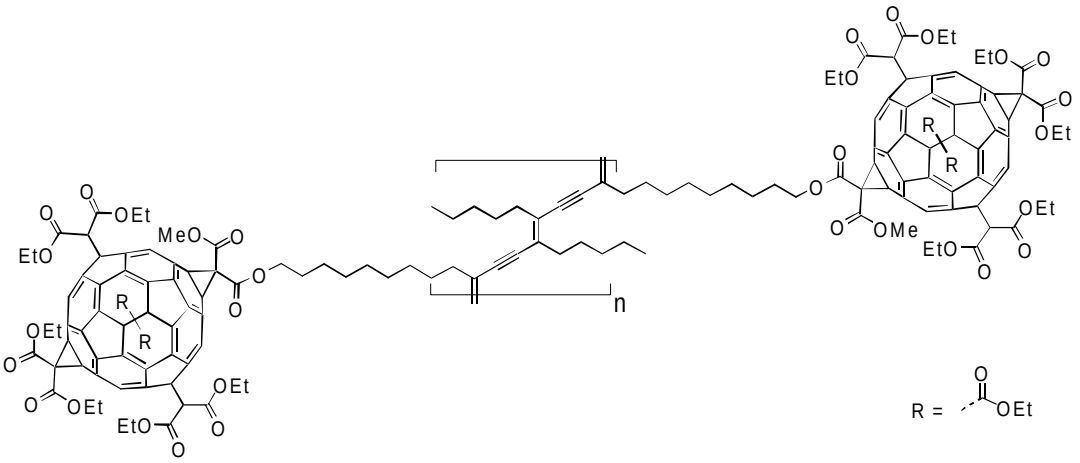

Figure 3.49. Polydiacetylene **104**.

The IR spectra of polymer **104** and its monomer unit **103** (figure 3.50) show similar profiles although the spectrum of **104** presents broader bands according to its polymeric nature.

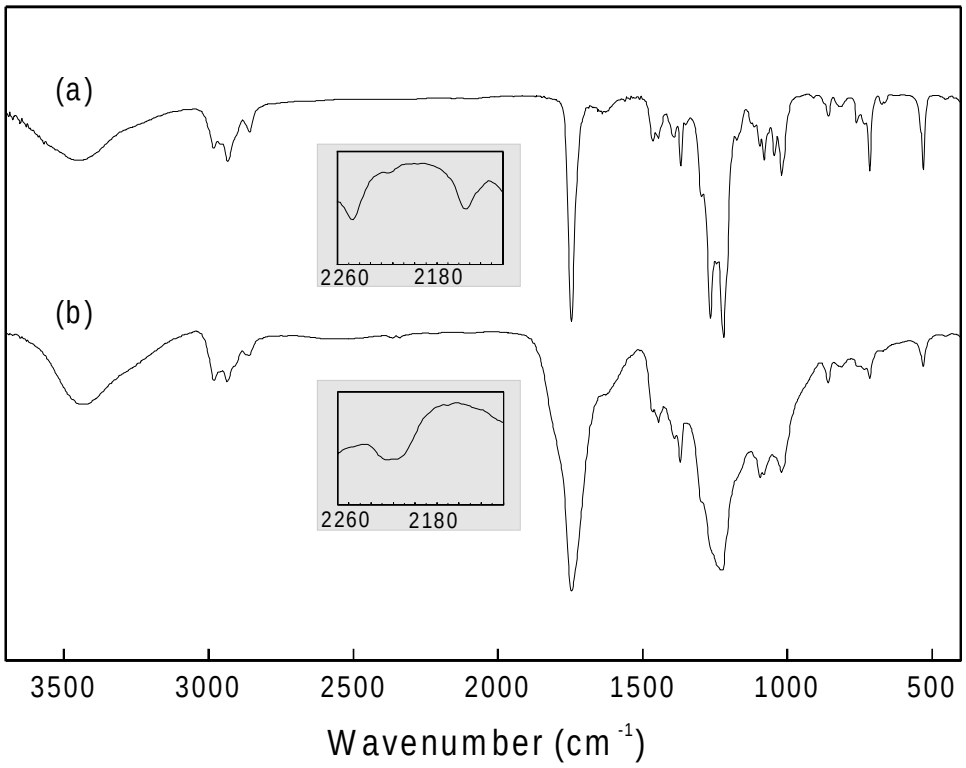

Figure 3.50. IR (KBr) spectra of: (a) monomer **103**; and (b) polymer **104**.

Also, some differences should also be stressed. The single butadiyne moiety **103** is shows two very weak bands at about 2250 and 2150 cm^{-1}, while polymer **104** displays a weak and a broad band centered at 2220 cm^{-1}. The double bonds present in the polydiacetylene chain are probably responsible for the broad band at 1700-1630 cm^{-1} in the IR spectrum of **104**.

MALDI-TOF mass spectrometry did not afford any information about the mass distribution of polymer **104** since no peak was obtained either in the positive or negative mode. Nevertheless, the color of the polymer suggest that also in this case the polydiacetylene chains are not very long. Further investigations are currently under way to study the structure and properties of this polymer.

3.5.5 Microscopic Beads of Three-Dimensionally Polymerized Lipo-Fullerene Derivatives Obtained in a Phospholipid Bilayer

The inclusion of the lipo-fullerene **99** into DPPC MLVs and its polymerization inside the phospholipid bilayer was studied in collaboration with Prof. T. Bayerl at University of Würzburg.

The DPPC/lipo-fullerene **99** MLV aggregates were successfully obtained according to the same procedure described above. Perdeuterated DPPC-d_{62} was used in these experiments to perform deuterium solid state NMR experiments. Freeze fracture electron microscopy studies together with DSC and ^{2}H-NMR experiments confirmed that lipo-fullerene monomers **99** exhibit self-assembly properties within the bilayer which are, at comparable DPPC/lipo-fullerene ratio, nearly identical to those described previously for non-polymerizable lipophilic [60]fullerene derivatives **85** and **86**.

The polymerization of **99** in multilamellar DPPC vesicles with a content in lipo-fullerene of 15 mol % was studied. The experiment was performed by submitting an aqueous dispersion of multilamellar DPPC vesicles containing 15 mol % lipo-fullerene **99** within a 2 ml quartz-glass cuvette to irradiation with an 8 watt lamp working at a wavelength of 256 nm under continuous gentle vortexing for 12 hours. According to the transition state temperature of plain DPPC MLVs (41.3 °C) (figure 3.39.c), the experiment was carried out at two different temperatures: (a) at 50 °C, this is above the transition state of DPPC MLVs (highly mobile fluid bilayer), and (b) at 5 °C, temperature below the transition state of DPPC MLVs (virtually immobile gel-phase bilayer).

Two control samples of pure DPPC MLVs were subjected to the same conditions and afterwards checked by DSC. No indication for thermic or irradiation damage of the DPPC was found. The phase transition temperature (41.3 °C) and width was unchanged to that measured before the UV-treatment.

In contrast, the DPPC/lipo-fullerene system shows significant changes after the UV irradiation at 50 °C with respect to the lipid molecular order and dynamic behavior, as is revealed by DSC and ^{2}H-NMR measurements.

Figure 3.51 shows the DSC measurements for DPPC MLVs containing 15 % mol of lipo-fullerene **99** prior and posterior to irradiation. Before polymerization occurs (figure 3.51.a), the plot shows a main phase transition corresponding to the melting of DPPC (T_m = 41 °C). The pre-transition phase of DPPC can also be observed for heating scans at T_p = 30.5 °C. No lipo-fullerene transition is observed since lipo-fullerene **99** is in the fluid state during the measurements. The high concordance between this result and the DSC measurement of plain DPPC MLVs (figure 3.39.c) is demonstrating the complete microscopic demixing between DPPC and the lipo-fullerene molecules. After irradiation the situation changes significantly as is shown in figure 3.51.b. Together with the main phase transition corresponding to unaffected DPPC MLVs (T_m = 41 °C), other processes are observed. Also, the pre-transition state observed before the polymerization process occurs is not detectable anymore. Obviously, the polymerization strongly alters the mechanical properties, resulting in shifts to higher transition temperatures. This observation could indicate a stiffening of the whole system.

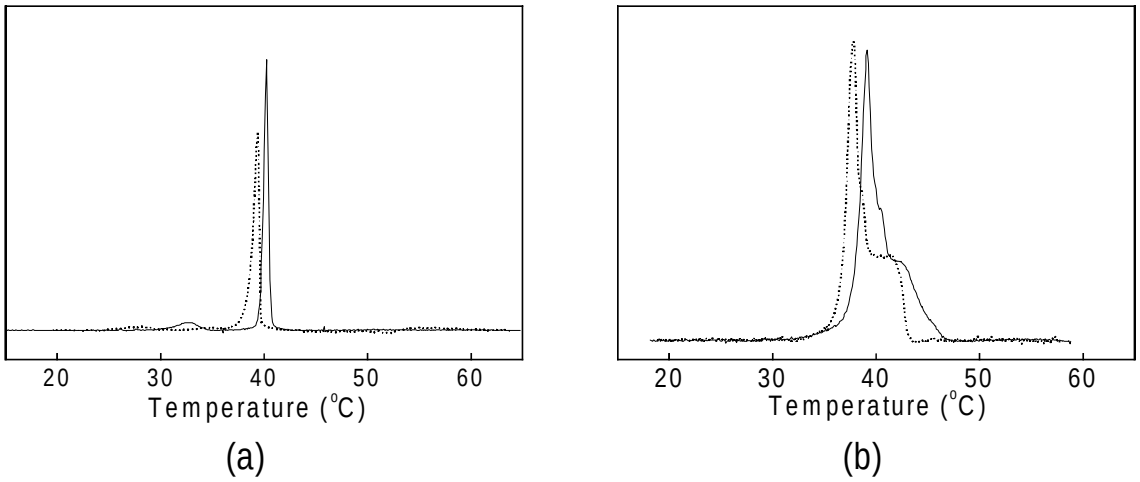

Figure 3.51. Endotherms (heating scans) and exotherms (cooling scans) corresponding to MLVs of DPPC containing 15 mol % of lipo-fullerene **99** (a) before, and (b) after irradiation. Solid curves correspond to the heating and the dashed ones to the cooling scans.

^{2}H-NMR experiments[103,104] also show that after irradiation, the molecular order along the DPPC tails is decreased and that the bilayer becomes less flexible as a result of the UV-irradiation. This indicates that the lipid parts become exposed to a less flexible moiety within

the bilayer, similar to the effect that is observed when a pure DPPC bilayer becomes attached to a solid support.

The result of the lipo-fullerene **99** polymerization within the DPPC bilayer under fluid bilayer conditions is revealed by freeze fracture electron microscopy (figure 3.52). While the sample before the polymerization (figure 3.52.a) shows the above mentioned rod-like structure of the bilayer surface with low spatial rod correlation owing to the mobility of the individual rods within the bilayer plane, the situation is completely different afterwards. Here, almost no rod-like structures and not even lipid vesicles are observed, but perfectly spherical objects (diameter range from 100 nm to several µm).

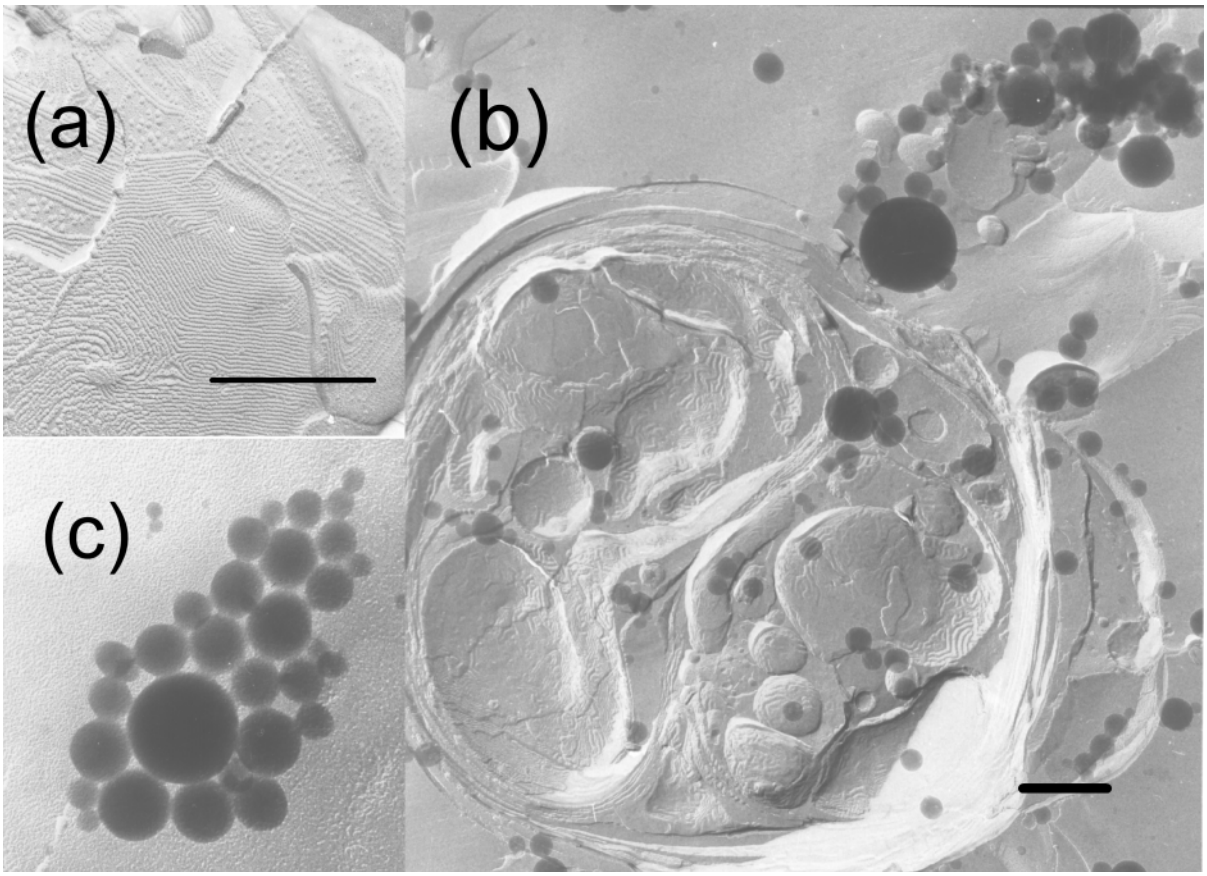

Figure 3.52. Freeze fracture transmission electron micrographs (TEM) of DPPC multilamellar vesicles containing 15 % mol of lipo-fullerene **99**: (a) before polymerization, (b) after polymerization, (c) TEM of pure poly-lipo-fullerene spheres obtained after extraction of the DPPC and subsequent drying. The bars represent a size of 0.5 µm.

The electron contrast of these spherical structures reveals that they consist essentially of poly-lipo-fullerene (figure 3.52.b). It is worth to emphasize that these spheres are not imaged from the platinum/carbon freeze fracture replica but from the real objects which stick to the replica.

Closer inspection shows that the smaller ones of these poly-lipo-fullerene spheres (those with diameters below 150 nm) are hollow as one can clearly observe the replica background below them with a position independent transparency over the whole sphere diameter. In contrast, the larger spheres are filled, rendering the core regions impenetrable to the electron beam.

An extraction of the templating DPPC by organic solvents and subsequent vacuum drying did not cause any significant change of the poly-lipo-fullerene spheres but allowed their transmission EM-inspection in absence of the freeze fracture replica. Here, aggregations of perfectly smooth and spherical objects with diameters between 50 nm - 10 µm were observed (figure 3.52.c). Similar diameters were observed for the DPPC/lipo-fullerene multilamellar vesicles prior to polymerization.

Atomic Force Microscopy (AFM) was used for an assessment of the surface of the spheres at a molecular scale after the extraction of the lipid. It was found that the surface of the spheres is surprisingly smooth with maximum amplitudes in height of 1.5 nm over lengths of several hundred nm (figure 3.53). The fullerene cages within the polymerized network are clearly resolved.

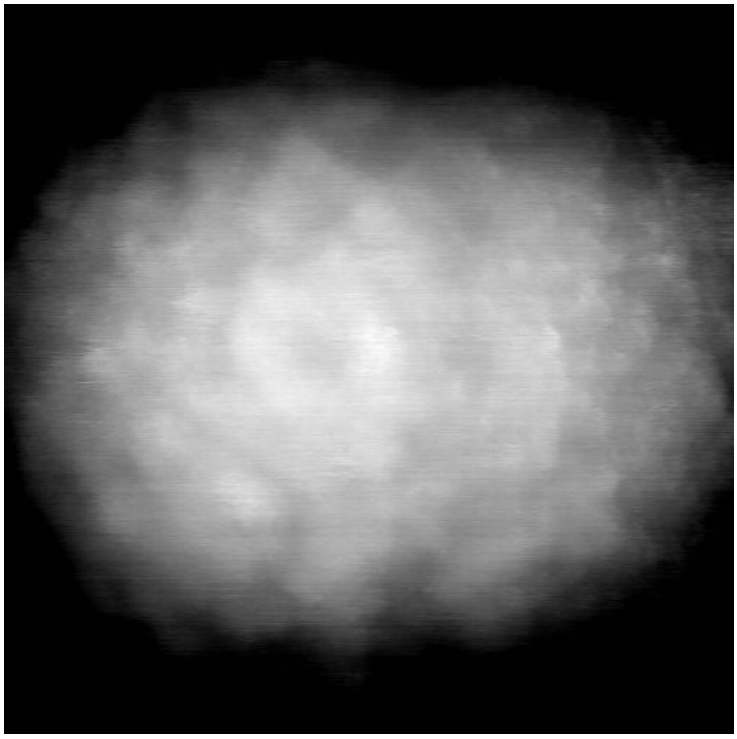

Figure 3.53. Atomic Force Microscopy of the poly-lipo-fullerene hollow spheres after extraction of the DPPC.

The importance of the fluid state of the bilayer and thus of the presence of collisions between adjacent fullerene rods for the formation of the above hollow spheres during polymerization

becomes obvious by the finding that under case b) conditions (gel phase bilayer) where all collective lateral rod mobility is prevented, no spheres are formed.

The poly-lipo-fullerene hollow beads seem to exhibit an unusually high mechanical strength. This is indicated by the finding that in all the microscopic studies carried out which comprised transmission (TEM) and scanning (SEM) electron microscopy as well as AFM, mechanically ruptured or otherwise damaged spheres were never observed in spite of the considerable forces to which the beads were subjected during the freeze fracture preparation procedure for TEM. Furthermore, the fact that one cannot observe any edge-darkening of the spheres in the transmission electron micrographs (figure 3.51) indicates that the wall thickness of the beads must be below the resolution limit of our TEM measurement, which is well below 10 nm. Taking into account the lateral [60]fullerene spacing measured by AFM, it was concluded that their wall is probably made up of one or just very few lipo-fullerene layers, thus representing a two-dimensional polymeric network which is spherically curved to a closed shell in the third dimension.

3.5.6 Microscopic Filled Beads of Three-Dimensionally Polymerized Lipo-Fullerene Derivatives Obtained by Polymerization in Solution

Recently, the polymerization of **99** in solution has been studied. The first experiments have been performed by irradiating a 5 mg/ml solution of **99** in decane at room temperature with an 8 watt lamp working at a wavelength of 256 nm. After a short time (30 minutes), the formation of shining brownish scales which remain stuck on the walls of the reactor is clearly visible. However, it was also possible to distinguish a suspension of small objects in the solution. The observation of these items by TEM showed that they consisted of the same kind of spherical polymers which were obtained when polymerization was carried out inside the MLVs. The only difference was that no hollow spheres were obtained in the first case. The average size of the polymer obtained in this case, was relatively bigger than before, with diameters ranging from some hundred nm to several μm.

These experiments are currently under way, but the first results obtained are of special interest in order to understand the mechanism that is involved in the formation of these spherical polymers. First, it was thought that MLVs were acting as templates for the polymerization process, but after these last results this should be reconsidered.

3.5.7 Differences in the Polymerization Processes: Conclusions

The perfect spherical shape of the polymers obtained when the polymerization is performed either in the membrane or in solution is surprising. This is certainly due to the three-dimensional pattern of the monomer unit. Functionalization of [60]fullerene provides a unique tool in organic chemistry for the construction of three-dimensional arrays.

It seems that the polymerization either in solution or inside the lipidic membrane is a diffusion controlled process. The monomer must diffuse either through the solution or inside the lipidic membrane to reach the point where polymerization is taking place. According to the polymerization mechanism described by Wegner et al[111-113], the unreacted diyne moiety must face the cumullene living polymer end, parallel and at the right distance. Then, it is not surprising, that formation of spherical polymers has never been observed when irradiation is carried out inside the lipidic membrane in the solid state (at temperatures below the DPPC MLVs transition temperature). Under these conditions, the diffusion of the lipo-fullerenes in a solid phase turns out to be difficult. Either in solution or in a mobile gel phase (inside a lipidic membrane at a temperature above the transition state MLVs DPPC) the situation is nearly identical. The lipo-fullerene diffuses through a solution in the first case, and through a lipidic fluid medium in the second. The main difference between these two cases is that only when polymerization takes places inside the MLVs, poly-lipo-fullerene spheres with diameters below 150 nm that appear hollow are obtained. It might be that these smaller hollow spheres are those generated in smaller vesicles. The content of lipo-fullerene in these smaller vesicles is obviously finite according to their size. Then, polymerization occurs yielding spherical polymers of small dimensions. The vesicle is limiting the extension of the polymerization process. When polymerization takes place in a big vesicle, the number of lipo-fullerene molecules involved is obviously much larger. Possibly, during the polymerization process, the membrane is subjected to local high pressure and therefore breaks. Once this happened, the polymer can continue growing if it gets in contact with other deposits of unreacted monomer. Since it is possible to create selectively small vesicles using filtration techniques, it would be interesting to see if the size distribution of the polymer gets affected by decreasing the average size of the MLVs.

In the polymerization of neat films of lipo-fullerene **98**, no diffusion process is involved. Due to the heat of the irradiation lamp during the polymerization, the sample is in the liquid state. Thus, the chains of lipo-fullerene are mobile and when getting in contact they combine to large scale shape polymers.

The poly-lipo-fullerene spheres may have some interesting applications in quite different fields. First, they may serve as model systems for two-dimensional polymers to test theoretical predictions of polymer physics like the suggested temperature induced transition between a flat and a crumpled phase. Furthermore, their shape, strength and elasticity may have potential for solvent free lubrication purposes. Besides that, in biotechnology they may serve as caging enzymes, for enhancing the mechanical stability of liposomes and for drug delivery systems.

3.5.8 Microscopic Arrangement of Low Concentration Unpolymerized Lipo-Fullerenes in Monovesicles: A Spectacular Reticular Structure

Quite recently, TEM has shown very particular arrangements of lipo-fullerene **99** in small DPPC MLVs containing under gel phase and diluted conditions (content of lipo-fullerene **99** lower than 5 mol %) (figure 3.54).

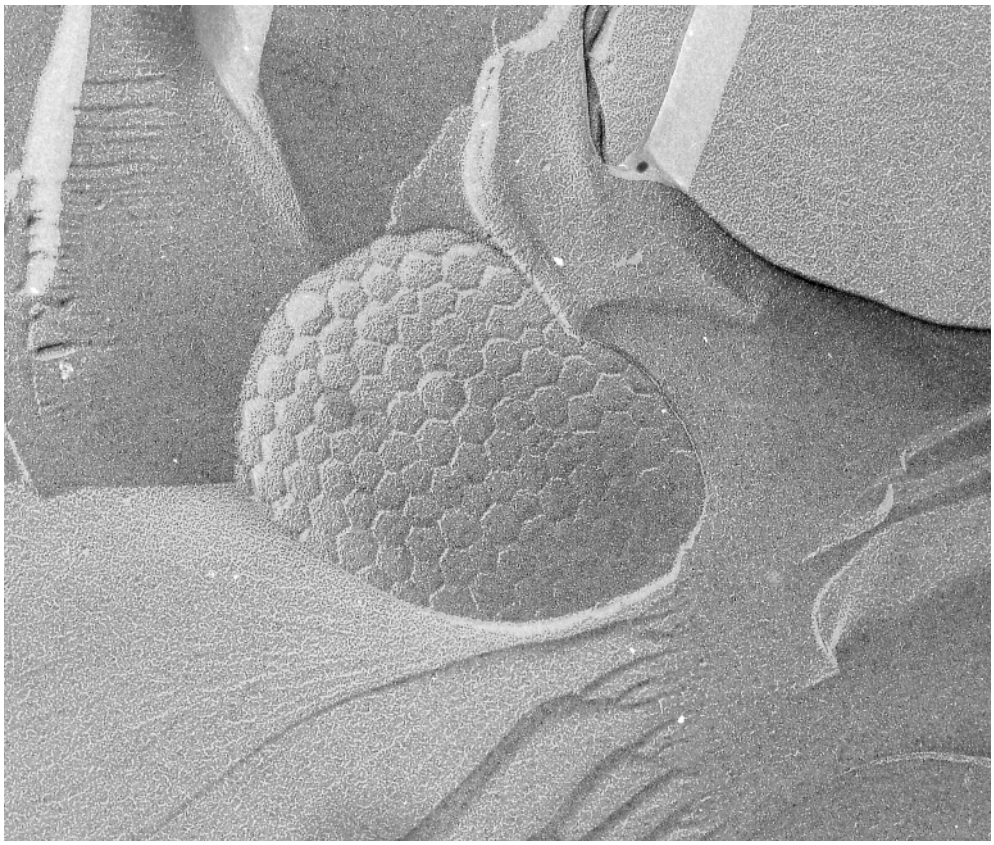

Figure 3.54. Freeze fracture transmission electron micrograph (TEM) of a DPPC unilamellar vesicle containing 3 % mol of lipo-fullerene **99** before polymerization.

Here, no long rod-like structures are observed, but a framework made of thin struts that covers the whole surface of the vesicle. The struts are interconnected forming mainly pentagons and

hexagons similar to the way in which the carbon atoms are connected in the fullerene molecules. This structure is probably caused by thin arrangements within the lipidic bilayer consisting of a discrete number of lipo-fullerene molecules.

Similar structures have often been observed in natural systems, and their construction obeys a common form of architecture known as tensegrity[115]. The term refers to a system that stabilizes itself mechanically by the way in which tensional and compressive forces are distributed and balanced within the structure. Tensegrity structures are mechanically stable not because of the strength of individual members but because of the way the entire structure distributes and balances mechanical stress. An increase in tension in one of the members results in increased tension in members throughout the structure, even in those on the opposite side.

3.6 New Perspectives: Biotinated Lipo-Fullerenes

3.6.1 Introduction: Biotin

It has been described above how lipo-fullerenes self-assemble giving rod-like structures of up to 30 nm diameter and of several µm length upon intercalation into synthetic lipidic bilayers. The solubility of lipo-fullerenes **85** and **86** within the DPPC vesicles has been shown surprisingly high: homogeneous systems containing more than 25% mol of both lipo-fullerenes have been easily achieved.

The technology developed clearly offers the possibility to introduce biological active moieties into the system. The fullerene core permits the design of lipo-fullerene derivatives with specific moieties placed in a desired position. As a first example, it would be interesting to build up transmembrane systems consisting of a lipo-fullerene carrying a biological active lipophobic substituent able to cross the membrane and to be placed in the surface of the vesicle. It was taken into consideration to use biotin as a biological active moiety for the goal pursued. D-(+)-Biotin (also referred to as vitamin H in humans) is an essential cofactor for a number of enzymes that have diverse metabolic functions (figure 3.55).

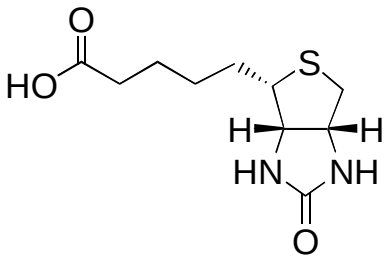

Figure 3.55. D-(+)-Biotin.

Biotin serves as a covalent bound CO_2 *mobile carrier* for reactions in which CO_2 is fixed into an acceptor by carboxylases[116]. Streptavidin is a protein isolated from *Streptomyces avidinii* that consists of four identical subunits, each containing a single biotin binding site[117]. The high affinity between streptavidin and biotin has made this system very popular in the field of labeling and affinity techniques.

It was planned to build-up a lipo-fullerene molecule containing a biotin subunit. Once introduced into the vesicles, this moiety could probably be able to cross the membrane according to its high polarity. This situation could be easily recognized taking advantage of the

high affinity between streptavidin and biotin. Thus it would be possible to label the biotin heads at the surface of the vesicle binding streptavidin proteins.

3.6.2 Planned Synthesis of a Biotin-Lipo-Fullerene Derivative

According to the previous considerations it was planned to synthesize the biotinated lipo-fullerene **105** depicted in figure 3.56. The lipidic chains should provide the required solubility of the resulting molecule in the interior of the vesicle with similar effects in the composite system as has been described above for the non biotinated lipo-fullerenes. The biotin moiety is placed at the outside of the macromolecule. It is connected to the fullerene core by a long aliphatic chain capped with a triethylglycol chain. This segment should provide extra lipophobicity in order to bring the capped biotin rest to the exterior of the vesicle.

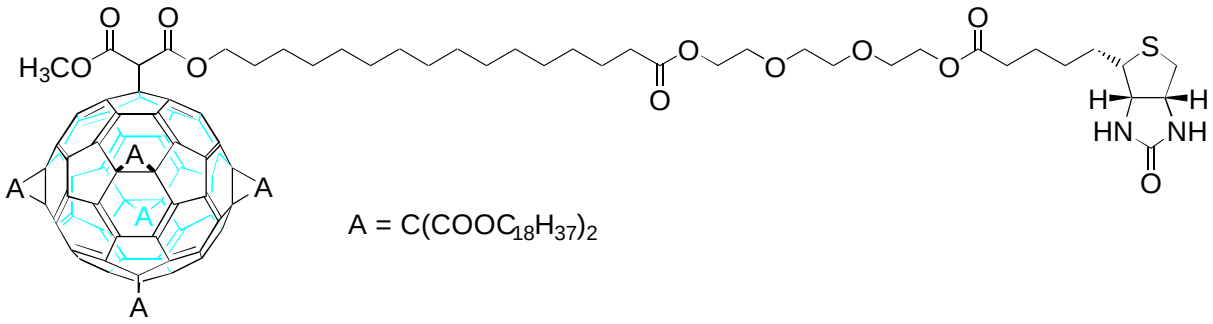

105

Figure 3.56. Biotinated lipo-fullerene **105**.

The synthesis of **105** was designed as described in scheme 3.24. The available hexadecandioic acid was quantitatively reduced with lithium aluminum hydride in THF. Treatment of malonyl chloride monomethyl ester with the dialcohol **106** and pyridine furnished the malonic alcohol **107** in a 25 % yield. Oxidation with PDC in DMF gave **108** in a good yield.

Triethylglycol was monoprotected as a THP ether in a 48% yield. The subsequent esterification of biotin with alcohol **109** is currently under study. Using DCC with catalytic amounts of DMAP as coupling agents produced a mixture consisting of the desired product **110** together with the side-product N-biotnyl-N,N´-dicyclohexylurea. The appearance of this side-product seems to indicate the low reactivity of the alcohol probably due to intramolecular hydrogen bonding. Other coupling procedures are to be examined.

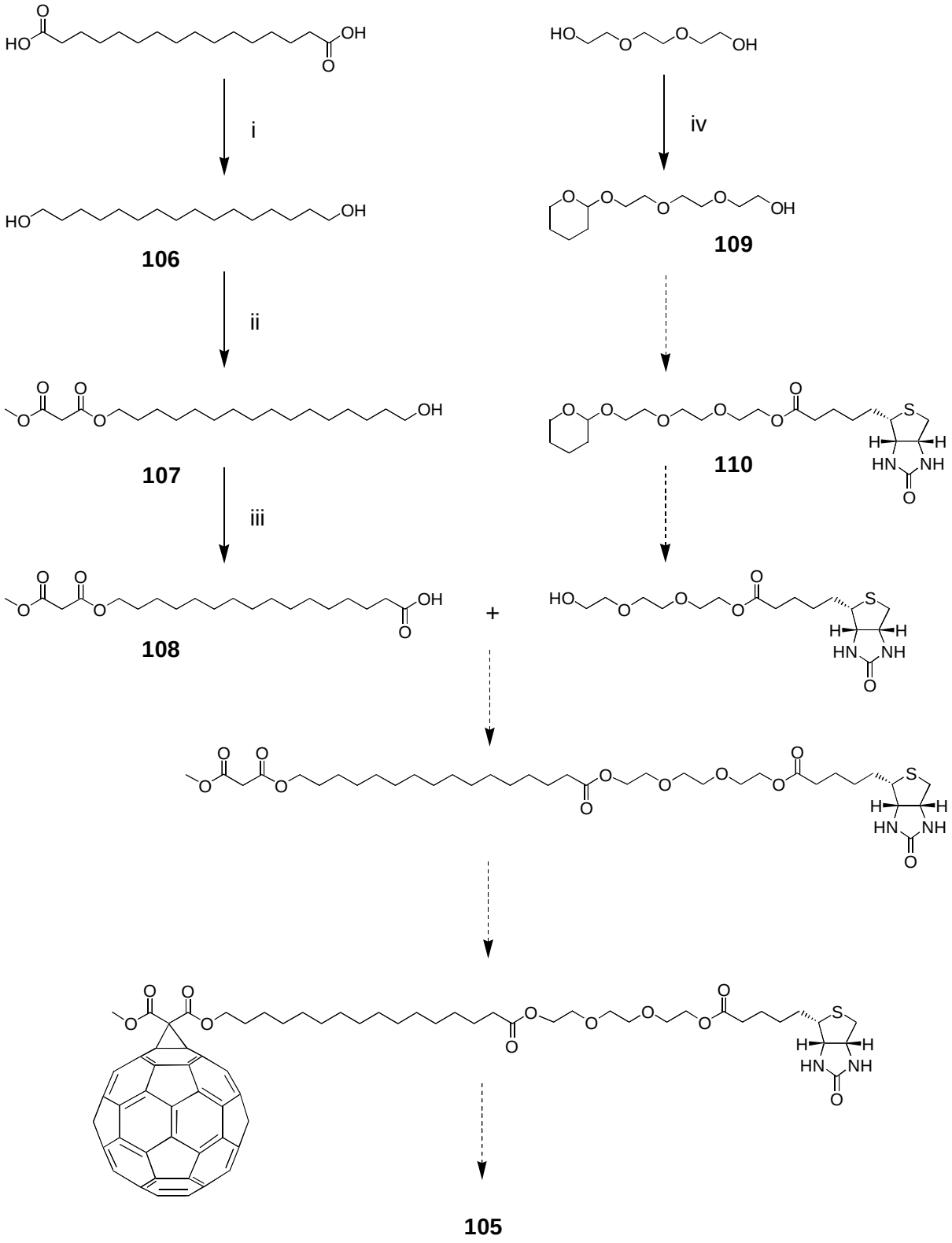

Scheme 3.24. i) $LiAlH_4$/THF (100 %); ii) Malonyl chloride monomethyl ester, Pyr/CH_2Cl_2 (25 %); iii) PDC/DMF (74 %); iv) DHP, PTSA/ CH_2Cl_2 (40 %).

3.7 Modification of the Bingel Reaction

3.7.1 Problems in the Syntheses of Bromo Malonates

It has been demonstrated in the previous chapters that cyclopropanation of fullerenes via the reaction with bromo malonates in the presence of base is one of the most efficient tools for the synthesis of methanofullerenes[24-29]. The advantages of this reliable method of fullerene functionalisation are: i) mild reaction conditions providing comparatively high yields; ii) exclusive formation of [6,6]-bridged adducts, and iii) facile one step access to higher adducts with a stereochemically defined addition pattern. For the present work, the template activation method with DMA[29,30] has been of special importance. Thus, taking advantage of this reaction, the synthesis of highly compact dendrimer structures containing [60]fullerene as a central building block has been possible.

Unfortunately, the preparation of pure bromo malonates has been complex in some cases. First of all, the yields in bromo malonates are limited due to the simultaneous formation of dibromo malonates. Moreover, the chromatographic properties of starting malonates, bromo- and dibromo malonates differ only slightly. For example, in the preparation of the 2nd and 3rd generation dendritic bromo malonates **27** and **28** no chromatographic conditions were found to isolate them. However, since the bromo malonates **27** and **28** were the only reactive species under the reaction conditions applied, the corresponding mixtures of malonate, bromo- and dibromo malonate was directly used as reagent for the [60]fullerene cyclopropanation process. Nevertheless, the final purification of the fullerene targets has been severely complicated due to the presence of unreacted dendritic malonate species.

3.7.2 Efficient Cyclopropanation of [60]Fullerene Starting from Malonates

A modification of this cyclopropanation, namely the direct treatment of C_{60} with malonates in the presence of iodine and base[118], works satisfactorily only in some cases, e.g. with diethyl malonate. This modification is based upon the *in situ* generation of iodo malonate species that are further reacting with [60]fullerene in the reaction mixture. However, when other malonates containing dendritic or long alkyl side chains were used, the yields in monoaddition products were very low and most of the C_{60} was converted into an unidentified material.

It was thought to look for conditions to generate reactive bromo malonates in the presence of DBU and [60]fullerene in order to achieve fullerene addition products in a one pot reaction. The reaction for preparing monoaddition [6,6]bridged methanofullerenes was designed in the following way: equimolar amounts of C_{60}, the desired malonate and CBr_4 would be disolved in toluene. Afterwards, two equimolar portions of DBU would be added. In a first step, bromo malonate would be formed, and this would further react with C_{60} in the presence of DBU.

Four different malonates were purchased (**111**) or synthesized (**90**, **112**, **24**) and used under the reaction conditions described above to check whether the conceived methodology was applicable (scheme 3.25).

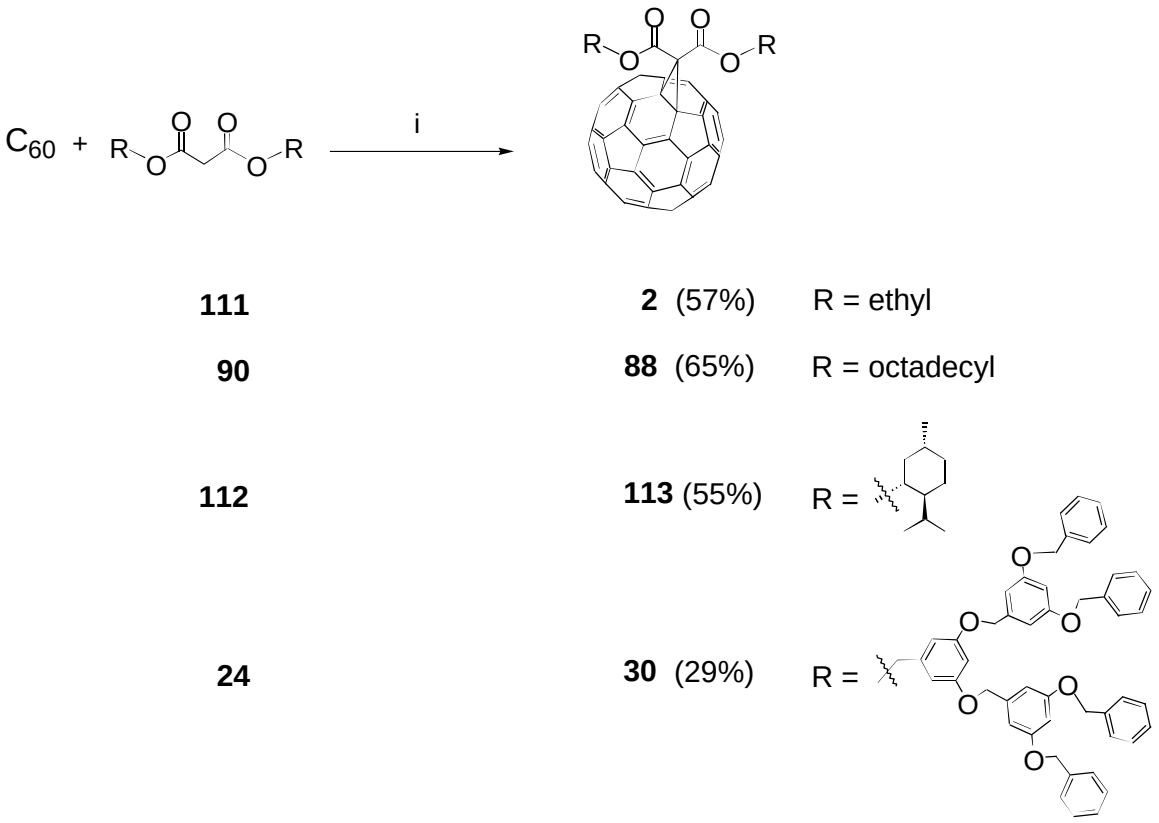

Scheme 3.25. Reagents and conditions: i) C_{60} (1 equiv.), $CH_2(CO_2R)_2$ (1.5 equiv.), CBr_4 (1.5 equiv.), DBU (3 equiv.), toluene, RT, 6 h.

Following this approach, clean conversion of C_{60} into the methanofullerenes **2**, **88**, **113**, and **30** was observed. In all cases the yields obtained were comparable to those achieved when starting with the corresponding bromo malonate under classical Bingel reaction conditions.

Once the broad applicability of this new approach to the synthesis of [6,6]bridged monoaddition methanofullerenes was demonstrated, it was tried to combine it with the template activation method used before. In that way, it would be possible to synthesize [60]fullerene hexaadducts with octahedral addition patterns starting from malonates. First, the

reversible addition of DMA to [60]fullerene results in activation of the corresponding octahedral positions. Then, generation of reactive bromo malonate species *in situ* would lead to the desired hexakis-addition products. The reaction was run with two different malonates: diethyl malonate (**111)** and dioctadecyl malonate (**90)** (scheme 3.26).

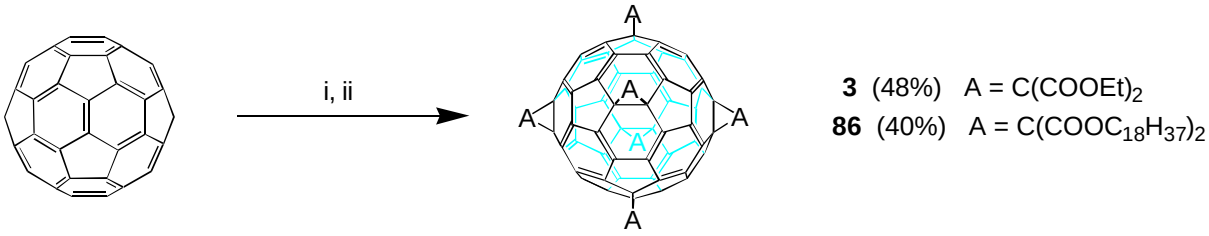

Scheme 3.26. Reagents and conditions: i) DMA (10 equiv.); ii) $CH_2(CO_2R)_2$ (10 equiv.), CBr_4 (10 equiv.), DBU (20 equiv.), toluene, RT, 48 h.

The yields in hexaadducts **3** and **86** were 48 % and 40 %, respectively, which are as high as those obtained with the original procedure using the corresponding bromo malonates.

Compounds **2**, **88**, **113**, **30**, **3**, and **86** were purified by chromatographic techniques and fully characterized.

It was assumed that in a first step the reaction mechanism involves the formation of the corresponding bromo malonate and bromoform through DBU catalysis. After that, the bromo malonate is reacting with C_{60} using stoichiometric amounts of DBU to yield the cyclopropanation product. After a more detailed investigation of the reaction conditions it was found that the use of 1.1 equiv. of DBU instead of 2 equiv. was sufficient to achieve the same yields in cyclopropantion products according to the proposed mechanism.

4 Summary

The central idea of the present work was to investigate and, later, to take advantage of, the unique geometrical properties of [60]fullerene making it a central tecton for the synthesis of well defined three dimensional macromolecules. [60]Fullerene with its spherical skeleton has an unsurpassable workspace for this purpose. No other building block offers such a versatility in organic chemistry as [60]fullerene does. The synthetic strategy was based on the nucleophilic cyclopropanation of C_{60} with bromo malonates together with the template activation method allowing for the preparation of octahedral hexakis-addition [60]fullerene derivatives. This methodology has been improved after the introduction of an alternative strategy. The direct treatment of C_{60} with malonates in the presence of CBr_4 and DBU leads to an efficient conversion to methanofullerenes. This has been demonstrated with the syntheses of monoadducts and highly symmetric hexaadducts in yields as good as when starting from the corresponding bromo malonates (chapter 3.7).

The convergent synthesis, complete characterization and molecular dynamics simulations of dendrimers involving [60]fullerene as core tecton and first to third generation benzyl ether based dendrons as branches has been successfully fulfilled. With dendrimer **32** the core branching multiplicity of 12, which is the highest known to date, is realized using a T_h-symmetrical substituted C_{60} core with an octahedral addition pattern. NMR investigations as well as molecular modelling studies have shown that due to high branching multiplicity, dendrimer **32** represents a globular and densely packed macromolecule (chapter 3.1.4).

The synthesis of mixed adducts containing different kinds of functionalities has also been studied. Addends with specific physical or chemical properties, or just positional blockers to enable the construction of distinct addition patterns within the fullerene core, have been employed. Of special interest has been the synthesis of the chiral bisoxazoline-dendrimer-[60]fullerenes **48**-**51**. These compounds have potential application as *chemzymes* for all those enantioselective reactions that are catalyzed by bisoxazolines themselves. In addition to the local C_2-symmetry of the chiral bisoxazoline addends, their screw-like C_3-symmetrical arrangement within the fullerene core provides a further effective scenario for chiral discrimination. The dendritic addends provide solubility and could also discriminate substrates

in the chiral regions. Eventually, the consecution of higher generation related products would result in nanoparticles that would offer the advantages of a homogeneous catalyst and could be removed from the reaction mixture by physical operations as easily as a heterogeneous one (chapter 3.1.5).

The synthesis of a porphyrin-dendrimer-fullerene **54** has been achieved starting from a porphyrin-fullerene monoadduct **53**. This compound represents a new class of models for hemeproteins with potential applications as catalysts. Nevertheless, the compound was obtained in a very low yield according to the bulkiness of the resulting system making the study of its properties difficult (chapter 3.1.6).

Despite the promising result, the low yields in which the highly substituted dendrimer-fullerenes obtained, made of necessary to introduce the *spacing* concept (chapter 3.2.2). The modification of the benzyl ether-type dendron by intercalating aliphatic chains providing spaciousness and flexibility has resulted in the development of a new dendritic system (chapter 3.2.3). After this modification, first and second generation porphyrin-dendrimer-fullerenes **71** and **72** have been achieved in acceptable yields. Small bathochromic shifts for the porphyrin chromophor in the UV spectra are observed for these compounds relative to the parent dyad **53**. This unequivocally reflects that interaction between the porphyrin and the dendrons occurs. The magnitude of this interaction is increasing with the generation number. The shifts might derive from microenvironmental effects and/or from the deviation from planarity that the porphyrin could suffer in the resulting crowded surroundings. The dendritic coverage within **71** and **72** is also influencing the redox potentials of the porphyrin moiety. The polar microenvironment helps to stabilize the different oxidation states within the porphyrin, while the first reduction step of the porphyrin moiety is energetically more disfavoured with increasing the size of the addends attached to the fullerene core (chapter 3.2.5).

The synthesis of dendrimer-[60]fullerenes via a divergent approach has been explored. For that proposal a dendritic system based on 3,5-dihydroxy-benzylalcohol capped with MEM protected hydroxyl groups has been developed. Unfortunately, all efforts made to cleave these protecting groups in the methanofullerene **81** were fruitless. Other kinds of protecting groups should be considered in order to explore the divergent synthesis of dendrimer-fullerenes. Of special interest would be the formation of water-soluble dendrimers with potential abilities as

molecular micelles, as hosts for the transport of biological guests, or as neuroprotective agents, or as drugs (chapter 3.3).

In the second part of this work, different fullerene derivatives have been synthesized by attaching long alkyl chains, giving the so-called *lipo-fullerenes* (chapter 3.4.2). The T_h-symmetrical [60]fullerene hexakisadducts containing six pairs of dodecyl (**85**) or octadecyl chains (**86**) have been introduced to lecithin artificial membranes changing the phospholipid bilayer to a composite system with new physical properties (chapter 3.4.3). From digital scanning calorimetry experiments (DSC) it could be concluded that the effect of both lipo-fullerenes **85** and **86** on the phase transition behavior of the multilamelar vesicles (MLVs) was surprisingly low. From these results it is possible to conclude that the phase transitions of dipalmitoyl-sn-glycero-3-phosphatidylcholine (DPPC) and of **85** or **86** are almost completely decoupled, indicating pronounced microscopic demixing. This is, the interaction between lipo-fullerenes and DPPC in the MLVs seems to be at least very small (chapter 3.4.3.2). Transmission electron microscopy has shown that lipo-fullerenes arrange in bilayers as rod-like structures, exhibiting long range ordered super-structures in the gel phase. This spatial correlation is drastically reduced or even lost in the fluid phase of the bilayer (chapter 3.4.3.3). ^{2}H-NMR experiments made clear that the lipo-fullerene rods stabilize the bilayer against deformation in a magnetic field in a similar fashion as a membrane cytoskeleton does. The important difference to point out is that the former seems to be located between the two layer leaflets, while the cytoskeleton is attached to the outside of the membrane (chapter 3.4.3.4).

Different lipo-fullerenes containing butadiyne moieties in the aliphatic chains able to polymerize have been prepared (chapter 3.5). Neat polymerization of **99** resulted in the formation of a polymer consisting of a net of polydiacetylene chains with pendant alkyl rests capped with substituted fullerenes. The fullerenes provide the inter-cross-linking to the resulting polymer. Molecular modeling suggests that due to sterical reasons it is difficult to achieve long polydiacetylene chains and that, certainly, not all the butadiyne moieties can take part in the polymerization process (chapter 3.5.3). Longer polydiacetylenes chains with pendant fullerenes have been made starting from **101**, a fullerene derivative containing a single diacetylene moiety (chapter 3.5.4).

The polymerization of the lipo-fullerene derivative **99** has been carried out inside artificial bilayers by irradiation with UV light. Polymerization occurs only at temperatures above the

transition state of the DPPC MLVs, when the diffusion of lipo-fullerene **99** and thus collision processes are faster. Perfectly spherical objects (diameter range from 0.1 µm up to several µm) are obtained in this case. The smaller ones of these poly-lipo-fullerene spheres (those with diameters below 150 nm) are hollow while the larger ones are filled (3.5.5).

When polymerization was carried out in solution large hollow and perfectly spherical poly-lipo-fullerenes are also obtained (chapter 3.5.6). It seems that the polymerization either in solution or inside the lipidic membrane is a diffusion controlled process. The monomer must diffuse either through the solution or inside the lipidic membrane to reach the point where polymerization is taking place. The perfect spherical shape of the polymers obtained when the polymerization is performed either in the membrane or in solution is certainly surprising. This is most likely due to the three-dimensional pattern of the monomer unit. The main difference between these two cases is that only when polymerization takes places inside the MLVs, poly-lipo-fullerene spheres with diameters below 150 nm, which appeared hollow, are formed. It might be that these smaller hollow spheres are those generated in smaller vesicles. The content of lipo-fullerene in these smaller vesicles is obviously limited by their size. Then, polymerization takes places yielding spherical polymers of small dimensions. The vesicle is limiting the extension of the polymerization process (chapter 3.5.7).

The poly-lipo-fullerene hollow beads seem to exhibit an unusually high mechanical strength. The poly-lipo-fullerene spheres may have some interesting applications in quite different fields. First, they may serve as model systems for two-dimensional polymers to test theoretical predictions of polymer physics like the suggested temperature induced transition between a flat and a crumpled phase. Furthermore, their shape, strength and elasticity may have a potential as solvent free lubrication purposes. Beside that, they may serve in biotechnology for caging enzymes, for enhancing the mechanical stability of liposomes and for drug delivery systems.

Lipo-fullerene **99** has been shown to arrange in a framework fashion within the bilayer made of thin struts that covers the hole surface of the vesicle. The struts are interconnected forming mainly pentagons and hexagons similar to the way how the carbon atoms are connected in the fullerene molecules. Similar structures have often been observed in natural systems, and their construction obeys a common principle of architecture known as tensegrity, although the mechanism that governs the formation of this kind of structure is still unknown (chapter 3.5.8).

The synthesis of lipo-fullerene **105** carrying a biotin rest has been started in order to build up transmembrane systems consisting of a lipo-fullerene and a biological active lipophobic substituent able to cross the membrane and to be placed on the surface of the vesicle. Once introduced in the vesicles, this moiety could probably be able to cross the membrane according to its high polarity. This phenomenon would be easily recognized taking advantage of labeling techniques (chapter 3.6).

4 Zusammenfassung

Das Ziel der vorgestellten Arbeit war die Untersuchung der geometrischen Eigenschaften von [60]Fulleren als zentrales Tekton für die Darstellung definierter dreidimensionaler Makromoleküle. C_{60}-Fulleren mit seinem sphärischen Kohlenstoffgerüst sollte für diesen Zweck eine ideale „workspace“ darstellen, denn kaum ein anderer Synthesebaustein in der Organischen Chemie bietet ähnliche Vielfältigkeit und Anwendungsmöglichkeiten. Die hier aufgezeigte Synthesestrategie basiert auf der nucleophilen Cyclopropanierung von C_{60} mit Brommalonestern und der Methode der Templat-Aktivierung zur Darstellung oktaedrischer Hexakis-Addditionsprodukte von [60]Fulleren. Diese Methode wurde durch direkte Reaktion von C_{60} mit Malonestern in Gegenwart von CBr_4 und DBU verbessert und führte zu einer effizienten Umwandlung von C_{60} in Methanofullerene. Die Synthese sowohl von Monoaddukten als auch von hochsymmetrischen Hexakisaddukten mit vergleichbaren Ausbeuten gegenüber der Originalmethode zeigt den Vorteil bzw. die Überlegenheit dieser Technik (Kap. 3.7).

Die konvergente Synthese von Dendrimeren unter Verwendung von [60]Fulleren als Core-Tekton und Benzylether-Dendronen der ersten bis dritten Generation als Äste einschlußlich gelang eine komplette Charakterisierung und Moleküldynamik-Simulation der Produkte. Dendrimer **32**, das mit einer Verzweigungsmultiplizität von 12 die bis dato höchsterreichte Verzweigung besitzt, läßt sich durch Verwendung eines T_h-symmetrisch substituierten C_{60}-Core mit oktaedrischem Substitutionsmuster realisieren. NMR-Untersuchungen sowie Molecular-Modelling Studien ergaben, daß verursacht durch seine hohe Multiplizität der Verzweigung das Dendrimer **32** ein globuläres und entsprechend dicht gepacktes Makromolekül darstellt (Kap. 3.1.4).

Auch die Darstellung gemischt-substituierter Addukte mit verschiedenen Funktionalitäten wurde untersucht. Dazu wurden Addenden mit spezifischen physikalischen oder chemischen Eigenschaften eingesetzt, oder solche, die als Positions-Blockade nur die Entstehung ungewünschter Additionsmuster am C_{60}-Core verhindern. Besonderes Interesse erweckte die Synthese chiraler Bisoxazolin-Dendrimer[60]fullerene. Diese Verbindungen bieten potentielle Anwendungsmöglichkeiten als *Chemzyme* für enantioselektive Reaktionen, die üblicherweise

durch Bisoxazoline alleine katalysiert werden. Zusätzlich zu der C_2-Symmetrie der chiralen Bisoxazolinaddenden liefert die schraubenartige C_3-symmetrische Substitutionsanordnung des Fullerenkerns einen effektiven Beitrag zu einer möglichen chiralen Diskriminierung. Die dendritischen Addenden fördern zum einen die Löslichkeit und können zum anderen Substrate in der chiralen Umgebung selektiv diskriminieren. Außerdem könnten mit der Darstellung von Dendrimeren höherer Generationen Nanopartikel zugänglich sein, die die Vorteile eines homogenen Katalysators besitzen und gleichzeitig sich so einfach wie üblicherweise nur heterogene Katalysatoren aus dem Reaktionsgemisch entfernen lassen (Kap. 3.1.5).

Die Synthese des Porphyrindendrimerfullerens **54** gelingt ausgehend von Porphyrin-Fullerenmonoaddukt **53**. Diese Verbindung gehört zu einer neuen Klasse von Hämprotein-Modellen mit Einsatzmöglichkeiten als Katalysator. Allerdings konnte die Verbindung nur in sehr geringen Ausbeuten gewonnen werden, die sicherlich aus der sterisch anspruchsvollen Gruppenanhäufung resultiert und die eine Bestimmung der Eigenschaften nicht mehr zuließ.

Trotz der vielversprechenden Resultate machten die niedrigen Ausbeuten der hochsubstitutierten Dendrimerfullerene die Einführung eines *Spacer*-Konzepts (Kap. 3.2.2) erforderlich. Durch Einbau aliphatischer Spacerketten reduziert man die Gruppenhäufung in den Benzylether-Ästen und erhält neue dendritische Systeme mit mehr Raumfreiheit und Beweglichkeit der Dendrimeräste (Kap. 3.2.3). Mit dieser Modifikation erhält man nun die Porphyrin-Dendrimerfullerene **71** und **72** der ersten bzw. zweiten Generation in akzeptablen Ausbeuten. Die Verbindungen zeigen eine schwache bathochrome Verschiebung im UV-Spektrum des Porphyrinchromophors relativ zur Ursprungsdiade **53**, die auf die Wechselwirkung zwischen dem Porphyrin und den Dendronästen zurückgeführt werden muß. Die Größe dieser Wechselwirkung wächst mit steigender Generationenzahl. Die bathochrome Verschiebung wiederum kann aus Mikroumgebungseffekten resultieren und/oder auf der Abweichung des Porphyrinsystems von der Planarität beruhen, hervorgerufen durch die dichte Packung der Umgebung. Die dendritische Bedeckung in **71** und **72** beeinflußt auch das Redoxpotential der Porphyrineinheit. Die polare Mikroumgebung trägt zur Stabilität der einzelnen Oxidationsstufen des Porphyrins bei, während die erste Reduktionsstufe der Porphyrineinheit energetisch weniger begünstigt wird (Kap. 3.2.5).

Auch die Darstellung von Dendrimer[60]fullerenen *via* einer divergenten Synthese wurde untersucht. Für diese Studie wurde ein dendritisches System entwickelt, basierend auf 3,5-Dihydroxybenzylalkohol als Baustein mit MEM-geschützten Endhydroxyfunktionen. Allerdings scheiterten alle Versuche, die Schutzgruppen von den Methanofullerenen **81** am Syntheseabschluß zu entfernen. Hier sollten in Zukunft andere Schutzgruppen herangezogen werden um eine divergente Synthese von Dendrimerfullerenen erfolgreich abzuschließen. Von besonderem Interesse sollte die Darstellung wasserlöslicher Dendrimerer mit der Möglichkeit zur Bildung molekularer Mizellen sein, die als Wirt für den Transport biologischer Gastmoleküle oder als neuroprotektives Agens und mögliche Pharmakon dienen könnten (Kap. 3.3).

Im zweiten Teil der vorliegenden Arbeit wird die Synthese einer Zahl verschiedender Fullerenderivate vorgestellt, die lange Alkylseitenketten am Fullerencore aufweisen und als *Lipofullerene* bezeichnet werden (Kap. 3.4.2). Die T_h-symmetrischen [60]Fulleren-Hexakisaddukte, die sechs Paare von Dodecyl- (**85**) bzw. Octadecylketten (**86**) enthalten, wurden in künstliche Lecithinmembranen eingeführt und überführen den Phospholipid-Bilayer damit in ein Composite-System mit neuen physikalischen Eigenschaften (Kap. 3.4.3). Aus Digital Scanning Kalorimetrie-Experimenten [DSC] konnte geschlossen werden, daß der Einfluß der beiden Lipofullerene **85** und **86** auf das Phasenübergangsverhalten der multilamellaren Vesikel [MLVs] erstaunlich gering war. Aus diesen Ergebnissen ließ sich schließen, daß die Phasenübergänge von Dipalmitoyl-*sn*-glycero-3-phosphatidylcholin [DPPC] und **85** oder **86** mehr oder weniger vollkommen entkoppelt sind und auf eine verstärkte mikroskopische Entmischung hinweisen. Dies bedeutet, daß die Wechselwirkung zwischen Lipofullerenen und DPPC in den MLVs zumindest sehr gering zu sein scheint (Kap. 3.4.3.2). Transmissionselektronenmikroskopie [TEM] ergab, daß sich die Lipofullerene in dem Bilayer in röhrenartigen Strukturen anordnen und über weite Distanzen eine geordnete Superstruktur in der semikristallinen Gelphase einnehmen. Diese räumliche Anordnung wird in der Flüssigphase drastisch reduziert oder geht ganz verloren (Kap. 3.4.3.3). ^{2}H-NMR-Experimente deuten darauf hin, daß die Lipofulleren-Röhren die Doppelschicht gegen Deformation im Magnetfeld ähnlich stabilisieren wie es das Membrancytoskelett bewirkt. Der entscheidende Unterschied zwischen beiden liegt jedoch in der Tatsache, daß die ersteren zwischen den beiden Schichten des Bilayers zu finden sind, während das Cytoskelett außerhalb der Membran-Bilayerschichten liegt (Kap. 3.4.3.4).

Es wurden Lipofullerene synthetisiert, die Butadiin-Einheiten in den aliphatischen Ketten und damit die Möglichkeiten zur lichtinduzierten Polymerisation besitzen (Kap. 3.5). Die Polymerisation von reinem **99** ergab ein Polymer bestehend aus einem Netz von Polydiacetylenketten mit abwechselnden Alkylresten, die mit substituierten Fullerenen abschließen. Das Fulleren ist verantwortlich für das inter-cross-linking zum resultierenden Polymer. Molekular Modelling läßt vermuten, daß aus sterischen Gründen die Ausbildung langer Polydiacetylenketten schwierig ist und daß sicherlich nicht alle Butadiin-Einheiten am Polymerisationsprozeß teilnehmen können (Kap. 3.5.3). Längere Polydiacetylenketten mit dazwischen liegenden Fullerenen wurden ausgehend von **101**, einem Fullerenderivat, das nur eine Diacetyleneinheiten beinhaltet, dargestellt (Kap. 3.5.4).

Die Polymerisation von Lipofullerenderivat **99** durch Belichtung mit UV-Licht wurde auch innerhalb der künstlichen Membran durchgeführt. Diese Polymerisation erfolgt bei Temperaturen oberhalb des Übergangspunkts der DPPC-MLVs, wenn die Diffusion des Lipofullerens **99** erhöht ist und Kollisionsprozesse häufiger auftreten. Perfekt sphärische Objekte (Durchmesser von 0.1 µm bis zu einigen µm) wurden erhalten. Die kleineren dieser Polylipofullerensphären (solche mit Durchmessern unter 150 nm) sind hohl, während die größeren gefüllt sind (Kap. 3.5.5).

Wenn man diese Polymerisation in Lösung ausführt, werden auch große, hohle und perfekt sphärische Polylipofullerene erhalten (Kap. 3.5.6). Es scheint, daß die Polymerisation sowohl in Lösung als auch innerhalb der Lipidmembran ein diffusionskontrollierter Prozeß ist. Das Monomer muß entweder durch die Lösung oder innerhalb der Membran diffundieren, um einen Punkt zu erreichen, wo die Polymerisation stattfinden kann. Die Ausbildung perfekt sphärischer Strukturen des Polymers sowohl innerhalb der Membran als auch in Lösung ist erstaunlich. Diese erfolgt höchstwahrscheinlich aufgrund der globulären, dreidimensionalen Struktur der Monomereinheiten. Der Hauptunterschied zwischen den beiden entstehenden Polymerstrukturen liegt darin, daß nur wenn die Polymerization in den MLVs stattfindet hohl scheinende Polylipofullerensphären mit Durchmessern unter 150 nm entstehen. Es wäre möglich, daß diese kleineren Hohlkugeln solche sind, die in kleineren Vesikeln gebildet werden. Der Inhalt von Lipofullerenen in diesen kleinen Vesikeln ist verständlicherweise begrenzt durch ihre Größe, und die Polymerisation ergibt daher nur sphärische Polymere kleiner Dimensionen. Das Vesikel ist der limitierende Faktor für das Ausmaß des Polymerisationsprozesses (Kap. 3.5.7).

Die hohlen Polylipofulleren-Kugeln scheinen eine ungewöhlich große mechanische Festigkeit aufzuweisen. Solche Lipofullerensphären können interessante Anwendungsmöglichkeiten auf verschiedenen Gebieten bieten. Zum einen könnten sie als Modellsysteme für zwei-dimensionale Polymere dienen, um gewisse theoretische Vorhersagen der Polymerphysik zu bestätigen, wie z.B. die der angenommenen temperaturinduzierten Übergänge zwischen flachen und gekrümmten Phasen. Desweiteren könnte ihre Form, Stärke und Elastizität ein Potential für lösungsmittelfreie Schmier- und Gleitmittelanwendungen darstellen. Ferner könnten sie in der Biotechnologie zum Einschluß von Enzymen eingesetzt werden, zur Erhöhung der mechanischen Stabilität von Liposomen und als Arzneimittel/Therapeutika-transportsysteme dienen.

Lipofulleren **99** ordnen sich innerhalb des Bilayers in gerüstartiger Weise als dünne Röhren an, die die gesamte Oberfläche des Vesikels überziehen. Die dünnen Röhren besitzen untereinander Anordnung Verbindungen, die hauptsächlich aus Fünfecken und Sechsecken bestehen, was an der Kohlenstoffatome in Fullerenen erinnert sind. Ähnliche Strukturen wurden häufig in natürlichen Systemen beobachtet, ihr Aufbau entspricht einem Prinzip der Architektur, das als *Tensegrität* bezeichnet wird, obwohl der Mechanismus, der zu dieser Art von Strukturen führt, noch unbekannt ist (Kap. 3.5.8).

Abschließend wurde die Synthese eines Biotin-Lipofullerens **105** begonnen, mit der Absicht, ein Transmembransystem aufzubauen, das aus einem Lipofulleren und einem biologisch aktiven, lipophoben Substituenten besteht, der die Membran durchdringen und sich auf der Oberfläche der Vesikel plazieren kann. Einmal in solche Vesikel eingeführt, könnte diese Lipofulleren-Untereinheit aufgrund ihrer Polarität die Membran durchstoßen und dieses anschließend durch bestimmte einfache *labeling*-Techniken nachgewiesen werden (Kap. 3.6).

5 Experimental Part

5.1 Instrumentation

Flash Chromatography (FC): Silica gel 60 (230-400 mesh, 0.04-0.063 nm) from Merk.

Thin Layer Chromatography (TLC): Macherey-Nagel, Alugram SIL G/UV_{254}. The compounds were visualized by irradiation with 254 or 366 nm light and/or staining with $KMnO_4$ (aq.) or I_2.

Preparative High Performance Liquid Chromatography (HPLC): i) Instrumental: Shimadzu Class-LC10 with Communication Bus Module CBM-10A, Auto Injector SIL-10A, Preparative Liquid Chromatograph LC-8A, UV-Vis Detector SPD-10A, and Fraction Colector FRC 10A. ii) Columns: Grom-Sil 100 Si, NP1, 5µ, 250x20 (20 mL/min), and Macherey-Nagel-Nucleogel GFC 500-10 (10 mL/min). iii) Solvents purchased from SDS.

Analytical High Performance Liquid Chromatography (HPLC): i) Instrumental: Shimadzu Class-LC10 with Communication Bus Module CBM-10A, Auto Injector SIL-10A, Liquid Chromatograph LC-10AT, and Diode Array Detector SPD-M10A. ii) Columns: Grom-Sil 100 Si, NP1, 5µ, 200x4 (1.5 mL/min), and Macherey-Nagel-Nucleogel GFC 500-5 (1 mL/min). iii) Solvents purchased from SDS.

IR Spectra: Bruker FT-IR IFS 88. The spectra were measured as KBr pellets or as thin films of neat compound. The absorptions are given in wavenumbers (cm^{-1}).

UV/Vis Spectra: Shimadzu UV 3102 PC. All spectra were measured as solutions in the indicated solvents. Absorption maxims (λ_{max}) are reported in nm and extinction coefficients (ε) in $M^{-1}cm^{-1}$. Shoulders are indicated (sh).

Mass Spectra: Finnigan MAT 900 FAB-modus (3-Nitrobenzylalcohol); Varian MAT 311 A EI-Modus; Fissons VG Tofspec, MALDI, negative and positive modus (α-cyano-4-hydroxycinnamic acid).

NMR spctra: JEOL JNM EX 400 and JEOL JNM GX 400 (^{1}H: 400 MHz, ^{13}C: 100.5 MHz), JEOL PMX 60 (^{1}H: 60 MHz). All spectra were recorded at room temperature (RT) in the indicated solvent containing $SiMe_4$ as standard reference. ^{1}H-NMR and ^{13}C-NMR spectra the chemical shift values are given in ppm relative to $SiMe_4$. The resonance multiplicity is

described as *s* (singlet), *d* (doublet), *t* (triplet), *q* (quartet), and *m* (multiplet). Broad resonances are indicated broad (br).

5.2 Chemicals

Reagents were of highest quality obtainable from either Aldrich, Fluka or Merck. Solvents were destilled and dried according to standard procedures[119]. HPLC solvents were purchased from SDS. Dipalmitoyl-*sn*-glycero-3-phosphatidycholine (DPPC), its fully chain-deuterated analog DPPC-d_{62}, and selectively chain-deuterated DPPC-d_8 [dipalmitoyl(7,8-$^2H_4$)-*sn*-glycero-3-phosphatidylcholine], and 10,12-octadecanoic acid were purchased from Avanti Polar Lipids (Alabaster, AL, USA). Stearic acid-d_{35} was purchased from Aldrich.

[60]Fullerene was obtained in either lab and gold grade from Hoechst.

[60]Fullerene derivatives **2**[24], **6**[30], **35-37**[25, 27], **43-46**[72], **52**[83], and dendrons **12-17**[55,61,120] were prepared according to literature procedures. Malonates (except **64**, **67**, and **80**) and bromo malonates (except **92**) were prepared according to a protocol described by F. Diederich et al.[62] with some modifications[121]. Starting from bromo malonates, [60]fullerene mono- and hexakisaddition products were obtained according the procedures described by C. Bingel[24] and A. Hirsch et al.[29] respectively. Starting directly from malonates, these were obtained according the protocols described in chapter 3.7[122].

5.3 Experimental Details

Bis[(3,5-dibenzyloxy)benzyl]malonate (23)

Pyridine (0.78 mL, 9.7 mmols) was added to a solution of 3.113 g (9.7 mmols) of [G1]-OH (**13**) in dry CH_2Cl_2 (20 mL) under Argon. The mixture was cooled with an ice bath and after that 0.47 mL (4.85 mmols) of malonyl dichloride was added dropwise within 10 min. After 2 h the ice bath was removed and the solution was stirred at room temperature overnight. The solution was extracted with water and the organic layer dried over Na_2SO_4. FC (SiO_2/CH_2Cl_2) gave 3,00 g of the malonic diesther **23**. Yield: 87 %.

^{1}H-NMR (400 MHz, RT, $CDCl_3$): δ = 3.47 (s, 2H, C*H*$_2$), 4.97 (s, 8H, ArC*H*$_2$O), 5.11 (s, 4H, C*H*$_2$O$_2$C), 6.55 (t, 2H, J = 2 Hz, Ar*H*), 6.58 (d, 4H, J= 2 Hz, Ar*H*), 7.29-7.40 (m, 20H, Ph*H*); ^{13}C-NMR (100.5 MHz, RT, $CDCl_3$): δ = 41.38 (*C*H$_2$), 66.97 (*C*H$_2$O$_2$C), 70.01 (Ar*C*H$_2$O), 101.91, 106.93 (arom. *C*H), 127.55, 128.03, 128.60 (Ph *C*H), 136.60 (Ph *C*), 137.53, 160.14 (arom. *C*), 166.22 (*C*=O); MS (EI): *m/z* = 708 (M^+), 617 (M-PhCH_2^+), 388, 320 ([G1]-OH^+),

211, 181, 91 ($PhCH_2^+$), 65, 28 (CO^+); IR (KBr): $\tilde{\nu}$ = 3088.3 cm^{-1}, 3061.6, 3031.6, 3006.7, 2985.8, 2940.8, 2894.6, 2863.4, 1751.0, 1719.5, 1596.5, 1444.7, 1332.0, 1289.1, 1195.4, 1163.6, 1061.8, 1026.8, 834.1, 809.1, 692.7.

Bis{[3,5-bis(3',5'-dibenzyloxy)benzyloxy]benzyl}malonate (24)

According to the synthesis of malonate **23**, the reaction was performed using 1.29 mL (16.0 mmols) of pyridine, 12.29 g (16.5 mmols) of [G2]-OH (**15**) in 75 mL of dry CH_2Cl_2, and 0.80 mL (8.25 mmols) of malonyl dichloride. Purification by FC (SiO_2/hexane:AcOEt 4:1 gradually increasing to hexane:AcOEt 1:1) gave 10.5 g of malonic diester **24**. Yield: 81.7 %.

^{1}H-NMR (400 MHz, RT, $CDCl_3$): δ = 3.48 (s, 2H, CH_2), 4.89 (s, 8H, ArCH_2O), 4.99 (s, 16H, PhCH_2O), 5.10 (s, 4H, ArCH_2OCO), 6.50 (t, 2H, J = 2.4 Hz, Ar*H*), 6.55 (t, 4H, J = 2.4 Hz, Ar*H*), 6.64 (d, 8H, J= 2.4 Hz, Ar*H*), 6.65 (d, 4H, J = 2.4 Hz, Ar*H*), 7.26-7.4 (m, 40H, Ph*H*); ^{13}C-NMR (100.5 MHz, RT, $CDCl_3$): δ = 41.45 (*C*H_2), 67.00 (*C*H_2O_2C), 69.90 (Ar*C*H_2O), 70.04 (Ph*C*H_2O), 101.56, 101.95, 106.37, 106.95 (arom. *C*H), 127.60, 128.03, 128.61 (Ph *C*H), 136.79 (Ph *C*), 137.53, 139.15, 160.05, 160.12 (arom. *C*), 166.27 (*C*=O); IR (film): $\tilde{\nu}$ = 3088.1 cm^{-1}, 3062.9, 3031.5, 2927.9, 2871.8, 1752.3, 1735.3, 1595.6, 1497.2, 1451.2, 1374.3, 1295.4, 1155.7, 1055.6, 831.7, 736.2, 696.3.

Bis{[3,5-bis[3',5'-bis(3'',5''-dibenzyloxy)benzyloxy]benzyloxy]benzyl}malonate (25)

According to the synthesis of malonate **23**, the reaction was performed using 0.27 mL (3.30 mmols) of pyridine, 5.264 g (3.30 mmols) of [G3]-OH (**17**), and 0.16 mL (1.65 mmols) of malonyl dichloride in 60 mL of dry CH_2Cl_2. Purification by FC (SiO_2/hexane:CH_2Cl_2 1:1 gradually increasing to CH_2Cl_2) gave 3.53 g of the malonic diester **25**. Yield: 65.7 %.

^{1}H-NMR (400 MHz, RT, $CDCl_3$): δ = 3.44 (s, 2H, CH_2), 4.82 (s, 4H, ArCH_2O), 4.86 (s, 8H, ArCH_2O), 4.94 (s, 16H, PhCH_2O), 5.06 (s, 2H, CH_2O_2C), 6.49 (t, 4H, J = 2.4Hz, Ar*H*), 6.52 (m, 10H, Ar*H*), 6.60 (d, 8H, J = 2.4 Hz, Ar*H*), 6.63 (m, 20H, J, Ar*H*), 7.20-7.53 (m, 80H, Ph*H*); ^{13}C-NMR (100.5 MHz, RT, $CDCl_3$): δ = 41.38 (*C*H_2), 66.78 (*C*H_2O), 68.17 (Ar*C*H_2O), 69.76 (Ar*C*H_2O), 69.88 (Ph*C*H_2O), 101.48, 101,78, 105.98, 106.30, 106.58, 106.69 (arom. CH), 127.48, 127.90, 128.48 (Ph *C*H), 136.74 (Ph *C*), 139.11, 139.19, 159.96, 160.00, 160.10 (arom. *C*), 166.13 (*C*=O); IR (film): $\tilde{\nu}$ = 3087.7 cm^{-1}, 3062.5, 3030.9, 3008.7, 2927.6, 2870.9, 1736.0, 1595.3, 1497.0, 1450.4, 1373.8, 1295.3, 1155.0, 1052.4, 831.1, 736.0, 696.1.

Bromo bis[(3,5-dibenzyloxy)benzyl]malonate (26)

A mixture of 2.807 g (3.96 mmols) of **23** and 0.59 mL (3.96 mmols) of DBU in 20 mL of dry THF was cooled to -78°C under argon. Then, a solution of 1.313 g (3.96 mmols) of CBr_4 in 5 mL of THF was added and the mixture stirred for 2h. The reaction was quenched with 50 mL 0.1 M HCl and the cooling bath removed. Et_2O (50 mL) was added, the organic layer extracted with sat. aq. $NaHCO_3$ (to pH ca. 6) and sat. aq. NaCl solutions, and dried over Na_2SO_4. FC (SiO_2/hexane:CH_2Cl_2 2:1) gave 2.23 g of **26** as a yellow oil and 165 mg of **23** were recovered. Yield: 71 %.

^{1}H-NMR (400 MHz, RT, $CDCl_3$): δ = 4.91 (s, 1H, C*H*Br), 4.97 (s, 8H, ArCH_2O), 5.16 (s, 4H, CH_2O_2C), 6.55-6.57 (m, 6H, Ar*H*), 7.29-7.40 (m, 20H, Ph*H*); ^{13}C-NMR (100.5 MHz, RT, $CDCl_3$): δ = 42.0 (*C*HBr), 68.39 (*C*H_2O_2C), 70.04 (Ar*C*H_2O), 102.17, 106.86 (arom. *C*H), 127.56, 128.07, 128.63 (Ph *C*H), 136.66 (Ph *C*), 136.81, 160.17 (arom. *C*), 164.30 (*C*=O); MS (EI): *m/z* = 788 (M^+), 708 (M-Br $^+$), 382, 320 ([G1]-OH^+), 303, 230, 211, 181, 91 ($PhCH_2^+$), 77 (Ph^+), 65, 51; IR (KBr): $\tilde{\nu}$ = 3091.7 cm^{-1}, 2931.4, 2872.7, 1744.6, 1596.6, 1527.7, 1351.3, 1203.4, 1158.7, 1044.4, 803.3, 732.2.

Bromo bis{[3,5-bis(3',5'-dibenzyloxy)benzyloxy]benzyl}malonate (27)

According to the procedure described for the synthesis of **26**, the reaction was performed starting with 9.5 g (6.1 mmols) of malonate **24**, and 0.91 mL (6.1 mmols) of DBU in 70 mL of THF, and a solution of 2.023 g (6.1 mmols) CBr_4 in 15 mL THF. After the work-up a not separable mixture of **27**, the corresponding dibromo malonate, and **24** was obtained with a content in **27** higher than 60 % (^{1}H-NMR). Since the dibromo malonate **27-Br** and **24** are inert against the conditions for the base catalyzed coupling to fullerenes this mixture was used for subsequent reaction with C_{60}.

Bromo bis{[3,5-bis[3',5'-bis(3'',5''-dibenzyloxy)benzyloxy]benzyloxy]benzyl}malonate (28)

A mixture of 3.28 g (1.01mmols) of malonate **25**, and 0.15 mL (1.005 mmols) of DBU in 50 mL of THF was treated with a solution of 0.335 g (1.01mmols) CBr_4 in 5 mL THF in the same way as described for compound **26**. After the work-up the crude mixture was not purify. An ^{1}H-NMR spectra showed a content of bromo malonate **28** in the crude mixture higher than 60 %.

1,2-Bis[(3,5-dibenzyloxy)benzyloxycarbonyl]methano-1,2-dihydro[60]fullerene (29)

Over a solution of 100 mg (0.139 mmols) of C_{60} in 50 mL of toluene, 165 mg (0.209 mmols) of bromo malonate **26** in 10 mL of toluene, and 35 mg (1.39 mmols) of sodium hydride were added. After 72 h stirring at room temperature the excess of sodium hydride was destroyed with sulfuric acid 2 N. The organic layer was dried over $MgSO_4$ and the solvent evaporated under reduced pressure. FC (SiO_2/toluene) afforded 5 mg (5 %) of C_{60}, 103 mg (52 %) of **29,** and 62 mg (21 %) of a mixture of regioisomeric bisadducts.

^{1}H-NMR (400 MHz, RT, $CDCl_3$): δ = 4.95 (s, 8H, ArC*H*$_2$O), 5.43 (s, 4H, C*H*$_2$O$_2$C), 6.56 (t, 2H, J = 2.5 Hz, Ar*H*), 6.70 (d, 4H, J = 2.5 Hz, Ar*H*), 7.28-7.39 (m, 20H, Ph*H*); ^{13}C-NMR (100.5 MHz, RT, $CDCl_3$): δ = 51.76 (methano bridge), 68.66 (*C*H$_2$O$_2$C), 70.08 (Ar*C*H$_2$O), 71.36 (C_{60}-sp^3 *C*), 102.28 , 107.53 (arom. *C*H), 127.60, 128.10, 128.63 (Ph *C*H), 136.59 (Ph. *C*), 136.90 (arom. *C*), 139.07, 140,92, 141.86, 142.20, 142.98, 143.01, 143.05, 143.10, 143.85, 144.56, 144.68, 144.89, 144.98, 145.11, 145.17, 145.24 (C_{60}-sp^2 *C*), 160.23 (arom. *C*), 163.39 (*C*=O); UV/VIS (CH_2Cl_2): λ_{max} = 271.0 nm, 327.0, 426.50; MS (FAB): *m/z* = 1427.5 (M^+), 719.9 (C_{60}^+); IR (KBr): $\tilde{\nu}$ = 3060.9 cm^{-1}, 3028.4, 2923.5, 2857.5, 1745.3, 1594.4, 1450.9, 1372.1, 1226.5, 1157.7, 1057.9, 831.3, 753.2, 695.5, 526.3.

1,2-Bis{[(3,5-bis(3',5'-dibenzyloxy)benzyloxy]benzyloxycarbonyl]methano-1,2-dihydro-[60]fullerene (30)

The reaction was performed as is described for **29** using 100 mg (0.139 mmols) of C_{60}, 340 mg of a mixture of **27**, **27-Br**, and **24** with a content in **27** bigger than 60 %, and 50 mg (2 mmols) of NaH. After the usual work-up, purification by FC (SiO_2/toluene gradually increasing to toluene:ethyl acetate 9:1) followed by preparative HPLC-GPC (Nucleogel GFC 500-10/ 10 mL/min toluene) gave 63 mg of **30**. Yield: 19.9 %.

^{1}H-NMR (400 MHz, RT, $CDCl_3$): δ = 4.80-4.93 (m, 28H, C*H*$_2$O), 6.49-6.65 (m, 18H, Ar*H*), 7.20-7.38 (m, 40H, Ph*H*); ^{13}C-NMR (100.5 MHz, RT, $CDCl_3$): δ = 48.59 (methano bridge), 70.05 (broad), 70.55 (*C*H$_2$O), 71.32 (C_{60}-sp^3 *C*), 101.64, 106.43, 106.49 (arom. *C*H), 127.6, 128.03, 128.61 (Ph *C*H), 136.77 (Ph *C*), 136.91 (arom. *C*), 139.02, 139.03, 140.92, 141.85, 142.18, 142,98, 143.04, 143.85, 144.52, 144.54, 144.67, 144.90, 144.95, 145.08, 145.11, 145.17, 145.22 (C_{60}-sp^2 *C*), 160.14, 160.22 (arom. *C*), 163.41 (*C*=O); UV/VIS (CH_2Cl_2): λ_{max} = 258.5 nm, 320.0, 420.5; MS (FAB): *m/z* = 2276.7 (M^+),1556.8 (M-C_{60}^+); IR (film): $\tilde{\nu}$ = 3066.3 cm^{-1}, 3033.6, 2926.2, 2855.0, 1745.8, 1647.9, 1596.8, 1497.5, 1452.8, 1374.2, 1343.7, 1322.9, 1295.7, 1269.1, 1211.0, 1159.0, 1058.1, 1029.6.

1,2-Bis{[(3,5-bis(3',5'-bis(3'',5''-dibenzyloxy)benzyloxy)benzyloxy]benzyloxycarbonyl}-methano-1,2-dihydro-[60]fullerene (31)

The reaction was performed as is described for **29** using 200 mg (0.277 mmols) of C_{60}, 1730 mg (>0.260 mmols) of bromo malonate crude mixture **28**, and 100 mg (4.17 mmols) of NaH. After the work-up, purification by FC (SiO_2/toluene:ethyl acetate 98:2) followed by preparative HPLC-GPC (Nucleogel GFC 500-10/ 10 mL/min toluene) afforded 473 mg of **31**. Yield: 42.9 %.

^{1}H-NMR (400 MHz, RT, $CDCl_3$): δ = 4.80-4.93 (m, 60H, C*H*$_2$O), 6.49-6.65 (m, 42H, Ar*H*), 7.20-7.38 (m, 80H, Ph*H*); ^{13}C-NMR (100.5 MHz, RT, $CDCl_3$): δ = 51.73 (methano bridge), 69.77 (broad), 69.88 (broad) (*C*H$_2$O), 71.29 (C_{60}-sp^3 *C*), 101.48, 101.61, 106.34, 106.42 (arom. *C*H), 127.50, 127.91, 128.49 (Ph *C*H), 136.73, 136.92 (Ph *C*, arom.*C*), 138.92, 138.98, 139.15, 140.76, 141.68, 142.00, 142.79, 142.87, 143.67, 144.37, 144.40, 144.48, 144.69, 144.83, 144.92, 144.96, 145.05 (C_{60}-sp^2 *C*), 160.03, 160.11 (arom. *C*), 163.23 (*C*=O); UV/VIS (CH_2Cl_2): λ_{max} = 426.0 nm, 327.0, 269.0; MS (FAB): *m/z* = 3974.5 (M^+); IR (film): $\tilde{\nu}$ = 3066.3 cm^{-1}, 3033.5, 2928.6, 2871.8, 1748.7, 1596.6, 1497.6, 1453.1, 1374.1, 1341.6, 1320.7, 1296.1, 1159.0, 1056.0, 908.8.

1,2:18,36:22,23:27,45:31,32:55,56-Hexakis{bis[3,5-(dibenzyloxy)benzyloxycarbonyl]-methano}-1,2,18,36, 22,23,27,45,31,32,55,56-dodecahydro[60]fullerene (32)

A mixture of 170 mg (0.236 mmols) of C_{60} and 487 mg (2.36 mmols) of DMA in 50 mL toluene was stirred at room temperature during 2h. Then, 1.654 g (2.10 mmols) of bromo malonate **26** in 20 mL of toluene and 360 mg (2.36 mmols) of DBU were added. After 96 h the solvent was evaporated under reduced pressure and the crude mixture separated by FC (SiO_2/toluene:AcOEt 98:2) followed by preparative HPLC (grom-Sil 100Si, NP1, 5μ/ 20 mL/min toluene:AcOEt 98:2) and preparative HPLC-GPC (Nucleogel GFC 500-10/ 10 mL/min toluene) to give 63 mg of the hexaadduct **32**. Yield: 5.4 %.

^{1}H-NMR (400 MHz, RT, $CDCl_3$): δ = 4.78 (s, 48H, ArC*H*$_2$O), 4.98 (s, 24H, C*H*$_2$O$_2$C), 6.42 (s, broad, 36H, Ar*H*), 7.19-7.32 (m, 120H, Ph*H*); ^{13}C-NMR (100.5 MHz, RT, $CDCl_3$): δ = 45.44 (methano bridge), 68.13 (C_{60}-sp^3 *C*), 69.25 (*C*H$_2$O$_2$C), 69.83 (Ar*C*H$_2$O), 102.27, 106.73 (arom. *C*H), 127.60, 127.90, 128.52 (Ph *C*H), 136.79 (Ph *C*), 136.80 (arom. *C*), 141.30, 145.98 (C_{60}-sp^2 *C*), 160.02 (arom. *C*), 163.37 (*C*=O); UV/Vis (CH_2Cl_2): λ_{max} = 282.5 nm, 319.0, 338.0, 384.0; MS (FAB): *m/z* = 4961 (M^+), 4254.1 (penta$^+$), 3547.5 (tetra$^+$), 2840.3

(tris$^+$); IR (film): $\tilde{\nu}$ = 3091.5 cm^{-1}, 3067.3, 3034.5, 2925.9, 2872.6, 1747.0, 1598.2, 1454.9, 1375.0, 1341.3, 1294.5, 1264.8, 1212.4, 1160.5, 1061.4, 933.1.

1,2:18,36:22,23:27,45:31,32-Pentakis{bis[3,5-(dibenzyloxy)benzyloxycarbonyl]methano}-55,56-(diethoxycarbonyl)methano-1,2,18,36,22,23,27,45,31,32,55,56-dodecahydro[60]-fullerene (33)

A mixture of 240 mg (0.273 mmols) of **2** and 563 mg (2.731 mmols) of DMA in 50 mL toluene was stirred at room temperature for 2 h. Then, 1.72 g (2.185 mmols) of bromo malonate **26** in 20 mL of toluene and 416 mg (2.731 mmols) of DBU were added. After 96 h the solvent was evaporated under reduced pressure and the crude mixture separated by FC (SiO_2/toluene:AcOEt 98:2) followed by preparative HPLC (grom-Sil 100Si, NP1, 5µ/ 20 mL/min toluene:AcOEt 99:1) to give 184 mg of the hexaaduct **33**. Yield: 15.3 %.

^{1}H-NMR (400 MHz, RT, $CDCl_3$): δ = 1.17 (t, 6H, J = 6.8 Hz, C*H*$_3$), 4.13 (q, 4H, J = 6.8 Hz, C*H*$_2$O$_2$C), 4.79 (s, 8H, ArC*H*$_2$O), 4.80 (s, 8H, ArC*H*$_2$O), 4.81 (s, 16H, ArC*H*$_2$O), 4.82 (s, 8H, ArC*H*$_2$O), 4.99 (s, 8H, C*H*$_2$O$_2$C), 5.02 (s, 4H, C*H*$_2$O$_2$C), 5.06 (s, 4H, C*H*$_2$O$_2$C), 5.12 (s, 4H, C*H*$_2$O$_2$C), 6.43-6.59 (m, 30H, Ar*H*), 7.21-7.40 (m, 100H, Ph*H*); ^{13}C-NMR (100.5 MHz, RT, $CDCl_3$): δ = 13.87 (*C*H$_3$), 41.43 (*C*H$_2$O$_2$C), 45.33, 45.36, 45.39, 45.56 (methano bridge), 62.81 (*C*H$_2$O$_2$C), 67.03, 68.14 (broad), 69.19, 69.21, 69.83, 70.04 (*C*H$_2$O$_2$C, Ar*C*H$_2$O, C$_{60}$-sp^3 *C*) 101.93, 102.27, 106.65, 106.71, 106.78, 106.96 (arom. *C*H), 127.61, 127.91, 128.07, 128.26, 128.51, 128.63 (Ph *C*H)**,** 136.71, 136.80, 136.84, 136.88 (arom. *C*, Ph *C*), 141.20, 141.23, 141.30, 141.48, 145.84, 145.89, 145.97, 146.02, 146.06 (C$_{60}$-sp^2 *C*), 163.40, 163.49, 163.63 (arom. *C*), 166.27 (*C*=O); UV/Vis (CH_2Cl_2): λ_{max} = 282.0 nm, 319.0, 337.5, 384.5; MS (FAB): *m/z* = 4435.12 (M+Na$^+$); IR (film): $\tilde{\nu}$ = 3067.0 cm^{-1}, 3034.4, 2935.3, 2873.2, 1746.9, 1597.9, 1498.0, 1453.7, 1374.7, 1343.1, 1320.5, 1294.2, 1264.6, 1209.5, 1160.7, 1080.2, 1061.9, 1029.6, 908.7.

Allyl 3,5-(dibenzyloxy)benzyl ether (58)

To a slurry of 7.8 g (195 mmols) NaH (60 % in paraffin-oil) in 150 mL THF, 31.23 g (94.47 mmols) of 3,5-(dibenzyloxy)benzyl alcohol (**13**) in 150 mL THF were added. The mixture was stirred under reflux for 30 min, and then 16.9 mL (195 mmols) of 3-bromoprop-1-ene were added at once. Then reflux was maintained for 24 h. H_2O was carefully added, the resulting mixture extracted 3 times with Et_2O, the combined extract dried over anhydrous Na_2SO_4 and

the solvent evaporated under reduced pressure[123]. FC (SiO_2/hexane:ethyl acetate 95:5) gave 34.64 g (98.6 %) of **58** as a colorless oil.

^{1}H-NMR (400 MHz, RT, $CDCl_3$): δ = 4.99 (dd, 2H, J_1= 6 Hz, J_2= 1.6 Hz, C*H*$_2$CH=), 4.45 (s, 2H, ArC*H*$_2$O), 5.01 (s, 4H, PhC*H*$_2$O), 5.17-5.21 (m, 1H, C*H*H=), 5.26-5.31 (m, 1H, CH*H*=), 5.88-55.99 (m, 1H, C*H*=CH$_2$), 6.54 (t, 1H, J= 2 Hz, Ar*H*), 6.62 (d, 2H, J= 2 Hz, Ar*H*), 7.29-7.42 (m, 10H, *Ph*); ^{13}C-NMR (100.5 MHz, RT, $CDCl_3$): δ = 69.96 (Ph*C*H$_2$), 71.02 (Ar*C*H$_2$), 71.89 (*C*H$_2$-CH=), 101.27, 106.49 (arom. *C*H), 117.17 (CH=*C*H$_2$), 127.54, 127.96, 128.56 (Ph *C*H), 134.67 (*C*H=CH$_2$), 136.90 (Ph *C*), 140.83, 160.07 (arom. *C*); MS (EI): *m/z* = 360 (M^+), 304, 181, 91; IR (film): $\tilde{\nu}$ = 3065.0 cm^{-1}, 3032.5, 2924.5, 2860.9, 1585.8, 1497.6, 1452.1, 1376.2, 1293.0, 1158.1, 1058.7, 926.0, 832.1, 737.1, 696.9.

3-[3',5'-Di(benzyloxy)benzyloxy]propanol (<u>59</u>)

A 500 mL three necked flask provided with addition funnel, argon inlet, reflux condenser, rubber septum, and stirring bar was charged with 100 mL of a 0.5 M solution (50 mmols) of 9-BBN in THF. Then a solution of 16.643 g (46.172 mmols) of **58** in 75 mL of THF was added dropwise at room temperature and the resulting mixture stirred for 14 h[124]. The intermediate organoboran was oxidized by adding successively 3 mL of ethanol, 1 mL of a 6 M aqueous solution of sodium hydroxide, and 2 mL of 30 % hydrogen peroxide (x10). The mixture was heated for 3 h at 50°C and after that cooled to room temperature. The aqueous layer was saturated with potassium carbonate[123]. Then the organic layer was separated, dried over Na_2SO_4 and the solvent evaporated under reduced pressure. FC (SiO_2/hexane:ethyl acetate 3:2) yielded 15.70 g of **59** as a colorless oil. Yield: 89.9 %.

^{1}H-NMR (400 MHz, RT, $CDCl_3$): δ = 1.81 (tt, 2H, J_1=J_2= 6 Hz, C*H*$_2$), 2.45 (br, 1H, O*H*), 3.58 (t, 2H, J= 6 Hz, C*H*$_2$O), 3.72 (t, 2H, J=6 Hz, C*H*$_2$OH), 4.42 (s, 2H, ArC*H*$_2$O), 4.99 (s, 4H, PhC*H*$_2$O), 6.53 (t, 1H, J= 2 Hz, Ar*H*), 6.30 (d, 2H, J= 2 Hz, Ar*H*), 7.27-7.41 (m, 10H, *Ph*); ^{13}C-NMR (100.5 MHz, RT, $CDCl_3$): δ = 32.02 (*C*H$_2$), 61.29 (*C*H$_2$OH), 69.86 (*C*H$_2$O), 69.89 (*C*H$_2$Ph), 72.92 (Ar*C*H$_2$), 101.22, 106.37 (arom. *C*H), 127.46, 127.90, 128.50 (Ph *C*H), 136.79 (Ph *C*), 140.61, 160.03 (arom. *C*); MS (EI): *m/z* = 378 (M^+), 320. 304, 211, 181, 127, 91, 71; IR (film): $\tilde{\nu}$ = 3415.3 cm^{-1}, 3089.3, 3064.4, 3032.8, 2928.0, 2869.6, 1595.8, 1497.8, 1452.7, 1375.4, 1293.1, 1214.4, 1156.6, 1059.4, 832.5, 738.4, 697.3.

3-Bromo-1-[3',5'-di(benzyloxy)benzyloxy]propane (60)

To a mixture of 9,335 g (24.665 mmols) of alcohol **59** and 9.8 g (29.55 mmols) of carbon tetrabromide in 150 mL THF, 7.75 g (29.60 mmols) of triphenylphosphine were added. The reaction was stirred at room temperature under Argon for 40 minutes. A TLC control showed the presence of starting alcohol **59** in the reaction mixture. Then, 0.818 g (2.47 mmols) of CBr_4, and 0.647 g (2.47 mmols) of PPh_3 were added and the reaction was stirred for another 40 minutes until TLC showed no starting material. The reaction mixture was then poured into water and extracted with CH_2Cl_2 (3x); the combined extracts were dried with Na_2SO_4, filtrated and evaporated to dryness[55]. FC (SiO_2/hexane:CH_2Cl_2 1:1) afforded 10.26 g of **60** as a yellow oil (94.2 %).

^{1}H-NMR (400 MHz, RT, $CDCl_3$): δ = 2.10 (tt, J_1=J_2= 6.4 Hz, *CH₂*), 3.50 (t, J=6.4 Hz, *CH₂*Br), 3.56 (t, J=6.4 Hz, *CH₂*O), 4.44 (s, 2H, C*H₂*Ar), 5.03 (s, 4H, C*H₂*Ph), 6.55 (t, 1H, J=2.4 Hz, Ar*H*), 6.58 (d, 2H, J=2.4 Hz, Ar*H*), 7.29-7.43 (m, 10H, *Ph*); ^{13}C-NMR (100.5 MHz, RT, $CDCl_3$): δ = 30.59 (*C*H_2), 32.78 (*C*H_2Br), 67.61 (*C*H_2O), 70.00 (*C*H_2Ph), 72.92 (*C*H_2Ar), 101.30, 106.44 (arom. *C*H), 127.53, 127.99, 128.60 (Ph *C*H), 136.90 (Ph *C*), 140.77, 160.10 (arom. *C*); MS (EI): *m/z* = 442 (M^+), 304, 181, 91; IR (film): $\tilde{\nu}$ = 3088.9 cm^{-1}, 3064.4, 3032.3, 2910.2, 2866.9, 1596.0, 1497.5, 1452.5, 1375.0, 1318.8, 1292.3, 1257.4, 1213.3, 1158.0, 1107.4, 1080.8, 1060.2, 1028.4, 832.4, 736.8, 697.1.

3,5-Bis[3'-[3'',5''-(dibenzyloxy)benzyloxy]propoxy]benzyl alcohol (61)

A solution of 1.71 g (12.20 mmols) of 3,5-dihydroxybenzyl alcohol, 10.8 g (24.47 mmols) of **60**, 4.215 g (30.5 mmols) of dried potassium carbonate, and 0.2 g (0.76 mmols) of 18-crown-6 in 80 mL of dry acetone was boiled stirring vigorously under nitrogen till no starting material or monoalkylated product was observed by TLC (72 h). The mixture was dried using reduced pressure, the residue divided between water and CH_2Cl_2, and the aqueous layer extracted with CH_2Cl_2 (x3). The combined organic layers were dried over Na_2SO_4 and evaporated to dryness[123]. FC (SiO_2/hexane:ethyl acetate 3:2) gave 10.15 g of alcohol **61**. Yield: 96.6 %.

^{1}H-NMR (400 MHz, RT, $CDCl_3$): δ = 2.00 (t, 4H, J=6 Hz, *CH₂*), 2.10 (t, 1H, J=5 Hz, -O*H*), 3.57 (t, 4H, J=6 Hz, *CH₂*O), 3.98 (t, 4H, J= 6 Hz, *CH₂*), 4.40 (s, 4H, C*H₂*Ar), 4.44 (d, 2H, J=5 Hz, C*H₂*OH), 4.93 (s, 8H, C*H₂*Ar), 6.37 (t, 1H, J=2.4 Hz, Ar*H*), 6.43 (d, 2H, J=2.4 Hz, Ar*H*), 6.51 (t, 2H, J=2.4 Hz, Ar*H*), 6.56 (d, 4H, J=2.4 Hz, Ar*H*), 7.24-7.37 (m, 20 H, *Ph*); ^{13}C-NMR (100.5 MHz, RT, $CDCl_3$): δ = 29.46 (*C*H_2), 64.62, 64.87, 66.62 (*C*H_2O), 69.80 (*C*H_2Ph), 72.70 (*C*H_2Ar), 100.34, 101.15, 104.95, 106.32 (arom. *C*H), 127.43, 127.84, 128.44

(Ph *C*H), 136.78 (Ph *C*), 140.84, 143.41, 159.93, 160.21 (arom. *C*); MS (FAB+): *m/z* = 860 (M^+); IR (film): $\tilde{\nu}$ = 3448.2 cm^{-1}, 3088.5, 3063.8, 3032.4, 2930.8, 2870.9, 1596.3, 1497.5, 1452.5, 1375.9, 1319.1, 1293.2, 1214.9, 1160.1, 1104.2, 1081.7, 1059.6, 832.6, 737.6, 697.4.

Allyl 3,5-bis[3'-[3",5"-(dibenzyloxy)benzyloxy]propoxy]benzyl ether (62)

According to the same procedure described for **58**, the reaction was performed using 10.052 g (11.674 mmols) of **61**, 0.8 g (20 mmols) of NaH (60 % in paraffin-oil), and 17.5 mL (20 mmols) of allyl bromide in 100 mL THF. FC (SiO_2/hexane:ethyl acetate 4:1) yielded 10.057 g of **62**. Yield: 95.6 %.

^{1}H-NMR (400 MHz, RT, $CDCl_3$): δ = 2.02 (tt, 4H, J_1= J_2= 6 Hz, *CH*$_2$), 3.59 (t, 4H, J= 6 Hz, *CH*$_2$OCH$_2$), 3.96 (ddd, 2H, J_1=5.6 Hz, J_2=J_3=1.6 Hz, C*H*$_2$-CH=), 4.38 (s, 2H, C*H*$_2$Ar), 4.23 (s, 4H, C*H*$_2$Ar), 4.97 24 (s, 8H, C*H*$_2$Ar), 5.17 (dtd, 1H, J_1=10.0 Hz, J_2=J_3=1.6 Hz, C*H*H=), 5.28 (dtd, 1H, J_1=17.6 Hz, J_2=J_3=1.6 Hz, C*H*H=), 5.91 (ddt, 1H, J_1=17.6 Hz, J_2=10 Hz, J_3=5.6 Hz, C*H*=CH$_2$), 6.39 (t, 1H, J=2 Hz, Ar*H*), 6.48 (d. 2H, J=2 Hz, Ar*H*), 6.52 (t, 2H, J=2 Hz, Ar*H*), 6.58 (d, 4H, J=2 Hz, Ar*H*), 7.26-7.39 (m, 20 H, *Ph*); ^{13}C-NMR (100.5 MHz, RT, $CDCl_3$): δ = 29.55 (*C*H$_2$), 64.70, 66.75, 69.86, 70.96, 71.87, 72.79 (*C*H$_2$O), 100.51, 101.21, 105.87, 106.32 (arom. *C*H), 117.01 (*C*H$_2$=CH-), 127.46, 127.88, 128.49 (Ph *C*H), 134.69 (CH$_2$=*C*H-), 136.86 (Ph *C*), 140.65 (CH$_2$=*C*H-), 140.92, 160.01, 160.22 (arom. *C*); MS (EI): *m/z* = 900 (M^+), 303, 213, 181, 163, 123, 91, 65; IR (film): $\tilde{\nu}$ = 3088.3 cm^{-1}, 3064.4, 3032.5, 2930.6, 2867.1, 1596.1, 1497.7, 1452.7, 1375.6, 1319.5, 1293.0, 1214.9, 1159.9, 1102.0, 1060.7, 929.1, 832.8, 737.4, 697.4.

3-{3',5'-Bis[3"-[bis(3"',5"'-dibenzyloxy)benzyl]propoxy]benzyloxy}propanol (63)

According to the same procedure described for **59**, the reaction was performed starting with 9.12 g (10.123 mmols) of allyl ether **62** dissolved in 100 mL THF, and 23 mL of 9-BBN 0.5M (11.5 mmols). After the oxidation step, the crude mixture was purified by FC (SiO_2/hexane:ethyl acetate 3:2) to furnish 8.09 g of **63** (87 %).

^{1}H-NMR (400 MHz, RT, $CDCl_3$): δ = 1.81 (tt, 2H, J_1=J_2= 6 Hz, C*H*$_2$), 2.03 (tt, 4H, J_1=J_2= 6 Hz, C*H*$_2$), 2.30 (bs, 1H, O*H*), 3.58 (t, 2H, J=6 Hz, C*H*$_2$OH), 3.60 (t, 4H, J=6 Hz, C*H*$_2$O), 3.73 (t, 2H, J=6 Hz, C*H*$_2$O), 4.02 (t, 4H, J=6 Hz, C*H*$_2$OAr), 4.37 (s, 2H, C*H*$_2$Ar), 4.44 (s, 4H, C*H*$_2$Ar), 4.98 (s, 8H, C*H*$_2$Ph), 6.38 (t, 1H, J=2 Hz, Ar*H*), 6.45 (d, 2H, J=2 Hz, Ar*H*), 6.53 (t, 2H, J=2.4 Hz, Ar*H*), 6.58 (d, 4H, J=2.4 Hz, Ar*H*), 7.27-7.40 (m, 20H, *Ph*); ^{13}C-NMR (100.5 MHz, RT, $CDCl_3$): δ = 29.54, 31.98 (*C*H$_2$), 61.57 (*C*H$_2$OH), 64.72 (*C*H$_2$OAr), 66.77, 69.04

(*C*H_2O*C*H_2), 69.90 (*C*H_2Ph), 72.81, 73.00 (*C*H_2Ar), 100.52, 101.20, 105.82, 106.36 (arom. *C*H), 127.51, 127.92, 128.52 (Ph *C*H), 136.86 (Ph *C*), 140.46, 140.91, 160.02, 160.27 (arom. *C*); MS (EI): *m/z* = 918 (M^+), 91, 65, 43; IR (film): $\tilde{\nu}$ = 3462.1 cm^{-1}, 3088.3, 3063.6, 3032.3, 3008.0, 2930.2, 2868.4, 1597.9, 1497.5, 1452.5, 1375.0, 1319.1, 1293.0, 1214.9, 1150.2, 1102.2, 1082.0, 1058.9, 832.3, 737.4, 697.3.

Bis{3-[3',5'-di(benzyloxy)benzyloxy]propyl}malonate (64)

To a slurry of 450 mg (11.25 mmols) NaH (60 % in paraffin-oil) in 20 mL of dry THF under Argon were added 4.05 g (10.70 mmols) of **59** in 50 mL of dry THF. The mixture was stirred at room temperature for 45 min and then added via double-ended needle to another flask which contained 0.51 mL (5.243 mmols) of malonyl dichloride in 20 mL dry THF under Argon[125]. The resulting mixture was stirred for 3 h at room temperature. After that 100 mL HCl 0.1M were carefully added and then the resulting mixture extracted 3 times with Et_2O. The combined extract was washed with saturated solution of $NaHSO_4$, dried over Na_2SO_4 and the solvent evaporated under reduced pressure. FC (SiO_2/hexane:ethyl acetate 3:1) gave 4.027 g (93.1 %) **64** as an oil.

^{1}H-NMR (400 MHz, RT, $CDCl_3$): δ = 1.92 (tt, 4H, J_1=J_2= 6 Hz, C*H*$_2$), 3.34 (s, 2H, C*H*$_2$), 3.50 (t, 4H, J= 6 Hz, C*H*$_2$O), 4.25 (t, 4H, J=6 Hz, C*H*$_2$OOC), 4.42 (s, 4H, ArC*H*$_2$O), 5.02 (s, 8H, PhC*H*$_2$O), 6.54 (t, 2H, J= 2 Hz, Ar*H*), 6.57 (d, 4H, J= 2 Hz, Ar*H*), 7.29-7.43 (m, 20H, *Ph*); ^{13}C-NMR (100.5 MHz, RT, $CDCl_3$): δ = 28.83, 41.46, 62.71, 66.42, 70.02, 72.88 (*C*H_2), 101.27, 106.48 (arom. *C*H), 127.58, 128.01, 128.61 (Ph *C*H), 136.92 (Ph *C*), 140.82, 160.12 (arom. *C*), 166.62 (*C*=O); MS (EI): *m/z* = 824 (M^+), 644, 577, 492, 446, 378, 304, 211, 181, 91, 65; IR (film): $\tilde{\nu}$ = 3089.2 cm^{-1}, 3064.4, 3032.9, 2929.7, 2868.1, 1734.1, 1595.9, 1497.9, 1453.7, 1375.0, 1331.0, 1293.0, 1244.7, 1157.6, 1107.6, 1085.5, 833.1, 738.8, 697.8.

Bromo bis{3-[3',5'-di(benzyloxy)benzyloxy]propyl}malonate (66)

According to the procedure described for the synthesis of **26**, the reaction was performed starting with 3.8 g (4.606 mmols) of malonate **64** and 0.69 mL (4.618 mmols) of DBU in 30 mL of THF, and a solution of 1.53 g (4.613 mmols) CBr_4 in 30 mL THF. FC (SiO_2/hexane:ethyl acetate 3:1) gave 3.02 g (72.5 %) of **66** as a yellow oil.

^{1}H-NMR (400 MHz, RT, $CDCl_3$): δ = 1.88 (tt, 4H, J_1=J_2= 6 Hz, C*H*$_2$), 3.48 (t, 4H, J= 6 Hz, C*H*$_2$O), 4.31 (t, 4H, J=6 Hz, C*H*$_2$OOC), 4.40 (s, 4H, ArC*H*$_2$O), 4.81 (s, 1H, C*H*Br), 5.00 (s, 8H, PhC*H*$_2$O), 6.54 (t, 2H, J= 2 Hz, Ar*H*), 6.56 (d, 4H, J= 2 Hz, Ar*H*), 7.27-7.41 (m, 20H,

Ph); ^{13}C-NMR (100.5 MHz, RT, $CDCl_3$): δ = 28.61 (*C*H_2), 42.06 (*C*HBr), 64.21, 66.00, 69.91, 72.81 (*C*H_2), 101.22, 106.49 (arom. *C*H), 127.47, 127.90, 128.51 (Ph *C*H), 136.84 (Ph *C*), 140.66, 160.04 (arom. *C*), 164.51 (*C*=O); MS (EI): *m/z* = 904 (M^+), 824, 664, 586, 304, 181, 91; IR (film): $\tilde{\nu}$ = 3089.0 cm^{-1}, 3064.0, 3032.4, 2959.5, 2927.2, 2867.7, 1742.1, 1595.7, 1497.7, 1452.9, 1376.0, 1293.6, 1156.5, 1107.6, 1059.3, 909.2, 832.7, 738.1, 697.4.

Bis-3-{3',5'-bis[3''-[bis(3''',5'''-dibenzyloxy)benzyl]propoxy]benzyloxy}propyl-malonate (67)

According to the same procedure described for **64**, the reaction was carried out with the following amounts of reagents: 5.02 g (5.462 mmols) of **63** and 220 mg (5.5 mmols) of NaH (60 % in paraffin-oil) in 30 mL THF, and 0.265 mL (2.724 mmols) of malonyl dichloride in 20 mL THF. FC (SiO_2/hexane:ethyl acetate 3:1) gave 2.389 g of **67** as a dense oil. Yield: 46.0 %.

^{1}H-NMR (400 MHz, RT, $CDCl_3$): δ = 1.90 (tt, 4H, J_1= J_2= 6 Hz, *CH*$_2$), 2.02 (tt, 8H, , J_1= J_2= 6 Hz, *CH*$_2$), 3.31 (s, 2H, CO*CH*$_2$CO), 3.46 (t, 4H, J= 6 Hz, *CH*$_2$OCH_2), 3.59 (t, 8H, J= 6 Hz, *CH*$_2$OCH_2), 4.01 (t, 8H,J= 6 Hz, *CH*$_2$OAr), 4.23 (t, 4H, J= 6 Hz, *CH*$_2$OOC), 4.35 (s, 4H, C*H*$_2$Ar), 4.24 (s, 8H, C*H*$_2$Ar), 4.96 (s, 16H, C*H*$_2$Ph), 6.38 (t, 2H, J=2.4 Hz, Ar*H*), 6.45 (d, 4H, J=2.4 Hz, Ar*H*), 6.52 (t, 4H, J=2.4 Hz, Ar*H*), 6.57 (d, 8H, J=2.4 Hz, Ar*H*), 7.25-7.40 (m, 40 H, *Ph*); ^{13}C-NMR (100.5 MHz, RT, $CDCl_3$): δ = 28.70, 29.52; 41.26 (*C*H_2), 62.61 (*C*H_2OOC), 64.67 (*C*H_2OAr), 66.31 (*C*H_2OCH_2), 66.73 (*C*H_2OCH_2), 69.83 (*C*H_2Ph), 72.75 (2x*C*H_2Ar), 100.37, 101.16, 105.80, 106.30 (arom. *C*H), 127.44, 127.85, 128.46 (Ph *C*H), 136.83 (Ph *C*), 140.58, 140.91, 159.97, 160.20 (arom. *C*), 166.47 (*C*=O); MS (FAB+): *m/z* = 2039 (M+Cs^+), 1906 (M^+); IR (film): $\tilde{\nu}$ = 3088.9 cm^{-1}, 3064.2, 3032.7, 2930.1, 2867.8, 1749.8, 1733.3, 1596.1, 1497.7, 1452.8, 1375.8, 1293.0, 1214.9, 1157.5, 1105.2, 1060.1, 910.1, 831.8, 737.9, 697.2, 666.0.

1,2-Bis{3-[3',5'-di(benzyloxy)benzyloxy]propoxycarbonyl}methano-1,2-dihydro-[60]fullerene (68)

The reaction was performed as is described for compound **29**, using 62 mg (0.086 mmol) of C_{60}, 110 mg (0.122 mmol) of bromo malonate **66**, and 20 mg (0.833 mmols) of NaH. Purification by FC (SiO_2/toluene:ethyl acetate 98:2) afforded 23 mg (36.5 %) of C_{60}, 55 mg (41.4 %) of **68**, and 31 mg (15.2 %) of a mixture of the corresponding bisadducts.

^{1}H-NMR (400 MHz, RT, $CDCl_3$): δ = 2.11 (tt, 4H, J_1=J_2= 6 Hz, C*H*$_2$), 3.59 (t, 4H, J= 6 Hz, C*H*$_2$O), 4.58 (t, 4H, J=6 Hz, C*H*$_2$OOC), 4.61 (s, 4H, ArC*H*$_2$O), 5.01 (s, 8H, PhC*H*$_2$O), 6.52 (t,

2H, J= 2 Hz, Ar*H*), 6.58 (d, 4H, J= 2 Hz, Ar*H*), 7.29-7.42 (m, 20H, *Ph*); ^{13}C-NMR (100.5 MHz, RT, $CDCl_3$): δ = 28.97 (*C*H_2), 52.28 (methano bridge), 64.57, 66.39, 70.03 (*C*H_2), 71.54 (C_{60}-sp^3 *C*), 73.02 (*C*H_2), 101.30, 106.43 (arom. *C*H), 127.61, 128.03, 128.62 (Ph *C*H), 136.89 (Ph *C*), 138.98 (C_{60}-sp^2 *C*), 140.72 (arom. *C*), 140.97, 141.89, 142.23, 143.02, 143.05, 143.90, 144.63, 144.66, 144.73, 144.93, 145.13, 145.23, 145.29 (C_{60}-sp^2 *C*), 160.16 (arom. *C*), 163.65 (*C*=O), UV/Vis (CH_2Cl_2): λ_{max} (ε) = 259.0 nm (126865), 327.5 (38775), 426.0 (2925), 484.5 (1725); MS (MALDI-TOF): *m/z* = 1543.71 (M^+); IR (KBr): $\tilde{\nu}$ = 3087.5 cm^{-1}, 3061.7, 3029.3, 2955.1, 2923.6, 2857.0, 1743.8, 1593.8, 1496.5, 1451.8, 1374.5, 1291.6, 1266.8, 1233.2, 1155.3, 1105.7, 1058.5, 830.1, 735.9, 696.1, 526.4.

1,2:18,36:22,23:27,45:31,32:55,56-Hexakis{bis{3-[3',5'-di(benzyloxy)benzyloxy]propoxy-carbonyl}methano}-1,2,18,36, 22,23,27,45,31,32,55,56-dodecahydro[60]fullerene (<u>69</u>)

According to the synthesis of **32**, the reaction was carried out with 130 mg (0.180 mmol) of C_{60}, 370 mg (1.804 mmol) of DMA, 1.5 g (1.667 mmol) of the bromo malonate **66**, and 0.276 mL (1.849 mmol) of DBU in 90 mL of toluene. After 72 h, The crude mixture was separated first by FC (SiO_2/toluene:AcOEt 98:2 increasing to 9:1) followed by preparative HPLC (Grom-Sil 100 Si, NP1, 5μ/ 20 mL/min toluene:ethyl acetate 95:5) to afford 130 mg of the hexaadduct **69** as a yellow glass. Yield: 12.7 %.

^{1}H-NMR (400 MHz, RT, $CDCl_3$): δ = 1.88 (tt, 24H, J_1=J_2= 6 Hz, C*H*$_2$), 3.40 (t, 24H, J= 6 Hz, C*H*$_2$O), 4.28 (t, 24H, J=6 Hz, C*H*$_2$OOC), 4.33 (s, 24H, ArC*H*$_2$O), 5.94 (s, 48H, PhC*H*$_2$O), 6.48 (t, 12H, J= 2 Hz, Ar*H*), 6.53 (d, 24H, J= 2 Hz, Ar*H*), 7.22-7.36 (m, 120H, *Ph*); ^{13}C-NMR (100.5 MHz, RT, $CDCl_3$): δ = 28.78 (*C*H_2), 45.37 (methano bridge), 64.27, 66.41 (*C*H_2), 69.14 (C_{60}-sp^3 *C*), 69.90, 72.84 (*C*H_2), 101.27, 106.41 (arom. *C*H), 127.51, 127.89, 128.53 (Ph *C*H), 136.93 (Ph *C*), 140.81 (arom. *C*), 141.22, 145.89 (C_{60}-sp^2 *C*), 160.03 (arom. *C*), 163.69 (*C*=O); UV/Vis (CH_2Cl_2): λ_{max} (ε) = 270.0 nm (99650), 281.5 (112680), 319.5 (52100), 337.0 (41650), 387.0 (5650); MS (MALDI-TOF): *m/z* = 5681 ($M+Na^+$), 5658 ($M^{+)}$; IR (KBr): $\tilde{\nu}$ = 3087.9cm^{-1}, 3062.7, 3031.3, 3006.8, 2956.1, 2924.6, 2865.3, 1743.9, 1595.4, 1497.3, 1452.8, 1375.2, 1292.1, 1264.8, 1214.5, 1156.1, 1106.9, 1079.9, 1059.3, 831.4, 737.0, 714.3, 697.2, 528.4.

1,2-Bis{3-{3',5'-bis[3''-[bis(3''',5'''-dibenzyloxy)benzyl]propoxy]benzyloxy}propoxy-oxycarbonyl}methano-1,2-dihydro-[60]fullerene (70)

To a mixture of 36 mg of C_{60} (0.05 mmols), 17 mg (0.05 mmols) of CBr_4, and 95 mg (0.05 mmols) of malonate **67** in 40 mL toluene, 9 µl (0.06 mmols) of DBU were added. After 24 hours the solvent was destilled under reduced pressure and the crude mixture was separated by FC (SiO_2/toluene increasing to toluene:ethyl acetate 9:1) to yield 55 mg of [60]fullerene monoadduct **70**. Yield: 42 %.

^{1}H-NMR (400 MHz, RT, $CDCl_3$): δ = 2.02 (tt, 8H, J_1= J_2= 6 Hz, *CH*$_2$), 2.10 (tt, 4H, , J_1= J_2= 6 Hz, *CH*$_2$), 3.56 (t, 4H, J= 6 Hz, *CH*$_2$OCH$_2$), 3.59 (t, 8H, J= 6 Hz, *CH*$_2$OCH$_2$), 4.01 (t, 8H, J= 6 Hz, *CH*$_2$OAr), 4.36 (s, 4H, C*H*$_2$Ar), 4.43 (s, 8H, C*H*$_2$Ar), 4.58 (t, 4H, J= 6 Hz, *CH*$_2$OOC), 4.98 (s, 16H, C*H*$_2$Ph), 6.36 (t, 2H, J=2 Hz, Ar*H*), 6.44 (d, 4H, J=2 Hz, Ar*H*), 6.52 (t, 4H, J=2.4 Hz, Ar*H*), 6.57 (d, 8H, J=2.4 Hz, Ar*H*), 7.23-7.40 (m, 40 H, *Ph*); ^{13}C-NMR (100.5 MHz, RT, $CDCl_3$): δ = 28.92, 29.63 (*C*H$_2$), 52.30 (methano bridge), 64.56 (*C*H$_2$COO), 64.80 (*C*H$_2$OAr), 66.37, 66.90 (*C*H$_2$OCH$_2$), 69.97 (*C*H$_2$Ph), 71.50 (C_{60}-sp^3 *C*), 72.87, 73.05 (*C*H$_2$Ar), 100.52, 101.23, 105.97, 106.39 (arom. *C*H), 127.57, 127.98, 128.58 (Ph *C*H), 136.90 (Ph *C*), 140.53 (arom. *C*), 140.92 (C_{60}-sp^2 *C*), 140.99 (arom. *C*), 141.84, 142.16, 142.96, 142.99, 143.84, 144.57, 144.60, 144.67, 144.87, 145.07, 145.16, 145.22, 145.26 (C_{60}-sp^2 *C*), 160.08, 160.13 (arom. *C*), 163.61 (*C*=O); UV/Vis (CH_2Cl_2): λ_{max} = 259.5, 326.5, 425.5, 489.5; MS (FAB+): *m/z* = 2756 (M+Cs$^+$); IR (film): $\tilde{\nu}$ = 3087.4 cm^{-1}, 3061.7, 3029.9, 2925.4, 2860.8, 1744.2, 1594.8, 1496.9, 1451.4, 1374.3, 1292.2, 1234.3, 1158.2, 1103.7, 1059.4, 830.5, 736.7, 696.5, 526.5.

1,2-{[1'-Methoxycarbonyl-1´-[2-[4-[5-[10,15,20-triphenylporphyrinatozinc(II)]]]-phenoxy]ethoxycarbonyl]methano}-18,36:22,23:27,45:31,32:55,56-pentakis{bis{3- [3',5'-di(benzyloxy)benzyloxy]propoxycarbonyl}methano}-1,2:18,36:22,23:27,45:31,32:55,56-dodecaahydro[60]fullerene (71)

A mixture of 100 mg (0.0642 mmols) of **52** and 120 mg (0.578 mmols) of DMA in 50 mL toluene was stirred at room temperature for 2 h. Then 523 mg (0.578 mmols) of bromo malonate **66** in 10 mL of toluene, and 86 µl (0.578 mmols) of DBU were added. After 4 days the solvent was evaporated under reduced pressure and the crude mixture separated by FC (SiO_2/toluene increasing to toluene:ethyl acetate 95:5) followed by preparative HPLC (grom-Sil 100Si, NP1, 5µ/ 20 mL/min toluene:ethyl acetate 95:5) to give 47 mg of the porphyrin-dendrimer-[60]fullerene **71**. Yield: 12.7 %.

^{1}H-NMR (400 MHz, RT, $CDCl_3$): δ = 1.87 (m, 20H, dendrimer C*H*$_2$), 3.41 (m, 20H, dendrimer C*H*$_2$), 4.13 (s, 3H, C*H*$_3$), 4.29 (m, 42H, C*H*$_2$ dendrimer, C*H*$_2$ porphyrin), 4.82 (br, 2H, C*H*$_2$ porphyrine), 4.89 (m, 40H, C*H*$_2$ dendrimer), 6.42 (m, 30H, dendrimer Ar*H*), 7.25 (m, 102H, dendrimer *Ph*, porphyrine *Ph*), 7.70 (m, 9H, porphyrin *Ph*), 8.09 (m, 2H, porphyrin *Ph*), 8.17 (m, 6H, porphyrin *Ph*), 8.91 (m, 8H, porphyrin *β*-Pyrrol); ^{13}C-NMR (100.5 MHz, RT, $CDCl_3$): δ = 28.52, 28.85 (*C*H$_2$), 45.20, 45.46 (methano bridge), 50.77 (*C*H$_3$O), 64.30, 65.98, 66.31, 66.42 (*C*H$_2$O), 69.18 (C$_{60}$-sp^3 *C*), 69.93, 72.87 (*C*H$_2$O), 101.23, 106.25, 106.39, 112.70 (arom. *C*H), 120.81, 120.90 (porphyrin bridge *C*), 126.47, 127.47, 127.85, 128.49 (Ph *C*H), 131.87, 131.96 (pyrrol *C*H), 134.48, 135.61 (Ph *C*H), 136.76, 136.79, 136.85 (Ph *C*), 140.422, 140.56, 140.69, 140.74, 140.92 (arom. *C*), 141.10, 141.19, 141.31 (C$_{60}$-sp^2 *C*), 142.97 (pyrrol *C*), 145.64, 145.87, 145.94, 146.13 (C$_{60}$-sp^2 *C*), 150.03, 150.33 (Ph *C*), 157.87, 159.82, 159.91, 159.95 (arom. *C*), 163.61, 164.14 (*C*=O); UV/Vis (CH_2Cl_2): λ_{max} = 270.5, 283.0, 314.5 (sh), 337.5 (sh), 400.0 (sh), 422.0, 551.0, 590.5; MS (MALDI-TOF): *m/z* = 5669 (M^+); 4844 (M-$C_{51}H_{50}O_{10}^+$).

1,2-{[1'-Methoxycarbonyl-1´-[2-[4-[5-[10,15,20-triphenylporphyrinatozinc(II)]]]-phenoxy]ethoxycarbonyl]methano}-18,36:22,23:27,45:31,32:55,56-pentakis{bis{3-{3',5'-bis[3"-[bis(3"',5"'-dibenzyloxy)benzyl]propoxy]benzyloxy}propoxycarbonyl}methano}-1,2:18,36:22,23:27,45:31,32:55,56-dodecaahydro [60]fullerene (72)

According the preparation of **71**, the reaction was performed starting with 90 mg (0.0578 mmols) of **52**, 107 mg of DMA, 1.102 g (0.578 mmols) of **67**, 192 mg of CBr_4 (0.579 mmols), and 172 µl (1.152 mmols) in 70 mL toluene. After 5 days, the solvent was evaporated under reduced pressure and the crude mixture separated by FC (SiO_2/toluene increasing to toluene:AcOEt 95:5)_followed by preparative HPLC (grom-Sil 100Si, NP1, 5µ/ 20 mL/min toluene:AcOEt 95:5) to give 12.8 mg of the [60]fullerene-porphyrin-dendrimer **72**. Yield: 2.0 %.

^{1}H-NMR (400 MHz, RT, $CDCl_3$): δ = 1.78-1.94 (m, 60H, dendrimer C*H*$_2$), 3.22-3.64 (m, 60H, dendrimer C*H*$_2$), 3.80-3.94 (m, 60H, dendrimer C*H*$_2$), 4.09-4.36 (m, 65H, dendrimer C*H*$_2$, porphyrin, CH$_2$, C*H*$_3$), 4.78 (br, 2H, C*H*$_2$ porphyrine), 4.91-4.82 (m, 80H, dendrimer C*H*$_2$), 6.22-6.53 (m, 90H, dendrimer Ar*H*), 7.16-7.32 (m, 202, dendrimer *Ph*, porphyrine *Ph*), 7.64-7.68 (m, 9H, porphyrin *Ph*), 8.05 (m, 2H, porphyrin *Ph*), 8.15 (m, 6H, porphyrin *Ph*), 8.87-8.91 (m, 8H, porphyrin *β*-Pyrrol); ^{13}C-NMR (100.5 MHz, RT, $CDCl_3$): δ = 28.85, 29.41, 29.63 (*C*H$_2$), 45.10, 45.33, 45.38, 45.68 (methano bridge), 50.88 (*C*H$_3$O), 63.72, 64.37, 64.74,

66.36, 66.53, 66.68, 66.91 (*C*H_2O), 69.17 (C_{60}-sp^3 *C*), 69.88, 72.48, 72.64, 77.78 (*C*H_2O), 100.24, 101.17, 105.89, 106.30, 112.61 (arom. *C*H), 120.60, 120.79, 120.87 (porphyrin bridge *C*), 126.42, 127.46, 127.87, 128.47 (Ph *C*H), 131.81 (pyrrol *C*H), 134.48, 135.65 (Ph *C*H), 136.76, 136.84 (Ph *C*), 140.49, 140.56, 140.67, 140.79, 141.02 (arom. *C*),, 141.23, 131.44, 141.47 (C_{60}-sp^2 *C*), 143.07, 143.10 (pyrrol *C*), 145.78, 145.95, 146.08, 146.12 (C_{60}-sp^2 *C*), 150.05, 150.10, 150.36 (Ph *C*), 157.94, 159.91, 159.99, 160.04, 160.13, 160.25 (arom. *C*), 163.72, 164.16 (*C*=O); UV/Vis (CH_2Cl_2): λ_{max} = 282.5, 318.0 (sh), 336.0 (sh), 401.5 (sh), 424.5, 513.5, 552.0, 594.0.

3,5-Bis[(2'-methoxyethoxy)metoxy]benzoate methyl ester (76)

To a slurry of 1.605 g (40.125 mmols) NaH (60 % in paraffin-oil) in 20 mL THF, 2.25 g (13.38 mmols) of 3,5-dihydroximethylbenzoate in 50 mL THF and 5 mL MEM-Cl (40.138 mmols) were added. The mixture was stirred under reflux for 24 h. H_2O was carefully added, the resulting mixture extracted 3 times with Et_2O, the combined extract dried over anhydrous Na_2SO_4 and the solvent evaporated under reduced pressure. FC (SiO_2/hexane:ethyl acetate 7:3 with 2 % Et_3N) gave 4.22 g of **76** as a colorless oil. Yield: 91.6 %.

^{1}H-NMR (400 MHz, RT, $CDCl_3$): δ = 3.38 (s, 6H, C*H*$_3$O), 3.56 (m, 4H, C*H*$_2$O), 3.82 (m, 4H, C*H*$_2$O), 3.89 (s, 3H, C*H*$_3$O$_2$C), 5.28 (s, 4H, OC*H*$_2$O), 6.94 (t, 1H, J=2 Hz, Ar*H*), 7.38 (d, 2H, J=2 Hz, Ar*H*); ^{13}C-NMR (100.5 MHz, RT, $CDCl_3$): δ = 52.15 (*C*H$_3$O$_2$), 58.97 (*C*H$_3$O), 67.82, 71.48 (*C*H$_2$O), 93.44 (OCH$_2$O), 109.71, 110.78 (arom. *C*H), 132.19, 158.13 (arom. *C*), 166.60 (*C*=O); MS (EI): *m/z* = 344 (M^+), 313, 89, 59, 45, 31; IR (film): $\tilde{\nu}$ = 3100.9 cm^{-1}, 2987.5, 2953.8, 2928.4, 2876.4, 2818.2, 2719.7, 1592.7, 1453.2, 1435.1, 1400.8, 1367.4, 1340.4, 1300.9, 1230.0, 1201.3, 1177.9, 1155.6, 1101.9, 1077.6, 1015.7, 937.2, 849.0, 771.5.

3,5-Bis[(2'-methoxyethoxy)metoxy]benzyl alcohol (77)

A solution of 3.95 g (11.47 mmols) of **76** in 50 mL of absolute ether was added dropwise over a well stirred suspension of 0.21 g (5.53 mmols) lithium aluminum hydride in 20 mL of absolute ether. The reaction was monitored by TLC and when it was completed (12 h) quenched drooping carefully water. The aqueous layer was extracted with ether (3x150 mL), the combined organic layers were dried over Na_2SO_4 and the solvent distilled under reduced pressure[120]. FC (SiO_2/ethyl acetate:hexane 6:4 with 2 % Et_3N) gave 3.375 g of **77** as a colorless oil. Yield: 93 %.

^{1}H-NMR (400 MHz, RT, $CDCl_3$): δ = 2.23 (t, 1H, J=6 Hz, O*H*), 3.37 (s, 6H, C*H*$_3$O), 3.55 (m, 4H, C*H*$_2$O), 3.81 (m, 4H, C*H*$_2$O), 4.60 (d, 2H, J=6 Hz, C*H*$_2$0H), 5.24 (s, 4H, OC*H*$_2$O), 6.65 (t, 1H, J=2 Hz, Ar*H*), 6.72 (d, 2H, J=2 Hz, Ar*H*); ^{13}C-NMR (100.5 MHz, RT, $CDCl_3$): δ = 58.90 (*C*H_3O), 64.90 (*C*H_2OH), 67.60, 71.49 (*C*H_2O), 93.39 (O*C*H_2O), 104.03, 107.96 (arom. *C*H), 143.67, 158.40 (arom. *C*); MS (EI): *m/z* = 316 (M^+), 89, 59; IR (film): $\tilde{\nu}$ = 3441.4 cm^{-1}, 2926.0, 2881.6, 2820.6, 1598.4, 1457.6, 1409.2, 1366.3, 1289.3, 1200.1, 1173.7, 1101.7, 1032.2, 991.9, 918.2, 846.6.

Allyl 3,5-bis[(2'-methoxyethoxy)metoxy]benzyl ether (78)

According to the synthesis of **58**, the reaction was carried out starting from 2.1 g (52.5 mmols) of NaH (60 % in paraffin-oil) in 20 mL of dry THF, 5.535 g (94.47 mmols) of **77** in 50 mL THF, and 4.5 mL (52 mmols) of allyl bromide. FC (SiO_2/hexane:ethyl acetate 1:1 containing 2 % Et_3N) gave 5.76 g (91 %) of **78** as an oil.

^{1}H-NMR (400 MHz, RT, $CDCl_3$): δ = 3.38 (s, 6H, C*H*$_3$O), 3.56 (m, 4H, C*H*$_2$O), 3.82 (m, 4H, C*H*$_2$O), 4.45 (s, 2H, ArC*H*$_2$0), 5.20 (m, 1H, C*H*H=), 5.25 (s, 4H, OC*H*$_2$O), 5.31 (m, 1H, CH*H*=), 5.90-6.00 (m, 1H, C*H*=CH$_2$), 6.67 (t, 1H, J=2 Hz, Ar*H*), 6.72 (d, 2H, J=2 Hz, Ar*H*); ^{13}C-NMR (100.5 MHz, RT, $CDCl_3$): δ = 58.94 (*C*H_3O), 67.62 (*C*H_2OH), 71.15, 71.52, 71.78, 93.42 (O*C*H_2O), 104.08, 108.83 (arom. *C*H), 117.17 (*C*H_2-CH-), 134.68 (CH$_2$=*C*H-), 140.88, 158.34 (arom. *C*); MS (EI): *m/z* = 356 (M^+), 300, 224, 89, 59; IR (film): $\tilde{\nu}$ = 3079.8 cm^{-1}, 2977.6, 2925.2, 2879.3, 2819.4, 2726.1, 1598.3, 1457.6, 1409.0, 1290.0, 1242.7, 1200.9, 1174.7, 1156.5, 1132.4, 1101.9, 926.8, 847.6.

3-[3',5'-Bis[(2''-methoxyethoxy)methoxy]benzyloxy]-propanol (79)

This compound was prepared following the same procedure described for the synthesis of **59**, starting from 40 mL of 9-BBN 0.5 M in THF (18 mmols) and a solution of 5.66 g (15.88 mmols) of allyl ether **78** in THF (30 mL). Flash chromatography (SiO_2/hexane:ethyl acetate 3:7 containing 2 % Et_3N) yielded 5.508 g of **79** as a colorless oil (92.6 %).

^{1}H-NMR (400 MHz, RT, $CDCl_3$): δ = 1.86 (tt, 2H, J = 6 Hz, C*H*$_2$), 2.38 (t, 1H, J = 6 Hz, O*H*), 3.38 (s, 6H, C*H*$_3$O), 3.56 (m, 4H, C*H*$_2$O), 3.65 (t, 2H, J = 6 Hz, C*H*$_2$O), 3.78 (td, 2H, J_1=J_2= 6 Hz, C*H*$_2$OH), 3.81 (m, 4H, C*H*$_2$O), 4.45 (s, 2H, ArC*H*$_2$0), 5.25 (s, 4H, OC*H*$_2$O), 6.64 (t, 1H, J=2 Hz, Ar*H*), 7.00 (d, 2H, J=2 Hz, Ar*H*); ^{13}C-NMR (100.5 MHz, RT, $CDCl_3$): δ = 32.08 (*C*H_2), 58.91 (*C*H_3O), 61.32, 67.62, 68.97, 71.51, 72.84 (*C*H_2O), 93.41 (O*C*H_2O), 104.16, 108.62 (arom. *C*H), 140.81, 158.38 (arom. *C*); MS (EI): *m/z* = 374.2 (M^+), 300, 224, 89, 59;

IR (film): $\tilde{\nu}$ = 3463.5 cm^{-1}, 2926.6, 2878.5, 2820.9, 1597.7, 1457.8, 1406.1, 1364.2, 1290.0, 173.9, 1152.8, 1101.3, 1035.3, 934.6, 846.4.

Bis{3-[3',5'-bis[(2''-methoxyethoxy)methoxy]benzyloxy]}propylmalonate (80)

According to the same procedure described for **64**, the reaction was carried out with the following amounts of reagents: 560 mg (14.0 mmols) NaH (60 % in paraffin-oil) and 4.971 g (13.276 mmols) of **79** in 60 mL of dry THF, and 0.615 mL (6.306 mmols) of malonyl dichloride and 1 ml (12.364 mmols) pyridine in 20 mL dry THF. FC (SiO_2/hexane:ethyl acetate 7:3 containing 2 % Et_3N) gave 2.51 g (48.6 %) **80** as a pale yellow oil.

^{1}H-NMR (400 MHz, RT, $CDCl_3$): δ = 1.95 (tt, 4H, J = 6 Hz, C*H*$_2$), 3.37 (s, 2H, CH_2), 3.38 (s, 12H, C*H*$_3$O), 3.54 (t, 4H, J=6 Hz, C*H*$_2$O), 3.56 (m, 8H, C*H*$_2$O), 3.81 (m, 8H, C*H*$_2$O), 4.42 (s, 4H, ArC*H*$_2$O), 5.24 (s, 8H, OC*H*$_2$O), 6.60 (m, 6H, Ar*H*); ^{13}C-NMR (100.5 MHz, RT, $CDCl_3$): δ = 28.84, 41.39 (*C*H_2), 58.97 (*C*H_3O), 62.73, 66.56, 67.66, 71.55, 72.75 (*C*H_2O), 93.46 (O*C*H_2O), 104.05, 108.76 (arom. *C*H), 140.87, 158.39 (arom. *C*); 166.61 (*C*=O); MS (EI): *m/z* = 816 (M^+), 740, 651, 374, 222, 89, 59; IR (film): $\tilde{\nu}$ = 2925.3 cm^{-1}, 2879.6, 2819.7, 1750.7, 1733.9, 1598.0, 1458.7, 1289.0, 1154.1, 1102.6, 1035.2, 847.0, 665.5.

1,2-Bis{3-[3',5'-bis[(2''-methoxyethoxy)methoxy]benzyloxy]}propoxycarbonyl}-methano-1,2-dihydro-[60]fullerene (81)

According to the synthesis of **70**, the reaction was performed using 200 mg of C_{60} (0.2775 mmols), 138 mg (0.416 mmols) of CBr_4, 340 mg (0.416 mmols) of malonate **80**, and 0.124 mL (0.830 mmols) of DBU in 120 mL toluene. FC (SiO_2/toluene increasing to toluene:ethyl acetate 1:1) yielded 121 mg of [60]fullerene monoadduct **81**. Yield: 28.4 %.

^{1}H-NMR (400 MHz, RT, $CDCl_3$): δ = 2.15 (tt, 4H, J = 6 Hz, C*H*$_2$), 3.38 (s, 12H, C*H*$_3$O), 3.56 (m, 8H, C*H*$_2$O), 3.63 (t, J = 6Hz, C*H*$_2$O), 3.81 (m, 8H, C*H*$_2$O), 4.43 (s, 4H, ArC*H*$_2$O), 4.62 (t, J = 6Hz, C*H*$_2$O), 5.24 (s, 8H, OC*H*$_2$O), 6.69 (m, 6H, Ar*H*); ^{13}C-NMR (100.5 MHz, RT, $CDCl_3$): δ = 28.97(*C*H_2), 52.26 (methano bridge), 58.98 (*C*H_3O), 64.61, 66.51, 67.68 (*C*H_2O), 71.55 (C_{60}-sp^3 *C* and *C*H_2O), 72.86 (*C*H_2O), 93.47 (O*C*H_2O), 104.04, 108.70 (arom. *C*H), 138.98, 140.78 (C_{60}-sp^2 *C*), 140.96 (arom. *C*), 141.91, 142.23, 143.01, 143.05, 143.90, 144.62, 144.67, 144.72, 144.92, 145.16, 145.22, 145.28, 145.31(C_{60}-sp^2 *C*), 158.44 (arom. *C*), 163.60 (*C*=O);.UV/Vis (CH_2Cl_2): λ_{max} = 258.0 nm, 325.5, 426.5, 481.0; MS (MALDI-TOF): *m/z* = 1536.5 (M^+); IR (film): $\tilde{\nu}$ = 2923.2 cm^{-1}, 2876.5, 2817.1, 1744.2, 1596.8, 1456.9, 1238.7, 1174.3, 1101.8, 1032.6, 846.8, 705.6, 526.5.

1,2:18,36:22,23:27,45:31,32:55,56-Hexakis{[di(dodecyloxycarbonyl)]methano}-1,2,18,36, 22,23,27,45,31,32,55,56-dodecahydro[60]fullerene (85)

According to the synthesis of **32**, the reaction was carried out with 125 mg (0.173 mmols) of C_{60}, 354 mg (1.716 mmols) of DMA, 1.00 g (1.925 mmols) of the bromo malonate **91**, and 0.256 mL (1.715 mmols) of DBU, in 60 mL of toluene. After 72 h, the solvent was evaporated under reduced pressure and the crude mixture separated by FC (SiO_2/toluene:hexan 3:1) followed by HPLC (grom-Sil 100Si, NP1, 5µ/ 20 mL/min CH_2Cl_2:hexan 3:2) to give 183 mg of the hexaaduct **85** (yellow oil). Yield: 31.5 %.

^{1}H-NMR (400 MHz, RT, $CDCl_3$): δ = 0.85 (t, 36H, J=6.8 Hz, C*H*$_3$), 1.16-1.44 (m, 216H, C*H*$_2$), 1.66 (tt, 24H, J_1=J_2=6.8 Hz, C*H*$_2$CH$_2$O), 4.21 (t, 24H, J=6.8 Hz, C*H*$_2$O); ^{13}C-NMR (100.5 MHz, RT, $CDCl_3$): δ = 14.04 (*C*H$_3$), 22.64, 25.80, 28.40, 29.23, 29.33, 29.53, 29.60, 29.63, 29.70, 31.89 (*C*H$_2$), 45.38 (methano bridge), 66.95 (*C*H$_2$), 69.10 (C_{60}-sp^3 *C*), 141.20, 145.84 (C_{60}-sp^2 *C*), 163.98 (*C*=O); UV/Vis (CH_2Cl_2): λ_{max} = 244.5 nm, 270.0, 281.0, 319.5, 336.0; MS (MALDI-TOF): *m/z* = 3378 (M+Na$^+$), 3354 (M$^+$); IR (film): $\tilde{\nu}$ = 2956.0 cm^{-1}, 2926.4, 2855.0, 1748.3, 1466.5, 1378.9, 1352.1, 1264.2, 1214.6, 1166.9, 1125.1, 1079.3, 1045.9, 996.3, 945.9.

1,2:18,36:22,23:27,45:31,32:55,56-Hexakis{[di(octadecyloxycarbonyl)]methano}-1,2,18, 36,22,23,27,45,31,32,55,56-dodecahydro[60]fullerene (86)

According to the synthesis of **32**, the reaction was performed starting with 150 mg (0.208 mmols) of C_{60} , 430 mg (2.08 mmols) of DMA, 1.40 g (2.05 mmols) of the bromo malonate **92**, and 0.31 mL (2.07 mmols) of DBU in 100 mL toluene. After 120 h the solvent was evaporated under reduced pressure and the crude mixture separated by FC (SiO_2/toluene:hexan 5:4 increasing to 5:3) followed by HPLC (grom-Sil 100Si, NP1, 5µ/ 20 mL/min CH_2Cl_2:hexane 1:1) gave 180 mg of the hexaadduct **86** as a yellow powder. Yield: 19.8 %.

^{1}H-NMR (400 MHz, RT, $CDCl_3$): δ = 0.88 (t, 36H, J=6.8 Hz, C*H*$_3$), 1.17-1.40 (m, 360H, C*H*$_2$), 1.68 (tt, 24H, J_1=J_2=6.8 Hz, C*H*$_2$CH$_2$O), 4.23 (t, 24H, J=6.8 Hz, C*H*$_2$O); ^{13}C-NMR (100.5 MHz, RT, $CDCl_3$): δ = 14.03 (*C*H$_3$), 22.62, 25.79, 28.39, 29.23, 29.31, 29.54, 29.62, 29.67, 29.70, 31.87 (*C*H$_2$), 45.35 (methano bridge), 66.93 (*C*H$_2$), 69.08 (C_{60}-sp^3 *C*), 141.17, 145.83 (C_{60}-sp^2 *C*), 163.97 (*C*=O); UV/Vis (CH_2Cl_2): λ_{max} = 245.0 nm, 271.5, 281.5, 317.0, 334.5; MS (MALDI-TOF): *m/z* = 4367 (M$^+$); IR (KBr): $\tilde{\nu}$ = 2956.3 cm^{-1}, 2918.2, 2850.0, 1736.0, 1469.3, 1396.0, 1378.9, 1351.2, 1265.8, 1242.6, 1215.9, 1164.2, 1073.7, 761.8, 718.3, 530.0.

1,2-Di(dodecyloxycarbonyl)methano-1,2-dihydro[60]fullerene (87)

The reaction was performed as is described for **29** using 100 mg (0.139 mmols) of C_{60}, 108 mg (0.208 mmols) of the bromo malonate **91**, and 35 mg (1.46 mmols) of sodium hydride in 60 mL toluene. After 48 h the usual work-up was performed. FC (SiO_2/hexan:toluene 65:35) gave 4 mg (0.005 mmols) of C_{60}, 101 mg (62.8 %) of **87**, and 69 mg (31.1 %) of a regioisomeric mixture of the corresponding bisadducts.

^{1}H-NMR (400 MHz, RT, $CDCl_3$): δ = 0.88 (t, 6H, J=6.8 Hz, C*H*$_3$), 1.20-1.50 (m, 36H, C*H*$_2$), 1.84 (tt, 4H, J_1=J_2=6.8 Hz, C*H*$_2$CH$_2$O), 4.49 (t, 4H, J=6.8 Hz, C*H*$_2$O); ^{13}C-NMR (100.5 MHz, RT, $CDCl_3$): δ = 14.06 (*C*H$_3$), 22.63, 25.94, 28.54, 29.20, 29.31, 29.57, 29.60, 29.65, 31.86 (*C*H$_2$), 52.38 (methano brigdge), 67.43 (*C*H$_2$), 71.65 (C_{60}-sp^3 *C*), 139.05, 140.98, 141.96, 142.25, 143.03, 143.06, 143.12, 143.93, 144.65, 144.71. 144.72, 144.92, 145.23, 145.30, 145.43 (C_{60}-sp^2 *C*), 163.74 (*C*=O); UV/Vis (CH_2Cl_2): λ_{max} = 257.5 nm, 325.5, 426.0; MS (MALDI-TOF): *m/z* = 1161 (M^+), 720 (C_{60}^+); IR (KBr): $\tilde{\nu}$ = 2955.7 cm^{-1}, 2921.3, 2850.4, 1746.5, 1540.1, 1461.1, 1428.8, 1376.6, 1261.4, 1232.5, 1204.3, 1185.0, 1095.6, 1058.8, 1018.8, 865.6, 800.4, 755.6, 727.3, 703.9, 670.8, 579.9, 552.6, 526.3.

1,2-Di(octadecyloxycarbonyl)methano-1,2-dihydro[60]fullerene (88)

The reaction was performed as is described for **29** using 150 mg (0.208 mmols) of C_{60}, 215 mg (0.312 mmols) of bromo malonate **92**, and 75 mg (3.125 mmols) of sodium hydride in 100 mL toluene. After 48 h the usual work-up was performed. FC (SiO_2/hexan:toluene 70:30) gave 32 mg (21.3 %) of C_{60} and 149.8 mg of monoadduct **88**. Yield: 54.2 %.

^{1}H-NMR (400 MHz, RT, $CDCl_3$): δ = 0.88 (t, 6H, J=6.8 Hz, C*H*$_3$), 1.22-1.49 (m, 60H, C*H*$_2$), 1.84 (tt, 4H, J_1=J_2=6.8 Hz, C*H*$_2$CH$_2$O), 4.49 (t, 4H, J=6.8 Hz, C*H*$_2$O); ^{13}C-NMR (100.5 MHz, RT, $CDCl_3$): δ = 14.06 (*C*H$_3$), 22.64, 25.96, 28.54, 29.20, 29.32, 29.58, 29.64, 29.67, 31.88 (*C*H$_2$), 52.43 (methano bridge), 67.46 (*C*H$_2$), 71.68 (C_{60}-sp^3 *C*), 139.05, 141.01, 141.98, 142.27, 143.05, 143.07, 143.15, 143.95, 144.67, 144.73, 144.75, 144.94, 145.25, 145.32, 145.46 (C_{60}-sp^2 *C*), 163.79 (*C*=O); UV/Vis (CH_2Cl_2): λ_{max} = 257.5 nm, 325.5, 426.0; MS (MALDI-TOF): *m/z* = 1328 (M^+); IR (KBr): $\tilde{\nu}$ = 2953.5 cm^{-1}, 2918.5, 2849.0, 1747.4, 1461.7, 1428.8, 1376.9, 1297.1, 1266.6, 1252.9, 1229.6, 1203.4, 1185.9, 1175.1, 1096.1, 1059.4, 1018.3, 995.1, 808.0, 728.9, 581.3, 525.8.

Didodecylmalonate (89)

According to the synthesis of malonate **23**, the reaction was performed using 4.155 mL of pyridine (51.37 mmols), 9.58 g (51.41 mmols) of 1-dodecanol, and 2.5 mL (25.70 mmols) of malonyl dichloride in 100 mL of CH_2Cl_2. FC (SiO_2/hexan:CH_2Cl_2 1:1) gave 9.61g of malonic diester **89**. Yield: 84.8 %.

^{1}H-NMR (400 MHz, RT, $CDCl_3$): δ = 0.88 (t, 6H, J=6.8 Hz, C*H*$_3$), 1.26-1.36 (m, 36H, C*H*$_2$), 1.64 (tt, 4H, J_1=J_2=6.8 Hz, C*H*$_2$CH$_2$O), 3.36 (s, 2H, C*H*$_2$), 4.13 (t, 4H, J=6.8 Hz, C*H*$_2$O); ^{13}C-NMR (100.5 MHz, RT, $CDCl_3$): δ = 13.92 (*C*H$_3$), 22.54, 25.66, 28.36, 29.10, 29.22, 29.40, 29.51, 29.53, 29.57, 31.80, 41.53, 65.50 (*C*H$_2$), 166.63 (*C*=O); MS (EI): *m/z* = 273 (M-$C_{12}H_{23}^+$), 169 ($C_{12}H_{25}^+$), 105, 69, 57, 43; IR (KBr): $\tilde{\nu}$ = 2956.1 cm^{-1}, 2922.4, 2854.9, 1756.2, 1739.0, 1476.5, 1412.4, 1379.5, 1330.9, 1271.3, 1181.6, 1149.6, 1011.4, 893.1, 722.4, 685.5, 584.3.

Dioctadecylmalonate (<u>90</u>)

According to the synthesis of malonate **23**, the reaction was performed using 3.32 mL of pyridine (41.05 mmols), 11.123 g (41.12 mmols) of 1-octadecanol, and 2 mL (20.56 mmols) of malonyl dichloride in 150 mL of dry CH_2Cl_2. FC (SiO_2/hexan:CH_2Cl_2 1:1) gave 11.1g of malonic diester **90**. Yield: 89 %.

^{1}H-NMR (400 MHz, RT, $CDCl_3$): δ = 0.88 (t, 6H, J=6.8 Hz, C*H*$_3$), 1.25-1.37 (m, 60H, C*H*$_2$), 1.64 (tt, 4H, J_1=J_2=6.8 Hz, C*H*$_2$CH$_2$O), 3.37 (s, 2H, C*H*$_2$), 4.14 (t, 4H, J=6.8 Hz, C*H*$_2$O); ^{13}C-NMR (100.5 MHz, RT, $CDCl_3$): δ = 14.04 (*C*H$_3$), 22.63, 25.74, 28.42, 29.18, 29.32, 29.48, 29.54, 29.62, 29.65, 31.88, 41.67, 65.66 (*C*H$_2$), 166.80 (*C*=O); MS (EI): *m/z* = 608 (M$^+$), 357; IR (KBr): $\tilde{\nu}$ = 2965.7 cm^{-1}, 2919.0, 2849.6, 1749.4, 1715.8, 1473.9, 1463.5, 1402.0, 1359.8, 1183.0, 1054.9, 1031.7, 1022.1, 1005.7, 730.2, 719.8, 684.6, 614.8, 594.0.

Bromo didodecylmalonate (<u>91</u>)

According to the procedure described for the synthesis of **26**, the reaction was performed starting with 6.35 g (14.41 mmols) of **89**, 2.15 mL (14.40 mmols) of DBU, and 4.78 g (14.41 mmols) of CBr_4 in 100 mL of dry THF. FC (SiO_2/hexan:CH_2Cl_2 1:1) gave 5.24 g of **91** as a pale yellow oil. Yield: 70.0 %.

^{1}H-NMR (400 MHz, RT, $CDCl_3$): δ = 0.82 (t, 6H, J=6.8 Hz, C*H*$_3$), 1.17-1.36 (m, 36H, C*H*$_2$), 1.61 (tt, 4H, J_1=J_2=6.8 Hz, C*H*$_2$CH$_2$O), 4.15 (t, 4H, J=6.8 Hz, C*H*$_2$O); 4.77 (s, 1H, C*H*Br); ^{13}C-NMR (100.5 MHz, RT, $CDCl_3$): δ = 13.89 (*C*H$_3$), 22.51, 25.50, 28.18, 29.00, 29.19, 29.34, 29.41, 29.48, 31.76 (*C*H$_2$), 42.28 (*C*HBr), 67.04 (*C*H$_2$), 164.53 (*C*=O); MS (EI): *m/z* =

439 (M-Br^+) 351, 273, 105, 83, 71, 57, 43; IR (film): $\tilde{\nu}$ = 2955.9 cm^{-1}, 2925.2, 2854.6, 1769.6, 1746.9, 1466.5, 1378.9, 1301.7, 1242.7, 1201.6, 1146.2, 1004.7, 911.1, 789.6, 733.8, 650.1, 574.7.

Bromo dioctadecylmalonate (92)

DBU (1.22 mL, 8.174 mmols) was added to a solution of 4.97 (8.16 mmols) of **90** in 100 mL of dry CH_2Cl_2 under Argon. After 20 minutes, bromine (0.42 mL, 8.173 mmols) was added and the reaction was stirred for 20 minutes at room temperature. Then, the reaction was quenched with 50 mL 0.1 M HCl, the organic layer extracted with sat. aq. $NaHCO_3$ (to pH ca. 6) and sat. aq. NaCl solutions, and dried over Na_2SO_4. FC (SiO_2/hexane:CH_2Cl_2 1:1) gave 3.88 g of **92** as a white solid. Yield: 69.1 %.

^{1}H-NMR (400 MHz, RT, $CDCl_3$): δ = 0.88 (t, 6H, J=6.8 Hz, C*H*$_3$), 1.18-1.40 (m, 60H, C*H*$_2$), 1.65 (tt, 4H, J_1=J_2=6.8 Hz, C*H*$_2$CH$_2$O), 4.22 (t, 4H, J=6.8 Hz, C*H*$_2$O) 4.83 (s, 1H, C*H*Br); ^{13}C-NMR (100.5 MHz, RT, $CDCl_3$): δ = 14.05 (*C*H$_3$), 22.63, 25.59, 28.26, 29.09, 29.31, 29.44, 29.51, 29.61, 29.64, 31.87 (*C*H$_2$), 42.44 (*C*HBr), 67.29 (*C*H$_2$), 164.75 (*C*=O); MS (EI): *m/z* = 689 (M^+), 608 (M-Br^+), 357, 149; IR (KBr): $\tilde{\nu}$ = 2956.4 cm^{-1}, 2918.3, 2850.1, 1767.3, 1744.8, 1468.6, 1380.8, 1304.5, 1241.9, 1201.8, 1147.8, 1063.7, 995.6, 928.0, 896.1, 821.5, 721.5, 649.9.

1-Octadecanol-*d*$_{37}$ (93)

Stearic acid-*d*$_{35}$ (2 g, 6.256 mmols) in ether (50 mL) was added via a pressure-equalizing dropping funnel to a slurry of lithium aluminum deuterid (2 g, 47.642 mmols) in ether (20 mL) under argon at room temperature. The mixture was refluxed for 12 h and left at room temperature for another 24 h until no starting acid was detected by GC[126]. Methanol (10 mL) in ether (50 mL) was added slowly at 0 °C to decompose the excess of deuteride, and the mixture was then treated with 1N H_2SO_4 until two clear layers formed. The two layers were separated, and the aqueous layer was extracted with three portions of ether (3x50 mL). The combined organic phase was washed with 5 % $NaHCO_3$ (100 mL), dried over $MgSO_4$ and the solvent destilled under reduced pressure to yield 1.925 g of octadecanol-d_{37} **93**. Yield: 100 %.

^{1}H-NMR (400 MHz, RT, $CDCl_3$): δ = 1.22 (s, 1H, CD_2O*H*); MS (EI): *m/z* = 288 (M-HDO)$^+$; IR (KBr): $\tilde{\nu}$ = 3299.6 cm^{-1}, 2917.2, 2890.8, 2881.4, 2850.6, 2193.4, 2156.5, 2088.5, 1151.0, 1108.9, 1086.7, 1056.8, 967.3, 950.2, 802.1, 681.7, 520.8.

Di(octadecyl-*d*$_{37}$)malonate (94)

According to the general procedure described for **23**, the reaction was performed starting with 1.935 g (6.301 mmols) of octadecanol-d_{37} (**93**), 0.51 mL (6.306 mmols) of pyridine, and 0.3 mL (3.084 mmols) of malonyl dichloride in 100 mL CH_2Cl_2. FC (SiO_2/heptan:CH_2Cl_2 1:1) yielded 1.545 g of **94** (yield:73.3 %).

^{1}H-NMR (400 MHz, RT, $CDCl_3$): δ = 3.38 (s, 2H, C*H*$_2$); ^{13}C-NMR (100.5 MHz, RT, $CDCl_3$): δ = 41.69 (*C*H$_2$), 166.85 (*C*=O); MS (EI): *m/z* = 682.97 (M^+-HDO); IR (KBr): $\tilde{\nu}$ = 2917.8 cm^{-1}, 2890.8, 2851.6, 2194.3, 2157.1, 2088.9, 1747.9, 1714.5, 1405.4, 1373.3, 1191.3, 1085.9, 997.5, 665.9, 590.0, 521.2.

1,2:18,36:22,23:27,45:31,32:55,56-Hexakis{[di(octadecyl-*d_{37}*-oxycarbonyl)]methano}-1,2,18, 36,22,23,27,45,31,32,55,56-dodecahydro[60]fullerene (95)

A mixture of C_{60} (160 mg, 0.222 mmols) and DMA (412 mg, 2 mmols) in toluene (75 mL) was stirred at room temperature for 2h. Then, di(octadecanyl-d_{37})malonate **94** (1.54 g, 2.253 mmols), CBr_4 (663 mg, 2 mmols), and DBU (0.6 mL, 4 mmols) were added in this order. After 36 h the solvent was evaporated under reduced pressure and the crude mixture separated by FC (SiO_2/hexane:CH_2Cl_2 1:1) followed by preparative HPLC (grom-Sil 100Si, NP1, 5µ/ 20 mL/min heptane:CH_2Cl_2 55:45) gave 205 mg of HAC_{18}-*d_{444}* **95**. Yield: 19.2 %.

^{13}C-NMR (100.5 MHz, RT, $CDCl_3$): δ = 45.36 (methano bridge), 69.08 (C_{60}-sp^3 *C*), 141.18, 145.82 (C_{60}-sp^2 *C*), 163.99 (*C*=O); UV/Vis (cyclohexane): λ_{max} = 244.5 nm, 269.5, 280.5, 318, 334.0, 384.0; MS (MALDI-TOF): *m/z* = 4801 (broad distribution) (M^+); IR (KBr): $\tilde{\nu}$ = 2918.7 cm^{-1}, 288.1, 2850.7, 2192.7, 2087.4, 1759.0, 1731.7, 1283.3, 1226.5, 1089.5, 1060.6, 717.4, 528.9.

10,12-0ctadecadiyn-1-ol (96)

10,12-Octadecanoic acid (2g, 7.236 mmols) in ether (50 mL) was added via a pressure-equalizing dropping funnel to a slurry of $LiAlH_4$ (2.1g, 55.104 mmols) in ether (20 mL) under Argon at room temperature. The mixture was refluxed for 12 h and left at room temperature for another 8 h. A GC control showed complete conversion[126]. Methanol (10 mL) in ether (50 mL) was added slowly to decompose the excess hydride. The mixture was then treated with 5 % H_2SO_4 until two clear layers formed. The two layers were separated, and the aqueous layer was extracted with three portions of ether (3x50 mL). The combined organic phase was washed with 5 % $NaHCO_3$ and dried over $MgSO_4$. Evaporation of the solvent gave 1.9 g (100 %) of pure 10,12-octadecadiyn-1-ol (**96**) as a white solid.

^{1}H-NMR (400 MHz, RT, $CDCl_3$): δ = 0.89 (t, 3H, J=7 Hz, C*H*$_3$), 1.25-1.60 (m, 21H, C*H*$_2$, O*H*), 2.24 (t, 4H, J=7 Hz, C*H*$_2$-≡-), 3.64 (t, 2H, J=7 Hz, C*H*$_2$OH); ^{13}C-NMR (100.5 MHz, RT, $CDCl_3$): δ = 13.81 (*C*H$_3$), 19.09, 19.07, 22.07, 25.61, 27.95, 28.23, 28.71, 28.91, 29.26, 29.32, 30.92, 32.69 (*C*H$_2$), 62.99 (*C*H$_2$OH), 65.19, 65.22, 77.45, 77.52 (sp *C*); MS (EI): *m/z* = 262 (M^+), 220, 205, 134, 119, 105, 91, 81, 67, 55, 41; IR (film): $\tilde{\nu}$ = 3347.0 cm^{-1}, 2929.7, 2855.7, 2257.0, 2156.0, 1465.6, 1427.1, 1378.3, 1324.4, 1058.0, 723.8, 665.4.

Di(10,12-octadecadiynyl)malonate (97)

According to the synthesis of **23**, the reaction was carried out starting from 1.9 g (7.24 mmols) of 10,12-octadecadiyn-1-ol, 0.59 mL (7.24 mmols) of pyridine, and 0.35 mL (3.62 mmols) of malonyl dichloride in 60 mL CH_2Cl_2. FC (SiO_2/hexane:CH_2Cl_2 1:1) afforded 1.345 g of malonate **97**. Yield: 62.7 %.

^{1}H-NMR (400 MHz, RT, $CDCl_3$): δ = 0.89 (t, 6H, J=7 Hz, C*H*$_3$), 1.25-1.57 (m, 36H, C*H*$_2$), 1.65 (tt, 4H, C*H*$_2$, J_1=J_2=7 Hz), 2.26 (t, 8H, J=7 Hz, C*H*$_2$-≡-), 3.38 (s, 2H, C*H*$_2$), 4.15 (t, 4H, J=7 Hz, C*H*$_2$O$_2$); ^{13}C-NMR (100.5 MHz, RT, $CDCl_3$): δ = 13.80 (*C*H$_3$), 19.06, 19.08, 22.06, 25.66, 27.95, 28.22, 28.36, 28.69, 28.90, 29.04, 29.22, 30.91, 41.59 (*C*H$_2$), 65.20, 65.27 (sp *C*), 65.56 (*C*H$_2$O$_2$), 77.35, 77.48 (sp *C*), 166.73 (*C*=O); MS (EI): *m/z* = 592 (M^+), 549, 536, 134, 91, 81, 67, 55, 41, 29; IR (film): $\tilde{\nu}$ = 2931.2 cm^{-1}, 2857.1, 2256.7, 2156.2, 1753.0, 1736.1, 1465.6, 1427.1, 1328.6, 1270.7, 1182.8, 1148.6, 1014.2, 724.3, 665.5.

1,2-Di(10,12-octadecadiynyloxycarbonyl)methano-1,2-dihydro[60]fullerene (98)

According to the synthesis of **70**, the reaction was performed using 100 mg of C_{60} (0.139 mmols), 69 mg (0.208 mmols) of CBr_4, 124 mg (0.208 mmols) of malonate **97**, and 62 µl (0.415 mmols) of DBU in 70 mL toluene. FC (SiO_2/toluene:hexane 1:1) yielded 70 mg of [60]fullerene monoadduct **98**. Yield: 38.5 %.

^{1}H-NMR (400 MHz, RT, $CDCl_3$): δ = 0.90 (t, 6H, J=7 Hz, C*H*$_3$), 1.25-1.56 (m, 36H, C*H*$_2$), 1.84 (tt, 4H, C*H*$_2$, J_1=J_2=7 Hz), 2.24 (t, 8H, J=7 Hz, C*H*$_2$-≡-), 4.49 (t, 4H, J=7 Hz, C*H*$_2$O$_2$).

^{13}C-NMR (100.5 MHz, RT, $CDCl_3$): δ = 13.87 (*C*H$_3$), 19.12, 19.16, 22.10, 25.91, 27.98, 28.26, 28.52, 28.77, 28.98, 29.12, 29.36, 30.94(*C*H$_2$), 52.40 (methano bridge), 65.27, 65.37 (sp *C*), 67.41 (*C*H$_2$O$_2$), 71.65 (C_{60}-sp^3 *C*), 77.61, 77.44 (sp *C*), 139.03, 141.00, 141.96, 142.26, 143.04, 143.15, 143.94, 144.66, 144.69, 144.75, 144.93, 145.22, 145.32, 145.42 (C_{60}-sp^2 *C*), 163.76 (*C*=O); UV/Vis (CH_2Cl_2): λ_{max} = 258.5 nm, 325.5, 425.0, 488.5; MS (FAB+): *m/z* = 1312 (M^+), 720 (C_{60}^+); IR (KBr): $\tilde{\nu}$ = 2927.2 cm^{-1}, 2854.1, 2282.5, 2253.1, 2190.8,

2154.6, 2132.7, 2080.3, 1745.3, 1462.8, 1427.1, 1267.0, 1234.2, 1206.3, 1186.2, 1097.3, 705.3, 526.

1,2:18,36:22,23:27,45:31,32:55,56-Hexakis{[di(10,12-octadecadiynyloxycarbonyl)]-methano}-1,2,18, 36,22,23,27,45,31,32,55,56-dodecahydro[60]fullerene (99)

According to the synthesis of **95**, the reaction was carried out starting with 108 mg (0.1499 mmols) of C_{60}, 310 mg (1.50 mmols) of DMA, 894 mg (1.50 mmols) of **97**, 497 mg (1.5 mmols) of CBr_4, and 0.448 mL (3 mmols) of DBU in 70 mL toluene. After 36 h the usual work-up was performed. FC (SiO_2/hexane:CH_2Cl_2 1:1) followed by preparative HPLC (grom-Sil 100Si, NP1, 5µ/ 20 mL/min CH_2Cl_2:heptane 7:3) gave 166 mg of **99**. Yield: 26.0 %.

^{1}H-NMR (400 MHz, RT, $CDCl_3$): δ = 0.90 (t, 36H, J=7 Hz, C*H*$_3$), 1.35-1.55 (m, 216H, C*H*$_2$), 1.68 (tt, 24H, C*H*$_2$, J_1=J_2=7 Hz), 2.24 (t, 48H, J=7 Hz, C*H*$_2$-≡-), 4.24 (t, 24H, J=7 Hz, C*H*$_2$O$_2$); ^{13}C-NMR (100.5 MHz, RT, $CDCl_3$): δ = 13.84 (*C*H$_3$), 19.09, 19.13, 22.09, 25.74, 27.98, 28.31, 28.36, 28.78, 28.99, 29.13, 29.31, 30.92(*C*H$_2$), 45.33 (methano bridge), 65.23, 65.26 (sp *C*), 66.92 (*C*H$_2$O$_2$), 69.06 (C_{60}-sp^3 *C*), 77.43, 77.48 (sp *C*), 141.15, 145.81 (C_{60}-sp^2 *C*), 163.92 (*C*=O); UV/Vis (CH_2Cl_2): λ_{max} = 270.5 nm, 280.5, 318.0, 336.0, 383.0; MS (MALDI-TOF): *m/z* = 4267 (M^+); IR (KBr): $\tilde{\nu}$: 2930.8 cm^{-1}, 2856.4, 2256.1, 2155.5, 1746.3, 1465.1, 1264.4, 1215.8, 1080.2, 715.7, 529.3.

10,12-0ctadecadiyn methylmalonate (101)

To a solution of 1.808 g (6.89 mmols) 10,12-octadecadiyn-1-ol and 0.56 mL (6.89 mmols) pyridine in 60 mL CH_2Cl_2 under Argon at 0 °C, 0.74 mL (6.89 mmols) of malonyl dichloride monomethyl ester were added within 10 min. After 2 h the ice bath was removed and the reaction stirred overnight. The solution was extracted with H_2O and the solvent evaporated under reduced pressure. FC (SiO_2/CH_2Cl_2:hexane 1:1) afforded 2.215 g of desired target **101**. Yield: 88.6 %.

^{1}H-NMR (400 MHz, RT, $CDCl_3$): δ = 0.90 (t, 3H, J=7 Hz, C*H*$_3$), 1.2-1.56 (m, 18H, C*H*$_2$), 1.64 (tt, 2H, C*H*$_2$, J_1=J_2=7 Hz), 2.24 (t, 4H, J=7 Hz, C*H*$_2$-≡-), 3.39 (s, 2H, C*H*$_2$), 3.75 (s, 3H, C*H*$_3$O), 4.14 (t, 2H, J=7 Hz, C*H*$_2$O$_2$); ^{13}C-NMR (100.5 MHz, RT, $CDCl_3$): δ = 13.81 (*C*H$_3$), 19.06, 22.05, 25.63, 27.94, 28.20, 28.32, 28.67, 28.88, 29.02, 29.21, 30.90, 41.31 (*C*H$_2$), 52.39 (*C*H$_3$O), 65.17, 65.23 (sp *C*), 65.64 (*C*H$_2$O$_2$), 77.39, 77.52 (sp *C*), 166.64, 167.11 (*C*=O); MS (EI): *m/z* = 362 (M^+), 320, 289, 187, 134, 119, 101, 79, 67, 55, 41, 29; IR (film):

$\tilde{\nu}$ = 2932.0 cm^{-1}, 2857.6, 2256.3, 2156.0, 1756.6, 1738.1, 1464.9, 1436.9, 1334.5, 1273.5, 1199.1, 1150.3, 1024.0, 725.0, 665.5.

1,2-[Methoxycarbonyl-10,12-(octadecadiynyloxycarbonyl)methano-1,2-dihydro[60] fullerene (<u>102</u>)

According to the synthesis of **70**, the reaction was performed with 200 mg (0.277 mmols) of C_{60}, 138 mg (0.416 mmols) of CBr_4, 151 mg (0.208 mmols) of malonate **101**, and 124 µL (0.831 mmols) of DBU in 125 mL of toluene. After 24 hours the solvent was destilled under reduced pressure and the crude mixture was separated by FC (SiO_2/toluene:hexane 1:1) to yield 165 mg of [60]fullerene monoadduct **102**. Yield: 55.0 %.

^{1}H-NMR (400 MHz, RT, $CDCl_3$): δ = 0.89 (t, 3H, J=7 Hz, C*H*$_3$), 1.25-1.55 (m, 18H, C*H*$_2$), 1.84 (tt, 2H, C*H*$_2$, J_1=J_2=7 Hz), 2.24 (t, 4H, J=7 Hz, C*H*$_2$-≡-), 4.09 (s, 3H, C*H*$_3$O), 4.50 (t, 2H, J=7 Hz, C*H*$_2$O$_2$); ^{13}C-NMR (100.5 MHz, RT, $CDCl_3$): δ = 13.84 (*C*H$_3$), 19.11, 19.14, 22.08, 25.86, 27.95, 28.23, 28.48, 28.73, 28.94, 29.06, 29.33, 30.91 (*C*H$_2$), 52.10 (methano bridge), 53.93 (*C*H$_3$O), 65.27, 65.38 (sp *C*), 67.45 (*C*H$_2$O$_2$), 71.49 , 77.42 (C_{60}-sp^3 *C*), 77.61 (sp *C*), 138.94, 139.15, 140.99, 141.92, 141.96, 142.25, 143.05, 143.11, 143.13, 143.92, 144.66, 144.72, 144.92, 145.14, 145.22, 145.30, 145.36 (C_{60}-sp^2 *C*), 163.65, 164.17 (*C*=O); UV/Vis (CH_2Cl_2): λ_{max} = 258.0 nm, 326.0, 425.5, 488.0; MS (FAB+): *m/z* = 1081 (M^+), 720 (C_{60}^+); IR (KBr): $\tilde{\nu}$ = 2924.7 cm^{-1}, 2852.1, 2282.5, 2253.1, 2189.1, 2153.5, 2130.5, 2078.6, 1744.8, 1460.2, 1428.8, 1265.8, 1234.4, 1185.2, 1096.7, 1061.1, 734.1, 704.7, 525.9.

1,2-[Methoxycarbonyl-10,12-(octadecadiynyloxycarbonyl)methano]-18,36:22,23:27, 45:31,32:55,56-pentakis[(diethoxycarbonyl)methano]-1,2:18,36:22,23:27,45:31,32:55,56-dodecaahydro[60]fullerene (<u>103</u>)

A solution of 160 mg (0.148) of **102** and 305 mg (1.48 mmols) of DMA in 120 mL toluene was stirred under Argon for 2 h. Then, 0.25 mL (1.48 mmols) of bromo diethylmalonate and 0.22 mL (1.47 mmols) of DBU were added. After 48 hours the solvent was destilled under reduced pressure and the crude mixture was separated by FC (SiO_2/toluene:ethyl acetate 9:1) followed by preparative HPLC (grom-Sil 100Si, NP1, 5µ/ 20 mL/min toluene:ethyl acetate 95:5) to give 97.5 mg of hexakisadduct **103**. Yield: 35.2 %.

^{1}H-NMR (400 MHz, RT, $CDCl_3$): δ = 0.89 (t, 3H, J=7 Hz, C*H*$_3$), 1.25-1.55 (m, 18H, C*H*$_2$), 1.33 (t, 30H, J=7 Hz, C*H*$_3$), 1.68 (tt, 2H, J_1=J_2=7 Hz, C*H*$_2$), 2.43 (t, 4H, J=7 Hz, C*H*$_2$-≡-), 3.86 (s, 3H, C*H*$_3$O), 4.26 (t, 2H, J=7 Hz, C*H*$_2$O$_2$), 4.34 (q, 20 H, J=7 Hz, C*H*$_2$O$_2$); ^{13}C-NMR

(100.5 MHz, RT, $CDCl_3$): δ = 13.82, 13.96 (*C*H_3), 19.09, 19.11, 22.08, 25.65, 27.96, 28.26, 28.29, 28.73, 28.94, 29.02, 29.26, 30.92 (*C*H_2), 45.22, 45.31 (methano bridge), 53.48 (*C*H_3O), 62.81 (*C*H_2), 65.21, 65.25 (sp *C*), 66.96 (*C*H_2O_2), 69.00, 69.05 (C_{60}-sp^3 *C*), 77.47, 77.53 (sp *C*), 140.99, 141.19, 145.67, 145.83, 145.87, 145.98 (C_{60}-sp^2 *C*), 163.89, 163.95, 164.43 (*C*=O);

UV/Vis (CH_2Cl_2): λ_{max} = 244.5 nm, 270.0, 281.0, 319.5, 336.0, 386; MS (FAB+): *m/z* = : 1872 (M^+), 720 (C_{60}^+); IR (KBr): $\tilde{\nu}$: 2981.1 cm^{-1}, 2933.7, 2857.3, 1745.4, 1464.6, 1445.7, 1390.6, 1367.7, 1264.8, 1220.6, 1094.7, 1079.3, 1043.8, 1018.6, 715.5, 529.0.

1,16-Hexadecandiol (<u>106</u>)

Hexadecanedioic acid (2 g, 6.983 mmol) in 50 ml dry THF was added dropwise to a slurry of lithium aluminum hydride (4.5 g, 120 mmol) in 40 ml dry THF under nitrogen at rt. The mixture was refluxed for 2 d and then stirred at room temperature till TLC showed complete conversion (4 d)[126]. A mixture of methanol and ether (1:5) was added to destroy the excess hydride. Dilute H_2SO_4 (5 %) was added until two clear layers were formed. The two layers were separated and the aqueous layer was extracted with three portions of ether (3x50 ml). The combined organic phase was washed with 5 % $NaHCO_3$ and dried over $MgSO_4$. Evaporation of the solvent gave 1.80 g (100 %) of 1,16-hexadecandiol as a white solid.

^{1}H-NMR (400 MHz, RT, $CDCl_3$): δ = 1.10-1.30 (m, 28H, C*H*$_2$), 3.34 (dt, 4H, J_1=7 Hz, J_2=4 Hz, C*H*$_2$OH), 4.31 (t, 2 H, J=4 Hz, O*H*); ^{13}C-NMR (100.5 MHz, RT, $CDCl_3$): δ = 25.49, 28.96, 29.03, 29.09, 32.52 (*C*H_2), 60.69 (*C*H_2OH); MS (EI): *m/z* = 259 (M^++1), 222, 194, 166, 152, 138, 124, 109, 96, 82, 69, 55; IR (KBr): $\tilde{\nu}$ = 3422.3 cm^{-1}, 2918.1, 2850.3, 2360.5, 1700.9, 1652.7, 1471.4, 1261.1, 1122.1, 801.9.

16-Hydroxyhexadecyl methylmalonate (<u>107</u>)

According to the synthesis of **101**, the reaction was performed using 0.85 ml (0.79 mmols) of malonyl dichloride monomethyl ester, 2.05 g (7.96 mmol) of **106**, and 0.65 ml (0.8 mmol) of pyridine in 60 mL dry CH_2Cl_2. FC (SiO_2/hexan:ethyl acetate 7:3) gave 725 mg of **107**. Yield: 25 %.

^{1}H-NMR (400 MHz, RT, $CDCl_3$): δ = 1.26-1.31 (m, 24H, C*H*$_2$), 1.56, 1.64 (2tt, 4H, J_1=J_2 =7 Hz, C*H*$_2$CH$_2$COOH, C*H*$_2$CH$_2$O), 3.39 (s, 2H, OCC*H*$_2$CO), 3.62 (t, 2H, J=7 Hz, C*H*$_2$OH), 3.75 (s, 3H, C*H*$_3$O), 4.140 (t, 2H, J_1=7 Hz, C*H*$_2$CO$_2$C); ^{13}C-NMR (100.5 MHz, RT, $CDCl_3$): δ = 25.57, 28.23, 28.99, 29.27, 29.30, 29.36, 29.43, 29.46, 32.58, 41.19 (*C*H_2), 52.28 (*C*H_3),

62.72 (*C*H_2OH), 65.58 (*C*H_2O), 166.58, 167.04 (*C*=O); MS (EI): *m/z* = 222, 149, 119; IR (KBr): $\tilde{\nu}$ = 3417.9 cm^{-1}, 3345.4, 3227.2, 2918.2, 2849.7, 1735.8, 1475.2, 1440.2, 1409.7, 1356.2, 1278.6, 1219.2, 1156.8, 1063.6, 1030.9, 995.6, 969.3, 929.3, 852.5, 806.1, 730.6, 720.3, 689.3, 611.3, 581.1, 471.5, 412.1.

15-Carboxypentadecyl methylmalonate (<u>108</u>)

Pyridinium dichromate (PDC) (2.665 g, 7.078 mmol) in 6 ml dry DMF was added to a solution of 725 mg 16-hydroxyhexadecyl methyl malonate (**107**) in 4 ml dry DMF[127]. After 7 h stirring at r.oom temperature, the mixture was poured into 100 ml H_2O and extracted with ether. FC (SiO_2/hexan:Et_2O 1:1) gave 556 mg of **108**. Yield: 74 %.

^{1}H-NMR (400 MHz, RT, $CDCl_3$): δ = 1.21-1.40 (m, 24H, C*H*$_2$), 1.59-1.66 (m, 4H, C*H*$_2$), 2.34 (t, 2H, J=7 Hz, C*H*$_2$COOH), 3.99 (s, 2H, C*H*$_2$), 3.75 (s, 3H, C*H*$_3$O), 4.14 (t, 2H, J=7 Hz, C*H*$_2$COO), 11.21 (COO*H*); ^{13}C-NMR (100.5 MHz, RT, $CDCl_3$): δ = 24.55, 25.65, 28.32, 28.95, 29.01, 29.31, 29.38, 29.44, 29.46, 29.50, 33.96, 41.29 (*C*H_2), 52.38 (*C*H_3), 65.69 (*C*H_2O), 166.68, 167.15 (*C*O_2R), 180.12 (*C*OOH); MS (EI): *m/z* = 354 (M^+-H_2O), 236, 119; IR (KBr): $\tilde{\nu}$ = 3454.8 cm^{-1}, 2921.0, 2850.9, 1738.3, 1722.1, 1701.2, 1465.7, 1440.6, 1335.7, 1299.5, 1199.5, 1154.2, 1022.6, 933.4, 807.7, 722.8, 684.5, 612.3, 587.9.

Triethyleneglycol 3,4,5,6-tetrahydro-2*H*-pyran-2-yl ether (<u>109</u>)

p-Toluenesulfonic acid monohydrate (0.3 mmol, 0.057 g) was added to a solution of 4 ml (29.964 mmol) of triethyleneglycol and 2.7 ml (29.59 mmol) 2,3-dihydropyran (DHP) in 200 ml of CH_2Cl_2[128]. After 48 h, triethylamine (60 mg, 0.6 mmol) was added and the mixture stirred for 30 min. FC (SiO_2/hexan:ethyl acetate 7:3) gave 3.37 g of monoprotected triethylene-glycol **109**. Yield: 48 %.

^{1}H-NMR (400 MHz, RT, $CDCl_3$): δ = 1.47-1.57 (m, 4H, THP-C*H*$_2$), 1.64-1.67 (m, 1H, C*H*H), 1.70-1.79 (m, 1H, C*H*H), 3.44-3.67 (m, 12H, C*H*$_2$), 3.80-3.86 (m, 2H, CH*H*, C*H*$_2$O), 4.59 (dd, 1H, J_1=J_2=4 Hz, OC*H*O); ^{13}C-NMR (100.5 MHz, RT, $CDCl_3$): δ = 19.09, 25.09, 30.19, 61.36, 61.89, 66.30, 70.09, 70.25, 70.35, 72.33 (*C*H_2), 98.68 (*C*H); MS (EI): *m/z* = 151, 121, 98, 89, 85 (THP^+); IR (film): $\tilde{\nu}$ = 3456.8 cm^{-1}, 2940.7, 2870.6, 2739.3, 2659.6, 1455.0, 1385.0, 1351.9, 1323.2, 1284.7, 1259.8, 1201.8, 1125.2, 1075.9, 1035.1, 988.3, 872.5, 814.

Di-(+)-menthylmalonate (<u>112</u>)

Acorrding to the preparation of **23**, the reaction was performed using 5 g (32.0 mmols) of (+)-menthol, 2.59 mL (32.02 mmols) of pyridine, and 1.55 mL (15.93 mmols) of malonyl dichloride in 75 mL CH_2Cl_2. FC (SiO_2/hexane:CH_2Cl_2 65:35) afforded 3.75 g of **112**. Yield: 65.3 %.

^{1}H-NMR (400 MHz, RT, $CDCl_3$): δ = 0.76 (d, 6H, J=6.8 Hz, C*H*$_3$), 0.90 (d, 6H, J=7.2 Hz, C*H*$_3$), 0.91 (d, 6H, J=6 Hz, C*H*$_3$), 1.04 (m, 2H, C*H*H), 1.35 (m, 2H, C*H*H), 1.50 (m, 4H, 2xC*H*), 1.70 (m, 4H, 2 x C*H*H), 1.91 (qqd, J_1=J_2=7.2 Hz, J_3=2.8, 2H, C*H*Me$_2$), 2.03 (ddd, J_1=11.6 Hz, J_2=J_3=3.2 Hz, 2H, C*H*H), 3.33 (s, 2H, CH2), 4.76 (ddd, J_1=J_2=11 Hz, J_3=4.4 Hz, 2H, C*H*O).

1,2-Bis(menthyloxycarbonyl)methano-1,2-dihydro[60] fullerene (<u>113</u>)

According to the synthesis of **70**, the reaction was carried out using 100 mg (0.139 mmols) of C_{60}, 69 mg (0.208 mmols) of CBr_4, 79.2 mg (0.208 mmols) of malonate **112**, and 62 µl (0.415 mmols) of DBU in 60 mL toluene. After 24 h, the usual work-up was performed. FC (SiO_2/toluene:hexane 1:1) yielded 84 mg of [60]fullerene monoadduct **113**. Yield: 55.1 %.

^{1}H-NMR (400 MHz, RT, $CDCl_3$): δ = 0.82 (d, J=6.8 Hz, 6H, C*H*$_3$), 0.92 (d, J=7.2 Hz, 6H, C*H*$_3$), 1.00 (d, J=6 Hz, 6H, C*H*$_3$), 1.22 (ddd, J_1=J_2=J_3=11 Hz, 2H, C*H*H), 1.13 (m, 2H, C*H*H), 1.61 (m, 4H, 2xC*H*), 1.76 (m, 4H, 2 x C*H*H), 2.10 (qqd, J_1=J_2=7.2 Hz, J_3=2.8, 2H, C*H*Me$_2$), 2.32 (ddd, J_1=11.6 Hz, J_2=J_3=3.2 Hz, 2H, C*H*H), 5.05 (ddd, J_1=J_2=11 Hz, J_3=4.4 Hz, 2H, C*H*O); ^{13}C-NMR (100.5 MHz, RT, $CDCl_3$): δ = 16.01 (*C*H$_3$), 22.02, 20.79, 23.08 (*C*H$_2$), 25.98, 31.49, (*C*H), 34.10, 40.66 (*C*H$_2$), 46.94 (*C*H), 53.01 (methano bridge), 71.92 (C_{60}-sp^3 *C*), 78.04 (*C*HO), 138.95, 140.94, 140.96, 141.88, 141.94, 142.23, 142.29, 143.02, 143.03, 143.09, 143.13, 143.92, 143.94, 144.55, 144.69, 144.74, 144.79, 144.88, 145.16, 145.24, 145.36, 145.40, 145.43,145.81 (C_{60}-sp^2 *C*), 163.12 (*C*=O); UV/Vis (CH_2Cl_2): λ_{max} = 257.5 nm, 325.5, 426.0, 496.0; MS (MALDI-TOF): *m/z* = 1098 (M^+); IR (KBr): $\tilde{\nu}$ = 2951.8 cm^{-1}, 2923.0, 2866.2, 1736.7, 1453.6, 1368.5, 1266.3, 1234.2, 1177.7, 112.6, 1095.0, 1054.4, 981.7, 946.4, 903.5, 736.7, 702.3, 526.5.

6 Literature

[1] a) E. Osawa, *Kagaku* **1970**, *25*, 854. b) Z. Yoshida, E. Osawa, *Aromaticity Kagakudojin*; Kyoto, 1971.

[2] H. W. Kroto, J. R. Heath, S. C. O´Brien, R. F. Curl, R. E. Smaley, *Nature* **1985**, *318*, 162.

[3] W. Krätschmer, L. D. Lamb, K. Fostiropoulos, D. R. Huffmann, *Nature* **1990**, *347*, 354.

[4] A. Hirsch, *The Chemistry of the Fullerenes.* Organic Chemistry Monograph Series, Georg Thieme Verlag, Stuttgart-New York, 1994.

[5] A. Hirsch, *Angew. Chem.* **1993**, *105*, 1189; *Angew. Chem. Int. Ed. Engl.* **1993**, *32*, 1138

[6] A. Hirsch, *Synthesis* **1995**, 895.

[7] a) A. F. Hebard, M. J. Rosseinsky, R. C. Haddon, D. W. Murphy, S. H. Glarum, T. T. M. Palstra, A. P. Ramirez, A. R. Kortan, *Nature* **1991**, *350*, 600. b) K. Holczer, O. Klein, S.-M. Huang, R. B. Kauer, K. J. Fu, R. L. Whetten, F. Diederich, *Science* **1991**, *252*, 1154.

[8] P. M: Allemand, K. C. Khemani, A. Koch, F. Wudl, K. Holczer, S. Donovan, G. Gruner, J. D. Thompson, *Science* **1991**, *253*, 301.

[9] S. H. Friedman, D. L. DeCamp, R. P. Sijbesma, G. Srdanov, F. Wudl, G. L. Kenyon, *J. Am. Chem. Soc.* **1993**, *115*, 6506.

[10] S. R. Sijbesma, G. Srdanov, F. Wudl, J. A. Castoro, C. Wilkins, S. H. Friedman, D. L. DeCamp, G. L. Kenyon, *J. Am. Chem. Soc.* **1993**, *115*, 6510.

[11] H. Tokuyama, S. Yamago, E. Nakamura, T. Shiraki, Y. Sugiura, *J. Am. Chem. Soc.* **1993**, *115*, 7918.

[12] J. L. Anderson, Y.-Z. An, Y. Rubin, C. S. Foote *J. Am. Chem. Soc.* **1994**, *116*, 9763.

[13] L. L. Dugan, D. M. Turtetsky, C. Du, D. Lobner, M. Wheeler, C. R. Almli, C. K.-F. Shen, T.-Y. Luh, D. W. Choi, T.-S. Lin, *Proc. Natl. Acad. Sci. USA* **1997**, *94*, 9434.

[14] a) H. W. Kroto, *Nature* **1987**, *329*, 529; b) T. G. Schmalz, W. A. Seitz, D. J. Klein, G. E. Hite, *Chem. Phys. Lett.* **1986**, *130*, 203.

[15] R. C. Haddon, *Science* **1993**, *261*, 1545.

[16] a) R. C. Haddon, *Chem. Phys. Lett.* **1986**, *125*, 231; b) R. C. Haddon, *J. Am. Chem. Soc.* **1987**, *109*, 1686.

[17] R. C. Haddon, L. E. Brus, K. Raghavachari, *Chem. Phys. Lett.* **1986**, *125*, 459.

[18] Q. Xie, E. Pérez-Cordero, L. Echegoyen, *J. Am. Chem. Soc.* **1992**, *114*, 3978.

[19] a) Z. Gasyna, P. N. Schatz, J. P. Hare, T. J. Dennis, H. W. Kroto, R. Taylor, D. R. M. Walton, *Chem. Phys. Lett.* **1991**, *183*, 283. b) S. Leach, M. Vervloet, A. Despres, E. Breheret, J. P. Hare, T. J. Dennis, H. W. Kroto, R. Taylor, D. R. M. Walton, *Chem. Phys.* **1992**, *160*, 451.

[20] S. J. Cyvin, E. Brendsdal, B. N. Cyvin, J. Brunvoll, *Chem. Phys. Lett.* **1990**, *170*, 167.

[21] H. Ajie, M. M. Alvarez, S. J. Anz, R. D. Beck, F. Diederich, K. Fostiropoulos, R. Huffman, W. Krätschmer, Y. Rubin, K. E. Schriver, D. Sensharma, R. L. Whetten, *J. Phys. Chem.* **1990**, *94*, 8630.

[22] a) B. Chase, P. J. Fagan *J. Am. Chem. Soc.* **1992**, *114*, 2252; b) A. L. Balch, D. A. Costa, J. W. Lee, B. C. Noll, M. M. Olmstead, *Inorg. Chem.* **1994**, *33*, 2071.

[23] a) P. R. Birkett, P. B. Hitchcock, H. W. Kroto, R. Taylor, D. R. M. Walton, *Nature* **1992**, *357*, 479; b) P. R. Birkett, A. G. Avent, A. D. Darwish, H. W. Kroto, R. Taylor, D. R. M. Walton, *J. Chem. Soc., Chem. Commun.* **1993**, 1230; c) A. G. Avent, P. R. Birkett, J. D. Crane, A. D. Darwish, G. J. Langley, H. W. Kroto, R. Taylor, D. R. M. Walton, *J. Chem. Soc., Chem. Commun.* **1994**, 1463.

[24] C. Bingel, *Chem. Ber.* **1993**, *126*, 1957.

[25] A. Hirsch, I. Lamparth, H. R. Karfunkel, *Angew. Chem.* **1994**, *106*, 453; *Angew. Chem. Int. Ed. Engl.* **1994**, *33*, 437.

[26] F. Djojo, A. Herzog, I. Lamparth, F. Hampel, A. Hirsch, *Chem. Eur. J.* **1996**, *2*, 1537.

[27] A. Hirsch, I. Lamparth, T. Grösser, H. R. Karfunkel, *J. Am. Chem. Soc.* **1994**, *116*, 9385.

[28] A. Hirsch, I. Lamparth, G. Schick, *Liebigs Ann.* **1996**, 1725.

[29] I. Lamparth, C. Mössmer, A. Hirsch, *Angew. Chem.* **1995**, *107*, 1755; *Angew. Chem. Int. Ed. Engl*. **1995**, *34*, 1607.

[30] I. Lamparth, A. Herzog, A. Hirsch, *Tetrahedron*, **1996**, *52*, 5065.

[31] a) L. Isaacs, R. F. Haldimann, F. Diederich, *Angew. Chem.* **1994**, *106*, 2434*; Angew. Chem. Int. Ed. Engl.* **1994**, *33*, 2439; b) L. Isaacs, R. F. Haldimann, F. Diederich, *ibid.* **1995**, *107*, 1636 and **1995**, *34*, 1466; c) J.-F. Nierengarten, V. Gramlich, F. Cardullo, F. Diederich, *ibid.* **1996**, *108*, 2242 and **1996**, *35*, 2101.

[32] R. Breslow, *Acc. Chem. Res.* **1980**, *13*, 170.

[33] B. Kräutler, T. Müller, J. Maynollo, K. Gruber, C. Kratky, P. Ochsenbein, D. Schwarzenbach, H.-B. Bürgi, *Angew. Chem.* **1996**, *108*, 1294; *Angew. Chem. Int. Ed. Engl.* **1996**, *35*, 1204.

[34] P. J. Kursic, E. Wasserman, P. N. Keizer, J. R. Morton, K. F. Preston, *Science* **1991**, *254*, 1183.

[35] D. A. Tomalia, A. M. Naylor, W. A. Goddard III, *Angew. Chem.* **1990**, *102*, 119; *Angew. Chem. Int. Ed. Engl.* **1990**, *29*, 138.

[36] G.R. Newkome, C. N. Moorefield, F. Vögtle, 'Dendritic Molecules, Concepts, Syntheses, Prespectives', VCH, Weinheim, 1996.

[37] S. E. Campbell, G. Luengo, V. I. Srdanov, F. Wudl, J. N. Israelachvili, *Nature* **1996**, *382*, 520.

[38] K. C. Hwang, D. Mauzerall, *Nature* **1993**, *361*, 138.

[39] N. Ardoin, D. Astruc, *Bull. Soc. Chim. Fr.* **1995**, *132*, 875.

[40] a) E. Buhleier, W. Wehner, F. Vögtle, *Synthesis* **1978**, 155; b) F. Vögtle, E. Weber, *Angew. Chem.* **1979**, *91*, 813; *Angew. Chem. Int. Ed. Engl.* **1979**, *18*, 753.

[41] J. Issberner, R. Moors, F. Vögtle, *Angew. Chem.* **1994**, *106*, 2507; *Angew. Chem. Int. Ed. Engl.* **1994**, *33*, 2413.

[42] a) J. F. G. A. Jansen, E. M. M. de Brabander-van den Berg, E. W. Meijer, *Science* **1994**, *226*, 1226; b) J. F. G. A. Jansen, E. W. Meijer, E. M. M. de Brabander-van den Berg, *J. Am. Chem. Soc.* **1995**, *117*, 4417.

[43] C. C. Mak, H.-F. Chow, *Macromolecules* **1997**, *30*, 1228 and ref. therein.

[44] D. A. Tomalia, P. R. Dvornic, *Nature* **1994**, *372*, 617.

[45] a) Z. Xu, M. Kahr, K. L. Walker, C. L. Wilkins, J. S. Moore, *J. Am. Chem. Soc.* **1994**, *116*, 4537; b) T. Kawaguchi, K. L. Walker, C. L. Wilkins, J. S. Moore, *J. Am. Chem. Soc.* **1995**, *117*, 2159.

[46] K. L. Wooley, C. J. Hawker, J. M. J. Fréchet, *J. Am. Chem. Soc.* **1991**, *113*, 4252.

[47] a) D. A. Tomalia, H. Baker, J. Dewald, M. Hall, G. Kallos, S. Martin, J. Roeck, J. Ryder, P. Smith, *Polym. J.* **1985**, *17*, 117; b) D. A. Tomalia, H. Baker, J. Dewald, M. Hall, G. Kallos, S. Martin, J. Roeck, J. Ryder, P. Smith, *Macromolecules* **1986**, *19*, 2466.

[48] a) G. R. Newkome, Z. Yao, G. R. Baker, V. K. Gupta, *J. Org. Chem.* **1985**, *50*, 2004; b) G. R. Newkome, G. R. Baker, M. J. Saunders, P. S. Russo, V. K. Gupta, Z. Yao, J.

E. Bouillion, *J. Chem. Soc., Chem. Commun.* **1986**, 752; c) G. R. Newkome, Z. Yao, G. R. Baker, V. K. Gupta, P. S. Russo, M. J. Saunders, *J. Am. Chem. Soc.* **1986**, *108*, 849.

[49] R. G. Denkewalter, J. F. Kolc, W. J. Lukasavage, *U.S. Pat. 4.410.688* **1983**; *Chem. Abstr.* **1984**, *100*, 103907.

[50] G. R. Newkome, A. Nayak, R. K. Behera, C. N. Moorefield, G. R. Baker, *J. Org. Chem.* **1992**, *57*, 358.

[51] C. J. Hawker, J. M. J. Fréchet, *J. Chem. Soc., Chem. Commun.* **1990**, 1010.

[52] T. M. Miller, T. X. Neenan, *Chem. Mater.* **1990**, *2*, 346.

[53] K. Wooley, C. J. Hawker, J. M. J. Fréchet, *J. Chem. Soc., Perkin Trans. 1* **1991**, 1059.

[54] T. Kawaguchi, K. L. Walker, C. L. Wilkins, J. S. Moore, *J. Am. Chem. Soc.* **1995**, *117*, 2159.

[55] C. J. Hawker, J. M. J. Fréchet, *J. Am. Chem. Soc.* **1990**, *112*, 7638.

[56] K. L. Wooley, C. J. Hawker, J. M. J. Fréchet, F. Wudl, G. Srdanov, S. Shi, C. Li, M. Kao, *J. Am. Chem. Soc.* **1993**, *115*, 9836.

[57] C. J. Hawker, K. L. Wooley, J. M. J. Fréchet, *J. Chem. Soc., Chem. Commun.* **1994**, 925.

[58] S. Shi, K. C. Khemani, Q. Li, F. Wudl, *J. Am. Chem. Soc.* **1992**, *114*, 10656.

[59] M. Prato, Q. C. Li, F. Wudl, V. Lucchini, *J. Am. Chem. Soc.* **1993**, *115*, 1148.

[60] The Notation of this dendrimers in a short form refers to that proposed by Fréchet and coworkers in ref. [55].

[61] D. Seebach, J.-M. Lapierre, G. Greiveldinger, K. Skobridis, *Helv. Chim. Acta* **1994**, *77*, 1673.

[62] A. Hermann, M. Rüttimann, C. Thilgen, F. Diederich, *Helv. Chim. Acta* **1995**, *78*, 1673.

[63] Hubert Schönberger, Diplomarbeit, Universität Erlangen-Nürnberg 1997.

[64] HYPERCHEM 4.5, Hypercube, **1995**, 419 Phillip Steet, Waterloo, Ontario N2l 3X2 (Canada).

[65] S. I. Khan, A. M. Oliver, M. N. Paddon-Row, Y. Rubin, *J. Am. Chem. Soc.* **1993**, *115*, 4919.

[66] All structures were pre-minimized with the MM^+ force field implemented in HYPERCHEM prior to the MD simulation. During the MD simulations the structures were heated to 1000 K and kept at this temperature for equilibration

before they were allowed to cool to 0 K for establishing the minimum energy structure. Conditions for the simulated annealing: heat time: 5 ps, run time: 15 ps, cool time: 50 ps, step size: 0.001 ps, starting temperature: 0 K, simulation temperature: 1000 K, final temperature: 0 K, in vacuo, data collection period: 1 time step.

[67] Andrea Herzog, Doktorarbeit, Universität Erlangen-Nürnberg, end of 1998.

[68] F. Diederich, C. Thilgen, A. Herrmann, *Nachr. Chem. Tech. Lab.* **1996**, *44*, 9.

[69] B. Gross, V. Schurig, I. Lamparth, A. Herzog, F. Djojo, A. Hirsch, *J. Chem. Soc., Chem. Commun.* **1997**, 1117.

[70] J. F. Nierengarten, V. Gramlich, F. Cardullo, F. Diederich, *Angew. Chem* **1996**, *108*, 2242; *Angew. Chem. Int. Ed. Engl.* **1996**, *35*, 2101.

[71] E. Nakamura, H. Isobe, H. Tokuyama, M. Sawamura, *J. Chem. Soc., Chem. Commun.* **1996**, 1747.

[72] F. Djojo, A. Hirsch, *Chem. Eur. J.* **1998**, *4*, 344.

[73] Francis Djojo, Doktorarbeit, Universität Erlangen-Nürnberg, 1999.

[74] a) A. Pfaltz, Acc. *Chem. Res.* **1993**, *26*, 339; b) D. A. Evans, M. M. Faul, M. T. Bilodeau, *J. Am. Chem. Soc.* **1994**, *116*, 2742; c) R. E. Lowenthal, S. Masamune, *Tetrahedron* **1991**, *32*, 7373; d) A. S. Gokhale, A. B. E. Minidis, A. Pfaltz, *Tetrahedron Lett.* **1995**, *36*, 1831; e) M. B. Andrus, A. B. Argade, X. Chen, M. Pamment, *Tetrahedron Lett*. **1995**, *36*, 2945; f) S. E. Denmark, N. Nakajiama, O. J. C. Nicaise, *J. Am. Chem. Soc*. **1994**, *116*, 8797; g) E. J. Corey, K. Ishihara, *Tetrahedron Lett.* **1992**, *33*, 6807; h) D. A. Evans, S. J. Miller, T. Lectka, *J. Am. Chem. Soc*. **1993**, *115*, 6460.

[75] R.-H. Jin, T. Aida, S. Inoue, *J. Chem. Soc., Chem. Commun.* **1993**, 1261.

[76] a) P. J. Dandliker, F. Diederich, M. Gross, C. B. Knobler, A. Louati, E. M. Sanford, *Angew. Chem.* **1994**, *106*, 1821; *Angew. Chem. Int. Ed. Engl.* **1994**, *33*, 1739; b) P. J. Dandliker, F. Diederich, J.-P. Gisselbrecht, A. Louati, M. Gross, *Angew. Chem.* **1995**, *107*, 2906; *Angew. Chem. Int. Ed. Engl.* **1995**, *34*, 2906.

[77] R. Sadamoto, N. Tomioka, T. Aida, *J. Am. Chem. Soc.* **1996**, *118*, 3978.

[78] P. Bhyrappa, J. K. Young, J. S. Moore, K. S. Suslick, *J. Am. Chem. Soc.* **1996**, *118*, 5708.

[79] B. Meunier, *Chem. Rev.* **1992**, *92*, 1411.

[80] a) B. R. Cook, T. J. Reinert, K. S. Suslick, *J. Am. Chem. Soc.* **1986**, *108*, 7281; b) K. S. Suslick, B. R. Cook, *J. Chem. Soc., Chem. Commun.* **1987**, 200.

[81] a) H. Imahori, Y. Sakata, *Adv. Mater. 1997*, **9**, 537; b) T. G. Linssen, K. Dürr, M. Hanack, A. Hirsch, *J. Chem. Soc.; Chem. Commun.* **1995**, *103*; c) K. Dürr, S. Fiedler, T. Linßen, A. Hirsch, M. Hanack, *Chem. Ber.* **1997**, *130*, 1375; d) M. G. Ranasinghe, A. M. Oliver, D. F. Rothenfluh, A. Salek, M. N. Paddon-Row, *Tetrahedron Lett*. **1996**, *37*, 4797; e) P. S. Baran, R. R. Monaco, A. U. Khan, D. I. Schuster, S. Wilson, *J. Am. Chem. Soc.* **1997**, *119*, 8363.

[82] Elke Dietel, Diplomarbeit, Universität Erlangen-Nürnberg, 1996.

[83] E. Dietel, A. Hirsch, *J. Chem. Soc., Perkin Trans. 2* **1998**, 1357.

[84] D. Seebach, J.-M. Lapierre, K. Skobridis, G. Greiveldinger, *Angew. Chem.* **1994**, *106*, 457; *Angew. Chem. Int. Ed. Engl.* **1994**, *33*, 440.

[85] P. Murrer, D, Seebach, *Angew. Chem.* **1995**, *107*, 2297; *Angew. Chem. Int. Ed. Engl.* **1995**, *34*, 2116.

[86] H. M. Müller, D. Seebach, *Angew. Chem.* **1993**, *105*, 483; *Angew. Chem. Int. Ed. Engl.* **1993**, *32*, 477.

[87] Molecular modeling was performed with the MM^+ method implemented in HYPERCHEM software package. Geometry optimization with the Newton-Raphson algorism was carried out connecting optimized addends to [60]fullerene in order to achieve optimized structures with high gradients.

[88] A 3 mm glassy carbon electrode as a working electrode and a silver/silver chloride electrode (Ag/AgCl) as a reference electrode were chosen for the electrochemical cell system. $TBAPF_6$ (tetrabutylamonium hexafluorophosphate) was used as supporting electrolyte. Dichlor-methane was used as a solvent.

[89] C. Gueutin, D. Lexa, M. Momenteau, J.-M. Saveéant, F. Xu, *Inorg. Chem.* **1986**, *25*, 4294.

[90] J.-H. Fuhrhop, J. Köning, 'Membranes and Molecular Assemblies: The Synkinetic Approach', Monographs in Supramolecular Chemistry, The Royal Society of Chemistry 1994, Cambridge.

[91] T. W. Green, P. G. M: Wuts, 'Protective Groups in Organic Synthesis', 2nd Edition, John Wiley & Sons, Inc., New York, 1991.

[92] J. Mayargue, M. Essamkaoui, H. Moskowitz, *Tetrahedron Lett.* **1989**, *30*, 6867.

[93] E. J. Corey, J.-L. Gras, P. Ulrich, *Tetrahedron Lett.* **1976**, 809.

[94] http://wsrv.clas.virginia.edu/~rjh9u/gif/cellmemb.gif

[95] H. Hungerbühler, D. M. Guldi, K.-D. Asmus, *J. Am. Chem. Soc.* **1993**, *115*, 3386.

[96] K. C. Hwang, D. Mauzerall, *J. Am. Chem. Soc.* **1992**, *114*, 9705.

[97] M. Hetzer, S. Bayerl, X. Camps, O. Vostrowsky, A. Hirsch, T. M. Bayerl, *Adv. Mater.* **1997**, *9*, 913.

[98] 'Comprehensive Supramolecular Chemistry', First Ed, Volume 8, pages 181-197, J. E. D. Davis, J. A. Ripmeester Volume Editors, Elsvier Science Ltd., Oxford, 1996.

[99] R. L. Biltonen, D. Lichtenberg, *Chem. Phys. Lipids* **1993**, *64*, 129.

[100] The DSC measurements were performed in the ascending and descending temperature mode using a Hart Calorimeter (Hart Scientific, UT, USA) at a scan rate of ±15 °C/h for all experiments. Control measurements at lower scan rates gave similar results.

[101] M. Hetzer, T. Gutberlet, M. Brown, X. Camps, O. Vostrowsky, A. Hirsch, T. M. Bayerl, manuscript in preparation.

[102] J. A. N. Zasadzinski, *Biochim. Biophys. Acta* **1998**, *946*, 235.

[103] S. König, W. Pfeiffer, T. M. Bayerl, D. Richter, E. Sackmann, *J. Phys. II (Paris)* **1992**, *2*, 1589.

[104] S. König, T. M. Bayerl, G. Coddens, D. Richter, E. Sackmann, *Biophys. J.* **1995**, *68*, 1871.

[105] T. Pott, E.J. Dufourc, *Biophys. J.* **1995**, *68*, 965.

[106] T. Brumm, A. Möps, C. Dolainsky, S. Brückner, T. M. Bayerl, *Biophys. J.* **1992**, *61*, 1018.

[107] M. Bloom, E. Sternin, *Biochem.* **1987**, *26*, 2101.

[108] M. Bloom, *Phys. Can.* **1992**, *48*, 7.

[109] C. Dolainsky, A. Möps, T. M. Bayerl, *J. Chem Phys.* **1993**, *98*, 1712.

[110] 'Phospholipids Handbook' Editor Gregor Cevc, Marcel Dekker, Inc., New York, Basel, Hong Kong, 1993.

[111] a) G. Wegner, *Z. Naturforsch.* **1969**, B*24*, 824; b) G. Wegner, *Chimia* **1974**, *28*, 475; c) G. Wegner, *Makromol. Chem.* **1972**, *154*, 35; d) G. Wegner, *Makromol. Chem. Suppl.* **1984**, *6*, 347; e) G. Wegner, *Angew. Chem.* **1981**, *93*, 352; *Angew. Chem. Int. Ed. Engl.* **1981**, *20*, 361.

[112] K. Takeda, G. Wegner, *Makromol. Chem.* **1972**, *160*, 349.

[113] 'Modern Acetylene Chemistry', Editors P. J. Stang, F. Diederich, VCH, Weinheim, 1995.

[114] H. S. Nalwa, *Adv. Mater.* **1993**, *5*, 341.

[115] D. E. Ingber, *Scientific American* **1998**, *1*, 30, and ref. therein; *Spektrum der Wissenschaft* **1998**, *3*, 32.

[116] H. Dugas, *Biorganic Chemistry, A Chemical Approach to Enzyme Action*, Third Edition, Springer Verlag, New York-Berlin-Heidelberg, **1996**.

[117] N. M. Green, *Adv. Protein Chem.* **1975**, *29*, 85; b) M. Wilchek, E. A. Bayer, *Methods Enzymol.* **1990**, *184*, 5.

[118] J.-F. Nierengarten, V. Gramlich, F. Cardullo, F. Diederich, *Angew. Chem.* **1996**, *108*, 2242; *Angew. Chem. Int. Ed. Engl.* **1996**, *35*, 2242; quoting C. Bingel.

[119] D. D. Perrin, W. L. F. Amarego, *Purification of Laboratory Chemicals.* 3rd edition, Pergamon Press, Oxford, 1988.

[120] E. Reimannn, *Chem Ber.* **1969**, *102*, 2881.

[121] A slightly modification from the original paper was the use of all reagents in stoichiometric amounts to avoid dibromination.

[122] X. Camps, A. Hirsch, *J. Chem. Soc., Perkin Trans. I* **1997**, 1595.

[123] J. M. Lapierre, K. Skobridis, D. Seebach, *Helv. Chim. Acta* **1993**, *76*, 2419.

[124] H. C. Brown, E. F. Knights, C. G. Scouten *J. Am. Chem. Soc.* **1974**, *96*, 7765.

[125] H. Pielartzik, B. Irmisch-Pielartzik, T. Eicher *Methoden der Organischen Chemie (Houben-Weyl)*, Vol. E5: Carbonsäauren und Carbonsäure-Derivate, Editor: Jürgen Falbe, Georg Thime Verlag, Stuttgart-New York, p.700, 1985, and references therein.

[126] E. S. Finne, J. R. Gunn, T. S. Sorensen, *J. Am. Chem. Soc.* **1987,** *109*, 7816.

[127] E. J. Corey, G. Schmidt, *Tetrahedron Lett.* **1979**, 5, 399.

[128] N. Miyashita, A. Yoshikoshi, P. A. Grieco, *J. Org. Chem.* **1977**, *42*, 3772.